Polymer Surface Modification via Noncovalent Binding of Functional (Macro)molecules: Investigation of Entrapment Strategy and Mechanism

Dissertation

Zur Erlangung des akademischen Grades

Dr. rer. nat.

des Fachbereichs Chemie

der Universität Duisburg-Essen

vorgelegt von Haofei Guo

geboren in Yangzhou, VR China

Essen, 2010

Datum der mündlichen Prüfung: 30 November 2010

Vorsitzender: Prof. Dr. Georg Jansen

Gutachter: Prof. Dr. Mathias Ulbricht

Prof. Dr. Christian Mayer

Abstract

Entrapment technique, served as one kind of polymer surface functionalization strategies, has been developed in recent decades. All previous studies focused on polar polymer surface modification. In this thesis, aiming to polymer surface hydrophilic and antifouling modification, a variety of (macro)molecules have been applied to entrap into polar polyestersulfone (PES) and nonpolar polypropylene (PP) surface respectively. It was found that the modification conditions for PES are not suitable for PP membrane surface; and the conditions for PP membrane are not exactly effective for PP film. Furthermore, the entrapment mechanism has been studied and discussed.

In the beginning of this thesis, polar PES microfiltration (MF) membrane has been used as base polymer. Two different routes, abbreviated as E1 and E2 have been tested for PES surface modification. In E1, the modifiers were anticipated to diffuse into swelling region in modifier solution, and then they were fixed into PES surface by deswelling in water (solvent extraction); in E2, the base polymer was swollen in solvent, and the modifiers were anticipated to entrap into PES surface quickly in water solution. Present studies revealed that PES surface can be hydrophilic modified via entrapment of poly(ethylene oxide) (PEO)-containing homo-/copolymers; and E1 showed much better efficiency than E2. Therefore, E1 was selected as the entrapment approach for the following studies of PP surface modification.

Then nonpolar PP surface was endowed with hydrophilicity, thermo-responsibility, as well as cationic charge after entrapment with corresponding modifiers respectively. For instance, it was validated that entrapment of small amphiphilic molecule octaethyleneglycol monooctadecylether ($C_{18}EO_8$) into Membrana PP MF membrane surface improved outer surface and inner surface hydrophilicity, as well as the corresponding antifouling properties.

Wettability and water flux of poly(butyl acrylate)-b-poly(N-isopropylacrylamide) (PBA-*b*-PNIPAAm) entrapment modified PP membrane surface were time-dependent, which had abrupt change at the lower critical solution temperature (LCST) of PBA-*b*-PNIPAAm. This thermo-responsive property could be further used for protein desorption. In addition, non-porous Membrana PP plate surface was also functionalized with the same procedure, and modified PP plates showed similar modification efficiency and surface properties as for porous PP membranes. Moreover, zeta potential measurement validated that the Celgard PP film surface showed cationic after entrapment with methyl and octyl groups quarternized poly(n-butyl acrylate)-block-poly(2-dimethylaminoethyl methacrylate) (PBA-*b*-P*q*DMAEMA).

The mechanism of entrapment behavior was further investigated in the final section of this thesis. In case of Membrana PP MF surface modification in nonpolar solution, entrapment of a variety of ethyleneoxide-containing substances into PP surface was studied. All results revealed that PEGs were ineffective, while many nonionic amphiphilic substances, especially some tri-block copolymers of poly(ethylene oxide) (PEO) and poly(propylene oxide) (PPO) were very effective for PP surface hydrophilic modification. The relationship between modifier structure and architecture and entrapment behavior was investigated by studying the reverse micellization of amphiphilic modifiers in nonpolar solutions via pyrene-probe fluorescence and ^{1}H NMR spectroscopy. The balanced structure of nonionic tri-block modifiers, the lowest reverse critical micelle concentration (RCMC) had been observed. It was concluded that a balance block copolymer structure and architecture promoting the self-association in the nonpolar solvent is the basis for a high entrapment efficiency. In case of modification in polar solution, the swelling degree for diffusion of modifier is one important factor. Moreover, the deswelling step in a second solvent is another important factor to entrap the modifier into base polymer surface.

This work was performed during the period from September 2007 to September 2010 at the Institute of Technical Chemistry (Lehrstuhl für Technische Chemie II), Department of Chemistry, Universität Duisburg-Essen, under the supervision of Prof. Dr. Mathias Ulbricht.

I declare that this dissertation represents my own work, except where due acknowledgement is made.

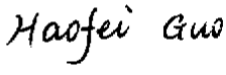

Haofei Guo

This thesis is dedicated

to my parents and sister

for their endless love and support.

Acknowledgement

The author wants first to express her deep gratitude to Prof. Dr. Mathias Ulbricht, who gave her constructive guidance and continuous support throughout her research work in DUE. Moreover, his respectable personality, patience and warm concerns on his students impressed her a lot.

The author also wants to especially appreciate Prof. Dr. Christian Mayer (Pysikalische Chemie, UDE), for his kind suggestions and professional comments on this thesis.

Moreover, the author would like to thank to all colleagues around her in group of Technische Chemie II, for their warm help, interesting discussion, fair competition as well as friendship. She will remember them and all those days with them. They are: Dongming, Heru, Tobias, Inge, Claudia, Frau Nordmann, Jun, Abdus, Monica, Halim, Marcel, Illing, Alex, Rafael, Qian, Eva, Nadia, Polina, Dongxu, Zhaoqing, Qianqian, Jing, Bintasan, Karin, Sebastian, Falk, Sven (Behnke), Sven (Frost), Christian (Kaul), Christian (Kuhn), Nico, David and Yan. In addition, the exchange students from U.S.A., Eric and Yang also contributed on some experiments of this thesis.

She would also like to thank many nice people in the department of chemistry for their technique support and very helpful discussion. They are: Herr Karwalt (ATR-FTIR, Anorganische Chemie), Herr Boukercha (SEM, Organishe Chemie), Herr Dr. Latz and Herr Gündel-Graber (XRD, Anorganische Chemie), Herr Bandmann, Dr. Schaller (NMR, Organishe Chemie) and Frau Brauner (Thermoanalysis, Anorganische Chemie).

Finally, she would love to give her deepest gratitude to her parents and sister for their endless support and concern throughout her life and study in Germany.

Content

List of Tables

List of Figures

Chapter 1

Introduction

1.1. Research background

As comprehensively reviewed by Ulbricht, polymeric membrane is one type of most important membranes in potential membrane separation process for liquid and gaseous mixtures (gas separation, reverse osmosis, pervaporation, nanofiltration, ultrafiltration, microfiltration) and in other important applications of membranes such as biomaterials, catalysis (including fuel cell systems) or lab-on-chip technologies [1]. Nevertheless, the performance of polymeric membrane is always limited by shortcoming of polymers such as low surface energy etc. For this reason, post-modification for imparting desirable functional species into polymer membrane surface is efficient way to minimize undesired (secondary) interactions (adsorption or adhesion) which reduce the performance (membrane fouling), or to introduce additional interactions (affinity, responsiveness or catalytic properties) for improving the selectivity or creating an entirely novel separation function (see Figure 1.1), without changing membrane bulk structure.

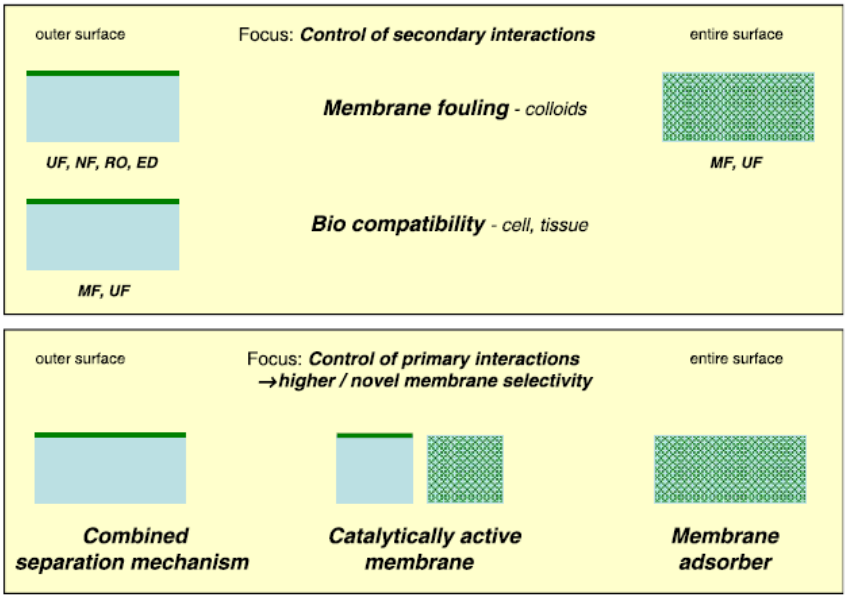

Figure 1.1. Improved or novel membrane performance via surface modification of membranes: a thin functional layer (green)—depending on pore structure and separation function either on the outer or the entire surface—leads to effective solutions for problems or to novel principles. 'Secondary' interactions (occurring also without a separation) should be controlled without sacrifying the separation function of the membrane. Controlling 'primary' interactions can be used to tailor the separation function of a membrane or to 'integrate' them with other processes [1].

By that means, hydrophilic, hydrophobic and ionic species are always used as modifiers in terms of specific application. In addition, applications of stimuli-responsive polymers attract more and more attention in recent two decades [2]. Because the reconstructable surfaces change their wettability and permeability, as well as their adhesive, adsorptive, mechanical and optical properties, emerging applications extend to materials with rapidly switchable adhesion to interacting materials and wetting (from wettable to non-wettable), with switchable appearance and coatings capable of rapid release of chemicals, such as protein desorption. Various architectures and responsive behavior of grafted stimuli-responsive polymers on surface are expressed in detail in Figure 1.2 [2].

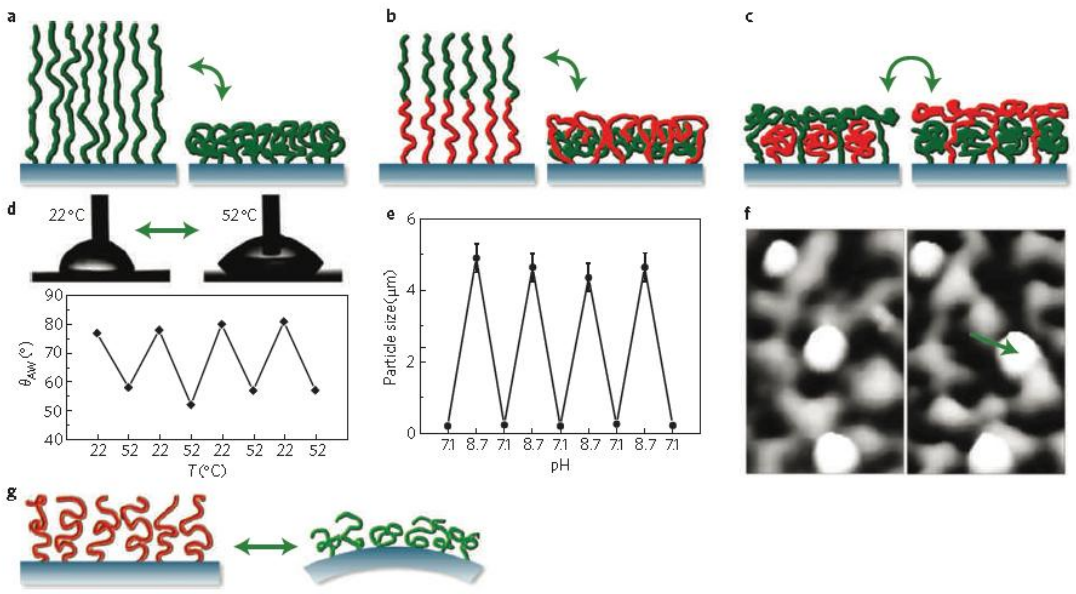

Figure 1.2. Cartoons and photographs illustrating various architectures and responsive behaviour of polymers. a. Single-component homopolymer brushes; b. Block copolymer brushes; c. Mixed brushes; d. Change of the wetting characteristics of zwitterionic 2-(methacryloyloxy)ethyldimethyl(3-sulphopropyl) ammonium hydroxide brushes after increasing the temperature from 22 °C to 52 °C, where θ_{AW} is the advancing water contact angle; e. Effective diameter of the silica particles and their aggregates covered with triblock poly(styrene-b-2-vinylpyridine-b-ethylene oxide) (PS-b-P2VP-b-PEO) copolymer brush as a function of pH. The error bars represent the standard deviation of the experimental data [3]; f. Atomic force microscopy (AFM) images acquired from the same area on the polystyrene-poly(methylmethacrylate) (PS-PMMA) mixed brush covered with silica nanoparticles after a cycle of topographical variation of the thin film in different solvents. The position of three silica spheres relative to the underlying patterns of the brush can be pursued over cycles. The green arrow indicates the displaced silica particle; g. Deflection of cantilever versus time. Bias applied at the same time. With the cantilever at negative bias, the charges on the chain are drawn towards the cantilever, leading to large surface stresses and strong bending. At opposite bias, the counterions move towards the surface, resulting in smaller stresses but bending in the same direction [2].

Polyethersulfone (PES) and polypropylene (PP) membranes have high chemical, thermal and mechanical resistance but the application is restricted by the weakly controlled surface

property of polymer material itself. The modification techniques can be physical, chemical or a combination. The choice of the specific type of surface modification depends on the chemical structure of the support membrane, and the desired characteristics of the modified surface.

In case of PES membrane, graft-polymerization can be initiated without a photoinitiator (see Figure 1.3), thus, UV-light is particularly useful for chemically attaching hydrophilic monomers to PES membranes for antifouling [4-9]. More interesting, PES membranes can be modified via a plasma generated by ionization of a gas or water. The active components generated in the plasma can activate the upper molecular layers of the PES membrane surface to increase the hydrophilicity, without affecting the bulk of the polymer. Possible gases include CF_4, Ar, O_2, H_2, He, Ne, N_2, and CO_2, in addition to H_2O [10-19]. The surface is bombarded with ionized plasma components to generate radical sites, and the generated radicals can subsequently react with gas molecules, schematically shown for O_2 in Figure 1.4. In addition, plasma treatment can be used as a source of radicals that act as active sites for graft-polymerization to avoid the loss of surface characteristics, which is due to surface rearrangement. Much work has been reported in the past decades. A wide variety of other surface modification methods can be found in the literature, such as grafting by corona induced grafting [20], ion beam irradiation [21], grafting after redox initiation [22] as well as surface coating [23] of hydrophilic species from aqueous solutions, but they are not as "mature" as the UV assisted and plasma induced polymerization.

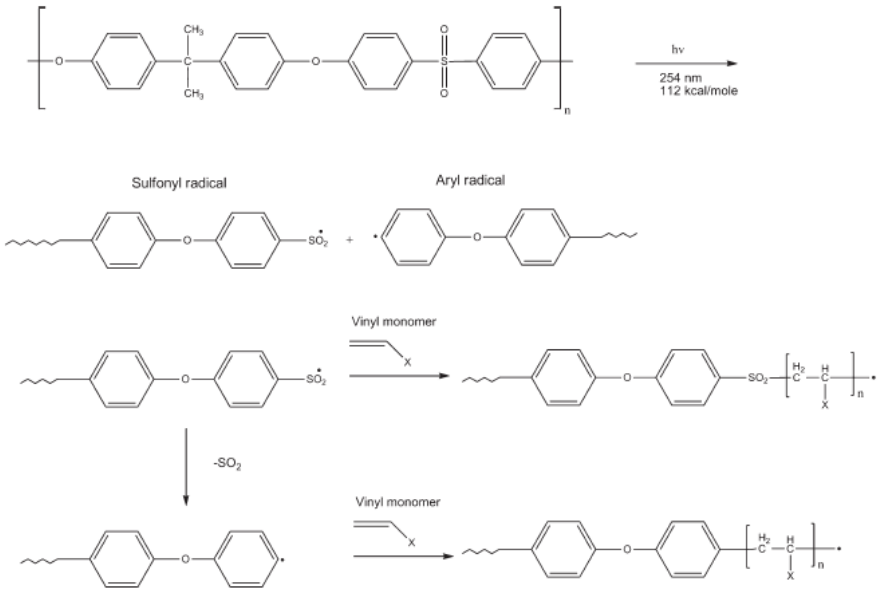

Figure 1.3. Mechanism of UV-induced grafting of a PES membrane [13].

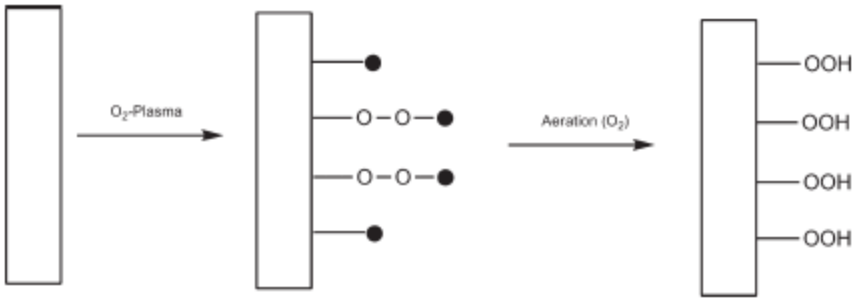

Figure 1.4. Schematical representation of O_2 plasma treatment of a membrane: —● and —○—○—● represent generated radicals [13].

Due to absence of active sites for further initiation and polymerization, for PP surface graft-polymerization and functionalization, it is necessary to introduce the reactive species onto or into PP membrane surface prior of modification. By this means, both gas-phase and solution-phase chemistry have been used. One called "the forgiving graft-on-a-graft" strategy was used by Tao et.al. to graft PAA and PTBA into CrO_3/H_2SO_4 pre-redox initiated PP surface [24,25]. More intense researches adopt the pretreatment way of gas-phase chemistry under high-energy irradiation with reactive gas(es) to initiate reactive groups for further reactive radical grafting [26], ion-induced grafting [27-31] and plasma polymerization [32-42];

preadsorption/preadhesion of desirable groups (monomers, initiators etc.) onto membrane surface for further photo initiated grafting is also widely applied [41,43-52]. Additional to surface grafting, polyelectrolytes and ionomers alternating (layer-by-layer) deposition onto PP membrane surface have been studied [53] and they are effective to achieve permanent modification, while the study focuses much on outer surface properties as mentioned by Meier-Haak et.al. Moreover, wetting of the pores of PP membranes with polar solvents, e.g., isopropanol, can temporarily increase hydrophilicity. Adsorption of various substances, especially amphiphilic polymers, from solutions in the pores has also been used, but the hydrophilization is also not stable [54]. One more sophisticated example to introduce a functional "skin" is to deposit Langmuir–Blodgett layers onto PP membrane surface [55], however this method is complicated to realize and only onto outer surface.

1.2. State of problems and strategy of this project

Intense research efforts for PES and PP MF membranes currently focus on covalent binding functional moieties into membrane surface. The resulting covalent functionalization can be more stable than that from many physical methods, but often undesired degradations of chemical or pore structure are observed (Figure 1.5). Many studies have confirmed that the plasma treatments, wet oxidative etching or grafting are less effective for PP membrane surface modification than for polyethylene (PE) [56]. The ineffectiveness of such chemistry reflects both the more reactive nature of PP surface and the chemistry that leads to ablative etching [57]. Some physical methods such as coating or adsorption can only achieve instable modification [23,54].

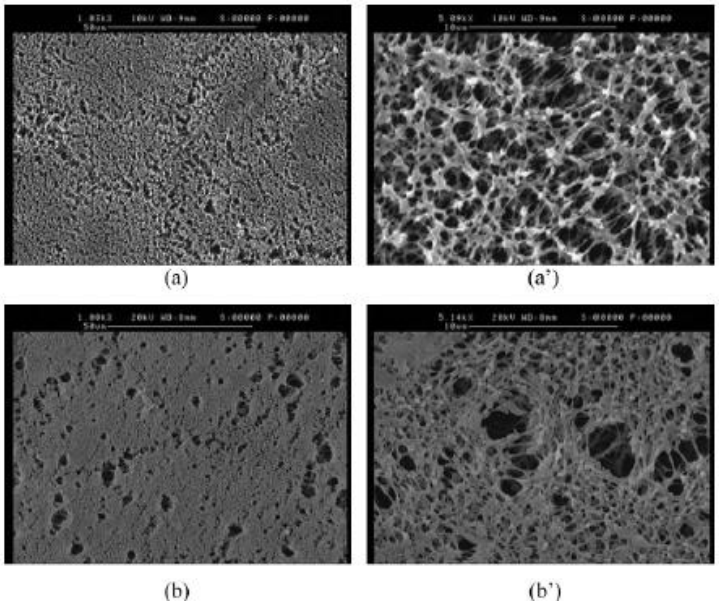

Figure 1.5. SEM images of the nascent (a) and modified PP microfiltration (MF) (PPMM) membrane (b: 2.58 wt% GAMA-grafted PPMMs), respectively (left 1000 ×, right 5000×) [52].

Considering the advantages and disadvantages of previously introduced modification approaches, it is interesting to extend one novel technique aiming to achieve less membrane pore damage than due to chemical modification and better long-term stability than surface coating; this is entrapment method. The definition of entrapment serving as polymer surface functionalization is derived from a two-liquid process deposition accomplished by surface physical interpenetration network (SPIN), to incorporate modifying species into the polymer surface region utilizing its reversible swelling property in solvent/nonsolvent of polymer substrate. The better control and stability of entrapment than adsorption to incorporate initiator into PP membrane surface has been validated indirectly by Ulbricht and Yang [51] (cf. Figure 2.10 in Section 2.4.3), however, the entrapment efficiency for additional/functional species into membrane surface was unclear. Therefore, in this project, more focus will be on the investigation of entrapment of various species into polymer (especially PP) membrane surface, to endow PES or PP surface with versatile functions.

1.3. Objective of this research

Research of this dissertation will focus on increasing hydrophilicity, temperature-responsive as well as charge property of PES and PP MF membrane surface modification in view of fouling reduction. For this goal, fabrication of functional membrane surfaces via entrapment of hydrophilic, nonionic amphiphilic, temperature-responsive as well as cationic amphiphilic (macro)molecules have been performed respectively. It is important to further confirm that the modification efficiency is dominated by entrapment efficiency rather than by adsorption/deposition or pore-blocking by modifiers during modification into polymer film surface. Moreover, the mechanism study of entrapment behavior could guide the application of this method in other polymer surface modification with specific aim.

More detailed tasks in this dissertation include:

i. Fabricate more hydrophilic surface for PES MF membrane via entrapment of PEO-containing homopolymer and amphiphilic polymer in order to find basic suitable entrapment route for the following studies;
ii. Fabricate hydrophilic surface for PP MF membrane via entrapment of small amphiphilic molecules in order to increase antifouling tendency with remaining membrane pore structure;
iii. Fabricate thermo-responsive surface for PP MF membrane via entrapment of homopolymer poly(*N*-isopropylacrylamide) (PNIPAAm) and block copolymer poly(*n*-butyl acrylate)-*block*-poly(*N*-isopropylacrylamide) (PBA-*b*-PNIPAAm), in order to change surface wettability and adhesion of protein on external stimuli (temperature);

iv. Fabricate cationic and hydrophilic surface for PP film via entrapment of methyl and octyl groups quaternized poly(n-butyl acrylate)-block-poly(2-dimethylaminoethyl methacrylate) (PBA-*b*-P*q*DMAEMA);

v. Investigate the influence of substrate difference (polarity of PES and PP, structure of PP membrane from Membrana and Celgard, PP plate, and PP film respectively) on entrapment efficiency under the identical modification condition;

vi. Investigate the effect of (macro)molecular structure on hydrophilic surface modification of PP MF membrane via entrapment.

1.4. Scope of this research

The feasibility of entrapping PEO-containing hydrophilic (macro)molecules into polar PES MF membrane has been studied initially. Detailed conditions such as mutual solvent for swelling, temperature, modifier, deswelling way and entrapment procedure have been studied in detail in terms of pore structure and surface wettability characterization. For the following entrapment studies with different polymer substrates and modifiers, the efficient entrapment approach has been hence selected and decided, which is a procedure of swelling during embedment in modification solution and subsequently deswelling during entrapment in water or specific organic solvent for solvent extraction.

To enhance the hydrophilicity and antifouling property of hydrophobic and nonpolar PP MF membrane surface, entrapment of small molecules octaethyleneglycol monooctadecylether ($C_{18}EO_8$) was performed. A comprehensive understanding of the effects of modification conditions on membrane physicochemical structure, outer surface and inner pores wettability,

membrane performance, antifouling capacity as well as stability of entrapment modified membrane in water at room temperature was investigated in detail.

Subsequently, one more application of entrapment of thermo-stimuli PNIPAAm-based polymer into PP MF membrane surface was proposed. The temperature responsive property of membrane surface and inner pores was studied by contact angle (CA) and water flux measurement and further applied for protein desorption/elution. Moreover, the identical condition was used for PP plate (same polymer for membrane preparation) surface modification to elucidate the influence of pore-blocking during entrapment modification.

Even polymerized from the same monomer, the polymer could have different physical properties such as molecular weight, crystalline degree, crystalline size and so on; moreover, different membrane preparation procedure produces different membranes (pore size, pore diameter, porosity etc.). Therefore, the effects of all of these physical parameters from PP film (FS 2500) and different membranes (PP membrane Celgard® 2500 and PP membrane 2E HF from Membrana) on entrapment feasibility and efficiency under same modification conditions have been studied besides the influence of membrane pores.

As a consequence, it was found that the swelling degree is one key factor for ‘attracting’ modifiers, whereas the solvent conditions for membranes was not strong enough for PP film. Therefore, to entrap one cationic block polymer into PP film surface, much stronger condition under high temperature with mutual solvent was used for swelling and embedment. Correspondingly, a series of deswelling methods/solvent systems were investigated and compared to avoid surface adsorption, for further confirming that the change of polymer surface property was from entrapment rather than pore-blocking and surface deposition.

As the study of embedment/entrapment behavior, entrapment a variety of ethyleneoxide-containing substances from nonpolar solutions into PP microfiltration membrane surface for

hydrophilic modification was performed. The results from gravimetric weight gain, surface characterization by contact angle measurements and ATR-IR spectroscopy, water flux measurements and protein adsorption revealed that PEGs were ineffective, while many nonionic amphiphilic substances, especially some tri-block copolymers of PEO and PPO were very effective for PP surface modification. The relationship between modifier structure and architecture and entrapment behavior was investigated by studying the micellization of the amphiphilic modifiers in nonpolar solutions via pyrene-probe fluorescence and ^{1}H NMR spectroscopy. We observed that the balanced structure of nonionic tri-block (macro)molecules tended to promote the formation of reverse micelles. This work provides more comprehensive insights in surface entrapment as an easy way to perform physical surface modification method for polymeric materials.

Chapter 2

State-of-the-art and theoretical background

2.1. Polymer structure

A polymer is a large molecule composed of repeating structural units typically connected by covalent chemical bonds, which was first proposed by Herman Staudinger in 1922. Therefore the term ‘macromolecule’ was then first used for a large molecule [58]. Knowing the polymer structure from the aspect of polymer chains configuration, conformation, or polymer aggregation is helpful to understand its behavior in solution and at surface.

2.1.1. Chain structure (random coil)

Long chain length of polymer allows entanglement (cf. Figure 2.1). The long chains in Figure 2.1 also illustrate the coiling if polymer chains are in the amorphous state. One of the most powerful theories in polymer science states that the conformations of amorphous chains in space are random coils; and the term “random coil” is often used to describe the unperturbed shape of the polymer chain in both dilute solution and in the bulk amorphous state. Until today, the random coil model has remained essentially the same with Guth’s and Mark’s concept, which is a “random walk” or “random flight” of the polymer chain, although many mathematical treatments, such as freely joined chains, freely rotating chains (including wormlike chains), chains with fixed bond angles and independent rotational potentials and with interdependent potential, including the rotational isometric state approximation etc. [59], have refined its exact definition. The random coil model has been used widely to explain rubber elasticity, dilute solution viscosities, as well as a host of other physical and mechanical

phenomena, such as melt rheology, diffusion, and the equilibrium swelling of crosslinked polymers.

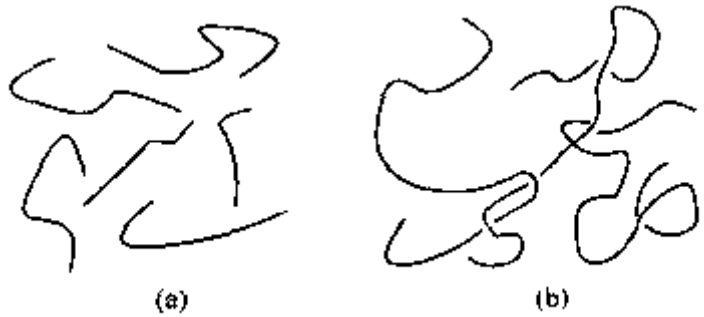

Figure 2.1. Entanglement of polymer chains. (a) Low molecular weight, no entanglement. (b) High molecular weight, chains entangle each other. The transition between the two is often at about 600 backbone chain atoms [59].

2.1.2. Polymer networks

A polymer network is a network in which all polymer chains are interconnected to form a single macroscopic entity by many crosslinks [60]. So far several mathematic models, such as affine network model, phantom network, and real networks [61, 62] have been set up for discussing polymer network theory.

Interpenetrating polymer networks (IPNs) are a unique type of polymer blend, synthesized by swelling a crosslinked polymer (I) with a second monomer (II), plus crosslinking and activating agents, and polymerizing monomer II in situ [63]. As expressed by IUPAC [60], an IPN is a polymer comprising two or more networks which are at least partially interlaced on a polymer scale but not covalently bonded to each other. The network cannot be separated unless chemical bonds are broken. The two or more networks can be envisioned to be entangled in such a way that they are concatenated and cannot be pulled apart, but not bonded to each other by any chemical bond (cf. Figure 2.2). It should be clarified that simply mixing

two or more polymers (mechanical blend polymer) does not create an IPN, nor does creating a polymer network out of more than one kind of monomers which are bonded to each other to form one network (heteropolymer or copolymer). More kinds of IPN related polymer networks such as semi-interpenetrating polymer networks (SIN) and pseudo-interpenetrating polymer network have been demonstrated in detail by Sperling [64-67]. As shown in Figure 2.3, those are also composed of two or more polymers, but have different architectures and 'binding way' in between polymer components. Some other IPN related polymers such as latex IPNs have been studied to simplify the IPN preparation procedure [65-71].

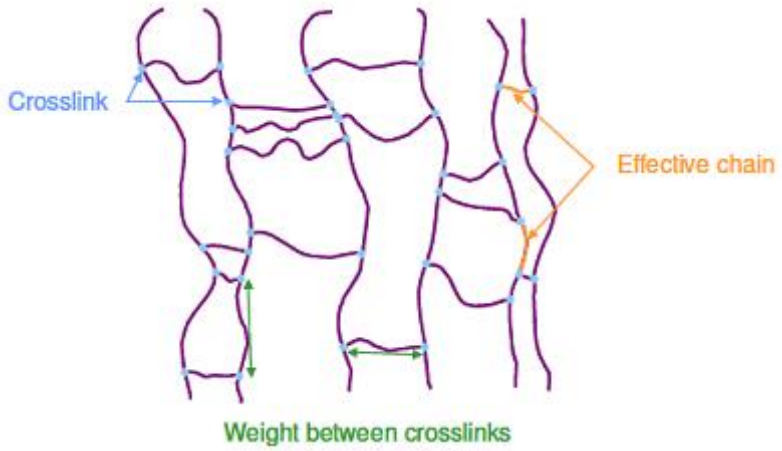

Figure 2.2. Schematic representation of a polymer network [72].

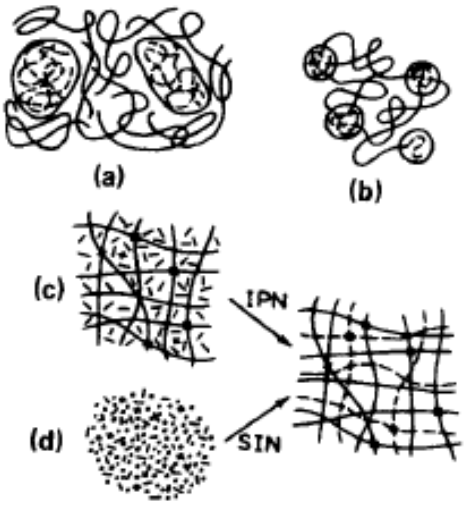

Figure 2.3. Schematic illustrations of molecular and phase domain morphologies in various types of polyblends. Polymer A: …….; Polymer B: — ; Crosslinks:  . Therein, (a) Mechanical blend. Particles of A dispersed in B. (b) A-B-A block copolymer. Blocks of B between domains formed by end blocks of A. (c) and (d) IPNs. In (c), monomer A and crosslinking agent swelled into crosslinked polymer B. A is polymerized to produce IPN; in (d), monomers A and B and crosslinking agents are mixed and simultaneously polymerized to produce similar result, designated SIN [64].

2.1.3. Aggregate structure

The solid state includes both amorphous and crystalline polymers. While amorphous polymers do not contain any crystalline regions, "crystalline" polymers generally are only semi-crystalline, which is actually a misnomer containing both crystalline domains and amorphous domains. When a crystalline polymer is melted, the melt is amorphous. The reason why polymers fail to attain 100% crystallinity is kinetic, resulting from the inability of the polymer chains to completely disentangle (long-chain nature) and line up properly in a finite period of cooling or annealing [73-76].

It had already been established that the polymer chain passed through many unit cells. Because of the known high molecular weight, the polymer chain was calculated to be even longer than the crystallites. Hence it was reasoned that they passed in and out of many crystallites. These findings led to the fringed micelle model. According to this model, the crystallites are about 10 nm long (cf. Figure 2.4). The disordered regions separating the crystallites are amorphous. The chains wander from the amorphous region through crystallites, and back into the amorphous region. The chains are long enough to pass through several crystallites, binding them together.

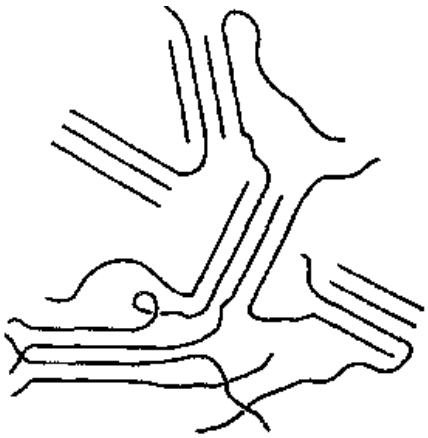

Figure 2.4. The fringed micelle model. Each chain meanders from crystallite to crystallite, binding the whole mass together [74].

2.2. Polymer in solution

2.2.1. Solubility parameter

The first step in the solution process of a polymeric material by a good solvent is a swelling. Providing the solvent is a good solvent, the intermolecular forces in linear and branched polymers are broken and the polymer dissolves [77]. Not every polymer will dissolve in every solvent, however. The solubility in solvent could be limited by molecular weight, crosslink structure as well as the crystalline structure etc. [73]. One of the simplest notions in chemistry is that "like dissolves like". "Like" may be defined in terms of similar chemical groups or similar polarities [78].

Quantitatively, solubility of one component in another is governed by the familiar equation of the free energy of mixing,

$$\Delta G_M = \Delta H_M - T\Delta S_M \quad (2.1)$$

Where ΔG_M is the change in Gibbs' free energy, T is the absolute temperature, and ΔS_M is the entropy of mixing. A negative value of ΔG_M indicates that the solution process will occur spontaneously. The term $T\Delta S_M$ is always positive because there is an increase in the entropy on mixing. The sign of ΔH_M is the enthalpy of mixing.

Surprisingly, the heat of mixing is usually positive, opposing mixing. And positive heats of mixing are the more usual case for relatively nonpolar organic compounds. On a quantitative basis, Hildebrand and Scott proposed that, for regular solutions,

$$\Delta H_M = V_M \left[\left(\frac{\Delta E_1}{V_1} \right)^{1/2} - \left(\frac{\Delta E_2}{V_2} \right)^{1/2} \right]^2 \phi_1 \phi_2 \tag{2.2}$$

Where V_M presents the total volume of the mixture, ΔE presents the energy of vaporization to a gas at zero pressure (i.e., at infinite separation of the molecules) and V is the molar volume of the components, for both species 1 and 2. The quantity Φ represents the volume fraction of component 1 or 2 in the mixture. The quantity $\Delta E/V$ represents the energy of vaporization per cm^3. This term is sometimes called the cohesive energy density. By convention, component 1 is the solvent, and component 2 is the polymer.

It should be noted that according to above equation, "like dissolves like" means that the two terms $\Delta E_1/V_1$ and $\Delta E_2/V_2$ have nearly the same numerical values. This equation also yields only positive values of ΔH_M. However, since the majority of polymer solutions do have positive heats of mixing, the theory has found very considerable application.

The square root of the cohesive energy density is widely known as the solubility parameter.

$$\delta = (\Delta E/V)^{1/2} \tag{2.3}$$

So that,

$$\Delta H_M = V_M [\delta_1 - \delta_2]^2 \phi_1 \phi_2 \tag{2.4}$$

And it can be seen that equations 2.3 and 2.4 break down for negative heats of mixing. The solubility parameter describes the enthalpy change on mixing of nonpolar solvents well but

does not give uniform results when extended to polar systems. Complete miscibility is expected to occur if the solubility parameters are similar and the degree of hydrogen bonding is similar between the components.

To take into account strong interactions, Hansen and coworkers [79-84] suggested to break the total solubility parameter into different components δ_d, δ_p and δ_h, which represent the energy from dispersion bonds, dipolar intermolecular force and hydrogen bonds between molecules, respectively, such that,

$$\delta = \sqrt{{\delta_d}^2 + {\delta_p}^2 + {\delta_h}^2} \tag{2.5}$$

Thus, "like dissolves like" means each of these three components should be equivalent for a solvent-solute pair.

While solubility of a polymer also depends on its molecular weight, the temperature, and so on, it is frequently found that polymers will dissolve in solvents having solubility parameters within about one unit of their own. It is interesting to note that although it is more accurate to use three-dimensional solubility parameters for evaluating the solubility of a polymer in a solvent, people prefer to use total solubility parameter because of its convenience and availability of data.

Overall, solubility parameter provides a simple method of correlating and predicting the cohesive and adhesive properties of materials from a knowledge of the properties of components only. Particularly for polymers, applications include finding compatible solvents for coating resins, predicting the swelling of cured elastomers by solvents, estimating solvent pressure in devolatilization and reactor equipment [85] and predicting polymer-polymer [86] polymer-binary-solvent [87], random copolymer [88], and multicomponent solvent equilibria [89-91].

2.2.2. Polymer-solvent interaction parameter χ

Many thermodynamic properties of polymer solutions such as solubility, swelling equilibria, and the colligative properties can be expressed in terms of the polymer-solvent interaction parameter χ. This unitless quantity was originally introduced by P.J. Flory [92] and M. L. Huggins [93-96] as an exchange interaction parameter in their lattice model of polymer solutions. In their definition, the quantity kTχ (k is the Boltzmann constant; T, the absolute temperature) is the average change in energy when a solvent molecule is transferred from pure solvent to pure, amorphous polymer. The reader is referred to Flory [97] for details. However, as explained in the following section, for χ is defined empirically, independent of the Flory–Huggins or any other model (cf. Equation 2.6).

$$\chi = \frac{(\mu_1 - {\mu_1}^0)^R}{{\emptyset_2}^2 RT} = \frac{(\mu_1 - {\mu_1}^0)}{{\emptyset_2}^2 RT} - \frac{\ln(1-\emptyset_2) + \emptyset_2(1-1/x)}{{\emptyset_2}^2} \tag{2.6}$$

Therein, R is the gas constant and ϕ_1 and ϕ_2 are the volume fractions of solvent and polymer, respectively, and $(\mu_1 - {\mu_1}^0)$ is the change that the chemical potential of the solvent undergoes on mixing, as expressed in Equation 2.7.

$$\mu_1 - {\mu_1}^0 = \left(\frac{\partial \Delta G_M}{\partial n_1}\right)_{T,P,n_2} = \left(\frac{\partial(\Delta H_M - T\Delta S_M)}{\partial n_1}\right)_{T,P,n_2} \tag{2.7}$$

Where, n_1 and n_2 represent the moles of solvent and amorphous polymer respectively.

For many systems, χ has been found to increase with polymer concentration and decrease with temperature with a dependence that is approximately linear with, but in general not proportional to, 1/T. According to Equations 2.6 and 2.7, for a given volume fraction ϕ_2 of polymer, the smaller value of χ, the greater the rate at which the free energy of the solution decreases with the addition of solvent. Consequently, liquids with the smallest χ are usually the best solvent for a polymer. Negative values of χ often indicate strong polar attractions between polymer and solvent. A simple principle to judge the solubility of polymer in solvent

with this unitless number is 1) if $\chi < 0.5$, the polymer should be soluble if amorphous and linear; 2) if the polymer is crystalline, it must be heated to near its melting temperature, so that the total free energy of melting plus dissolving is negative. For many nonpolar polymer-solvent systems, χ is in the range of 0.3-0.4 [98].

2.3. Polymer at surfaces

The starting point is to consider the interaction energy between the atoms or molecules making up this third component with those between the solvent and macromolecular species. Using the concept of the Flory parameter χ, a value for the interaction with the surface by considering the interaction energy between the polymer-solvent, polymer-surface and solvent-surface can be assigned from χ [99]. So, if $\chi < \chi_{surf}$, the polymer will not absorb (where χ_{surf} is the polymer-surface value). Conversely, if $\chi > \chi_{surf}$, the polymer will adsorb. Detailed modeling has been carried out by Scheutjens and Fleer [100], who used the lattice model at a surface and varied the χ parameter over the first few layers (cf. Figure 2.5). This enabled predictions of concentration profiles to be made for both adsorbed homopolymers and adsorbed copolymers.

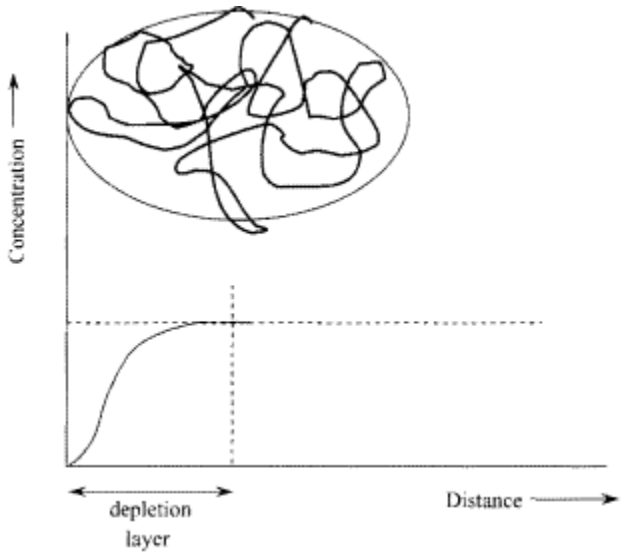

Figure 2.5. Illustration of the closest approach of a non-adsorbing polymer coil to a surface, showing the reduction in the local polymer concentration close to the surface from the acreage value in solution – the region is termed the depletion layer [101,102].

To obtain a uniform polymer concentration right up to the interface, the number of conformations in parts of the polymer would have to be reduced as that part of the coil close to the surface became more concentrated. This is energetically unfavorable without a competing attraction from the interface and the result is a depletion layer where the local concentration is lower than the global average within a distance of ~R_g away from the surface. When the enthalpy for the adsorption, coupled with the increase in entropy of solvent molecules displaced from the surface, is greater than the decrease in entropy due to the restriction on polymer conformation, the free energy is favorable for adsorption and the polymer will stick to the surface. Figure 2.6 illustrates the type of conformation that occurs for a polymer adsorbed from a θ- or better solvent. In a poor solvent, of course, the polymer will adsorb in a dense layer on the surface. Figure 2.7 shows the concentration profile in the surface layer. Note that the tails project further into the solution phase than the loops and so the total concentration profile falls to that of the tails at the outer periphery.

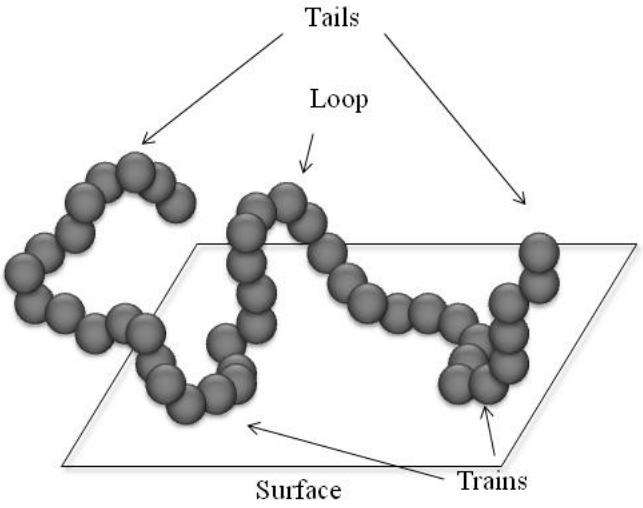

Figure 2.6. Three-dimensional representation of the conformation of a polymer adsorbed at an interface, showing the features of ‘tails’, ‘loops’ and ‘trains’ [99].

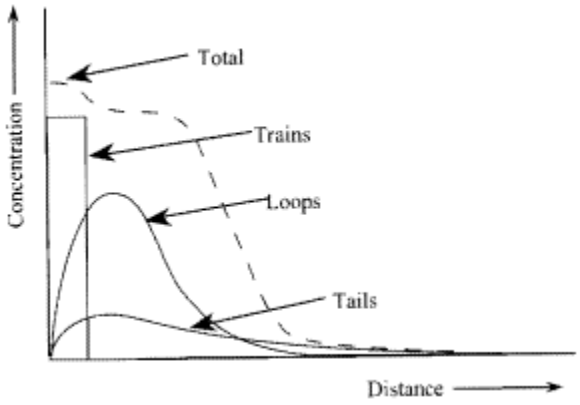

Figure 2.7. Illustration of the concentration profile of an adsorbed polymer [99].

The amphiphilic polymers, like short-chain surfactants composed of hydrophilic (“water-loving”) and hydrophobic (“water-hating”) parts, can form micelles or reverse micelles under certain concentration, are thereafter applied in surface modification as deposition. More interesting, their well-defined self-aggregation structure can be utilized to form pattern on surface (cf. Figure 2.8) [103-112].

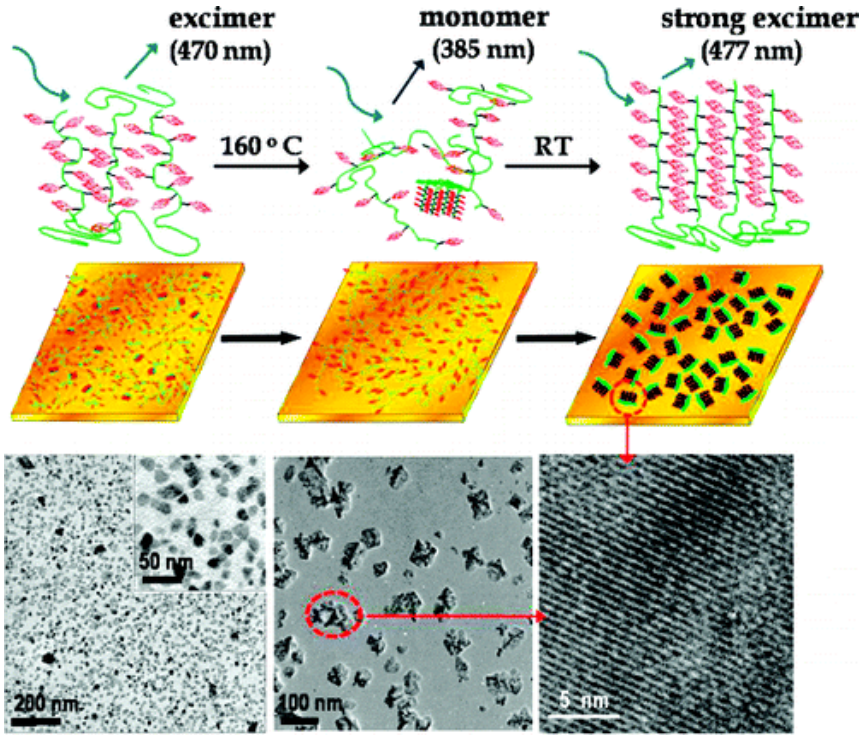

Figure 2.8. Schematic illustration of the generation of well-ordered pyrene structure of poly(methyl methacrylate)-*b*-poly(1-pyrenyl methacrylate) (PMMA-*b*-PPY) and mechanism of excimer intensity control by temperature [103].

So far, many investigations are focused on non-ionic amphiphilic polymers with a molecular weight in the range 1×10^3-3×10^3 Da. PEO chains are a common choice for the hydrophile as this polymer has good water solubility at molecular weights > 10^3 Da. On the other hand, poly(propylene oxide) (PPO) has poor water solubility at this molecular weight and is therefore a useful choice as a hydrophobe, either alone or in conjunction with other hydrophobic molecules. A variety of structures are produced, with the various types and their uses given in a review by Hancock [113]. The structures can vary from simple linear block structures to sophisticated branched structures resembling brushes or combs [99].

2.4. Entrapment of functional species as a polymer surface modification method

2.4.1. Theoretical development from the evolution of definition

Entrapment, a functionalization strategy to incorporate modifying species into the polymer surface region utilizes its reversible swelling property (transition from solid to gel-like state). The definition has been introduced by Desai and Hubbell [114,115], but it had initially derived from an idea of Ruckenstein and Chung [116]. In order to obtain surfaces of polymer materials with good biocompatibility, Ruckenstein et al. designed a series of experiments, named ‘‘two-liquid deposition process”, to introduce water-soluble diblock copolymers onto hydrophobic surfaces. Therein, one of the liquids was a solvent for the block copolymer as well as for the hydrophobic polymeric substrate, while the second liquid was water, a nonsolvent for the polymeric substrate. It was anticipated that the block copolymers are deposited onto the hydrophobic surface in such a way that the hydrophobic block is embedded into the solid while the hydrophilic block remains exposed at the surface. Few years later, Hubbell et al. set up a similar system ‘‘surface physical interpenetration network (SPIN)”, therein, they employed water-soluble homopolymer (WSP) as modifier instead of an amphiphilic polymer. They mentioned this was one of phase-mixed structure, in which PEO entangled in the base polymer and present at higher concentrations near the polymer surface. This structure was given the name surface physical interpenetrating network to reflect the similarity between the synthesis of this structure and that of a semi-interpenetrating polymer network. In the latter, monomer of component II (corresponding here to the PEO) is diffused into a cross-linked network of component I (corresponding to the base polymer) and is allowed to polymerize without cross-linking to itself or to the network of component I. By contrast, in the former SPIN (or SIN), a polymer (rather than monomer)

is diffused into a noncross-linked (rather than cross-linked) base polymer; Hubbell et al. added the descriptor “physical” to emphasize the absence of chemical cross-links in the system. Additionally, the impregnating polymer is localized near the surface of the base polymer, hence the descriptor “surface”. The structure is actually a polymer blend, but they used the name SPIN because the blend is not synthesized by normal blending procedures but is prepared by procedures somewhat similar to those for semi-IPNs. Moreover, in Hubbell’s system, they emphasized the different functions of two solvents with compared Ruckenstein’s theory. The solution with WSP can slightly swell the base polymer; fine control can be obtained over solvent properties by diluting a good mutual solvent with a miscible solvent for only WPS. And then the swollen base polymer containing WPS was placed into a nonsolvent for base polymer but a solvent for PEO which is also miscible with the solvent used for the swelling step. They mentioned, the second solvent served for rapid deswelling or collapse of the base polymer, and entangling the PEO near the surface [115].

It seems that both groups used the same modification process (two-liquid process) and the difference is only the modifier. However, an intrinsic difference had been implied by their discussions: Ruckenstein et al. mentioned that the hydrophobic–hydrophobic interaction between the amphiphilic modifier and the substrate is the main driving force for deposition, while Hubbell et al. emphasized the macromolecular chain entanglement between PEG and the polymer substrate. Later, with reference to Hubbell’s work, Shakesheff and coworkers gave this modification process a simple and more intuitive name, i.e., ‘‘entrapment”, and they also realized the surface engineering of poly(lactic acid) (PLA) by entrapment of different PEGs [117,118]. Thereafter, entrapment has been used as one approach for surface functionalization, especially for applications in the biomaterials and biomedical fields [119-123]. However, when the modifier is an amphiphilic polymer, the ‘‘entrapment” of the modifier into the base polymer should also occur. Nevertheless, there is not yet experimental

evidence whether surface modification effects are dominated by deposition or by entanglement. Actually, Ruckenstein et al. called their process ‘‘two-liquid adsorptive entrapment with amphiphilic modifier” recently, and referred a ‘soft’ polymer substrate was formed during entrapment process, that means, the polymer substrate was swollen in its good solvent [124].

Irrespective the names and implied mechanisms, the modification processes which had evolved are always the same: the first step is swelling the polymer substrate to allow the modifier species to embed into its surface, and the second step is deswelling by water so that the modifier species can be fixed, i.e., entrapped into the polymer substrate. So far, some comparison studies have been done to identify the different modification efficiency with water soluble homopolymers (PEG) or amphiphilic PEG copolymers as modifiers [124,125], but no further mechanistic investigations for exploring the reasons of such differences have been performed.

2.4.2. Research development

So far not too much work has been done on entrapment technique for polymer surface modification. The main applications of this method in the past two decades focus on fabricating biocompatible surfaces for biomaterials such as biosensor, scaffold etc. (see Table 2.1).

Table 2.1. An overview of entrapment research for polymer surface modification.

Year	Research group	Base polymer	Modifier species	Destination or Application
1988, 2003	E. Ruckenstein et al. [116,124]	PMMA, PSt, PVA, PANI	PEO-PPO, PV-*b*-PVA, PV-PS, Pluronic®	Biocompatible, biosensor etc.
1991~1992	J.A. Hubbell et al. [114,115]	PEG (5~100 kg/mol), PVP, PEOx	PET, PUR, PMMA	Biocompatible or cell-non-adhesion
2000~2003	K.M. Shakesheff et al. [117,118,120]	PEG 18.5 kg/mol, PLL 29.3 kg/mol, PEG and PLL-RGD	PLA	Tissue engineering
2002	J.C. Shen et al. [121,122]	Chitosan, chitosan–aspartic acid, chitosan–phenylalanine, chitosan–arginine, chitosan–lysine, gelatin, alginate	PDL-LA	Cell growth, scaffold, biomimetic engineering
2007	C.R. Zhou et al. [123]	Chitosan, carboxymethyl chitosan, NPC	PL-LA	Osteoblasts-like compatibility, cytocompatibility

Aiming to fabricate a biocompatible surface or a practical biomaterial, which has a very low interfacial free energy between the solid and the environmental liquid, Ruckenstein et al. selected a series of A-B block copolymers (where A is more hydrophilic than B, i.e., PEO-PPO, poly(N-vinylpyrrolidone)-*b*-poly(vinyl acetate) (PV-*b*-PVA), poly(N-vinylpyrrolidone-styrene) (PV-PS)) to be modifier to incorporate into the various nonbiodegradable polymers possessing suitable mechanical properties (i.e. PMMA, PS and PVA) respectively under two-liquid deposition process in his early studies. A contact angle technique was employed to evaluated the polar and dispersion components of the surface free energy of the solid, and to confirm that the deposited block copolymers were not extracted during long exposures to the aqueous medium (7 days). They found the biocompability of the modified surface could be

enhanced through the reduction of the solid-liquid interfacial free energy, and through the inhibition of protein adsorption by the steric repulsion created by the polymeric chains [116]. Recently, they used similar method to entrap Pluronic® triblock copolymer on the surface of polyaniline (PANI) film surface by first immersing the latter in NMP solution of one of the Pluronic® for short time, and then dipping the softened swelling film into water (nonsolvent for PANI). So finally the Pluronic® entrapped films became more hydrophilic and decreased the amount of BSA adsorption. By reducing the biofouling, the life of the modified PANI can be extended when the latter is employed as a biosensor [124].

For biomedical applications, Hubbell et al. immobilized water-soluble polymers instead of amphiphilic polymers, such as PEG, PVP, PEOx etc., into polymeric biomaterials surface, i.e. polyethylene terephthalate (PET), polyurethane (PUR, Pellethane®), PMMA etc. Water contact angle analysis, protein adsorption studies, fibroblast adhesion assays and whole blood perfusions over these polymers showed that the surface modified with PEG 18,500 was the most effective in reducing all the tested biological interactions [114]. The structure of, for instance, PET/PEG 18,500 surface physical interpenetrating networks (SPIN) system was investigated and considered to be a phase-mixed nonequilibrium surface structure, and kinetically stable below the T_g for PET for 3 months in aqueous environment. However, PEG leaching occurred upon incubation in water at temperatures near the T_g of PET as well as upon swelling the PET with organic solvents at room temperature [115].

With the development of tissue engineering, biocompatibility and drug delivery, engineering PLA surface based on the entrapment of molecules during the reversible swelling of the polymer surface region in the application field of PLA-based devices have been developed in recent 10 years [126]. Quick et al. immobilized PEG (M_w = 18,500 g/mol) and poly($_L$-lysine) (PLL) (M_w = 29,300 g/mol) into PLA in 2,2,2-trifluoroethanol (TFE)/water mixture respectively, and the swelling was then reversed by the addition of a large excess of the

nonsolvent for PLA, water [117] (cf. Figure 2.9). XPS of PLA/PEG 18,500 system revealed that control over the PEG surface density may be achieved by using predetermined process conditions, such as a particular solvent/nonsolvent ratio or a set polymer treatment time, and that surface coverage of around 75% is possible [118]. Micro- and macrothermal analysis of such bioactive surface-engineered polymer demonstrated that the entrapped PEG was in a miscible state with, and homogeneously distributed into, the PLA. The amount of PEG entrapped in the modified region was 18 wt% and the physical properties of PLA surface and near surface have been modified by the entrapment of PEG [120]. Cell adhesion studies showed that even in serum-containing media PEG entrapment will prevent attachment, with a 95% reduction in cell number compared to unmodified poly($_L$-lactic acid) (PL-LA). And this modification strategy was also further used to coentrap both PEG and poly($_L$-lysine)-GRGDS (PLL-RGD) with the PLA surface region. The attachment of cells to this material shows that the entrapment approach may be used to create highly selective biomaterial surfaces that are able to prevent unwanted cell or protein adhesion yet actively promote specific cellular interaction [117,118].

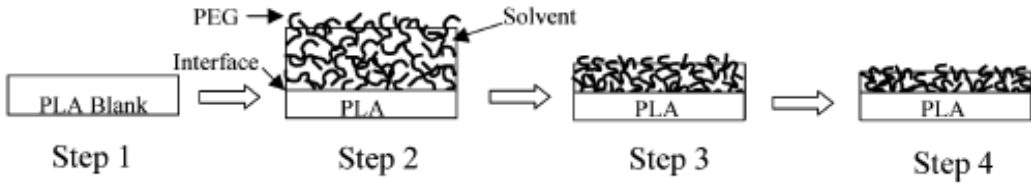

Figure 2.9. Schematic of the sample preparation processes: Step 1 is the formation of a PLA blank disk. Step 2 involves swelling the PLA disk and diffusing PEG molecules into the disk substrate in a PEG/TFE/water solution. In step 3, the PEG molecules are entrapped inside the PLA by deswelling the swollen disk by addition of a large excess of water into the solution. Step 4 is the removal of the possible residual TFE and water from substrate by drying [120].

On the basis of the above investigations, further applications for the promotion of chondrogenesis have been studied by Zhu et al., who realized the entrapment of chitosan-amino acid based derivatives, gelatin and alginate into PDL-LA surface with the entrapment areas of approximately 10-20 μm in depth [122]. Similar work has been confirmed by Liu et al. later. They incorporated chitosan and chitosan-based derivatives into PL-LA surface to promote osteoblasts-like compatibility respectively [123].

2.4.3. Potential application of entrapment technique in polymeric (membrane) surface modification

Entrapment technique serving as a surface modification method possesses one specific advantage to introduce desirable functional groups into such base polymer, which lacks any functional groups for covalent grafting of surface-modifying species, such as PLA. With this regard, entrapment of species into PP surface could be possible. One selective and less degrading strategy for PP membrane surface modification, mainly developed by Ulbricht et al., is to adsorb a photo-initiator on or into the membrane surface, and to perform a subsequent UV initiated graft copolymerization to yield tethered polymer chains on the PP surface [45,51] (cf. Figure 2.10). It had been demonstrated that such "grafting-from" functionalization can be better controlled by entrapping the photo-initiator in the surface layer of the PP membrane pores (via swelling the PP in an initiator solution in an apolar solvent and then immobilizing it by deswelling the PP in a polar solvent), rather than by an adsorption process [44]. However, to our knowledge, no published work aims to investigate the entrapment efficiency directly so far. Furthermore, it can be imagined that the membrane surface properties could be changed by the entrapment procedure itself.

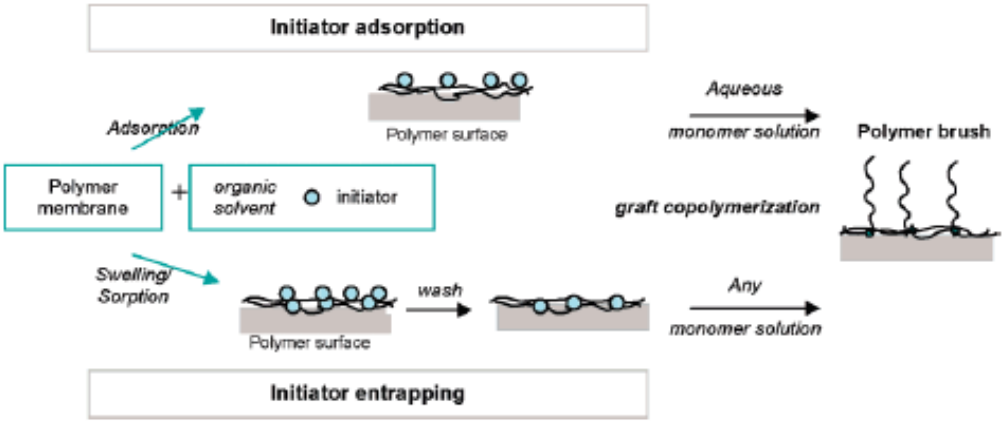

Figure 2.10. Schematic description of surface-initiated graft copolymerization via adsorption and entrapping methods for initiator immobilization [51].

2.4.4. A so-called "entrapment technique for polyolefin surface modification"

Bergbreiter et al. have demonstrated one so-called entrapment way for polyolefin surface modification, that relies on mixing small amounts of a preformed PP or PE block cooligomer with an excess of a host PP or PE to produce a surface-modified polyolefin film that is in turn amenable to further chemistry [127-133]. One example in Figure 2.11 showed the modification route. It seems that this way is more like blend, and because of the quantity difference, the large amount component is considered to be the 'host' or 'base', and the small amounts of e.g. terminally functionalized oligomers is considered to be the modifier, and the final blend structure is small amount modifiers existing in the 'surface' of 'base' polymer. This method seems more similar with "blending" (accompanied by surface segregation) rather than "entrapment" described by Hubbell et al. (a post modification). It is necessary to clarify the difference of this research and this on-going project related to polymer surface (including PP) entrapment modification before our investigation.

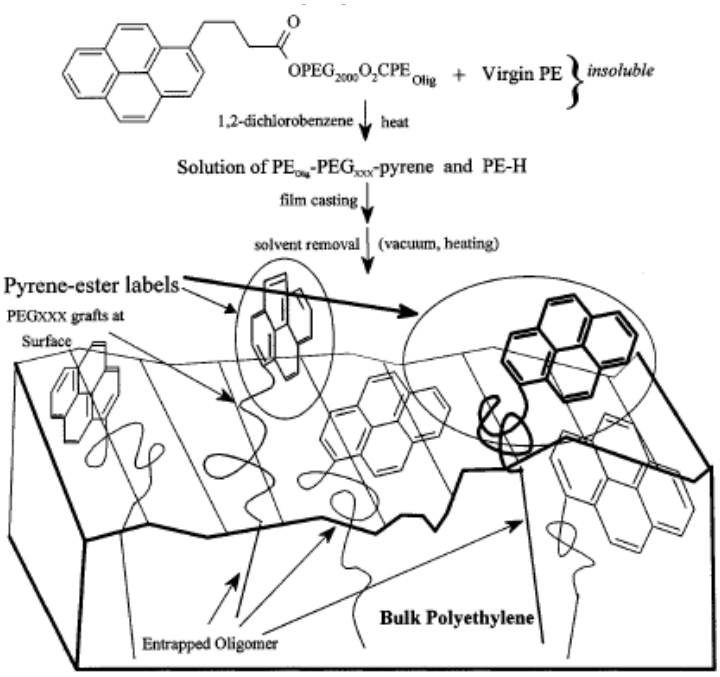

Figure 2.11. So-called entrapment functionalization of labeled block cooligomers as a route to surface-functionalized polyethylene films [128].

Chapter 3

Experiments

3.1. Materials

3.1.1. Polymer substrates

Asymmetric PES microfiltration membrane (type MicroPES® 2F) prepared via NIPS process [134] with a nominal pore diameter of 0.2 μm and a thickness of 100 μm from Membrana GmbH, was employed for investigating the feasibility of entrapment of homo- and block polymer into polar polymer membrane surface.

Symmetric hydrophobic PP microfiltration membrane (type ACCUREL® PP 2E HF (R/P)) with a nominal pore diameter of 0.2 μm, a porosity of 70 % and a thickness of 190 μm purchased from Membrana GmbH was used as substrate for investigating the feasibility, stability as well as the mechanism of entrapment of a series of commercial (macro)molecules and thermo-responsive block copolymers for membrane surface hydrophilic and antifouling modification.

Symmetric hydrophobic PP microfiltration membrane (type Celgard® 2500) with a total pore volume of 0.195 mL/g, porosity in the range of 37 ~ 48%, pore dimension of 0.05 × 0.19 μm and thickness of 25 μm from Polypore [60,135-137] was used for investigating the feasibility of entrapping small amphiphilic molecules ($C_{18}EO_8$ and $C_{18}EO_8C_{18}$).

Hydrophobic PP plates were prepared from PP pellets (type Piolen TO 2A 12, from Membrana GmbH). The pellets were molten at about 250 °C for 30 min on a clean glass plate

(Duran, Germany) and then manually pressed with another hot glass plate for few minutes to obtain a PP plate. Six PP plate samples were selected for the experiments. They had a diameter of 18 mm and a weight in the range of 30 ~ 35 mg. The thickness at 5 ~ 7 different positions was measured and the average value was then calculated ignoring the maximum and minimum data. The average density was calculated from the thickness, the area (2.245 cm^2) and the weight of each plate. The used samples had an average thickness of 0.204 ± 0.095 mm as well as an average density of 788.8 ± 59.5 mg/cm^3. The plates were used for entrapment of thermo-responsive block copolymer PBA-*b*-PNIPAAm to study the influence of membrane pore structure during the modification.

Hydrophobic PP film (type FS 2500) with a surface tension of 19 mN/m and thickness of 28 µm from Membrana was used for entrapment of small amphiphilic molecules ($C_{18}EO_8$ and $C_{18}EO_8C_{18}$) and charged block copolymer PBA-*b*-P*q*DMAEMA.

3.1.2. Modifiers

The commercial PEO block containing (macro)molecules, including homopolymers and block copolymers as well as other amphiphilic molecules, were used as modifiers. PEG (M_w = 400, 1500, 3000, 6000, 10,000, 12,000 g/mol) from Fluka, and PEG with a molar mass of 200,000 g/mol was from Acros. $C_{18}EO_8$, $C_{18}EO_jC_{18}$ (j = 8, 136) were from Polysciences, Inc.. A series of Pluronics®, i.e., PE10100 ($EO_4PO_{54}EO_4$), PE10300 ($EO_{17}PO_{60}EO_{17}$), PE10500 ($EO_{37}PO_{56}EO_{37}$, solid and 18 wt% aqueous solution), PE6400 ($EO_{13}PO_{30}EO_{13}$), and RPE1740 ($PO_{14}EO_{24}PO_{14}$) were used as received from BASF, Ludwigshafen, Germany. Pluronic® F127 ($EO_{100}PO_{65}EO_{100}$) was purchased from BASF and Pluronic® F108 ($EO_{132}PO_{50}EO_{132}$) was from Aldrich. The thermo-responsive PNIPAAm containing homo- and block polymers, such as PNIPAAm (M_w = 37.8 kg/mol, abbreviated as hP), PBA-*b*-

PNIPAAm (M_w = 42.3 kg/mol, $M_{wPNIPAAm}$:M_{wPBA} = 1:0.8 (calculated from element analysis), abbreviated as cP1) and cP2 (M_w = 46.1 kg/mol, $M_{wPNIPAAm}$:M_{wPBA} = 1:2.5 (calculated from element analysis)) as well as PBA-*b*-P*q*DMAEMA (M_w = 81.5 kg/mol, M_{wPBA}:$M_{wPDMAEMA}$ = 1:5.1(calculated from element analysis)) were prepared in our lab [138,139].

3.1.3. Good solvent for polymer substrate and modifier

Selection of suitable solvent, which should be good solvent for either polymer substrate or the modifier, was the first important step for entrapment modification. Some solvents and mutual solvents were tested in the experiment. Therein, carbon tetrachloride, DCE (99.8+%, extra pure), DMSO, Tetraline, THF, o-xylene, 1-propanol (99.5%, a.p.) as well as isopropanol (a.p.) were purchased from Acros; DMF (a.p.) was from AppliChem; DMAc, TEG (anhydrous, > 99%) and benzene were from Fluka; chloroform was from Fischer Scientific; NMP (NMP^1, purity is 65.5%; NMP^2, purity is 99.5%.) from Merck; cyclohexane and ethanol (p.a.) were from VWR respectively.

3.1.4. Other chemicals

In addition, other chemicals and solvents required for some special measurements or for cleaning, preparing buffer solutions, protein solutions were used. D-chloroform (99.8 atom % D) was from Aldrich. Pyrene (98%), Ponceau S and acetone were from Acros. Disodium hydrogenphosphate dihydrate and potassium dihydrogenphosphate were from Fluka. 5-Sulfosalicylic acid was from Serva, acetic acid from Fischer, potassium hydroxide from Merck, while 1 M KOH and KCl were from Bernd Kraft GmbH, sodium hydroxide from Roth, 1 M HCl from Waldeck and HCl (conc.) from Riedel de Haen, and the Pierce BCA

Protein Assay kit was purchased from Thermo Science. BSA (fraction V, fatty acid free) was from ICN Biomedicals, Inc.. Ultrapure water from a Milli-Q system (Millipore Inc.) with a 18.2 *MΩ* resistivity was used in all experiments.

3.2. Entrapment functionalization procedure

Utilizing the gel-like property of polymer in certain solvent, the hydrophilic or amphiphilic modifier is anticipated to embed into swelling region of polymer substrate to entangle with polymer chains. Thereafter the modifier could implant into polymer substrate during deswelling step. Based on this idea, two procedures have been considered. One way, the polymer substrate was immersed directly into the solution with anticipated modifier for swelling and embedment at the same time, and the subsequent deswelling step was under the condition of vacuum oven before immersed into water for 20 min (Figure 1, E1). The other way was set up to swell polymer substrate in certain solvent (solvent1) firstly, and then it was placed into modifier's aqueous solution for implantation of modifier and deswelling of polymer substrate simultaneously, and finally removed into vacuum oven at 45 °C for 48 h to completely deswell and dry (Figure 1, E2). Before the modification, PP and PES samples were pretreated by acetone and acetone/water (3/7, v/v) for 48 h respectively, in order to elute residual solvent from manufacturing and possible fatty from fingers, and then dried and weighed. The general modification conditions with respect to different polymer substrates and modifiers are listed in Table 3.1 and Table 3.2. After modification and before measurement, all entrapment treated samples were washed by fresh water for 2.5 h to remove excessive outer surface absorbed modifiers. It is necessary to notify that E_PP/$C_{18}EO_8C_{18}$ was eluted at 40 °C due to the weak water solubility of $C_{18}EO_8C_{18}$ at room temperature.

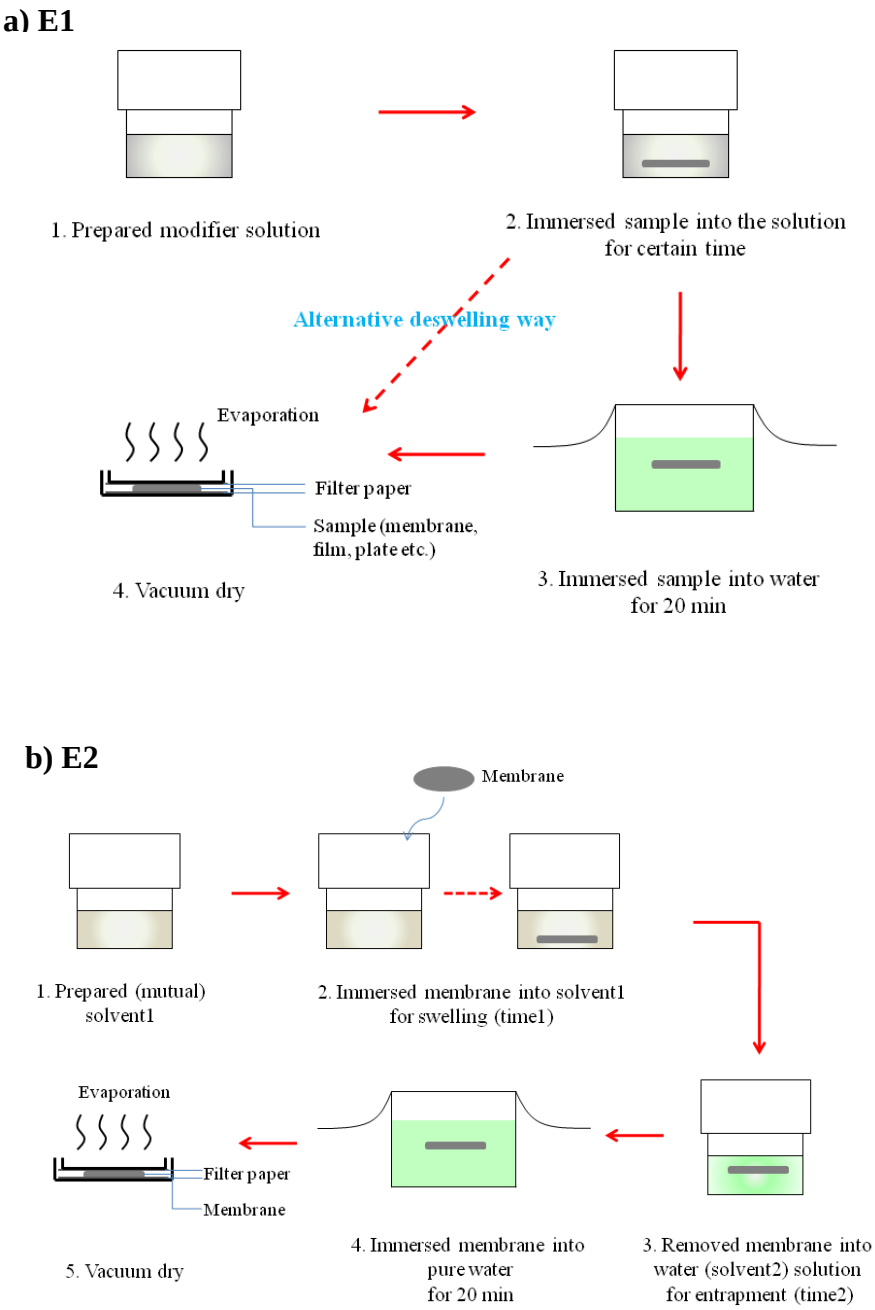

Figure 3.1. Entrapment procedures: a) one-solvent step (E1) and b) two-solvent step (E2).

Table 3.1. General modification conditions in terms of different polymer substrates (E1).

Substrate	Modifier	Solvent	Conc. (g/L)	Temp. (°C)	Time	Deswelling way
PES 2F	PEG6K, PEG35K, $C_{18}EO_8$, $C_{18}EO_8C_{18}$, $C_{18}EO_{136}C_{18}$, PE10100, F108, F127	NMP[2]/H_2O DMF/H_2O DMSO/H_2O DMAc/H_2O	1~20	20, 30	16 h 18 h 20 h	Directly dried or soaked into water for 20 min before vacuum dry
PP 2E HF	PEGs (400 ~ 200,000 g/mol) $C_{18}EO_8$, $C_{18}EO_8C_{18}$, $C_{18}EO_{136}C_{18}$, PE10100, PE10300, PE10500, F127, F108, PE6400, RPE1740	DCE	1~25	20	~20 h	Same as above
PP 2E HF	hP, cP1, cP2	DCE Chloroform Carbontetra -chloride Benzene, THF	10 , 20 25	20, 40	3~20 h	Same as above
Cel 2500	$C_{18}EO_8$, $C_{18}EO_8C_{18}$	DCE	25	20	20 h	Soaked into water for 20 min before vacuum dry
FS 2500	$C_{18}EO_8$, $C_{18}EO_8C_{18}$	DCE	25	20	20 h	Same as above
PP plate	cP1	DCE	20	20	20 h	Soaked into water for 20 min before vacuum dry
FS 2500	PBA-*b*-PqDMAEMA	O-xylene/1-propanol (6/4~8/2 , v/v)	10 ~25	101.7± 0.1	1 min	D, SD-1, S'SD-1, SD-2, S'SD-2, S"SD-2 [1]

[1] The abbreviations of deswelling approaches are corresponding to the following condition respectively:

1) Immediately vacuum dry at 45 °C (D);

2) immersed sample into the corresponding mutual **s**olvent (o-xylene/1-propanol) for 5 min, then **d**ried (SD1);

Table 3.2. Two-step modification conditions for PES 2F membrane (E2).

Modifier	Swelling step		Entrapment		Conc. (g/L)	Temp. (°C)	Deswelling way
	Solvent1	Time1 (h)	Solvent2	Time2 (h)			
PEG 6K, PEG 35K, PE10500, F127, F108 L64, RPE1740	NMP[2]/H_2O (7/3, v/v)	0.5~22 h	Water	0.5~4, 144	20	20, 30	1) immediately dried; 2) soaked into water for 20 min before vacuum dry

3.3. Characterization and analyses

3.3.1. Surface characterization

Attenuated total reflection infrared spectroscopy (ATR-IR). ATR-IR method is simple and efficient to obtain surface chemical structure information. A Varian 3100 spectrometer (USA), equipped with a MCT detector and an ATR unit with a Ge crystal (60°), was employed to acquire ATR-IR spectra. A total of 64 scans were performed at a resolution of 4 cm^{-1}.

(continued)

3) immersed sample into a modifier **s**olution at room temperature for 5 min, and then removed into the corresponding mutual **s**olvent (o-xylene/1-propanol) at room temperature for 5 min, then **d**ried (S'SD1);

4) immersed sample into pure **s**olvent (o-xylene) for 5 min, then **d**ried (SD2);

5) immersed sample into modifier **s**olution at room temperature for 5 min, subsequently removed into pure **s**olvent (o-xylene) for 5 min, then **d**ried (S'SD2);

6) immersed sample into 30 g/L **s**olution (higher concentration than modifier solution but with identical components) at room temperature, and then removed into pure **s**olvent (o-xylene) for 5 min, finally **d**ried (S"SD2).

Contact angle (CA). Static CA measurement is always used to analyze surface wettability. Here it was carried out by a contact angle goniometer (OCA 15 Plus, Dataphysics GmbH, Filderstadt, Germany) equipped with a video camera and an image analysis system. Two different measuring modules were employed with respect to the specific condition and request of surface, which were water sessile drop and air captive bubble respectively. 5 ~ 7 drops of 5 μL water drops were injected onto dried surface for calculating the average contact angle at room temperature (20 °C). The captive air bubble under water was employed for studying the hydrophilic PES membrane and temperature-responsive property of some modified surfaces, and the temperature was controlled by surrounding water temperature. The water temperature for prewetting membrane pores was also taken into account: that should be the same with measuring temperature.

Zeta potential. Zeta potential (ζ-potential) is electric potential in the interfacial double layer (DL) at the location of the slipping plane versus a point in the bulk fluid away from the interface, which is widely used for quantification of the magnitude of the electrical charge at the double layer to evaluate surface charge property. A flat–sheet tangential flow module was used for outer surface zeta potential measurement [140] and the cell set-up for trans-membrane zeta potential has been described by Staude et al. [141,142]. The streaming potential was measured using the system at 25 °C with circulated electrolyte solution (0.001 M KCl, pH adjusted with 1 M KOH or HCl) by using a pressure difference less than 1 bar. For each pH value, a variation of pressures was done. The zeta potential can be calculated from Helmholtz–Smoluchowski equation, that is

$$\zeta = \frac{k \cdot \eta}{\varepsilon_0 \cdot \varepsilon_r} \cdot \frac{\Delta E}{\Delta P} \tag{3.1}$$

where k is the liquid conductivity, η is the liquid viscosity, ε_0 and ε_r are the dielectric constant of vacuum and liquid, respectively. Therein, $\varepsilon_0 = 8.854 \times 10^{-12} C^2 \cdot J^{-1} \cdot m^{-1}$, ε_r

of water is used for very low concentration KCl solution (0.001 N) [143]. *ΔE* is the potential difference, and *ΔP* is the hydrodynamic pressure difference, therefore, the slop of *ΔE/ΔP* means streaming potential. In addition, to study temperature-responsive property of zeta potential, the relationship of between η and ε_r to temperature were respectively calculated as:

$$\eta = -5E^{-4} \ln T + 0.0025, R^2 = 0.9995 \quad (3.2)$$

$$\varepsilon_r = -0.3613T + 87.58, R^2 = 1 \quad (3.3)$$

3.3.2. Membrane characterization

Membrane structure including membrane pore size distribution, membrane specific surface area, membrane outer surface and cross section morphology have been characterized respectively. The membrane performances of modified membrane were evaluated from water flux, static adsorption/staining, protein filtration etc. In addition, the stability of modified PP membrane was tested.

Pore size distribution. Pore size distributions of membranes in the dry state were determined by the wetting fluid displacement technique with Capillary Flow Porometer CFP-34RTG8A-X-6-L4 (PMI Inc., Ithaca, NY, USA) [144]. The gas flow was measured as a function of the trans-membrane pressure, first through a dry membrane and then after wetting the membrane with 1,1,2,3,3,3-hexafluropropene ("Galwick", PMI, surface tension 16 dyn·cm^{-1}). The pore size distribution was then deduced from the comparison of the two experiments by using PMI software.

Specific surface area. Specific surface area of the membrane was determined by using the surface area analyzer SA 3100 (Beckmann-Coulter GmbH, Krefeld, Germany) for measuring the nitrogen adsorption BET (Brunauer, Emmett and Teller) isotherm. 130 ~ 140 mg

membrane samples were used for measurement. The BET equation permits us to extract from a multilayer adsorption theory that volume of adsorbed gas which would saturate the surface if the adsorption were limited to a monolayer [145]. Therefore, V_m may be interpreted in the same manner that the limiting value of the ordinate is handled in the case of monolayer adsorption, and which has been expressed on a 'per gram' basis in writing Eq. (3.4).

$$V_m = \frac{A_{sp} M_V}{N_A \sigma^0} \tag{3.4}$$

Where, V_m is the volume of monolayer, A_{sp} is the specific surface area, M_v is the gram molecular volume (22,414 cm^3/mol), N_A is Avogadro constant and σ^0 is the cross sectional area occupied by each adsorbate molecule.

If the area occupied per molecule on the surface is known, the specific surface or BET surface area in (m^2/g) is then determined from the following expression:

$$A_{sp} = \frac{V_m N_A \sigma^0}{M_V} \tag{3.5}$$

For Nitrogen BET determinations, σ^0 is assumed to be 0.162 nm^2 [146].

Membrane morphology. Images of the top surface and cross-section of membranes were taken by scanning electron microscopy (SEM; Quantas 400 FEG, USA) after sputter coating with gold/palladium using a sputter coater K 550 (Emitech, UK).

Water flux. One standard microfiltration process was carried out using 25 mm diameter dead-end stirred ultrafiltration cell (10 ml, Amicon Model 8010, Millipore), with an additional feed reservoir connected to a nitrogen gas tank. The active membrane surface area was 3.14 cm^2. For water flux experiment, the stirred cell and feed reservoir were filled with water. The unmodified PP membrane was pre-wetted with ethanol and the modified membranes were pre-wetted by water, each for 5 min to completely fill the pores, and then pressurized at ca. 4.1 kPa/cm^2 for 50 min till the water flux became stable (this indicated that

in case of unmodified PP membranes, the water had completely replaced the ethanol from the pores). Then the pressure was decreased gradually to 4.0, 3.0, 2.0, 1.0, 0.5 and 0.25 kPa/cm^2, and the corresponding water fluxes were recorded.

Using the same set-up, another way to measure the permeability was recording the flux values per fixed interval time under a constant pressure. The unmodified PP membranes were pre-wetted with ethanol and the modified membranes were pre-wetted with water, and then precompacted at 3 kPa/cm^2 for 15 min to make sure that all pores of samples were entirely penetrated by water. Subsequently, the pressure was released to 1.2 kPa/cm^2 (still higher than pressure used for measuring water flux) for 0.5 h for further pre-compaction of the membranes. Then, the pressure was kept at 1.0 kPa/cm^2 for 0.5 h; thereafter, the water flux was measured at 1.0 kPa/cm^2 for 2 h. The weight of the permeated water was recorded with a balance every 5 min.; the water flux was calculated from the final stable average value, i.e., time-independent values which were reached within up to 2 h.

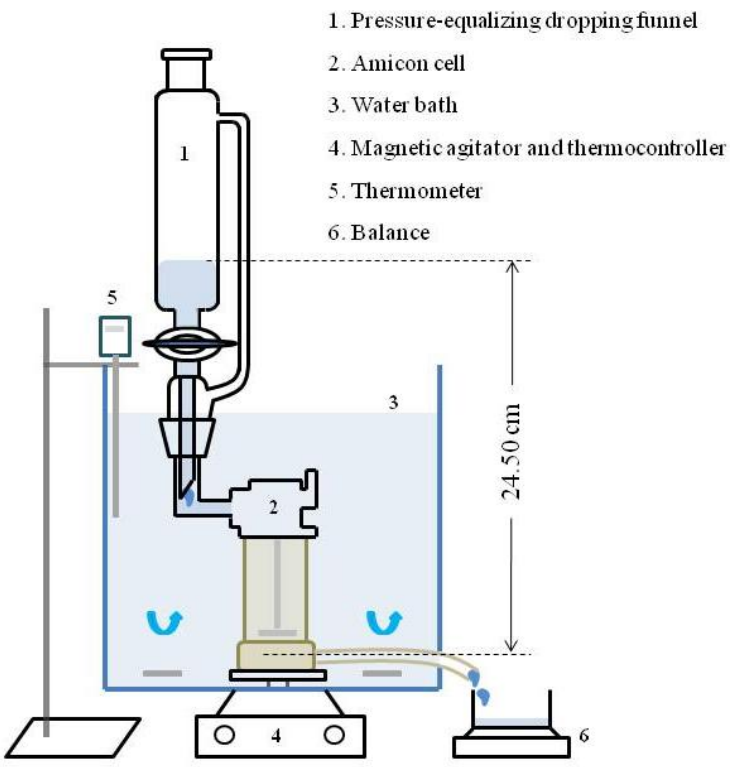

Figure 3.2. Hydraulic water flux apparatus.

To study the temperature-responsive water flux, the filtration experiments were performed using a 25 mm diameter thermostated dead ended Amicon cell (10 mL, Millipore Inc., USA), which was connected to a pure water-filled pressure-equalizing dropping funnel (100 mL) as a feed reservoir as well as to control the trans-membrane pressure to be constant at 0.024 bar (water height was 24.5 cm). The active membrane area was 3.14 cm^2. The unmodified PP membranes were prewetted with ethanol and the modified membranes were prewetted with water, which were then precompacted at ca. 0.1 bar for 0.5 h to make sure that all pores of the samples were entirely penetrated by water. Subsequently, the pressure was released to 0.04 bar (still higher than measuring pressure) for 0.5 h for further precompaction of the membranes. Then the pressure was kept at 0.024 bar for 0.5 h to be constant before the measurement. The weight of the permeated water was recorded with a balance every 5 min and repeated 3 times at each temperature. The temperature was controlled by thermo-meter from room temperature to 40 °C.

Protein adsorption, fouling and cleaning. BSA was used as a model protein. Solutions with 1 g/L BSA were prepared in phosphate-buffered saline solution (PBS, pH 5).

As to static adsorption, pre-wetted PP membranes (0.13 cm^2) were immersed into 2 mL, 1 g/L protein solutions for 3 h and then washed with phosphate-buffered saline solution. Two methods have been employed to quantify the adsorbed protein amount with respect to the membrane property. One was BCA dye from Thermo Science, which has a standard working range of 125 ~ 2000 μg/ml. Aliquots of the supernatant solutions were mixed with BCA protein assay reagent, and shaken for 2 h at room temperature. Analysis of BSA concentration was done by measuring the UV-Vis absorbance at the wavelength of 562 nm and comparison with calibration curves. The other way was Ponceau S staining for microgram adsorption analysis [147], which is even sensitive in protein concentration range of 25 ~ 350 μg/ml [148]. After BSA adsorption, PP membranes were put into 20 g/L Ponceau

S in 30 wt% trichloroacetic acid and 30 wt% sulfosalicylic acid for 1 h, washed with Milli-Q water 3 times; then washed with 5 vol% acetic acid for 1 h and rinsed 3 times with water. To remove the BSA/Ponceau S complex from membrane surface, the samples were eluted with 3.0 ml 100 mM NaOH for 1 h; equilibration of the membranes with each solution was enforced by a Vortex mixer. The solution was removed from the membrane sample, 50 µl 6 M HCl were added to neutralise the solutions, and absorbance was measured at 515 nm. Calibrations had been done with known BSA amounts (0.001-1 mg) applied to unmodified PP membranes.

Temperature-responsive protein adsorption-desorption study of PNIPAAm containing block copolymer modified PP membrane was performed after static adsorption in 10 mL, 2 g/L BSA PBS solution (pH = 5) at 40 °C for 3 h. The excessive protein solution on membrane surface had been rinsed away with 40 °C water; then water flux was measured at 40 °C, 25 °C and again 40 °C, successively, for eluting the adsorbed protein. To detect the protein desorption, the pure water permeability at each temperature was measured for up to 2 h until stable values had been obtained.

The capacity of microfiltration of BSA solutions and also the cleaning efficiency of $C_{18}EO_8$ modified PP membrane were investigated as a comparison with unmodified PP. Pre-wetted membranes were pressurized at 1.2 kPa/cm^2 for 0.5 h, and then the pressure was decreased to 1.0 kPa/cm^2 (as the measuring pressure) for 0.5 h to make sure both the condition and the membrane became stable. Fluxes during BSA filtration and washing steps were measured gravimetrically in the following order: 1) pure water flux, 2) 1 g/L BSA (pH 5) filtration, 3) PBS (pH 5) filtration, and 4) pure water filtration. For each stage a constant trans-membrane pressure of 1.0 kPa/cm^2 was used for 1 h.

Stability study. $C_{18}EO_8$ modified PP membrane samples were incubated into water and shaken at room temperature for up to eight weeks. Fresh water was changed every day. The changes of surface properties were evaluated by gravimetric, static CA, ATR-IR, and also by the BSA filtration cum elution filtration experiment, similar to description in previous.

3.3.3. Polymer structure characterization

Polymer crystalline structure was analyzed by X-ray diffraction (XRD) as well as differential scanning calorimetry (DSC). Water content of polymer was analyzed by thermogravimetrie analyse (TGA) plus fourier transform infrared (FT-IR) (TG-IR). And the molecular and polymer structure in solution (micelle and reverse micelle) were analyzed by pyrene-based fluorescence and ^{1}H nuclear magnetic resonance (^{1}H NMR).

XRD was carried out using a STOE transmission diffractometer STADIP (2003-10, STOE & Cie GmbH, Germany) with a Cu Kα (λ=0.1542 nm) generator at 50 kV and 30 mA.

DSC was carried out using a DSC 204 (NETZSCH-Gerätebau GmbH Thermal Analysis, Germany) in the temperature range of -50 ~ 200 °C, temperature increase rate of 20 °K/min and the measuring atmosphere of air.

Pyrene probe fluorescence was carried out using a Cary Eclipse Fluorescence spectrophotometer (Varian Inc., USA). Series of 10 mL solutions for each modifier in water or 1,2-dichloroethane ranging from 10^{-6} ~ 100 g/L, each containing 50 µL 0.02 mM pyrene ethanol solution, were prepared. From fluorescence spectra, the intensities of the peaks centered at 372 and 384 nm, referred to as “peak I” and “peak III”, respectively, were measured. The intensity ratio of “peak III” to “peak I” (III/I) was calculated and plotted as a function of polymer concentration [149].

^{1}H NMR was carried out using a Bruker DMX-300 (300 MHz) spectrometer at room temperature. Nonaqueous solutions of Pluronics® PE 10500, F127 and F108 were prepared by dissolving the polymer in d-chloroform and step-wise diluting to the desired concentrations (0.1 ~ 100 g/L).

Chapter 4

Results

The experimental results, which can be classified into following five parts with respect to different polymer substrates, modifiers and destinations, are presented in this chapter: (i) study of entrapment of a variety of hydrophilic polymers into PES MF membrane surface; (ii) study of entrapment of nonionic PEG400-containing amphiphilic molecules into PP 2E HF MF membrane surface, (iii) study of entrapment of nonionic and thermo-responsive macromolecules into PP 2E HF MF membrane and plate surface; (iv) study of entrapment of nonionic and cationic amphiphilic (macro)molecules into PP film surface; (v) study of entrapment mechanism via macromolecular configuration analyses in nonpolar environment.

4.1. Entrapment of hydrophilic (macro)molecules into PES membrane surface

4.1.1. Effect of solvent and temperature on membrane integrity and structure before modification

Effect of solvent. Although the nominal pore diameter of PES (MicroPES® 2F) is 0.2 μm [134], four PES samples measured in our lab showed different pore diameters, as shown in Figure 4.1. It was found that the general average pore diameter with maximum distribution of four samples was in the range of 0.40 ~ 0.45 (cf. right up column Figure in Figure 4.1).

The PES samples should be eluted before using. Water and ethanol elution under room temperature for 16 h will not damage the membrane structure (Figure 4.2). Their average

pore diameters were around 0.45 µm, this value seemed a little bit higher than that of O_PES, but this slight difference was allowed and could be due to the inhomogeneous of PES product. However, in acetone the white porous PES membrane became a transparent dense film in a few minutes. Therefore, acetone and water mutual solvent was used for cleaning PES membrane to decrease the solubility capacity of acetone. For example, when the acetone/water volume ratio was 7/3, the average pore diameter had slightly decline but could general keep the pore structure as that of O_PES (Figure 4.2). Compared a series of different mixture ratios of acetone and water, it can be found 7/3 (v/v) acetone/water could be a critical ratio to clean PES membrane (Figure 4.3) and avoid damaging pore structure, otherwise, the membrane was deformed by too strong solvent treatment. Some organic solvents, such as NMP, DMAc, DMF, DMSO, TEG etc., for swelling PES membrane showed similar impact like acetone from either appearance or PMI data (see Figure 7.1 in Appendix). Pure NMP, DMAc, DMF, DMSO and even TEG can dissolve or damage membrane. Therefore, the nonsolvent of PES membrane, water was used to decrease the dissolving or swelling tendency of the above solvents, however, high organic content of water diluted solvent could deform membrane. From appearance and PMI data, it was generally concluded that 8/2 (v/v) was a critical mutual solvent ratio of NMP/H_2O, DMAc/H_2O, DMF/H_2O and DMSO/H_2O to PES membrane at room temperature (cf. Figure 4.4). Additionally, the influence of solvent temperature on membrane structure was studied, as shown in Figure 4.5 and Figure 7.2, and it was found that the temperatures (~ 40 °C) had not much influence on membrane structure.

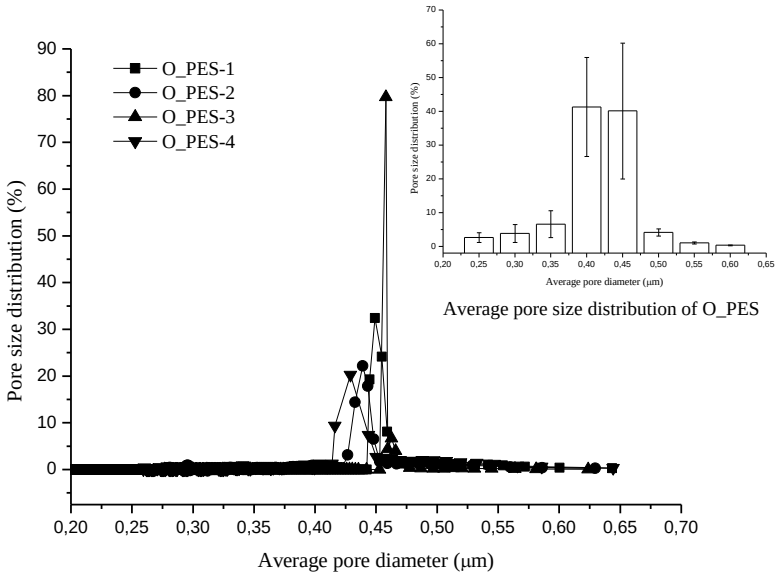

Figure 4.1. Relative abundance as a function of average pore diameter of O_PES membranes.

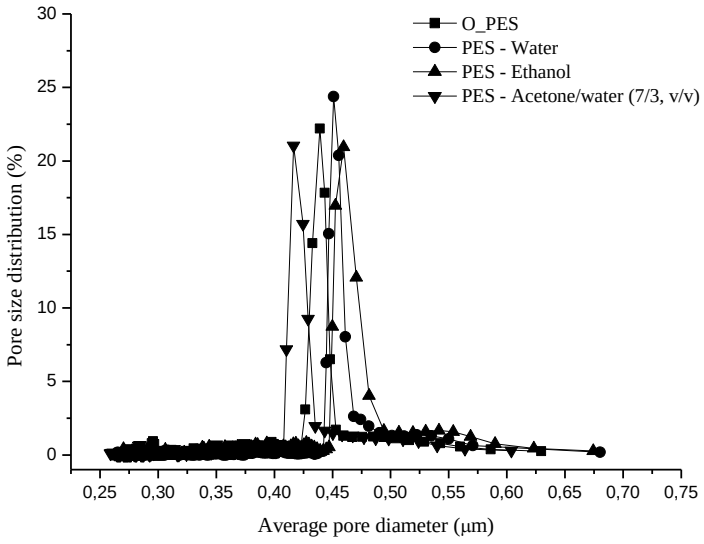

Figure 4.2. Effect of pretreatment solvent on membrane structure at 20 °C for 16 h.

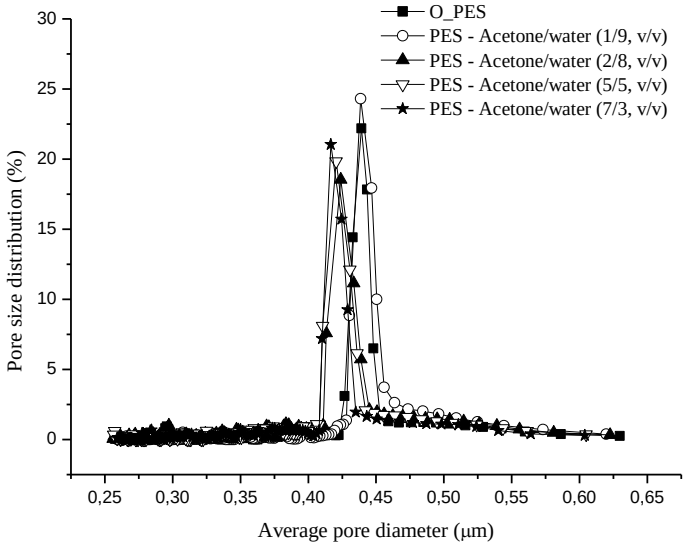

Figure 4.3. Effect of mixture content (volume ratio of acetone/water, 1/9 ~ 7/3(v/v)) on membrane structure (16 h, 20 °C, other mutual solvent effects are listed in Figure 7.1).

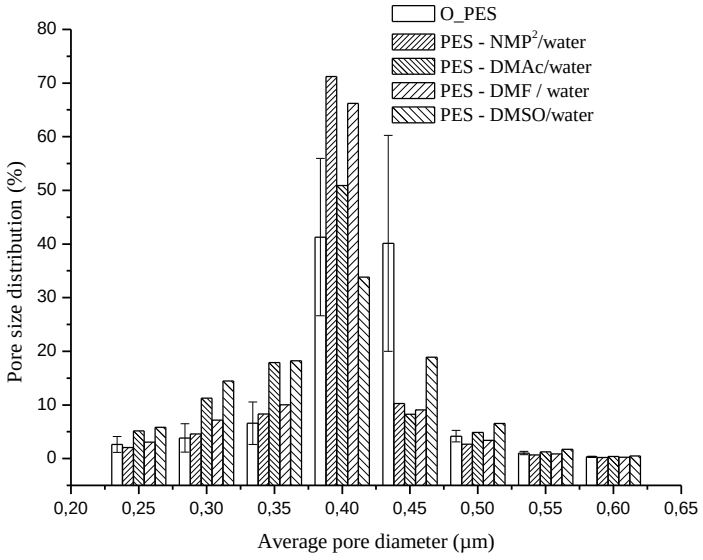

Figure 4.4. Effect of organic solvent on membrane structure (8/2 (v/v), 16 h, 20 °C).

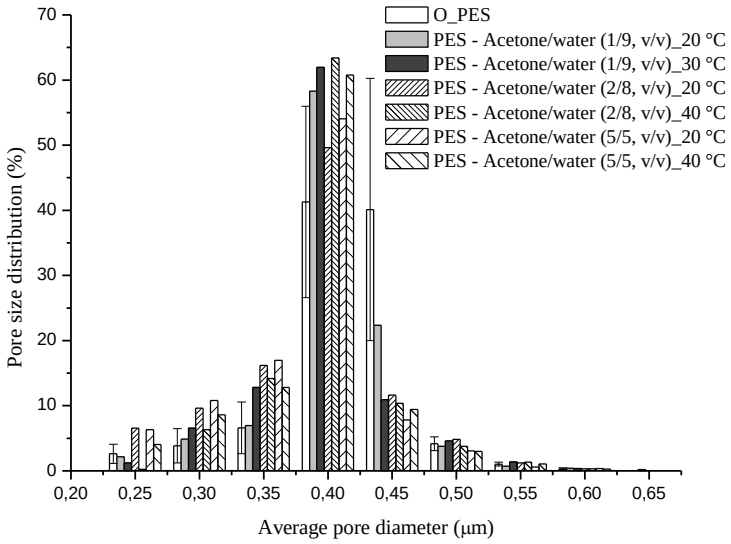

Figure 4.5. Effect of solvent temperature on membrane structure (16 h, 20 ~ 40 °C).

4.1.2. Effect of modification conditions on membrane structure and surface property

In this section, two different modification procedures (E1 and E2) have been tested (cf. Figure 3.1). The modification treated samples with corresponding numbers, as used in the following context, can be seen in Table 7.3 and 7.4. All the relevant factors, such as mixture ratio of mutual solvent, modifiers, concentration, modification time, deswelling way etc., which could influence the modification efficiency, were investigated, respectively. The overview on such factors has been listed in Table 3.1 and Table 3.2. More details on modifiers (structure, PEO content) can be seen in Table 4.14 (refer also to page 114).

4.1.2.1. Factors of E1 procedure

E1 procedure was performed under modification solution for swelling and embedment of modifiers into polymer surface firstly, and the good solvent was removed out of swollen membrane through vacuum dry or solvent exchange subsequently, to fix the modifier into polymer surface, as depicted in Figure 3.1a.

Effect of mutual solvent/solution. Figure 4.6 shows a membrane structure comparison of unmodified and entrapment treated sample. Therein, the average pore diameter and pore size distribution of 20 g/L PEG6000/DMSO&water (6/4, v/v) treated sample (337#) decreased evidently (Figure 4.6a), while 20 g/L PEG6000/DMSO&water (5/5, v/v) (Figure 4.6a, 338#) and 20 g/L PEG6000 distearate/TEG&water (Figure 4.6b 371# & 372#) treated sample still kept membrane structure very well. However, it was also found that 337# was somehow deformed after vacuum drying, and the corresponding water contact angle values of 371# and 372# were almost the same as for O_PES (Table 4.1). In addition, in Table 4.1 and Figure 4.7, some other samples treated with low organic content solution, such as 3/7 DMSO/water (v/v) (340#, 349#), 4/6 DMSO/water (v/v) (339#) and 3/7 NMP^2/water (350#) showed lower water contact angle than O_PES. DMSO/water seemed more effective than NMP^2/water.

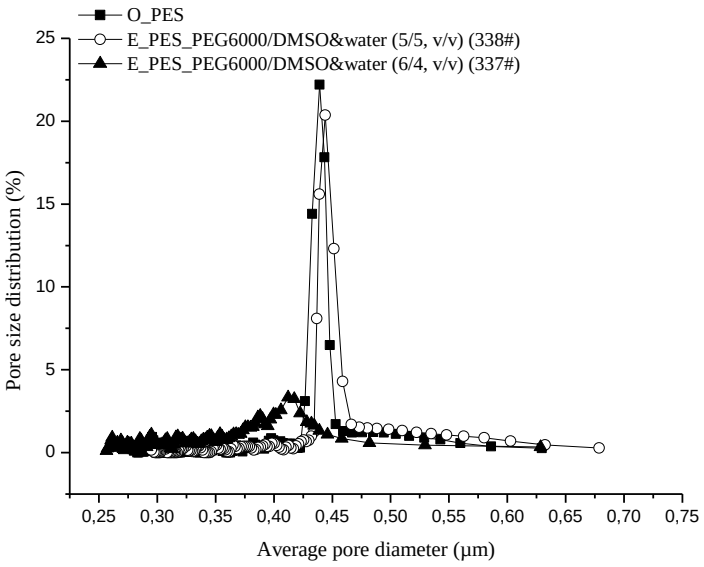

a)

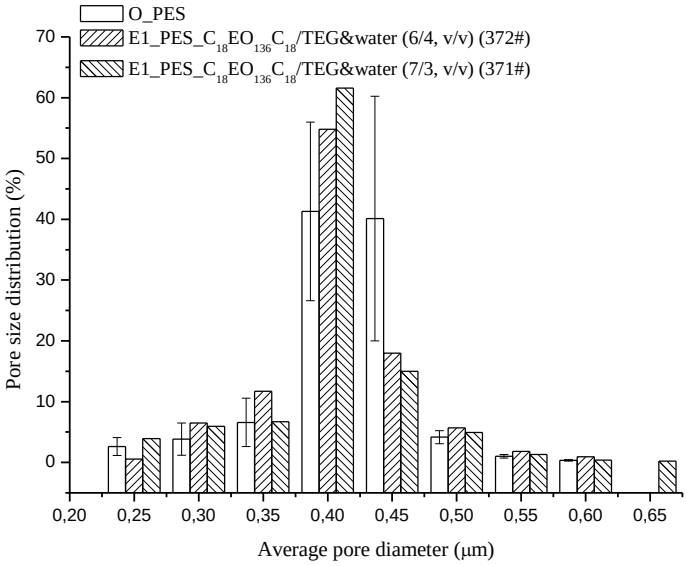

b)

Figure 4.6. Effect of solution on membrane structure: a). 20 g/L PEG 6000/DMSO&water, 18 h, 30 °C, vacuum dry directly; b). 20 g/L $C_{18}EO_{136}C_{18}$/TEG&water, 20 h, 30 °C, vacuum dry directly.

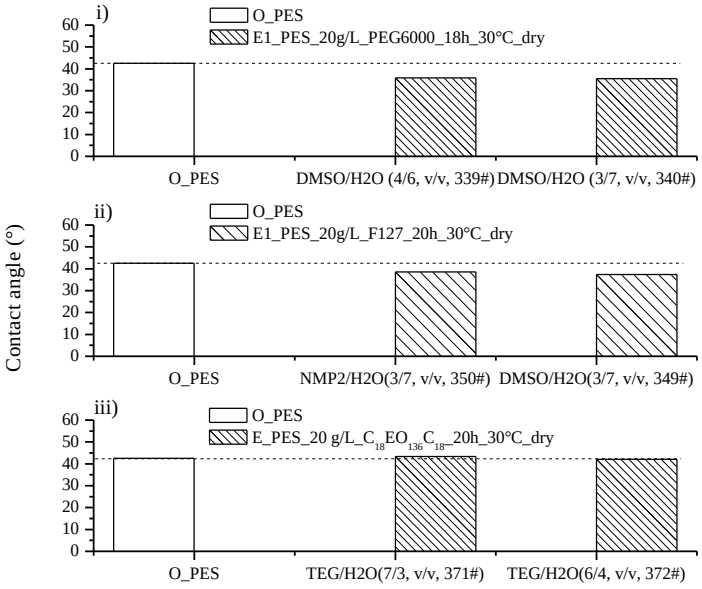

Figure 4.7. Effect of different solvents on surface wettability (vacuum dry immediately).

Table 4.1. Contact angle of original PES and different modifiers entrapment treated E1_PES samples.

Sample	Modifier	CA (°)
O_PES	-	42.5
PES-339#	PEG6000	35.9
PES-340#	PEG6000	35.5
PES-349#	F127	37.4
PES-350#	F127	38.6
PES-371#	$C_{18}EO_{136}C_{18}$	43.4
PES-372#	$C_{18}EO_{136}C_{18}$	42.0

Effect of modifier. Figure 4.8 shows water contact angle of E1_PES treated by two kinds of 1 g/L solution conditions with a series of water soluble polymers. And these samples have been immersed into water for 20 min before vacuum dry. It can be seen either homopolymer PEG 35,000 or amphiphilic macromolecules with various PEO chain length treated E1_PES, showed similar contact angle values and smaller than that of O_PES. Moreover, CA of E1_PES modifier with DMSO/water (8/2, v/v) solution was at least 5° less than E1_PES modified with DMF/water (8/2, v/v) solution. Figure 4.9 compares the effect of different modifier structure on surface wettability. Sample 307# was modified with $C_{18}EO_8$ containing short hydrophilic chain length (M_{wPEG} = 400 g/mol), but showed similar and even better surface hydrophilicity than 311#, a sample modified with a larger amphiphilic molecule containing longer PEG chain length (M_{wPEG} = 6000 g/mol). Sample 314# and 316# were modified under similar conditions but with different modifiers, these two modifiers (PEG6000 and $C_{18}EO_{136}C_{18}$ (M_{wPEG} = 6000 g/mol)) have same PEG chain length but both showed weak modification efficiency from CA (still higher than 40°).

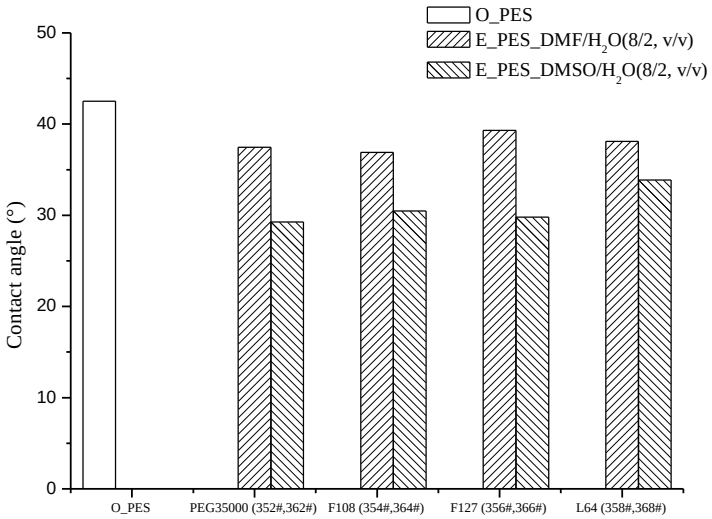

Figure 4.8. Effect of PEG chain-length on surface wettability (1 g/L solution, 18 h, 30 °C, water 20 min for deswelling).

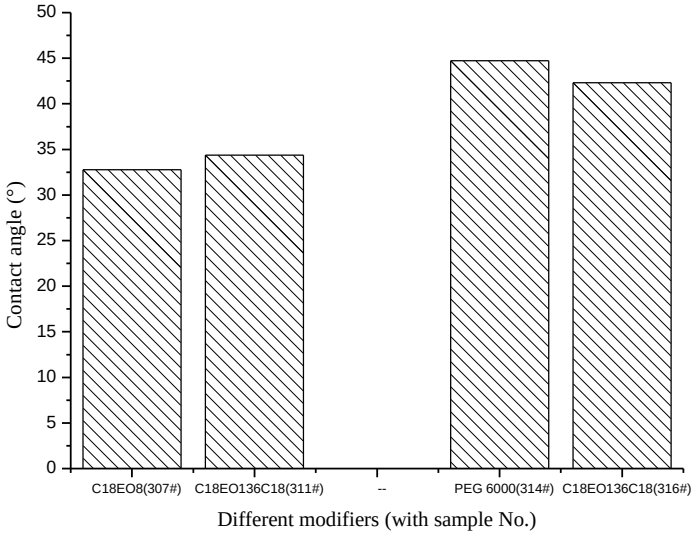

Figure 4.9. Effect of modifier structure on surface wettability.

Effect of concentration. Table 4.2 shows CA of E1_PES treated with three modification systems of different concentration (1 ~ 20 g/L) respectively. 358# and 360# showed similar contact angle and less modification efficiency compared with PE10100/DMSO&H_2O and PEG200,000/DMSO&H_2O modification efficiency. From 374#, 376#, 378# and also 380#,

382#, it is clear to see the higher concentration, the lower surface contact angle. Even though, 1 g/L concentration seemed somehow effective to improve PES surface hydrophilicity. As shown in Figure 4.10, the 1 g/L F108/DMSO&H_2O (v/v) modified E1_PES expressed low CA of about 30°, whereas the water flux had not clear decrease as expected. This might be due to the large pore sizes and high water flux (cf. Figure 4.1), as well as the good wettability of O_PES membrane. Hence, the difference of water flux value of O_PES and E1_PES was not so obvious.

Table 4.2. Effect of concentration on contact angle: E1_PES.

Modifier solution, time, temperature and deswelling way	Concentration (g/L) (With sample No.)	CA (°)
L64/DMSO&H_2O (8/2,v/v)_18h_30°C_water 20 min	1 (358#)	38.9
	20 (360#)	38.6
PE10100/DMSO&H_2O (8/2,v/v)_20h_20°C_water 20 min	1 (374#)	27.2
	10 (376#)	19.2
	20 (378#)	13.3
PEG200,000/DMSO&H_2O (8/2,v/v)_20h_20°C_water 20 min	1 (380#)	26.5
	10 (382#)	19.3

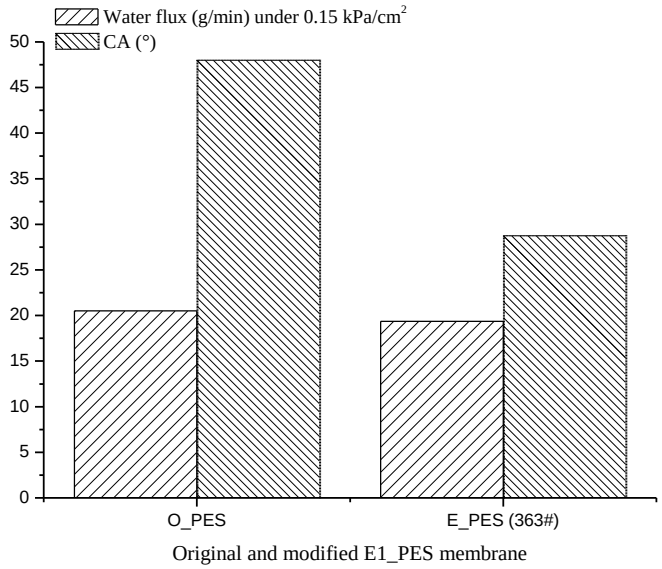

Figure 4.10. Wettability of outer surface and pore wall of O_PES and low concentration modified E1_PES.

Effect of adsorption/desorption (& deswelling way). One disadvantage of E1 procedure is the existence of adsorption or deposition of excessive modifier onto membrane surface or pores when immediately drying the swelling PES membrane. CA values of immediately dried E1_PES samples increased ~ 10° after water elution for 2.5 h (cf. Figure 4.11). As tested by coating and washing, it was found this elution time is enough for dissolve adsorbed water soluble modifiers considering their good solubility in water.

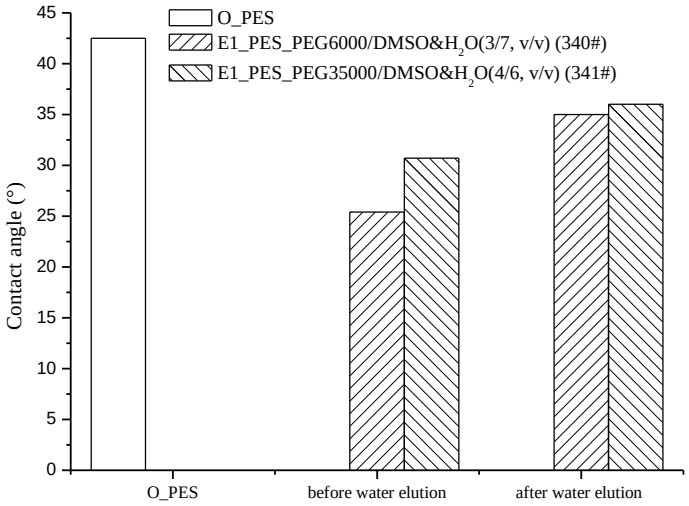

Figure 4.11. Effect of adsorption of modifier on contact angle (20 g/L PEG solution, 18 h, 30 °C, vacuum dry directly).

To avoid or reduce the adsorption affect, nonsolvent of PES, water was used to replace mutual solvent for deswelling pre-modified PES membrane. The detailed comparison of vacuum evaporation (dry immediately) and water replacement deswollen E1_PES from CA and IR spectrum are shown in Figure 4.12 and 4.13 respectively. From CA, it is hard to conclude which deswelling way is better for surface hydrophilic modification. It was anticipated to find the C-O peak from PE10100 at about 1100 cm^{-1} of modified PES IR spectra, however, this peak overlapped with O_PES peak. More detailed observation showed that the strength of ether peak for E1_PES was stronger than that of O_PES, but there was not much difference of 369# and 370#, two modified PES samples treated with different deswelling way.

In addition, before the modification experiment, it was found that 7/3 (v/v) NMP[2]/water was a critical mixture ratio to avoid damage membrane structure. However, the swelling membranes with corresponding modifier solution were seriously damaged during immediately dry process.

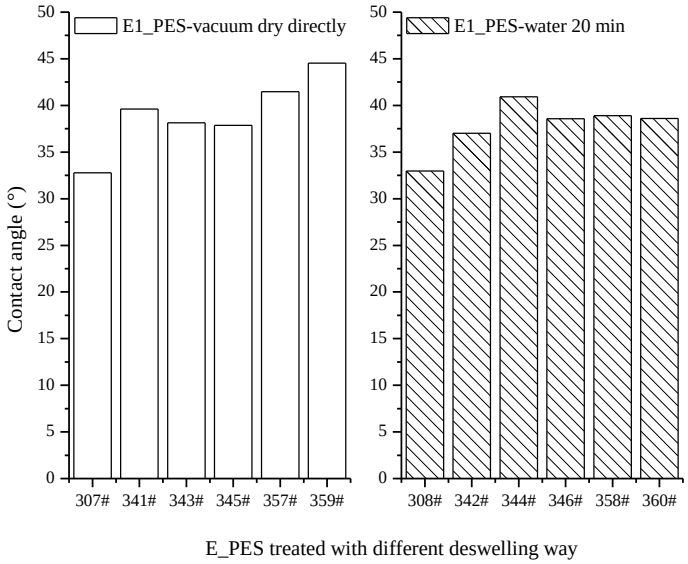

Figure 4.12. Effect of deswelling way on contact angle.

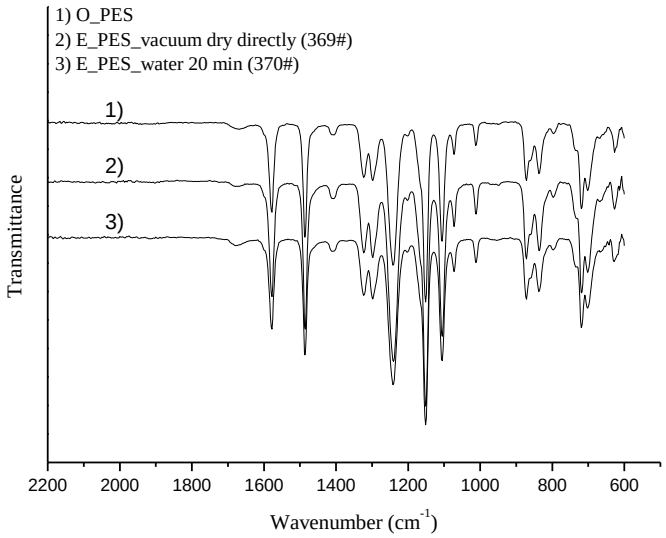

Figure 4.13. IR spectrum of original and E1_PES membrane treated with different deswelling way (1 g/L PE10100/DMSO&water (8/2, v/v), 18 h, 30 °C).

4.1.2.2. Factors of E2 procedure

E2 procedure was performed under the certain solvent for swelling firstly; thereafter the modifiers were entrapped into PES surface in the aqueous solution rapidly, as depicted in Figure 3.2b.

As validated in E1 procedure, NMP^2/water (7/3, v/v) was strong enough for swelling PES membrane. Therefore, in this part, NMP^2/water (7/3, v/v) was selected as good solvent for swelling PES membrane, water solutions of a series of different modifiers were carried out as modification solution. The details of tested sample IDs are listed in Table 7.4 in Appendix. The effects of temperature, embedment time as well as deswelling way were generally studied.

Figure 4.14 shows CA of E2_PES entrapped with 20 g/L F127/water for 2 h at 20 °C and 30 °C respectively. 30 °C modified sample (399#) showed better surface hydrophilicity than 20 °C modified sample (402#). Figure 4.15 is CA of E2_PES entrapped with a series of water soluble polymer at 20 °C for 2 h (PEG35,000, F128, F127, PE10500, L64 and RPE1740, see samples 400# ~ 405#). The surface hydrophilicity has not obviously improvement or change under this modification condition, and it seems that long PEO chain length and structure of amphiphilic polymer have no obvious effect on modification efficiency.

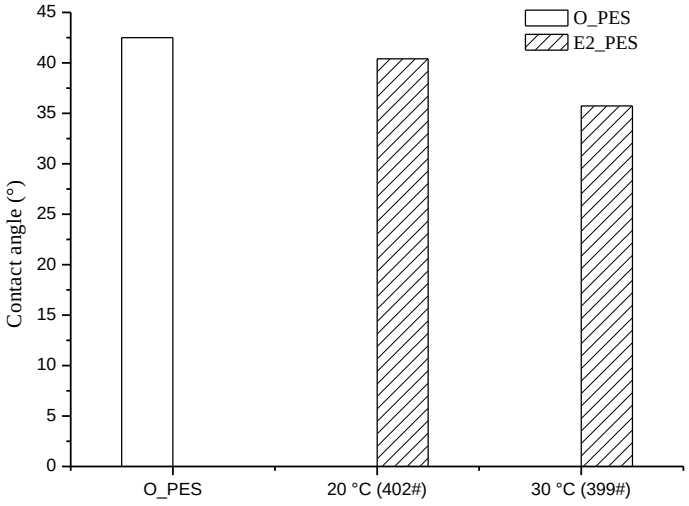

Figure 4.14. Effect of embedment temperature on surface wettability: swelling in NMP^2/water (7/3, v/v) for 20 h; entrapment in 20 g/L F127/H_2O solution for 2 h; then vacuum dry.

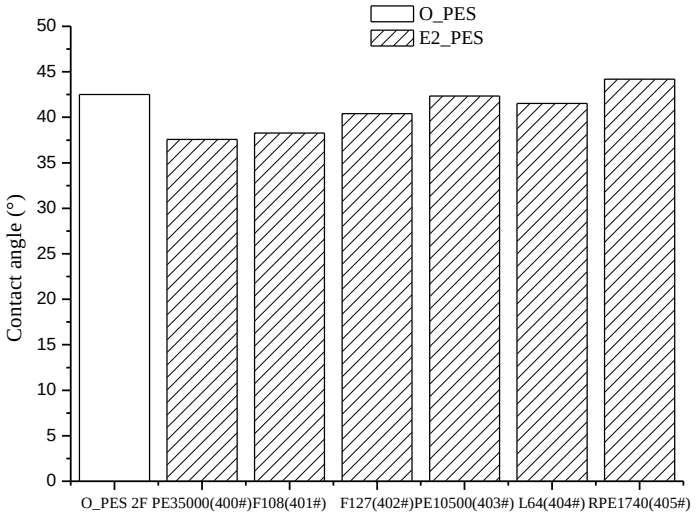

Figure 4.15. Effect of modifiers on contact angle: swelling in NMP^2/water (7/3, v/v) for 20 h; entrapment in 20 g/L aqueous solution for 2 h; then vacuum dry (for 393#, PE10500 was water solution with the concentration of about 18 %).

In E2 procedure, the embedment process was anticipated to deswell swollen membrane with water solution replacing organic solvent. Therefore, this process was also called as deswelling1, the subsequent dry process was called deswelling2. It was found that the embedment time from 0.5 ~ 4 h has not so much influence on modification efficiency (Table 4.3). Moreover, CA under vacuum dry was lower than water 20 min deswollen E2_PES.

For PEG6000 as modifier, CAs of E2_PES samples, which were modified under a variety swelling time and embedment time respectively, are listed in Table 4.4. All samples were dried immediately after entrapment process. The CA values decreased to 3 ~ 8°. CAs of 383 ~ 387# were similar; this further confirmed that embedment time was not the dominant fact of the entrapment efficiency. Samples 388 ~ 390#, which underwent longer swelling time (> 16 h) than 383 ~ 387# (< 10 h) showed lower CA and better wettability.

Table 4.3. Effect of embedment time, "deswelling2" on CA.

Time (h) (With sample No.)	CA under different deswelling2 processes(°)	
	Vacuum dry 24 h	Water 20 min
0.5 (401#, 402#)	31.0	37.3
2.5 (403#, 404#)	30.7	39.1
4.0 (405#, 406#)	28.0	31.7

Table 4.4. CAs of PEG 6000 modified E2_PES memebrane (different swelling time (Time 1) in NMP2/H2O and entrapment time (Time 2) in aqueous solution).

Sample No.	383#	384#	385#	386#	387#	388#	389#	390#
Time 1 (h)	0.5	1	3	6	10	19	22	16
Time 2 (h)	0.5	2	3	4	15	3	5	144
CA (°)	43.10	39.33	38.32	36.16	38.06	35.06	33.77	34.58

4.2. Entrapment of small ampiphilic molecules into Membrana PP membrane surface

C_iEO_j

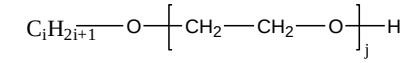

i = 18; j = 8

$C_iEO_jC_i$

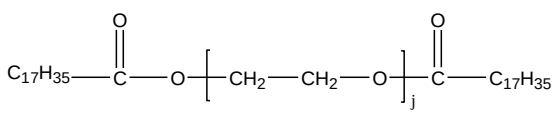

i = 18; j = 8, 136

Scheme 4.1. Chemical structure of C_iEO_j-containing amphiphilic molecules.

From this section, E1 procedure would be employed for further entrapment study. Modifiers of a series of small amphiphilic molecules containing same low alkyl chain (C_{18}) but different structures were anticipated to entrap into PP microfiltration membrane surface here. Detailed modification conditions, such as solvent, temperature, embedment time as well as concentration were studied, thereafter the optimized modification condition was decided with respect to CA results. Then, a series of characterizations of $C_{18}EO_8$ modified E_PP were carried out to comprehensive understand the feasibility and efficiency of entrapment technique on membrane surface property, antifouling property, membrane performance and stability. Therein, the effects of modification condition on membrane and polymer structure were investigated as well.

4.2.1. Effect of modification conditions

Solvent. Effect of acetone, which was used to elute residual solvent from manufacturing [52], on the membrane structure was studied initially. The membrane structure kept well after acetone treatment for 24 h at room temperature (see Figure 4.16).

After initial screening of solvents (e.g., carbon tetrachloride, 1,2-dichloroethane, xylene, 1,2,3,4-tetrahydronaphthalene), 1,2-dichloroethane had been selected because this solvent had the smallest influence on PP membrane structure according to macroscopic observation. From Figure 4.17, it was found that the average pore diameter slightly decreased at higher temperature in 1,2-dichloroethane. Moreover, all average pore diameters of 1,2-dichloroethane treated membranes became smaller with time than that of O_PP, however, there was not so much difference from 3 h to 20.5 h (Figure 4.18). Hence, 16 h at room temperature were finally selected for the modification experiment.

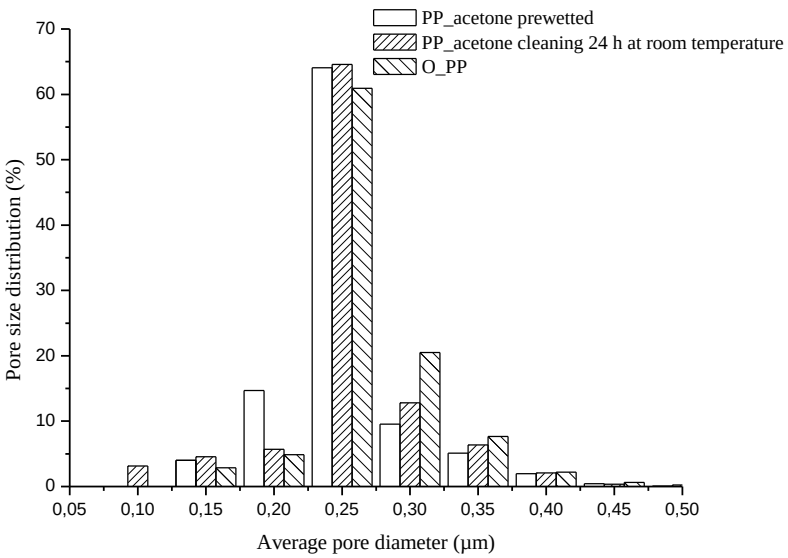

Figure 4.16. Effect of acetone on PP membrane structure.

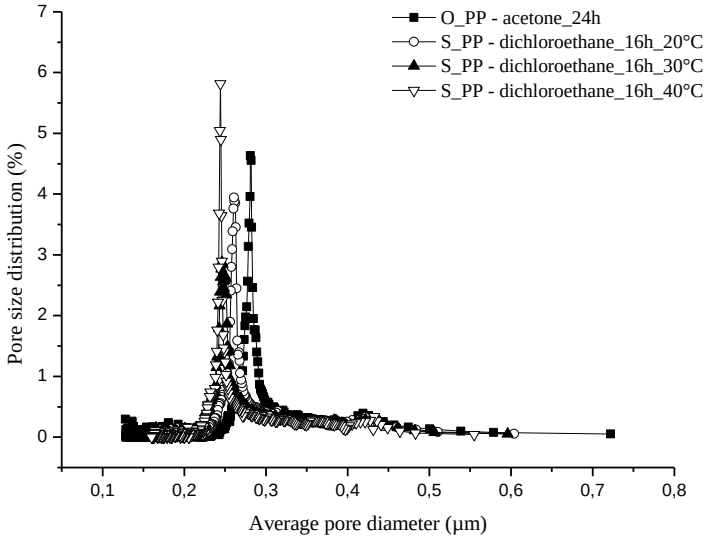

Figure 4.17. Effect temperature on PP membrane structure (in organic solvent).

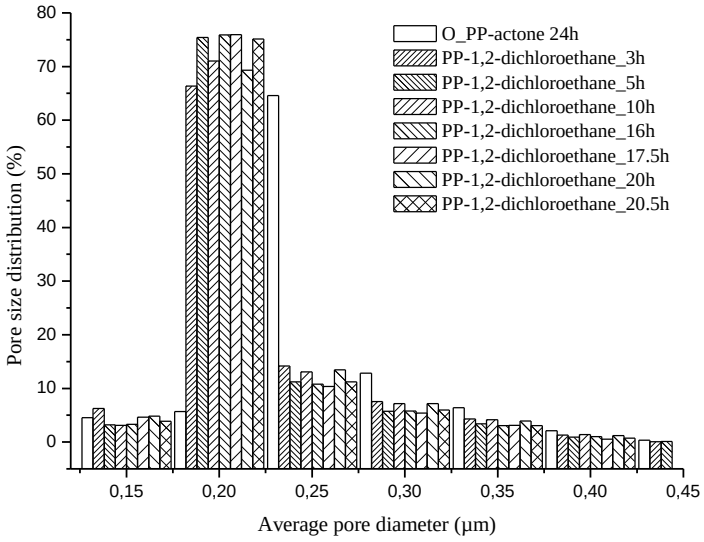

Figure 4.18. Effect of immersing time in dichloroethane on PP membrane structure, 20 °C.

Concentration. As seen in Table 4.5, CA showed weak modification efficiency at low concentration ~ 8 g/L (e.g. PP 2EHF-1 ~ 15#), irrespective the modifier structure ($C_{18}EO_8$, $C_{18}EO_8C_{18}$) and PEO chain length ($C_{18}EO_8C_{18}$, $C_{18}EO_{136}C_{18}$). The unexpected evaporation of solvent happened in PP membrane samples 16 ~ 18#, which made the concentration unknown, however, these sample surfaces acquired very well surface hydrophilicity: the water drop spread out quickly and penetrated into membrane pores except $C_{18}EO_{136}C_{18}$ treated PP (PP 2EHF-18#). Therefore, continully increased concentration of $C_{18}EO_8$/1,2-dichloroethane to 20 g/L (cf. PP 2EHF-19#), and the corresponding CA was only 12°. However, it was also found this surface hydrophilicity disappeared quickly when immersed sample into ethanol (cf. PP 2EHF-20#).

Detailed effect of concentration of $C_{18}EO_8$/1,2-dichloroethane on surface wettability (time dependent CA) is shown in Figure 4.19. After modification, water drop on dried membrane surface decreased with measuring time, and high concentration resulted in lower contact angle and quicker spreading tendency. As to unmodified PP, the contact angle kept almost stable (140° ~ 135°) in the measuring time range of ~ 20 min, which was only slightly

influenced by water evaporation and decrease of drop volume. As a conclusion, the higher concentration, the better surface wettability.

Table 4.5. Water contact angle of PP membrane treated under a series of conditions.

Sample No.	Modification conditions	CA (°)
PP 2EHF-1#	20 °C, 1 g/L $C_{18}EO_8$/DCE, 16 h, vacuum dry 48 h	132.7
PP 2EHF-2#	20 °C, 1 g/L $C_{18}EO_8C_{18}$/ DCE, 16 h, vacuum dry 48 h	134.7
PP 2EHF-3#	20 °C, 1 g/L $C_{18}EO_{136}C_{18}$/ DCE, 16 h, vacuum dry 48 h	138.2
PP 2EHF-4#	20 °C, 1 g/L $C_{18}EO_8$/ DCE, 16 h, ethanol 10 min	109.6
PP 2EHF-5#	20 °C, 1 g/L $C_{18}EO_8C_{18}$/ DCE, 16 h, ethanol 10 min	138.3
PP 2EHF-6#	20 °C, 1 g/L $C_{18}EO_{136}C_{18}$/ DCE, 16 h, ethanol 10 min	130.2
PP 2EHF-7#	20 °C, 3 g/L $C_{18}EO_8C_{18}$/ DCE, 16 h, vacuum dry 48 h	140.7
PP 2EHF-8#	20 °C, 3 g/L $C_{18}EO_8C_{18}$/ DCE, 16 h, ethanol 10 min	139.1
PP 2EHF-9#	20 °C, 3 g/L $C_{18}EO_8C_{18}$/ DCE, 16 h, vacuum dry 48 h	128.4 ~ 81.1
PP 2EHF-10#	20 °C, 3 g/L $C_{18}EO_8C_{18}$/ DCE, 16 h, ethanol 10 min	134.2
PP 2EHF-11#	20 °C, 1 g/L $C_{18}EO_8C_{18}$/ DCE, 10 h, vacuum dry 48 h	134.9
PP 2EHF-12#	20 °C, 3 g/L $C_{18}EO_8C_{18}$/ DCE, 10 h, vacuum dry 48 h	124.2
PP 2EHF-13#	20 °C, 8 g/L $C_{18}EO_8C_{18}$/ DCE, 10 h, vacuum dry 48 h	63.8
PP 2EHF-14#	20 °C, 3 g/L $C_{18}EO_{136}C_{18}$/ DCE, 10 h, vacuum dry 48 h	139.0
PP 2EHF-15#	20 °C, 3 g/L $C_{18}EO_8C_{18}$/ DCE, 10 h, ethanol 10 min	139.0
PP 2EHF-16#	20 °C, evaporated, $C_{18}EO_8$/ DCE, 10 h, vacuum dry 48 h	Spread & penetrated
PP 2EHF-17#	20 °C, evaporated, $C_{18}EO_8C_{18}$/ DCE, 10 h, vacuum dry 48 h	20.3 (90 s)
PP 2EHF-18#	20 °C, evaporated, $C_{18}EO_{136}C_{18}$/ DCE, 10 h, vacuum dry 48 h	Spread without penetration
PP 2EHF-19#	30 °C, 20 g/L $C_{18}EO_8$/ DCE, 20 h, vacuum dry 48 h	11.2
PP 2EHF-20#	30 °C, 20 g/L $C_{18}EO_8$/ DCE, 20 h, vacuum dry 48 h, eluted by ethanol 2.5 h at room temperature	140.4

Note: If there is no special notification, all PP samples were eluted by water at room temperature for 2.5 h before characterization.

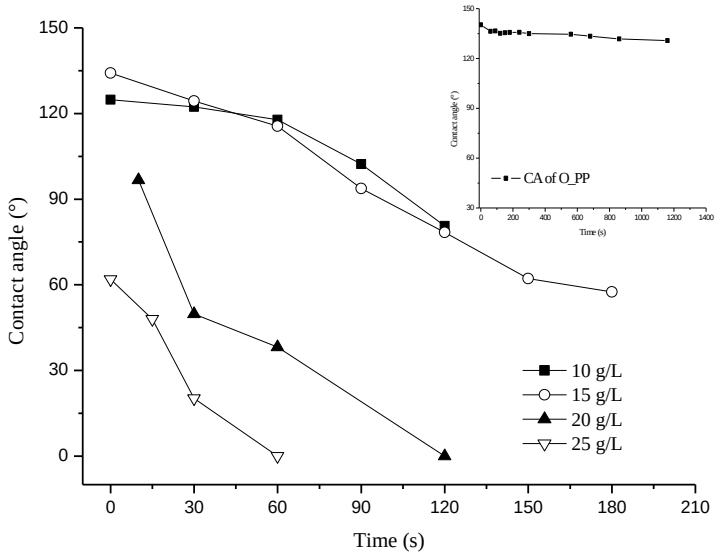

Figure 4.19. Effect of concentration (15 ~ 25 g/L) on time dependent CA: $C_{18}EO_8$/1,2-dichloroethane at room temperature for 20 h, water 20 min, then dry.

Modification time (swelling/embedment time). Furthermore, the effect of modification time (swelling/embedment time) in the range of 3 ~ 20 h was studied for 25 g/L $C_{18}EO_8$/1,2-dichloroethane at 20 °C. The original time-dependent CA data from different positions of every sample are shown in the Figure 4.20. It can be seen that when the swelling/embedment time was 3 h, membrane surface showed part hydrophilic, and most area was hydrophobic. Prolonged time to 5 h, CA continually decreased continuously with measuring time, and the values tended to be stable after 90 s. The final water contact angles were lower than 90°. 16 h modified sample surface still showed inhomogeneous hydrophilicity, but showed lower CA (e.g., at 90 s) than 5 h modified PP membrane. For 20 h modified sample, all the water drops decreased and spread quickly in 1 min, and even penetrated into membrane pores.

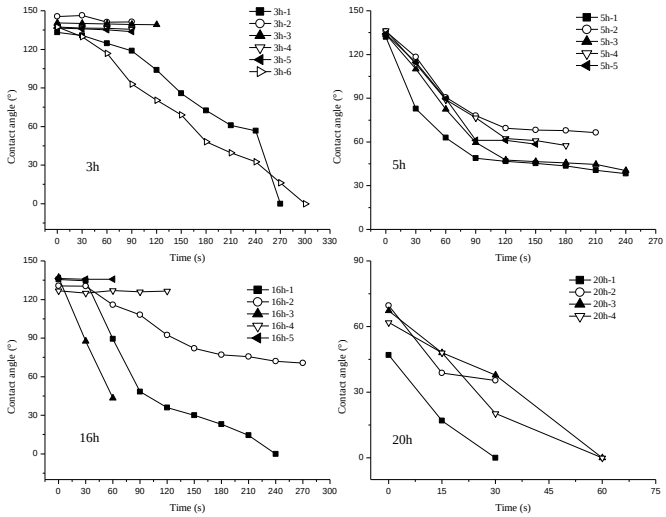

Figure 4.20. Effect of modification time (3 ~ 20 h) on time dependent CA: 25 g/L $C_{18}EO_8$/1,2-dichloroethane at room temperature, water 20 min, then dry.

Temperature. Effect of temperature on membrane surface wettability has been studied and their time-dependent CA trends are shown in Figure 4.21. Due to the different time interval of records and spreading speed of water drop on surface, it is impossible to obtain the average value for every sample; additionally, the values and tendency in Figure 4.21 can be simply used to judge whether the surface was homogeneous or not. Figure 4.21a and b are from different modification solution (20 g/L $C_{18}EO_8C_{18}$/1,2-dichloroethane, 25 g/L $C_{18}EO_8$/1,2-dichloroethane) with same modification process. Even though, Figure 4.21a and b showed that temperature of 20 ~ 30 °C has not evident influence on surface wettability.

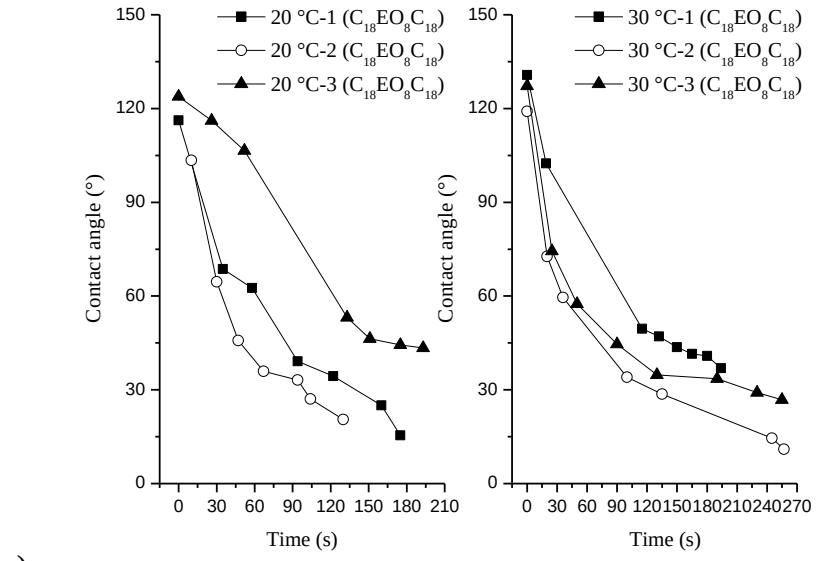

a)

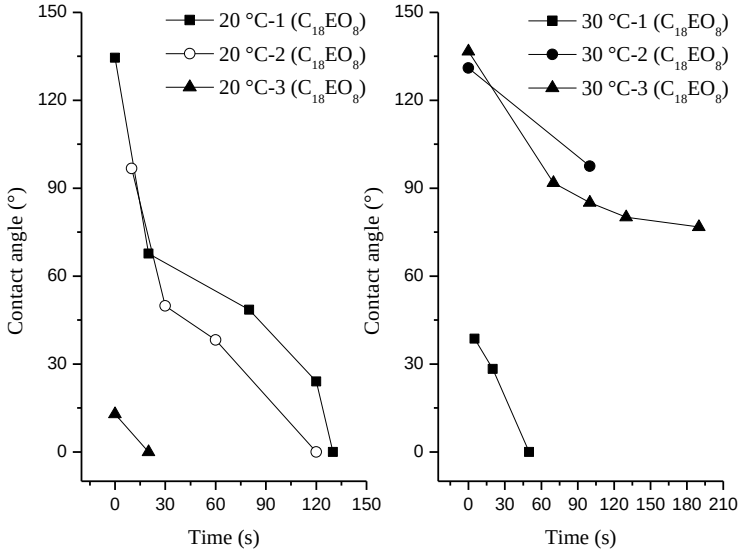

b)

Figure 4.21. Effect of temperature on time dependent CA: a) 20 g/L $C_{18}EO_8C_{18}$/1,2-dichloroethane for 19 h and b) 25 g/L $C_{18}EO_8$/1,2-dichloroethane for 20 h, water 20 min, respectively.

Adsorption/deposition. Different with other hydrophilic PEO-containing modifiers, $C_{18}EO_8C_{18}$ is water insoluble at room temperature, but it has good solubility in water at 40 °C. Hence, E_PP/ $C_{18}EO_8C_{18}$ sample should be eluted by water at 40 °C. Water elution results under 20 °C and 40 °C have been compared by time dependent CA and FTIR respectively (cf. Figure 4.22). It can be seen that the characteristic signals from $C_{18}EO_8C_{18}$ (ether group near 1111 cm^{-1} and ester group near 1736 cm^{-1}) became weaker when eluted at

40 °C (cf. Figure 4.22a), while the surface wettability did not change so much (cf. Figure 4.22b).

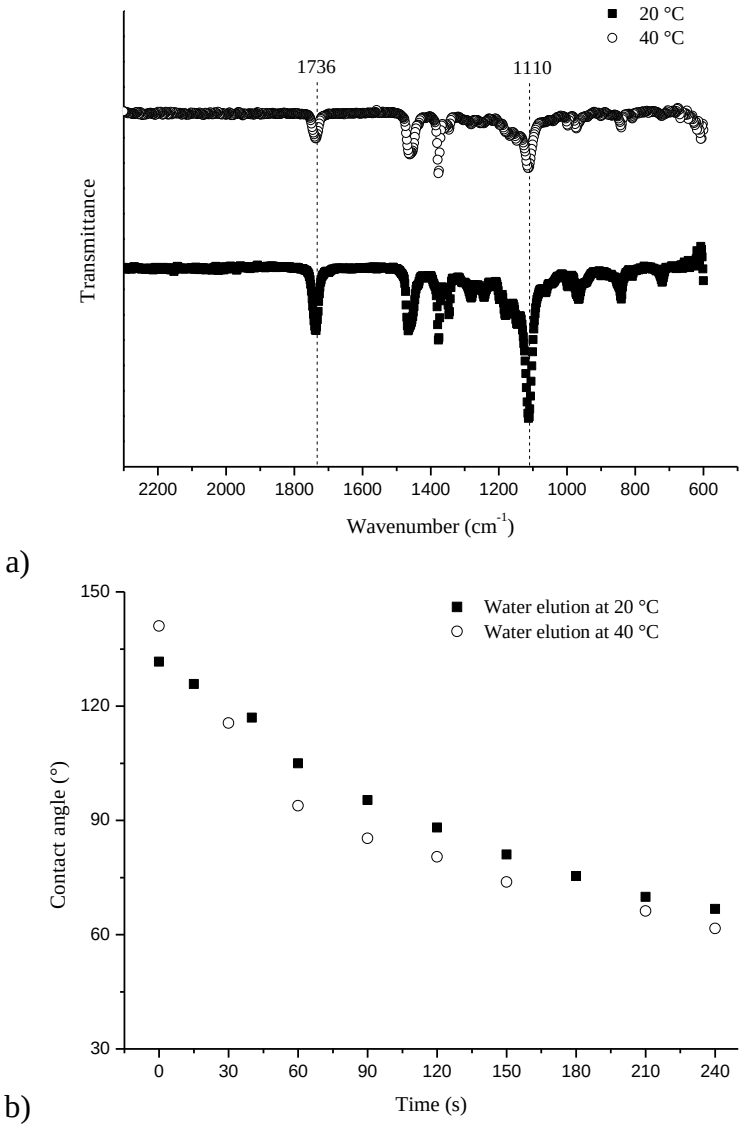

Figure 4.22. Effect of adsorption on surface property: a) IR; b) Time dependent CA. (25 g/L $C_{18}EO_8C_{18}$/1,2-dichloroethane for 20 h, water 20 min).

4.2.2. Entrapment of $C_{18}EO_8$ into PP membrane surface

Membranes were modified in terms of the E1 procedure shown in Figure 3.1 under conditions of 25 g/L $C_{18}EO_8$/1,2-dichloroethane solution for 20 h at room temperature. Water

immersion for 20 min before vacuum dry was proceeded and water elution for 2.5 h before characterization to further elute surface adsorbed modifier.

Membrane pore structure. The specific surface area of the membranes decreased from 29.6 m^2/g for O_PP to 25.6 m^2/g for E_PP. The increase of E_PP/$C_{18}EO_8$ in weight was 20.30 ± 0.04%. Gas permeability decreased for the modified membrane. Figure 4.23 shows the pore size distributions in dry state of original PP (O_PP), only solvent treated PP (to assess the effects of the entrapment modification conditions; S_PP) and modified PP membranes (E_PP). Compared with the data for O_PP, there was slight shift to lower values of average pore diameter and the slight broadening of the size distribution for S_PP. However, there was a much stronger change for E_PP; average pore diameter was reduced by more than 50 nm, and the size distribution was also broader. Moreover, the pore morphology is rather complex. The outer surface morphologies of membranes O_PP, S_PP and E_PP were compared (Figure 4.24). Solvent treatment alone had no influence on pore morphology (cf. Figure 4.24a vs. b). Apparently, a relatively smooth "cover-layer" had formed on the modified membrane surface and some pores appeared to be blocked (cf. Figure 4.24c). PP membrane was too soft to be frozen and broken, so that it was impossible to obtain smooth broken side. Hence, it is hard to recognize the difference between O_PP and E_PP from cross-section images (cf. Figure 4.25). Thereafter, with help of element analysis corresponding to the cross-section image (Energy dispersive analysis system of X-ray, EDS/EDX), it was found O wt% content increased after modification, and the values at different depth of E_PP were similar (cf. Figure 4.26, Table 4.6).

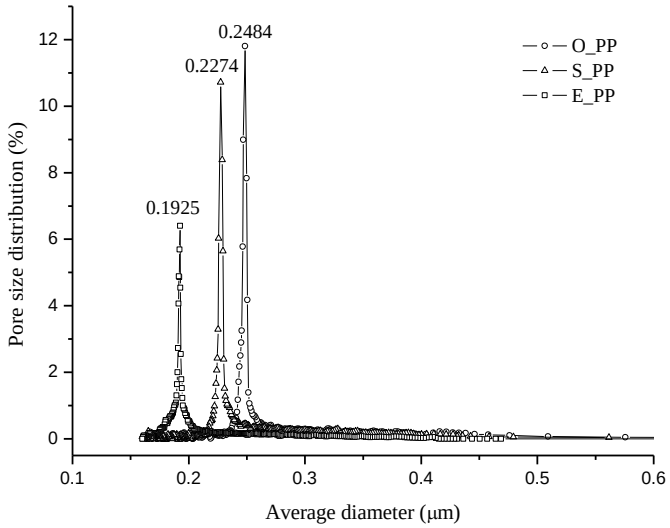

Figure 4.23. Pore size distribution as a function of average diameter of various PP samples (O_PP: original PP, S_PP: PP treated with 1,2-dichloroethane at 20 °C for 20 h, E_PP: PP modified with solution 25 g/L $C_{18}EO_8$/dichloroethane at 20 °C for 20 h).

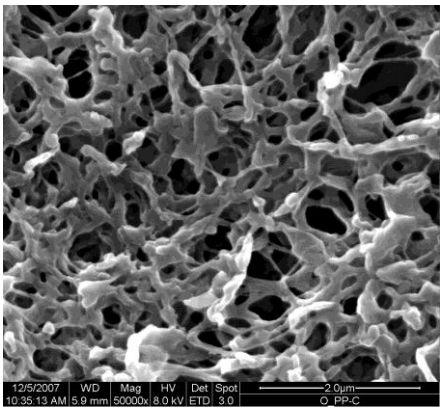

a. O_PP

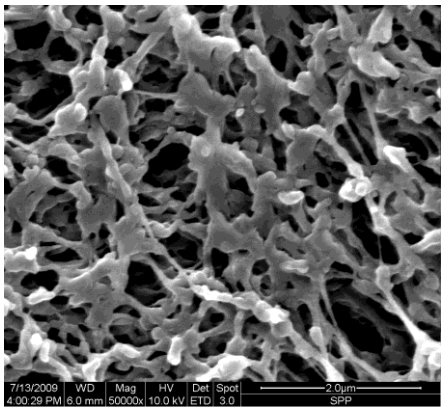

b. S_PP

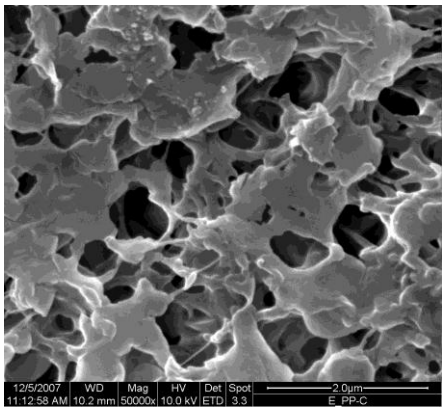

c. E_PP/$C_{18}EO_8$

Figure 4.24. Outer surface morphology for original (O_PP), 1,2-dichloroethane treated (S_PP) and $C_{18}EO_8$-modified membrane (E_PP).

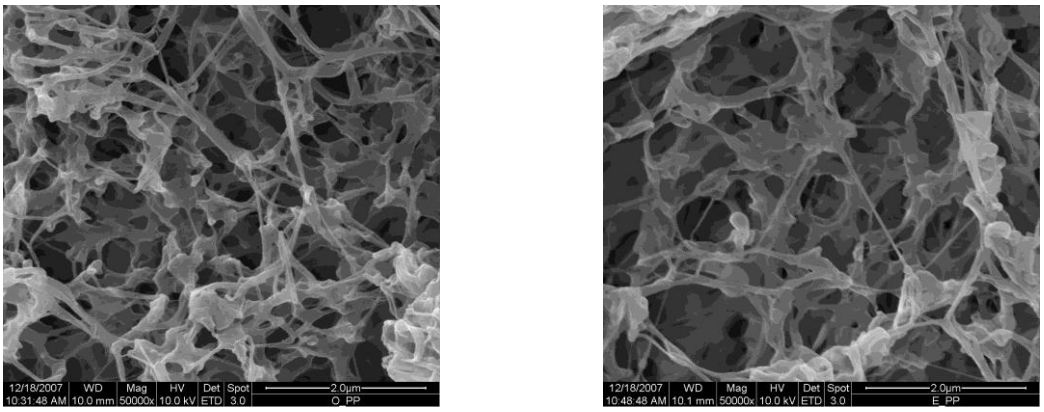

a. O_PP b. E_PP

Figure 4.25. Cross-section morphology for original (O_PP), and $C_{18}EO_8$-modified membrane (E_PP).

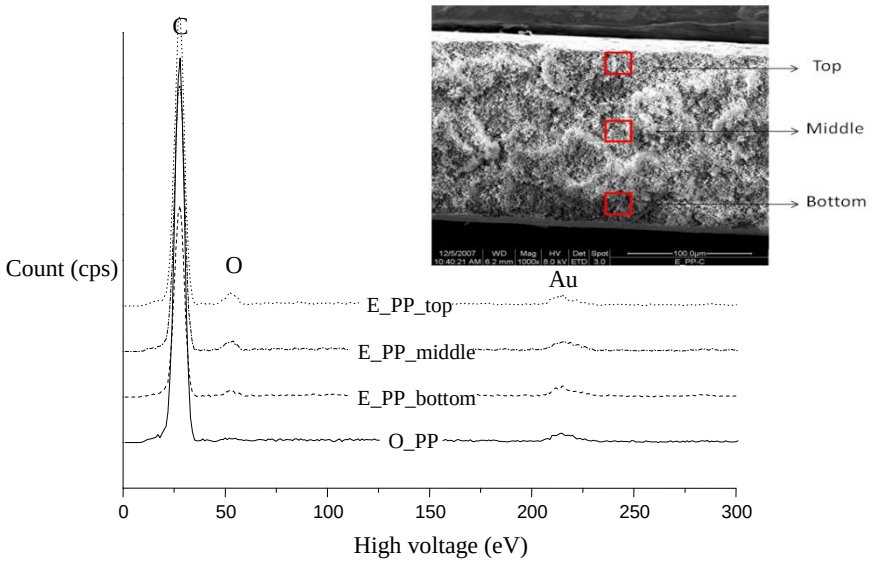

Figure 4.26. EDS (energy dispersive spectroscopy) spectrum of original and $C_{18}EO_8$-modified PP membrane with different measuring depth.

Table 4.6. Important elements of PP 2E HF membranes corresponding to Figure 4.26.

Sample	Element, wt%	
	C	O
O_PP	98.5	1.5
E_PP/$C_{18}EO_8$-bottom	95.7	4.3
E_PP/$C_{18}EO_8$-middle	94.7	5.3
E_PP/$C_{18}EO_8$- top	93.8	6.2

Physicochemical structure. The X-ray crystal structures of membranes O_PP and S_PP were measured to study the influence of solvent on the PP solid state structure (Figure 4.27). It can be seen that the primary crystal structure of the PP such as crystalline lattice [150] did not change. Only slight shifts and broadening of the characteristic peaks in membrane S_PP at 14.2°, 16.8°, 18.4° and 21.6° confirmed that the crystallite structure of membrane O_PP was almost preserved. Overall, the degree of crystallinity of the PP membrane decreased from 62.7% for O_PP to 53.8% for S_PP after the treatment with the pure solvent under embedding conditions (cf. Table 4.7). However, the apparent degree of crystallinity of E_PP, calculated from the XRD spectrum, was 57.6%, a little higher than that of S_PP. In addition, it was found that 4 new peaks appeared in the spectrum of E_PP, which completely correspond to the characteristic peaks in the spectrum of $C_{18}EO_8$.

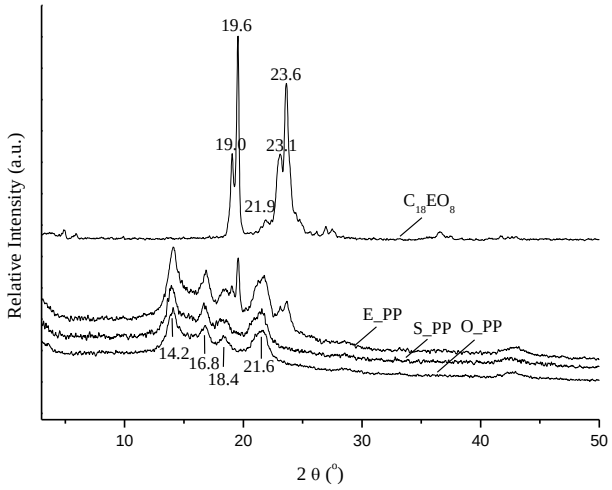

Figure 4.27. XRD spectra of membranes O_PP, S_PP and E_PP/$C_{18}EO_8$ as well as the modifier $C_{18}EO_8$.

Table 4.7. Integrated area and crystalline degree (Xc) from XRD spectrum.

Samples	Ac	A	Xc (%)
O_PP	12182	19424	62.7
S_PP	10760	20001	53.8
E_PP/$C_{18}EO_8$	22111	38420	57.6

Figure 4.28 shows the DSC of O_PP and E_PP. For O_PP, the first endothermic peak came out at 3.8 °C; and the first exothermic peak came out at 145.6 °C, with an enthalpy of -33.86 J/g; moreover, the second endothermic peak at 162.3 °C was 18.79 J/g. By contrast, for E_PP, there was one new sharp endothermic peak with the enthalpy of 22.15 J/g at 36.6 °C following the first endothermic peak at 5.5 °C; and the exothermic peak at 129.7 °C had the enthalpy of -408.4 J/g; when the heating temperature reached 154.9 °C, the other endothermic peak came out, with an enthalpy of 388.8 J/g. The change is evident after modification with $C_{18}EO_8$: a new exothermic peak came out at 36.6 °C and much more enthalpy produced or consumed of E_PP during phase transition (crystal formation, glass transition etc.). It can be deduced that this difference might be contributed by the existence of another crystal phase, $C_{18}EO_8$, as confirmed in Figure 4.27.

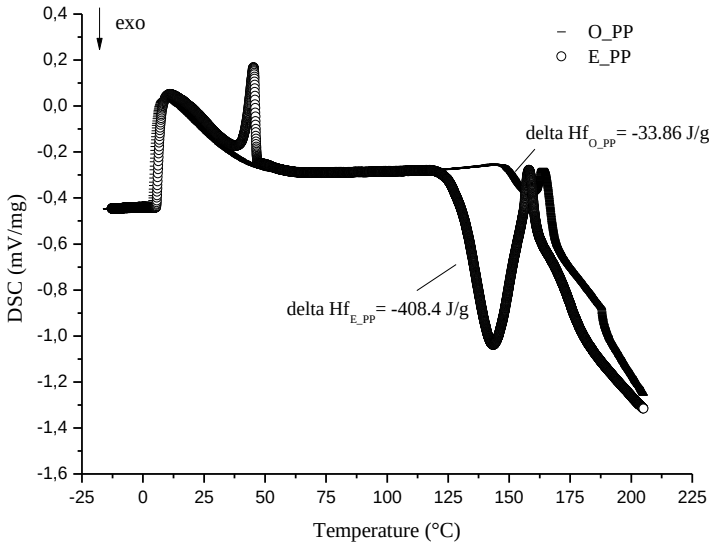

Figure 4.28. DSC spectra of membranes O_PP and E_PP modified with $C_{18}EO_8$.

Figure 4.29 presents IR spectra of membranes O_PP, S_PP and E_PP. The peaks at 973 and 998 cm^{-1} can be assigned to the amorphous and the crystalline domains of PP, respectively [74]. For original PP membrane (O_PP), the intensity of the 973 cm^{-1} peak was slightly higher than that of the 998 cm^{-1} peak; and this ratio did not significantly change after solvent

treatment. For the modified membrane E_PP, the intensity of 973 cm^{-1} peak was more than two times higher than that at 998 cm^{-1}. Moreover, the surface chemical composition from IR showed that the band at about 1115 cm^{-1}, corresponding to ether groups, was very strong in the spectrum of membrane E_PP (cf. Figure 4.29).

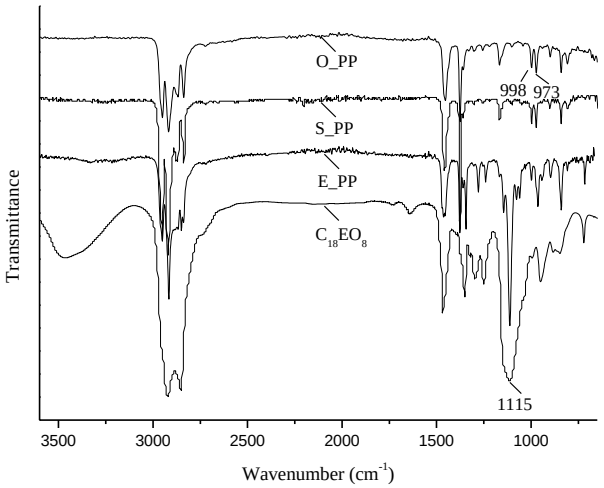

Figure 4.29. IR spectra of membranes O_PP, S_PP and E_PP as well as of the modifier $C_{18}EO_8$.

Membrane outer surface property. PP has low surface energy high CA over 140°. For E_PP/$C_{18}EO_8$, the 5 µl water drop could spread out quickly in 10 s so that the pores in this wetted area were completely penetrated (cf. Figure 4.30). The CA with adsorbed $C_{18}EO_8$ has been compared, as seen the captive bubble CA of pore-filled swollen PP (cf. Figure 4.31). CA of $C_{18}EO_8$ in the interface of H_2O/1,2-dichloroethane is more than 35°, which is larger than CA showed in first column (corresponding to Figure 4.30b). That means the water sessile drop measurement for membrane is influenced by pore structure.

a. O_PP b. E_PP/$C_{18}EO_8$

Figure 4.30. Profiles of 5 µl water drops 10 s after application onto membranes O_PP and E_PP.

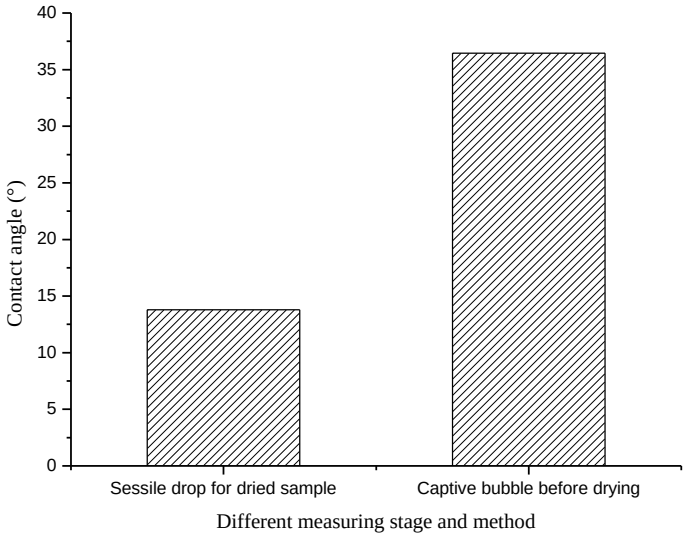

Figure 4.31. Different CAs of PP modified with 20 g/L $C_{18}EO_8$/1, 2-dichloroethane at room temperature for 20 h: captive bubble was from the 'swelling' sample before immersing into water; sessile drop was normal CA of water 20 min treated and then dried sample.

Inner pore property. Water fluxes as function of trans-membrane pressure are shown in Figure 4.32. A linear dependency was observed for both membranes. After modification, the water permeability evidently increased from 3500 to 9400 $L/h \cdot m^2 \cdot bar$, and the intercept of the curve with the x-axis was shifted from ~ 0.25 bar to 0 bar. Gas flow/liquid dewetting measurements (cf. Figure 4.23, where 1,1,2,3,3,3-hexafluoropropene with a surface tension of 16.0 dyn/cm had been used) were also done with the membrane pores wetted with water

(surface tension 72.8 dyn/cm; Figure 4.33). It was found that the pressure where the largest change of flux was observed (i.e., the pressure to dewet the largest fraction of barrier pores) was shifted by about 0.8 bar to lower values.

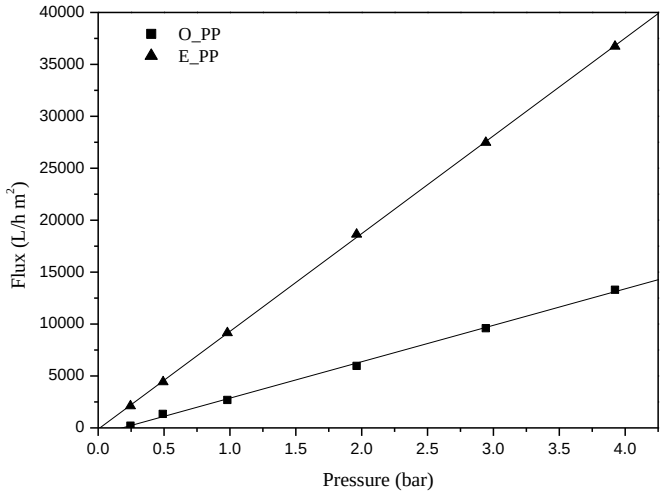

Figure 4.32. Water flux as function of trans-membrane pressure for membranes O_PP and E_PP/$C_{18}EO_8$.

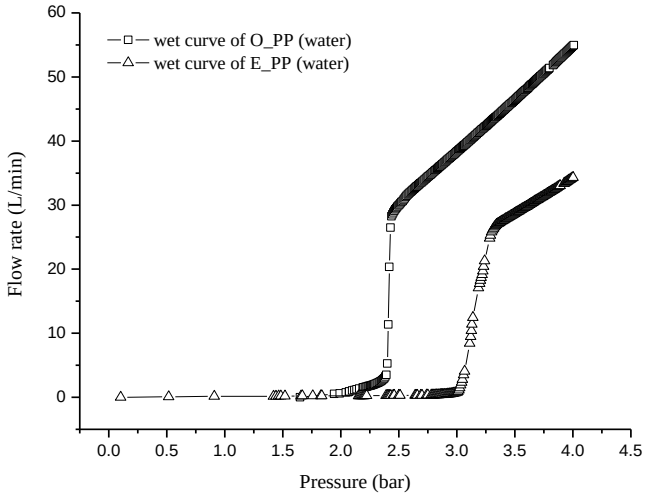

Figure 4.33. Gas flow due to pore dewetting for water filled membranes O_PP and E_PP/$C_{18}EO_8$.

Analysis of the modification of the inner membrane pore walls was further realized through trans-membrane streaming potential measurements (cf. Figure 4.34). The non-charged PP showed a negative zeta potential when the pH was higher than 3.9. This was because of

selective adsorption of ions from the neutral electrolyte solution: in the used electrolyte, anions have stronger tendency for adsorbing onto hydrophobic surfaces [151-153]. It could be anticipated that a neutral hydrophilic surface should have a lower adsorption tendency than the neutral hydrophobic surface. Indeed, we obtained the corresponding result that the absolute zeta potential value of membrane E PP, containing the non-ionic amphiphilic surfactant $C_{18}EO_8$, was significantly lower than that of the unmodified PP membrane.

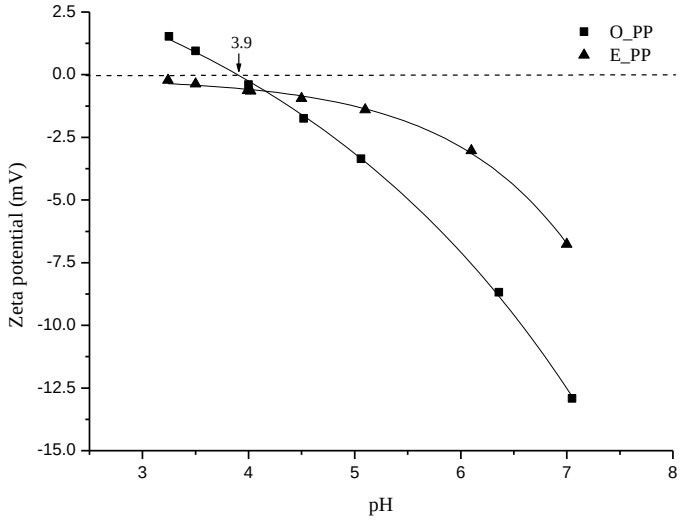

Figure 4.34. Trans-membrane zeta potential as function of pH for membranes O_PP and E_PP/$C_{18}EO_8$.

Protein adsorption and microfiltration of protein solution (fouling). Resistance to protein adsorption is another important parameter to be evaluated, and BSA was used as model protein. The aromatic azo dye Ponceau S was used to form a stoichiometric complex with adsorbed BSA; protein and dye were then eluted with concentrated sodium hydroxide solution, and the dye was quantified [154]. With this method, the amounts of adsorbed BSA from a solution with 1 g/L (pH 5) were 225 g/cm^2 for the original PP membrane, and only 60 g/cm^2 for the modified membrane (E_PP), both relative to outer membrane area. The data for the original membrane corresponds to 80 ng/cm^2, relative to the specific surface area; this is

somewhat lower than typical values for a BSA monolayer on planar substrates (100 ~ 200 ng/cm^2) [155], but this may be related to the porous membrane structure.

In applications for separation, fouling, especially irreversible fouling caused by protein adsorption and deposition, decreases the performance of membranes considerably. Microfiltration of a solution of BSA (0.1 ~ 1 g/L, pH 5) cum water elution at constant trans-membrane pressure was investigated (cf. Figure 4.35, Figure 7.3). First, the pure water flux was measured for 1 h; then BSA solution was filtered through the membrane until the flux became stable (after another hour); thereafter, PBS buffer flux and pure water were measured. The permeability of both original and modified membrane had a strong tendency to decrease during BSA filtration; then it increased during PBS filtration (pH 5), and it further increased during filtration of water (pH 6.5). This strong fouling had been caused by the high BSA concentration and the high initial flux. Consequently, the elution efficiency by just using buffer and water without back-flushing was relatively low. Nevertheless, distinct differences between membranes O_PP and E_PP could be still observed. Water permeability of E_PP was much higher than of O_PP (but lower than 9400 $L/h \cdot m^2 \cdot bar$ as deduced from data in Figure 4.32; for O_PP, the water permeability was influenced by the residual prewetting solvent, ethanol, therefore, the value was not exactly the same in each experiment). During BSA filtration, the initial permeability decrease for membrane E_PP was 15%, much lower than 54% for membrane O_PP, and it took much longer to reach the filtrate flux which was controlled by the fouling layer. In particular for the modified membrane, the initial filtrate flux was much beyond the typical range of critical or sustainable flux [156], leading to a very high fouling tendency. Also, it should be kept in mind that, due to the much higher initial flux, the mass of protein filtered through the modified membrane was much larger than for the unmodified one. The elution efficiency for membrane E_PP was significantly higher than for O_PP (cf. Table 4.8). And the SEM images revealed that, in contrast to the original PP

membrane, the protein cake layer was mostly removed from the outer surface of the modified PP membrane (cf. Figure 4.36b). In conclusion, the improvements seen for membrane E_PP relative to original PP were due to the increased hydrophilicity (high surface energy) after the entrapment modification.

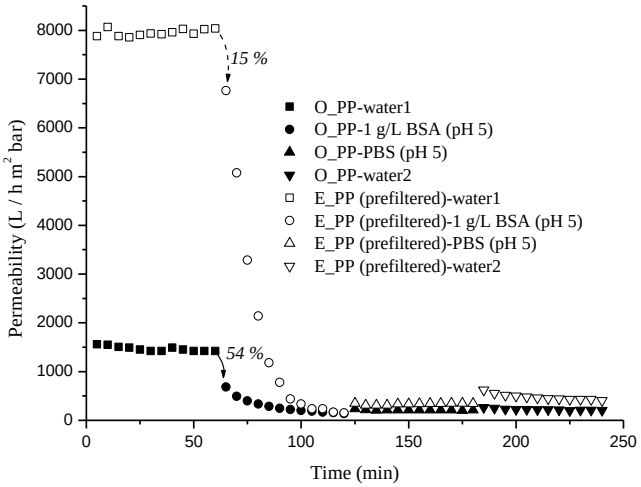

Figure 4.35. Subsequent measurements of fluxes for water, for 1 g/L BSA solution (pH = 5), for buffer (PBS, pH 5) and again for water, through original (O_PP) and modified membranes (E_PP/$C_{18}EO_8$), at a constant transmembrane pressure (1 bar), respectively.

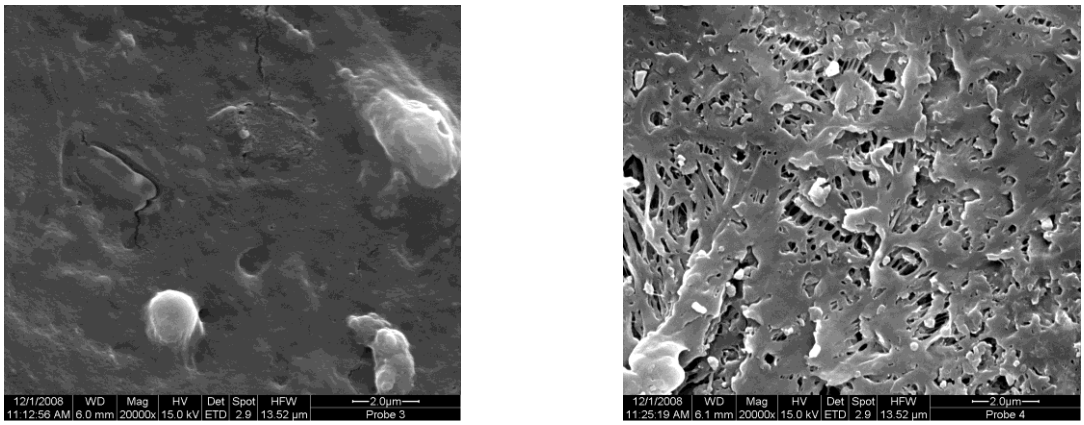

a. O_PP + 1 g/L BSA (pH 5)

b. E_PP/$C_{18}EO_8$ + 1 g/L BSA (pH 5)

Figure 4.36. Cake layer morphology for original and modified PP membranes after microfiltration of a 1 g/L BSA solution (pH 5) followed by measurement of buffer (PBS, pH 5) and water flux (cf. Figure 35).

Table 4.8. Final permeability values for water, 1 g/L BSA solution (pH 5) and PBS solution (pH 5) during microfiltration at 1 bar, relative water flux recovery after BSA microfiltration by filtration with water and PBS buffer, and filtered BSA amounts in 1 h, for original (O_PP) and $C_{18}EO_8$–modified (E_PP) PP membranes, soaked in water for 0, 4 and 8 weeks[1].

	Permeability, L/h·m^2·bar				Relative flux recovery[3]	Filtered BSA amount (g/h)
	Water 1[2]	Final BSA Solution	PBS buffer (pH 5)	Water 2[2]		
O_PP	1420	139	200	207	1.5	90
E_PP (prefiltered)	7951	155	347	434	2.8	533
E_PP (4 weeks)	7114	123	172	220	1.8	503
E_PP (8 weeks)	6408	182	269	348	1.9	404

1: data from experiments shown in Figures 8 and 13; 2: "water 1" and "water 2" represent the water flux before and after microfiltration of a 1 g/L BSA solution (pH 5), respectively; 3: the relative flux recovery was calculated from the ratio of final water flux ("water 2") and final BSA solution flux.

Stability study. E_ PP membranes measured by water permeability at 1.0 kPa/cm^2 for 2 h were utilized for stability study. Thereafter they had then been soaked in water at room temperature for up to 8 weeks. In general, with prolonging soaking time for up to 8 weeks, the gravimetrically determined weight gain (compared with O_PP) decreased (Figure 4.37), the contact angle increased (Figure 4.38), the ether peak of the modifier in the IR spectra became much weaker (Figure 4.39), and the antifouling capacity declined (Figure 4.40). However, the weight gain due to modification became constant after 7 ~ 8 weeks immersion in water (cf. Figure 4.37). Consequently, the water drop was still slowly spreading with time on the modified membrane after 8 weeks in water, while the slight change for membrane O_PP was only from a decrease of the volume due to evaporation from the drop (cf. Figure 4.38). In addition, water permeability was much higher than of O_PP, and protein fouling effects were lower than for O_PP (cf. Figure 4.40, Table 4.8).

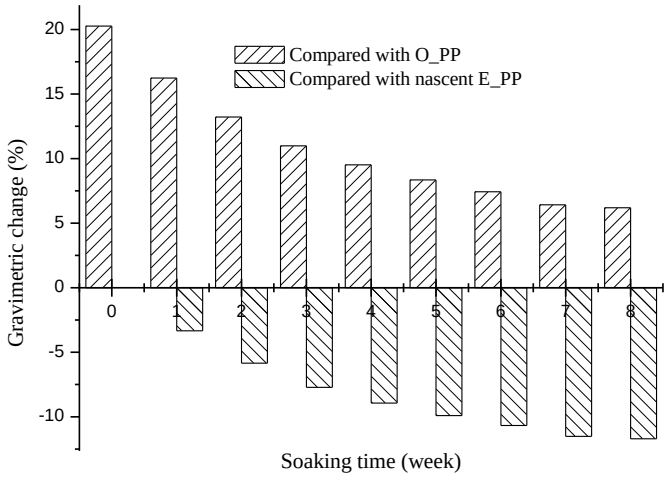

Figure 4.37. Gravimetric change with soaking time in water at room temperature for $C_{18}EO_8$-modified PP membrane (E_PP).

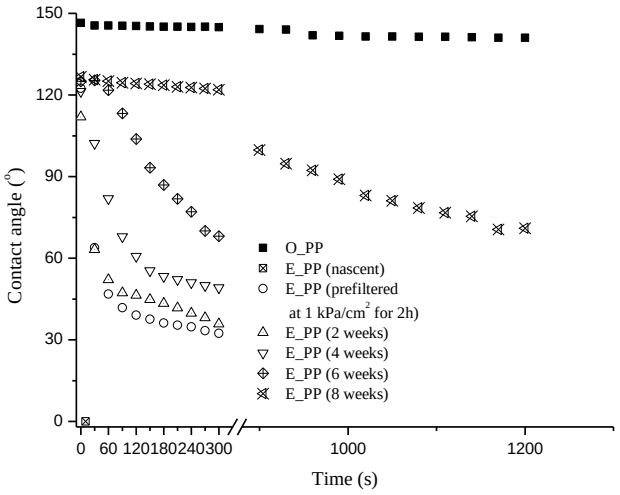

Figure 4.38. Time dependence of water contact angle for original (O_PP) and a series of $C_{18}EO_8$-modified membranes (E_PP) after various times of soaking in water at room temperature.

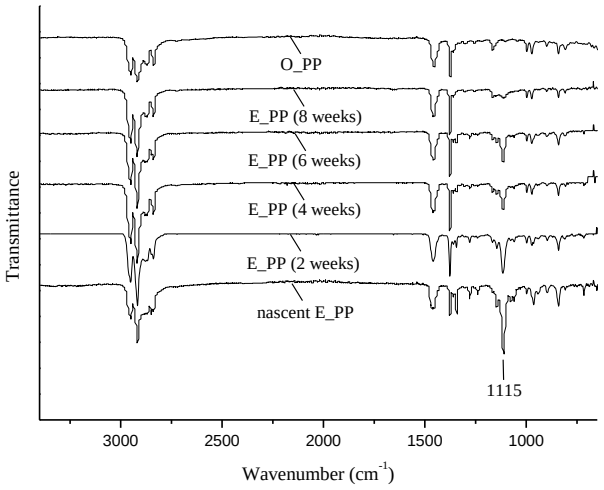

Figure 4.39. IR spectra for original (O_PP) and $C_{18}EO_8$-modified membranes (E_PP) after various times of soaking in water at room temperature.

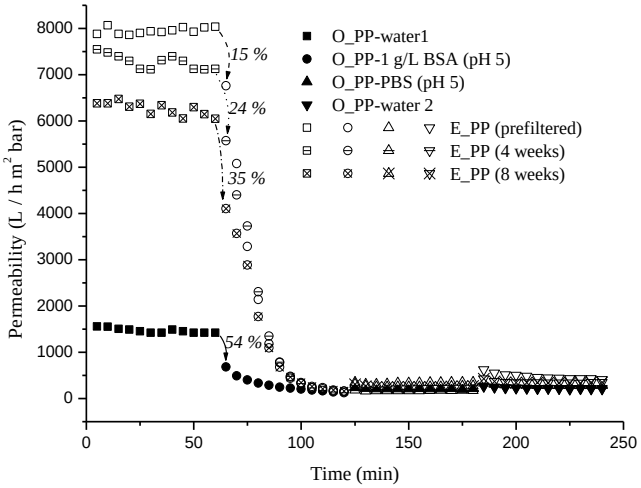

Figure 4.40. Subsequent measurements of fluxes for water, for a 1 g/L BSA solution (pH = 5), for buffer (PBS, pH 5) and again for water, at a constant transmembrane pressure (1 bar), through original (O_PP) and a series of $C_{18}EO_8$-modified membranes (E_PP), soaked in water at room temperature for 0, 4 and 8 weeks.

4.3. Entrapment of PNIPAAm-based macromoleclues into PP membrane and plate surface

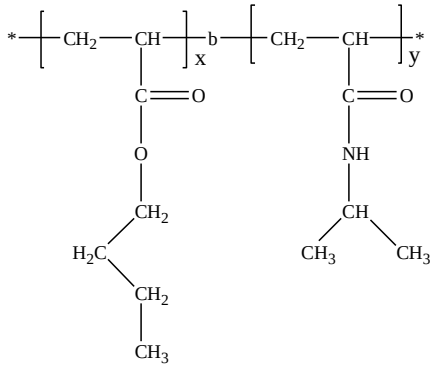

Scheme 4.2. Chemical structure of PBA-*b*-PNIPAAm.

4.3.1. PP MF membrane modified with entrapment of PNIPAAm-based macromolesules

Homopolymer PNIPAAm (hP) and two block copolymers PBA-*b*-PNIPAAm with different block ratio (cP1 and cP2) have been used as modifier species. Five solvents were selected as good solvents for PP with respect to their low polarity and solubility parameters (see Table 4.9). It should be noticed that PP solubility parameter values are different - in the range of 7.90 ~ 9.40 $(cal \cdot cm^{-3})^{1/2}$ or 16.60 ~ 19.90 $(MPa)^{1/2}$ - in different reports [157,158], which could be related to different molecular weights and crystalline contents, as confirmed by experiments [73]. In Table 4.9, the absolute difference between solvent and PP was calculated from 9.20 $(cal \cdot cm^{-3})^{1/2}$ or 18.80 $(MPa)^{1/2}$ for PP [159]. The target concentrations of modifier in the solvents were from 10 g/L to 25 g/L, according to previous experience with entrapment modification (Section 4.2). The effects of conditions (cf. Table 3.1) on modification efficiency have been evaluated based on contact angle characterizations. Because the CA of PNIPAAm-containing modified membrane surfaces showed time dependency, all the CA in this section were recorded at 60 s.

Table 4.9. Hansen solubility parameters of selected solvents and polypropylene at 25 °C.

	δ	δ *(SI)*	$\lvert\delta_{PP} - \delta_{solvent}\rvert$	
	$\sqrt{cal \cdot cm^{-3}}$	$\sqrt{MPa}$	$\sqrt{cal \cdot cm^{-3}}$	$\sqrt{MPa}$
PP	9.20 (7.90 ~9.40)	18.80 (16.60~19.00)		
1,2-dichloroethane	9.80	18.20	0.60	0.60
Chloroform	9.21	18.70	0.01	0.10
Carbon tetrachloride	8.65	18.00	0.55	0.80
Tetrahydrofuran (THF)	9.52	19.40	0.32	0.60
Benzene	9.15	18.70	0.05	0.10

SI: standard international unit; conversion is by δ ($MPa^{1/2}$) = 2.0455 δ ($cal^{1/2}$ $cm^{-3/2}$)

At a fixed modification temperature of 20 °C, PP membrane samples were immersed into solution of cP1 (20 g/L) for 20 h, then immersed into water for 20 min, and finally dried. The effect of different solvents on resulting contact angle is shown in Figure 4.41. It was found that after entrapment treatment, all sample surfaces showed much smaller CA than O_PP. Benzene and THF solution treated sample surfaces showed lowest CA. However, it was also found that in such high concentration, not all solvents can dissolvent cP1 completely, as shown in Table 4.10. Consequently, the modifications with solutions in 1,2-dichloroethane, carbontetrachloride and benzene had not good repeatability. In comparison, modifier solution in THF was much more reliable due to well repetitive property. Moreover, THF is the solvent which can entirely dissolve all homo- and block copolymers. In addition, $|\delta_{PP} - \delta_{THF}|$ is 0.60, this value confirms that THF should possess good swelling ability for PP. Therefore, THF has been selected as the best suited solvent.

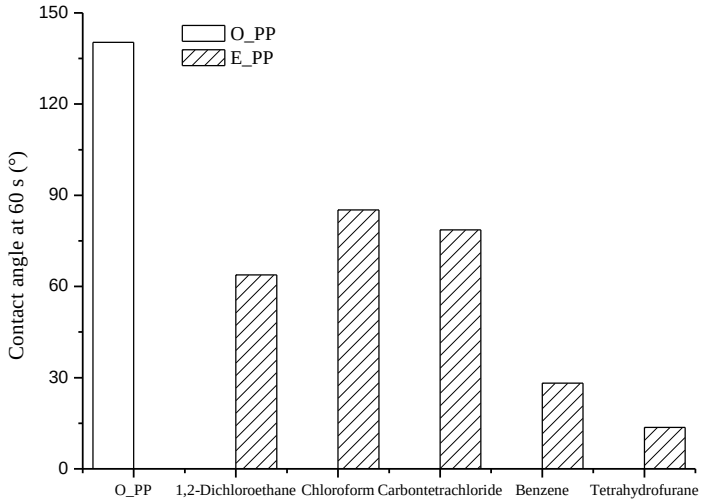

Figure 4.41. Effect of solvent on surface wettability (20 °C, cP1, 20 g/L for 16 h, water 20 min, then dry).

Table 4.10. Solubility table of modifiers in some organic solvents.

	1,2-dichloroethane	Chloroform	Carbontetrachloride	Benzene	THF
hP	-	+	-	-	+
cP1	-	+	-	-	+
cP2	+	+	-	+	+

Note: + soluble / - insoluble of polymer in solvent

Figure 4.42 compares the two parameters, modifier structure and deswelling way, under the conditions of 20 °C and 20 g/L solution in THF. The two types of deswelling treatment processes yielded much different results. After directly drying in vacuum, the CA for E_PP/hP was lower than for E_PP/cP1, and E_PP/cP2 membranes were still hydrophobic. In comparison, after 20 min water treatment, both hP- or cP1-modified E_PP showed very good hydrophilicity (~ 15°), while E_PP/cP2 still showed hydrophobicity (> 100°). M_w of homopolymer hP was 37.8 kg/mol. $M_{wPNIPAAm}$ of copolymer cP1 was 23.5 kg/mol and $M_{wPNIPAAm}$ of cP2 was 13.2 kg/mol, and cP2 had a much lower PNIPAAm content than cP1. Therefore, low modification efficiency for E_PP/cP2 might be due to its long hydrophobic

PBA block and the not well balanced hydrophilic/hydrophobic structure. Nevertheless, the similar CA values for E_PP/hP and E_PP/cP1 after treatment with water indicated that the hydrophilic chain length is probably not the dominant reason to influence surface wettability. The details of surface configuration status with hP or cPs influenced by dry or water treatment will be discussed in Chapter 5.

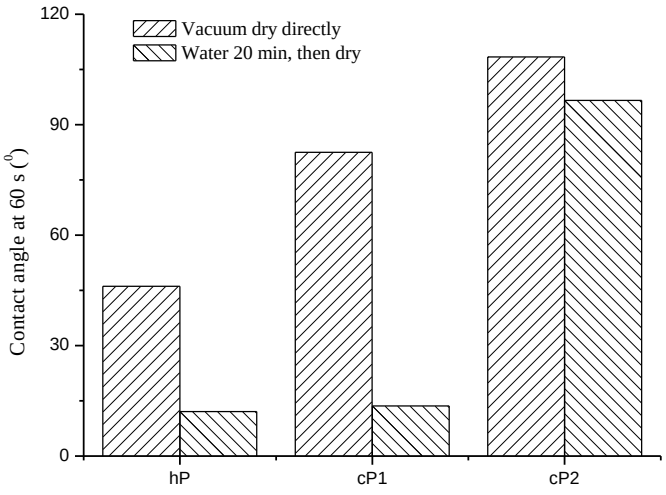

Figure 4.42. Effect of modifier and deswelling way (20 °C, THF, 20 g/L, 20 h).

Finally, under the condition selected above (cP1/THF and exposure to water for 20 min), the influences of modifier concentration and temperature have been studied (see Figure 4.43). As anticipated, the higher the concentration had been, the lower was the contact angle. 20 g/L was high enough to improve surface hydrophilicity significantly. The modification temperature of 20 °C was better suited than 40 °C to achieve pronounced hydrophilicity, although PP should swell more at higher temperature.

Overall, 20 °C, 20 g/L cP1/THF for 20 h and exposed into water 20 min before dry were selected to be the optimize conditions for PP membrane surface modification. The following comprehensive study will focus on E_PP modified under such conditions.

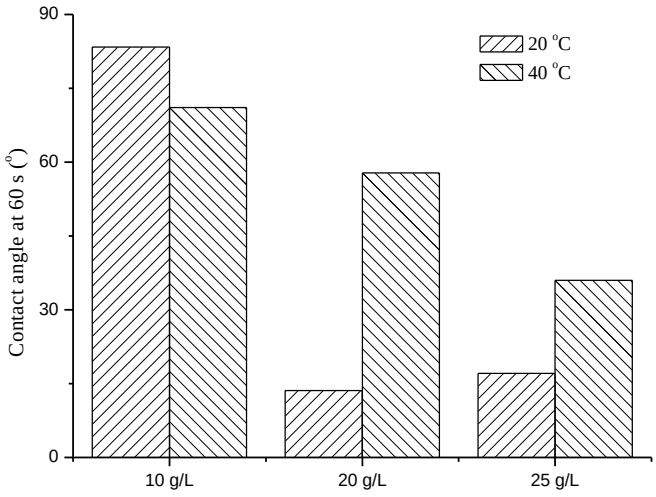

Figure 4.43. Effect of temperature and concentration on surface wettability (cP1, THF, 20 h, water 20 min, and then dry).

4.3.2. Structure and thermo-responsive study of PBA-*b*-PNIPAAm modified PP membrane

4.3.2.1. Effect of solvent and PBA-b-PNIPAAm on pore size distribution

Effects of THF and modification with cP1 according to Section 4.3.1 on PP membrane pore structure have been investigated initially. Figure 4.4 shows the pore size distributions in dry state of unmodified PP (O_PP), only solvent treated PP (S_PP) and cP1 modified PP (E_PP/cP1), which were determined by porosimetry. It can be seen that the solvent treated PP had the same average pore diameter as O_PP, while for modified PP, the average pore diameter reduced by about 10 ~ 40 nm and the pore size distribution became much broader. In the study of entrapment modifications with $C_{18}EO_8$ (M_w less than 1000 g/mol), the shift had been similar but the distribution remained sharp; the data had been related to a significant contribution of deposition to the pore wall (see Section 4.2.3, Section 5.1.2.2). Considering

the much larger size of the coil (collapsed in dry state) of the high molecular weight modifier cP1 used in this study, the observed changes might be due to surface-anchored macromolecular aggregates of cP1 rather than due to deposition of a polymer layer on the membrane pore walls.

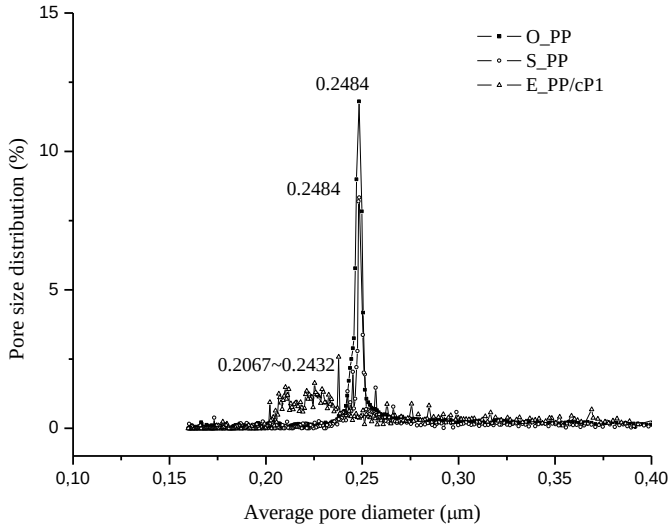

Figure 4.44. Pore size distribution from gas flow/wetting fluid displacement for various PP membranes (O_PP: original PP; S_PP: PP treated with THF at room temperature for 20 h; E_PP/cP1: PBA-*b*-PNIPAAm modified PP obtained with solution of 20 g/L cP1 in THF at room temperature for 20 h followed by immersion in water and drying).

4.3.2.2. Membrane surface properties

Membrane surface properties have been characterized by IR spectroscopy and static water contact angle. Figure 4.45 shows the FTIR spectrum of unmodified and modified PP membranes. Compared with O_PP, the characteristic peaks of PBA-*b*-PNIPAAm were identified at 1254, 1540 and 1650 cm^{-1} from E_PP spectrum, which were assigned to the methyl group in $CH(CH_3)_2$, amide II, amide I, respectively [160]. In addition, the peak around 3342 cm^{-1} was the stretching vibration of –NH from PNIPAAm, and the absorption at 1734 cm^{-1} was from C=O stretching vibration due to the ester group of the PBA block [161].

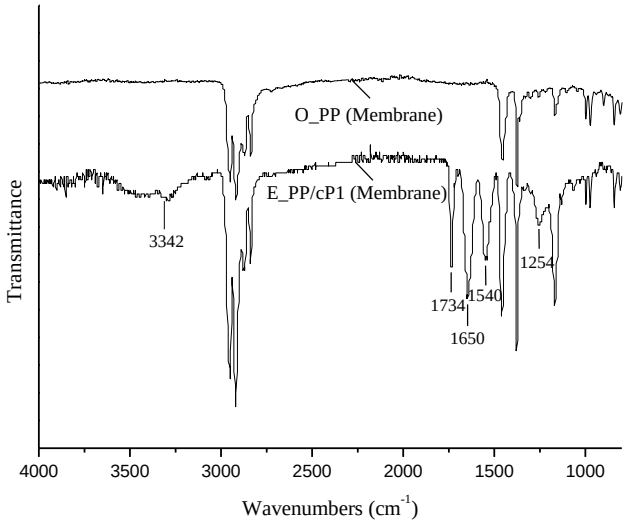

Figure 4.45. IR spectra of original and modified PP membranes.

With respect to the surface properties after modification, static water contact angle as a function of measuring time has been measured. As shown in Figure 4.46, the sessile drop water contact angle of modified PP had a sharp decrease with time and the water spread out completely within 1 min. In contrast, water contact angle of O_PP surface was relative stable even after prolonging the measuring time to the third minute. The combination of contributions of the roughness of membrane surface [162] might be possible reasons for such effect. However for the modified membrane of E_PP/cP1, it was observed that in a few minutes, the membrane area in contact with the water drop became almost transparent because the water spread out and penetrated into the membrane pores. Therefore, it is quite sure that this time-dependent wetting is dominated by a hydrophilic pore surface (cf. Section 4.2.2).

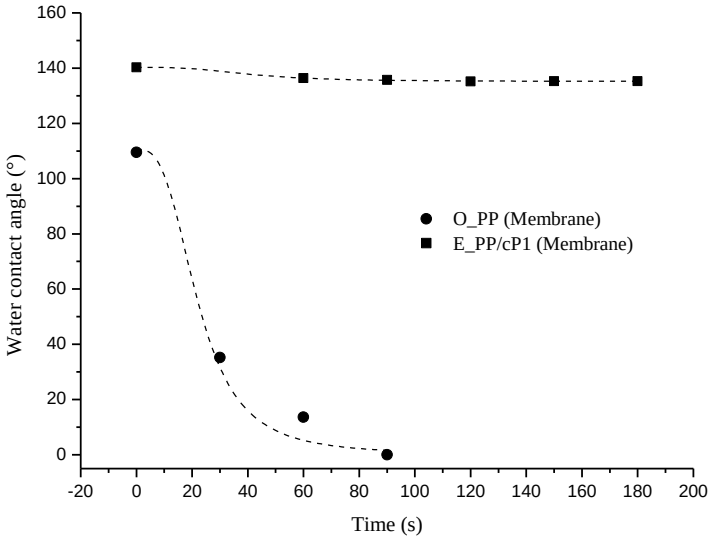

Figure 4.46. Time-dependent water contact angle of original and modified PP membranes at room temperature.

4.3.2.3. Thermo-responsive property of outer and inner surfaces of modified PP membranes

Thermo-responsive CA of E_PP/cP1 surface was evaluated via controlling water temperature under air captive bubble measurement mode (Figure 4.47). The captive bubble CA of E_PP was relative stable with measuring time compared with water sessile drop result. The slight increase with time might due to the penetrating of bubble into water existed into membrane pores, or the small crack in between water and membrane pores. More importantly, the air captive bubble contact angles at 20 °C were smaller than those at 40 °C, and the angle difference was more than 10°. This result implied that the PP membrane surface underwent a wettability change to be less hydrophilic with increasing temperature to 40 °C, which was higher than LCST of PNIPAAm.

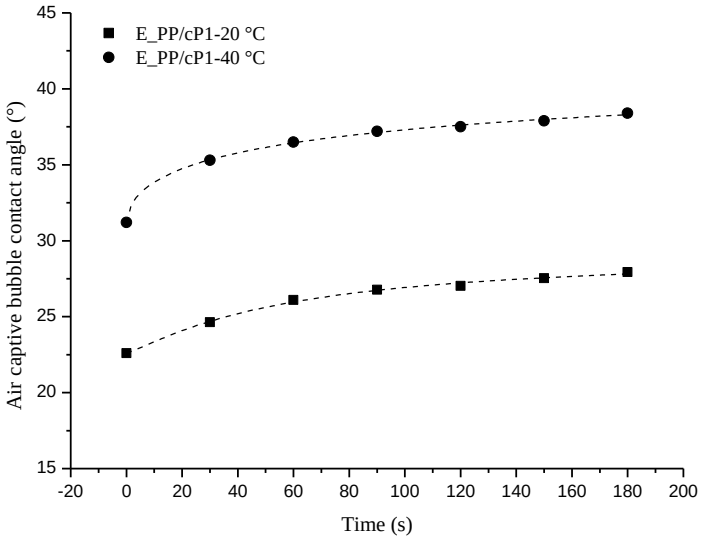

Figure 4.47. Time-dependent air-captive bubble contact angle in water of modified PP membrane at 20 °C and 40 °C, respectively.

Figure 4.48 shows the water permeability as a function of temperature. It can be seen that the water permeability of both unmodified and modified PP membranes increased with temperature, this apparent increase could be explained by Darcy's Law in pressure-driven membrane operations [163,164]. The viscosity decreases with temperature, that means, the water flux would increase with temperature, as verified by Figure 4.48. However, compared with the continuously increasing tendency for unmodified PP, the water permeability of modified PP increased discontinuously due to an abrupt increase at 31 ~ 32 °C and changed slope of the curve beyond that temperature. Water permeability of modified PP increased with temperature as 165 (L/h·m^2·bar)/K in the temperature range below 31 °C. This was much larger than the increase of 88 (L/h·m^2·bar)/K for original PP. When the temperatures were above 32 °C, the water permeability of modified PP increased with temperature as 135 (L/h·m^2·bar)/K. The differences implied first that the modified PP pore surface had a better wettability than PP, as already confirmed by contact angle and wetting data (cf. Section 4.3.2.2). It had been found and discussed before, that the wetting of submicrometer-size pores

by water has also an influence of water flux under otherwise identical conditions [165,166]. Second, above LCST, the wettability seemed to have been reduced, and this is also in line with contact angle and wetting data (cf. 4.3.2.2). More information can be deduced from this figure; the absolute water permeability of the modified membrane was smaller than for original PP but at 30 °C (below LCST) the values were already almost identical; but the permeabilities were significantly higher when temperature was over 32 °C. The cP chain configuration state as a function of temperature (around LCST) and the effect on surface wettability and water permeability will be discussed in Chapter 5.

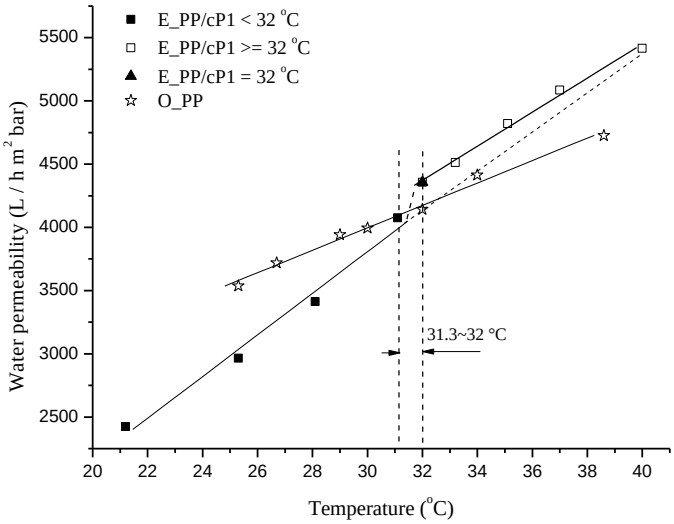

Figure 4.48. Temperature-dependent water permeability of original and modified PP membranes from 20 °C to 40 °C.

Figure 4.49 shows a variation of trans-membrane zeta potential with temperature of unmodified and modified PP membranes. It was observed that the relative zeta potential became more positive after modification; however, the change of relative zeta potential with temperature was not very obvious for both membrane samples. Especially for unmodified PP membrane, the relative trans-membrane zeta potential decreased initially from 23 °C to 27 °C, and then kept almost stable.

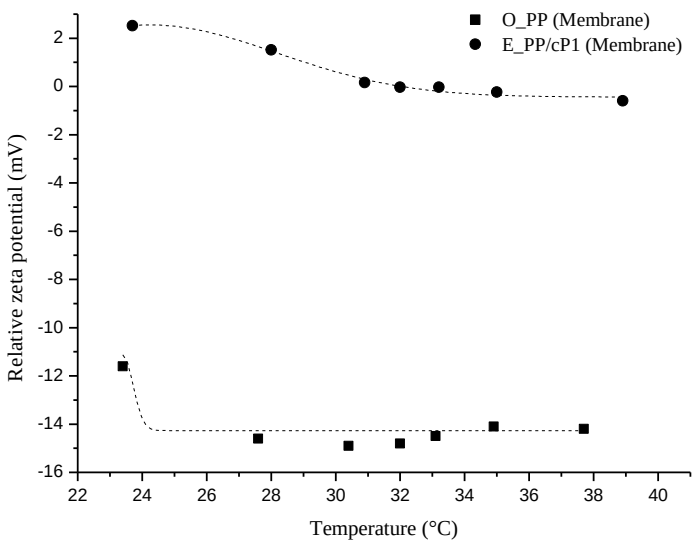

Figure 4.49. Temperature-dependent relative trans-membrane zeta potential of original and modified PP membranes (pH 5.65 ~ 5.85).

Moreover, the hydration/dehydration transition property of PNIPAAm is interesting for separation. Hence the effect of this transition on protein binding/release as a function of temperature has been studied here. The final stable water permeability of virgin and BSA adsorbed modified PP membranes at 25 °C and 40 °C has been measured respectively, data are shown in Figure 4.50. After protein adsorption, first water permeability at 40 °C had decreased. At the temperature below LCST (25 °C), water permeability was still lower than for the virgin membrane, but the flux recovery increased to 98%; thereafter, in the second measurement at 40 °C, water permeability had slightly increased compared with the first value after adsorption, the corresponding water flux recovery increased from initial 94% to 97%.

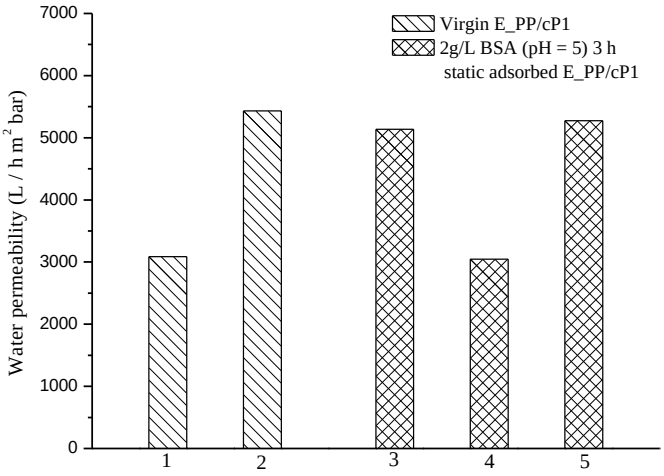

Figure 4.50. Water permeability of PBA-*b*-PNIPAAm modified PP membrane (EPP/cP1) in virgin state (columns 1 and 2) and after static adsorption of BSA (2 g/L; pH = 5, 3 h) (columns 3 ~ 5) measured subsequently at two temperatures around LCST: 1. 25.5 °C; 2. 40 °C; 3. 40 °C; 4. 25.5 °C; 5. 40 °C.

4.3.3. Modification of non-porous plates by entrapment of PBA-*b*-PNIPAAm (cP1)

Entrapment of cP1 into non-porous PP plates surface have been performed with the analogous process as Section 4.3.2. Physical parameters of thickness, density and gravimetry have been measured for estimating the effect of modification condition on self-made PP plates, and the correlated information can be seen in Figure 4.51. It was found that the thickness and density (Figure 4.51a & b) of E_PP/cP1 (Plate) plates almost remained as O_PP, but the average thickness of modified sample was slightly decreased to 0.0194 ± 0.0086 cm, so that the average density increased to 820.6 ± 49.6 mg/cm^3. In accordance to these results, Figure 4.51c shows the gravimetric decrease after modification, even when the PP surface could present modified polymers (deduced from Figure 4.52 ~ 54), and the average decrease degree was in the range of -2.3 ± 1.5 %.

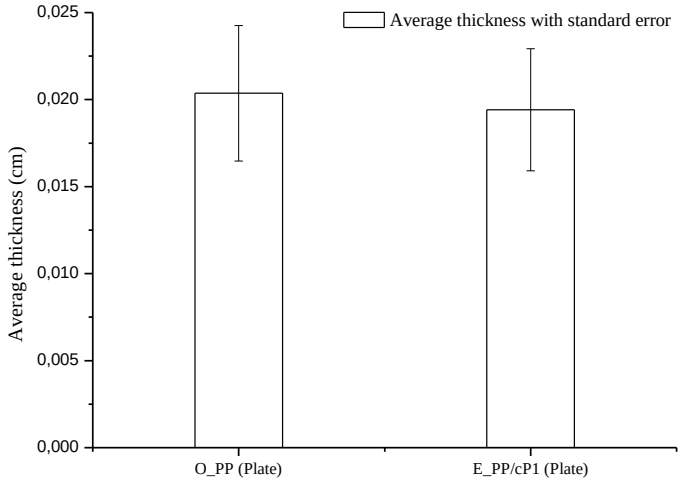

a).

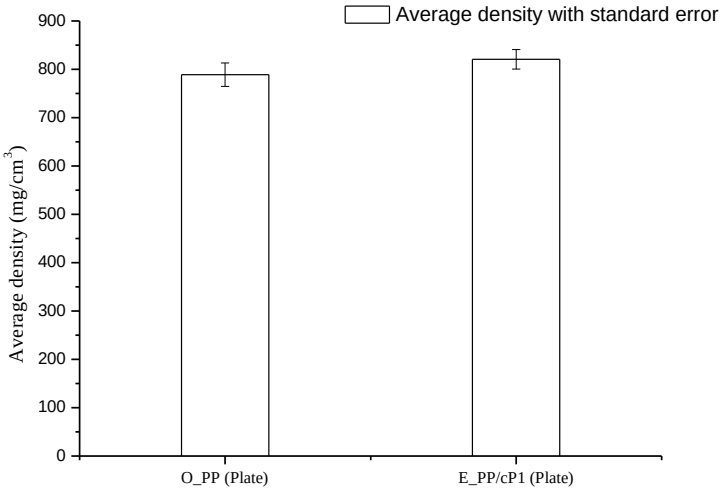

b).

Figure 4.51. Physical parameters of self-made original and modified PP plates: a) thickness; b) density.

The surface properties have been studied by IR (Figure 4.52) and time-dependent water sessile drop at room temperature (Figure 4.53). IR spectrum of modified PP plate surface was similar to data for modified PP membrane in Figure 4.45, which confirmed the existence of PBA-*b*-PNIPAAm in PP surface. Similar with the results for PP membrane surface modification, the water contact angle showed also significant time-dependence, the values strongly decreased in the initial 60 s by about 30 ~ 40°. Thereafter, the much slower further

decrease of water contact angle had been mainly caused by the volume decrease when water from the drop evaporated gradually. The average water contact angle at 60 s was 38.8 ± 11.0°, which is much smaller than that of unmodified surface (98.6 ± 14.0°) (cf. Figure 4.53).

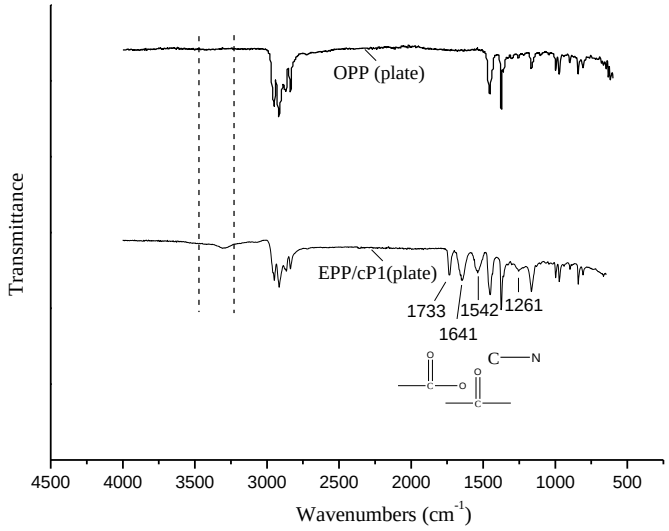

Figure 4.52. IR spectra of original and a series of modified PP plates.

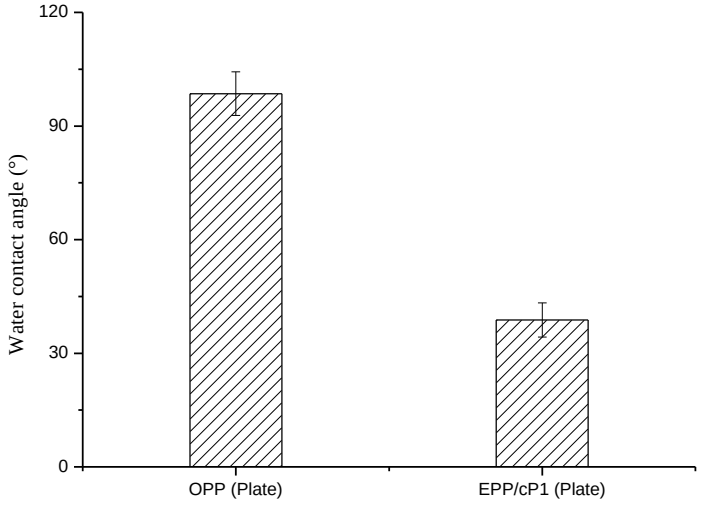

Figure 4.53. Time-dependent water contact angle of unmodified and modified PP plates.

Comparing with trans-membrane zeta potential of modified PP membrane, outer surface zeta potential for modified PP plate showed more obvious difference around LCST of PNIPAAm. As shown in Figure 4.54, modified PP surface was much less negative compared with unmodified PP, and the relative zeta potential decreased with temperature from 30 °C. As a

function of temperature, the absolute zeta potential of unmodified PP decreased 0.9 mV from 30 °C to 40 °C, but the general decrease tendency was not very regular; while for modified plate, it was clear to see an obvious decrease of outer surface zeta potential at 30.3 °C, which decreased 1.1 mV in the temperature range of 30.3 ~ 34.1 °C, and successively decreased but only 0.4 mV when the temperature was increased to 40 °C. Therefore, the abrupt change of zeta potential around LCST confirmed the existence of PBA-*b*-PNIPAAm on membrane surface.

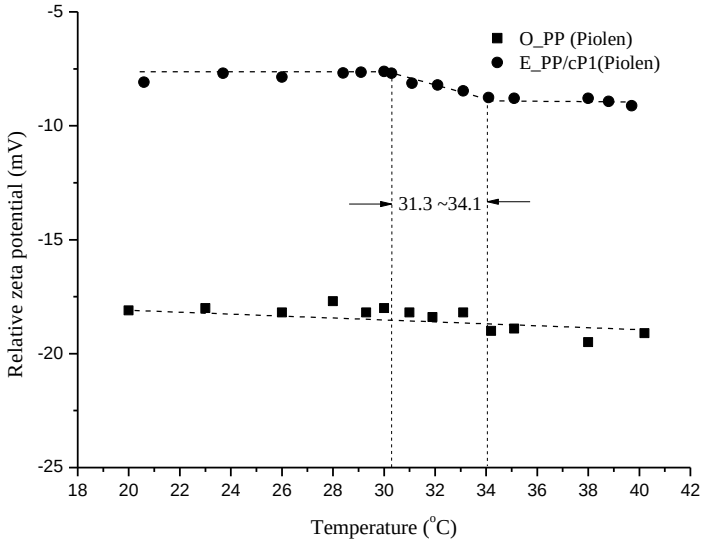

Figure 4.54. Temperature-dependent relative outer surface zeta potential of original and modified PP plates (pH 5.97 ~ 6.10).

4.4. Entrapment of nonionic and cationic macromolecules into PP membrane and film surface

4.4.1. Entrapment of small amphiphilic molecules into Celgard PP membrane and film surface

As described in section 4.2, it was confirmed that 25 g/L $C_{18}EO_8$ or $C_{18}EO_8C_{18}$/1,2-dichloroethane solution, 20 h swelling/embedment time at 20 °C, and incubated into water for 20 min before vacuum dry was the best suited condition to acquire well hydrophilic surface. Same condition was applied into Celgard PP membrane (Celgard 2500) and film (FS 2500). Contact angles of three different E_PPs have been compared in Figure 4.55. On one hand, it was found that $C_{18}EO_8$ modified surface showed the lowest CA. On the other hand, it was noticed that both PP membrane surfaces obtained better wettability than unmodified PP, while this modification condition for Membrana PP membrane had been much more efficient than for Celgard PP membrane. However, Celgard PP film, which was produced from the same material used for Celgard PP membrane, did not show the same improvement of wettability like Celgard PP membrane.

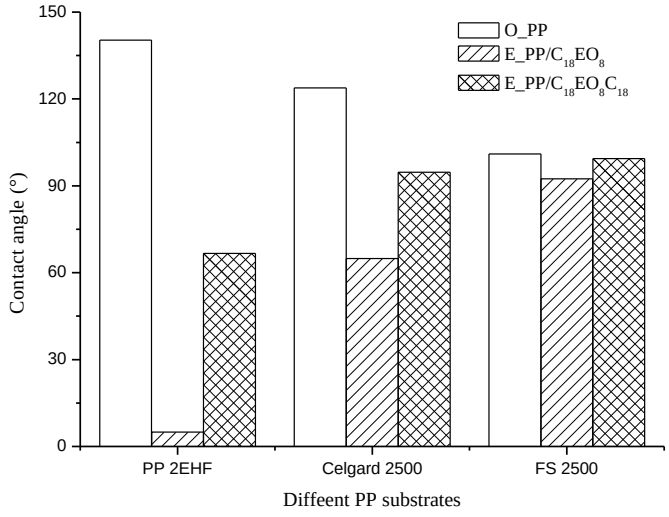

Figure 4.55. Contact angle of different PP substrates modified with same condition: room temperature, 25 g/L $C_{18}EO_8$ or $C_{18}EO_8C_{18}$ /1,2-dichloroethane for 20 h, then immersed into water for 20 min, vacuum dry.

The worst modification efficiency for Celgard PP film might be because of the weak swelling degree of PP film in 1,2-dichloroethane. Therefore, some other solvents, such as carbon tetrachloride, xylene and tetraline have been tested as good solvent for PP film, and the

relationship between swelling degree of PP film in these solvents and temperature as well as incubating time have been tested respectively(see Table 4.11 and Figure 4.56).

The weight increase/decrease during swelling/deswelling states of membrane has been measured respectively. As shown in Table 4.11, the weight increased after swelling, this might due to the existing of solvent in swelling region of PP film and possible residual absorbed solvent on film surface. Supposing the weight increase was only from the solvent in swelling region, the volume of such solvent was calculated to avoid the effect of solvent density on gravimetric change. Therein, tetraline treated PP showed the largest volume increase, and these values increased with swelling temperature. However, the dried samples generally showed weight decrease. The gravimetric change in the range of ± 0.3% could be caused by measuring error (ca. ± 0.04 g), while such big decrease (> 0.5 %) shown in Table 4.11 implied a possible leaching of residual solvent or amorphous part of polymer into organic solvent from Celgard PP film. To sum up, tetraline at 40 °C seemed most efficient for swelling PP film compared with 1,2-dichloroethane and other solvents.

Table 4.11. Swelling capacity of solvent on Celgard PP film at different temperature for 6 h.

	Carbon tetrachloride		1,2-Dichloroethane		O-xylene		Tetraline	
	20 °C	40 °C	20 °C	40 °C	20 °C	40 °C	20 °C	40 °C
Gravimetric change of swollen PP, %	4.50	3.80	0.85	0.23	1.12	1.22	5.10	8.21
Nominal data to PP volume, $*10^{-3}$ cm^3	0.38	0.31	0.088	0.024	0.22	0.24	0.66	1.10
Gravimetric change of deswollen PP, %	-0.75	-1.23	0.00	-0.62	-0.67	-0.99	-0.56	-1.15

PP films were then incubated into tetraline from 1 ~ 344 hours under 20 °C and 40 °C respectively, the final swelling degree was evaluated from gravimetric change (see Figure 4.56). Generally speaking, the longer swelling time and higher temperature were, the more

swelling degree and possible damage had the film. For instance, "40 °C_25 g/L $C_{18}EO_8C_{18}$/tetraline_6h" modified PP showed better surface hydrophilicity than "20 °C_25 g/L $C_{18}EO_8C_{18}$/tetraline_20h" modified PP film (CA = 93°, hydrophobic). In addition, carbon tetrachloride might be used to be the good solvent for PP film considering its large gravimetric decrease (cf. Table 4.11), but the surface wettability had not obvious improvement after modified in 25 g/L $C_{18}EO_8C_{18}$/carbon tetrachloride (cf. Figure 4.57).

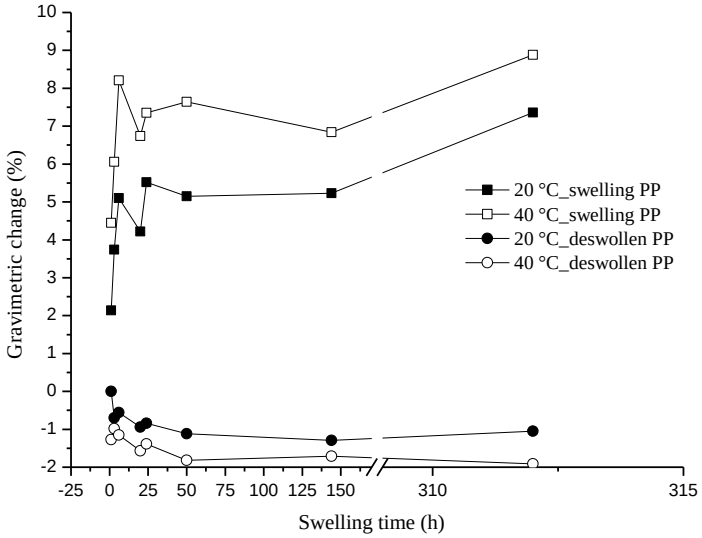

Figure 4.56. Effect of swelling time and temperature of tetraline on PP film swelling capacity of tetraline on PP film from gravimetric change (%).

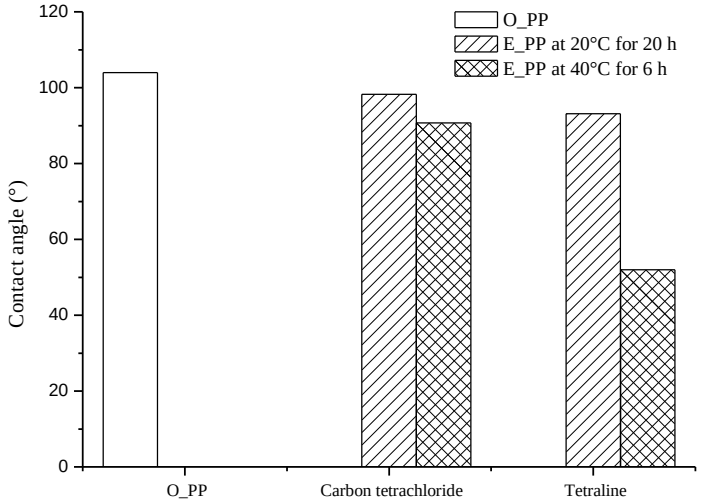

Figure 4.57. Effect of both swelling temperature and time on modification efficiency of PP film (FS 2500) surface (25 g/L $C_{18}EO_8C_{18}$ solution, water 20 min under 40 °C).

4.4.2. Entrapment of cationic amphiphilic macromolecules into Celgard PP film surface

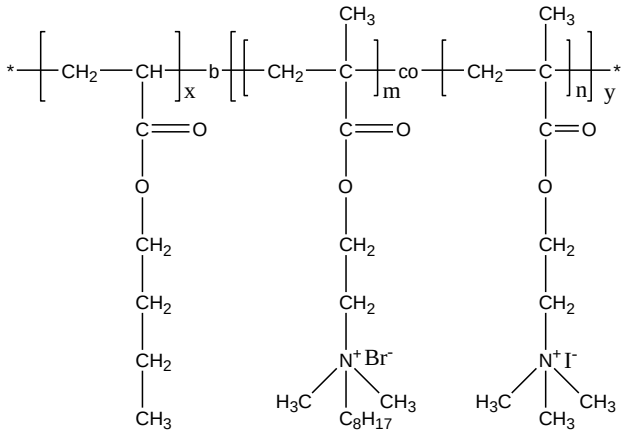

Scheme 4.3. Chemical structure of PBA-*b*-P*q*DMAEMA.

Solvent selection for PBA-*b*-P*q*DMAEMA is strictly limited by the quaternized part, which is composed of alkylated methyl and octyl group onto the tertiary nitrogen of DMAEMA. PBA-*b*-P*q*DMAEMA cannot be dissolved by neither water nor tetraline. Therefore, the modification condition for PP film surface modification, as concluded from section 4.4.1, is not suitable in this case. It was considered to adopt mutual solvent for preparing modifier solution. Different components in mutual solvent should be good solvent for both modifier and PP films, and they should be miscible each other. One component for swelling PP film has been searched firstly. As confirmed in the section 4.4.1, high temperature is effective to increase swelling degree. Meanwhile, the temperature should not be too high to avoid dissolving PP films. The dissolution temperatures of PP films in some organic solvents should be taken into account (see Table 4.12), and some literatures showed o-xylene can also dissolve PP at around 120 °C rather than p-xylene [167]. Considering the influence of solubility parameter and high boiling point of a solvent on swelling, a nonpolar o-xylene was preferred as good solvent for PP film rather than p-xylene. The other solvent component for dissolving PBA-*b*-P*q*DMAEMA was mainly up to the solubility of methyl and octyl groups

of quarternized parts. Hence, some alcohols such as ethanol, isopropanol and 1-propanol could be the alternatives. Mutual solvent with these two or more components containing o-xylene and alcohols solvent have been prepared. The influence of different components and mixture ratios of mutual solvents on swelling of PP film, solubility of PBA-*b*-P*q*DMAEMA and boiling point are generally listed in Table 4.13.

The boiling points of mutual solvents were tested firstly, and the results and phenomena are shown in Table 4.13. It was found that the temperatures were always not stable and tended to increase 5 ~ 10 °C during adding PP film, when the second component (i.e. ethanol, cyclohexane/ethanol) had lower boiling temperature than the heating temperature. By contrast, the boiling temperature of mutual solvents was relative stable when the second component was isopropanol or 1-propanol, which has the higher boiling points than ethanol and cyclohexane/ethanol. However, it was still observed that the boiling point increased with o-xylene ratio. The appearance (e.g. soft) of PP film treated by these two types of mutual solvents confirmed that the o-xylene/1-propanol was stronger than o-xylene/isopropanol when compared with same volume ratio. Finally, o-xylene/1-propanol mixture was selected as good solvent for modification. Moreover, o-xylene/1-propanol mutual solvents with volume ratio in between 7/3 ~ 8/2 at their 'boiling point' could be critical to retain film shape.

Table 4.12. Dissolution temperatures of PP films in organic solvents (10 g/L).

Solvent	δ at 25 °C [a] ($\sqrt{cal \cdot cm^{-3}}$)	T dissol. (°C)
Toluene	8.90	105
p-xylene	8.75	102
Cyclohexane	8.20	85
Methylcyclohexane	7.85	94
Isooctane	6.85	> l00 [b]

[a] Data of Hildebrand and Scott [168].

[b] Solvent boils before dissolution occurs.

Table 4.13. Solvent selection for both PP film and also the modifier PBA-*b*-P*q*DMAEMA.

Mutual solvent (v/v)	Boiling point (°C)	Solubility of modifier (10 g/L)	PP film in mutual solvent and appearance out of solvent
o-xylene/ethanol (9/1)	98.7 ~ 102.0	Soluble	Insoluble; Transparent; T increased by 5 ~10 °C
o-xylene/ethanol (8/2)	95.7 ± 0.2	Soluble	Same as above
o-xylene/ethanol (7/3)	88.5 ± 0.1	Soluble	
o-xylene/ethanol (6/4)	84.9 ± 0.1	Soluble	
o-xylene/ethanol (5/5)	83.0	Soluble	
o-xylene/ethanol (4/6)	81.7 ~ 8	Soluble	
o-xylene/ethanol (2/8)	80.2 ~ 3	Soluble	
o-xylene/ cyclohexane/ ethanol (6/3/1)	85.0	Soluble	Same as above
o-xylene/ cyclohexane/ ethanol (7/2/1)	103.8 ± 0.2	Soluble	Same as above
o-xylene/isopropanol (9/1)	114.1	Soluble	Dissolved
o-xylene/isopropanol (8/2)	97.6	Soluble	Insoluble; transparent.
o-xylene/isopropanol (7/3)	92.8	Soluble	Same as above
o-xylene/isopropanol (6/4)	90.1	Soluble	
o-xylene/isopropanol (5/5)	89.5	Soluble	
o-xylene/isopropanol (4/6)	87.5	Soluble	
o-xylene/isopropanol (2/8)	84.7	Soluble	
o-xylene/1-propanol (9/1)	110.0	Soluble	Dissolved
o-xylene/1-propanol (8/2)	106.0	Soluble	Nearly dissolved
o-xylene/1-propanol (7.5/2.5)	104.2 ± 0.1	Soluble	Nearly dissolved
o-xylene/1-propanol (7/3)	103.5 ± 0.2	Soluble	Nontransparent; very soft
o-xylene/1-propanol (6.5/3.5)	103.0 ± 0.3	Soluble	Ca. 70 % Transparent
o-xylene/1-propanol (6/4)	101.6 ~ 102.3	Soluble	Transparent
o-xylene/1-propanol (5/5)	100.2 ± 0.1	Soluble	Transparent
o-xylene/1-propanol (4/6)	99.4	Soluble	Same as above
o-xylene/1-propanol (2/8)	97.5	Soluble	

Note: it was found that for o-xylene/ethanol and o-xylene/ cyclohexane/ ethanol mixtures, the liquid temperature could increase by ca. 5 ~ 10 °C when adding PP.

Overall, to avoid dissolving PP film, the temperature lower than their boiling point was set up and the volume ratio in the range of 6/4 ~ 8/2 o-xylene/1-propanol were used for PP film surface modification.

Modification was processed under the conditions of 25 g/L PBA-*b*-P*q*DMAEMA in o-xylene/1-propanol at temperature of 101.6 ± 0.1 °C for a few minutes. A variety of deswelling methods had been tested, as depicted in footnotes attached to Table 3.1. Generally speaking, they can be classified into three approaches except directly drying: 1) pure solvent to replace modification solvent (SD1, SD2); 2) dipping swollen PP film impregnating modifier solution into corresponding solution at room temperature, and followed by pure solvent replacement (S'SD1, S'SD2); 3) dipping swollen PP film with modifier solution into a higher concentration solution at room temperature before solvent-extraction in o-xylene (S''SD2). In SD1, S'SD1, o-xylene/1-propanol mutual solvent with the volume ratio accordant to the modification solution was used for extraction of swelling solvent; while in SD2, S'SD2 and S''SD2, o-xylene was used as the extraction solvent. However, in the following of results will be explained from two aspects according to the type of deswelling solvent: single o-xylene or mutual solvent of o-xylene/1-propanol. For comparison, the effect of solvent/mutual solvent corresponding to deswelling solvent/mutual solvent on film had been firstly studied before modification. It was found that the weight of PP film decreased after mutual solvent treatment and even the modified films (before water elution), although the weights of E_PP films were slightly bigger than S_PP samples (cf. Figure 4.58). It can be concluded that the higher o-xylene content was, the larger was gravimetric decrease tendency.

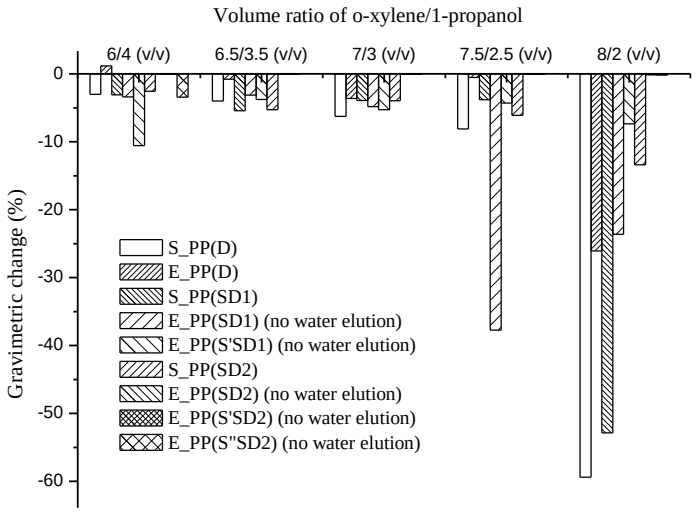

Figure 4.58. Gravimetric change of PP film after solvent or 25 g/L solution treatment at 101.6 ± 0.1 °C, 1 min, respectively (modified PP had not eluted by water before measurement).

Similar to Figure 4.58, Figure 4.59 shows the gravimetric change as functions of mixture ratio of mutual solvent and deswelling way, but the modified PP films had been eluted by water for 2.5 h before the measurement. It was found that most modified samples had the gravimetric change in the range of ca. ± 0.5%, this difference was not that big and could mainly be due to the measuring error. Different with the previous study of section 4.2, in which there was ca. 1 mg/cm^2 decrease degree for water elution $C_{18}EO_8$ modified PP membranes, the water elution for PBA-*b*-P*q*DMAEMA modified PP film was not obvious (Figure 4.59 vs. Figure 4.58). This is mainly due to the non-water soluble property of PBA-*b*-P*q*DMAEMA. So water used here aimed to change the surface configuration of entrapped block copolymers, not for eluting modifiers.

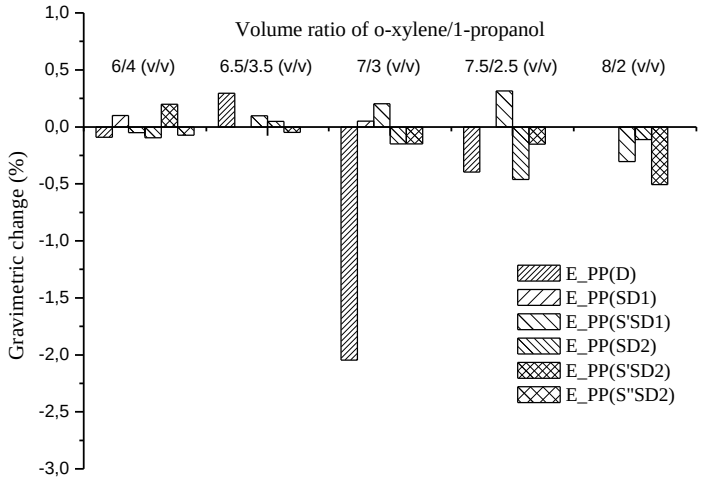

Figure 4.59. Gravimetric change of modified PPs with 25 g/L solution treatment at 101.6 ± 0.1 °C, 1 min, respectively (E_PPs had been eluted by water at room temperature for 2.5 h).

Factors affecting modification efficiency have been studied via CA measurement, as seen in Figure 4.60 and 4.61. Taking E_PP (D) samples as example, the relationship between contact angle and concentration is shown in Figure 4.60. It was found that the solvent treated PP (S_PP) surface showed larger CA than unmodified PP surface, this might because S_PP surface became coarse after treatment at high temperature. However, the modifier solution treated PP (E_PP) under same condition showed more hydrophilic, and surface wettability improved with concentration, so that concentration of 25 g/L was chosen as the best suited concentration.

Furthermore, the effects of mutual ratio of o-xylene/1-propanol and deswelling way on surface wettability had been investigated, as shown in Figure 4.61. On one hand, S_PP and E_PP samples, which had been treated by the mutual solvent or solution with mixture ratio of o-xylene/1-propanol in the range of 6/4 ~ 7/3 (v/v), exhibited similar contact angle; while 7.5/2.5 ~ 8/2 (v/v) o-xylene/1-propanol solvent or solution treated samples showed larger CAs. This might be due to the roughness of surface affected by strong organic solvent [162],

similar results caused by this reason were also shown in Figure 4.58. On the other hand, comparing different deswelling way, it was found that E_PP(D) samples acquired hydrophilicity; CAs of E_PP(SD1) deswollen by o-xylene/1-propanol (6/4 ~ 7/3 ,v/v) had about 40° decrease, but E_PP (S'SD1) surfaces, which were cooled in room temperature solution before mutual solvent extraction, showed somehow better wettability than E_PPs(SD1). For E_PP(SD2), E_PP(S'SD2) and E_PP(S''SD2), which were treated by pure o-xylene instead of o-xylene/1-propanol in step of solvent replacement, did not show very good modification efficiency, except 25 g/L PBA-*b*-P*q*DMAEMA 6/4 o-xylene/1-propanol(v/v) solution modified samples (E_PP(SD2) and E_PP(S''SD2)). Therefore, S'SD1 seemed to be the most efficiency way for deswelling and surface modification.

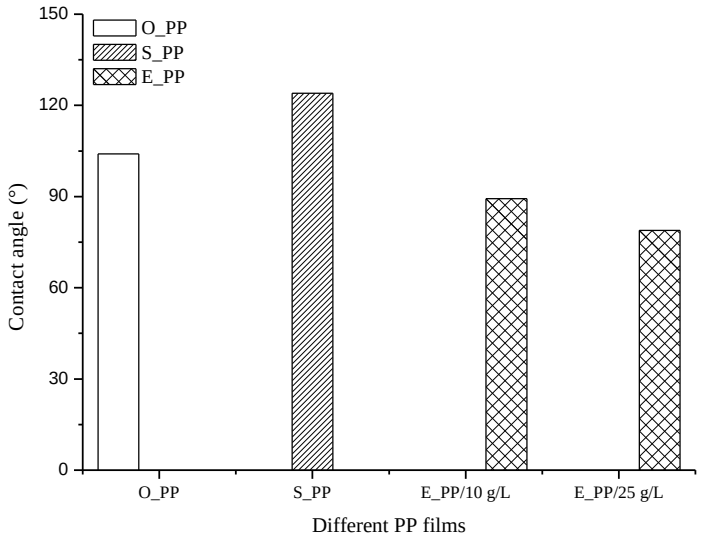

Figure 4.60. Effect of concentration on PP film surface hydrophilicity : 6.5/3.5 o-xylene/1-propanol (v/v), 101.6 ~ 8 °C, 1 min, vacuum dry.

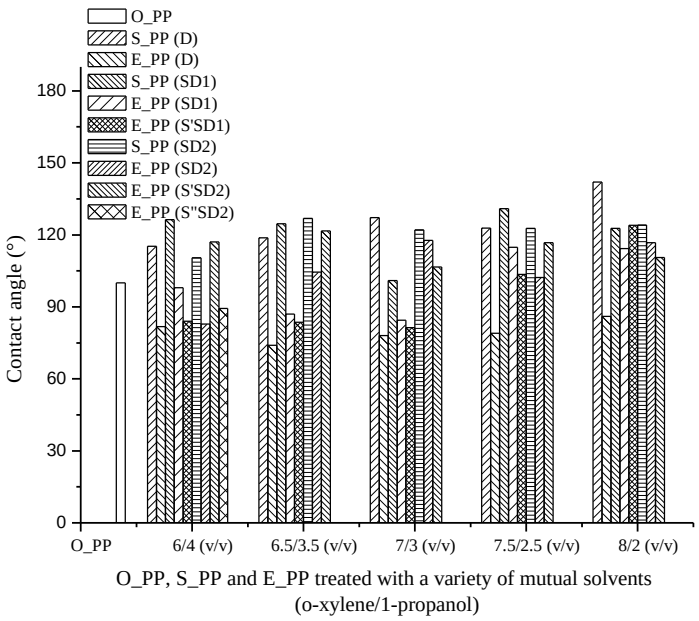

Figure 4.61. Effect of mixed volume ratio of o-xylene/1-propanol and deswelling methods on surface hydrophilicity: 101.6 ± 0.1 °C, 25 g/L PBA-*b*-P*q*DMAEMA/mutual solvent (o-xylene/1-propanol, v/v), 1 min).

Thereafter, surface chemical group composition of a series of E_PP(S'SD1) modified samples treated with different mutual ratio solutions (6/4 ~ 7.5/2.5, v/v) were characterized (see Figure 4.62). Compared to unmodified PP and modifier, it was clear to observe the ester peak close to 1730 cm^{-1} from 6.5/3.5 ~ 8/2 (v/v) modifier solution treated E_PPs, whereas it was surprising to see there was no corresponding signal appearing from 6/4 (v/v) solution modified sample, although this sample surface showed low CA and good hydrophicility. Generally speaking, the solvent extraction efficiency of o-xylene was worse than that of mutual solvent.

Surface charge of the same modified samples used for measuring data presented in Figure 4.62 had been characterized (see Figure 4.63). All the modification treated samples showed more positive surface than original PP, including 6.0/4.0 o-xylene/1-propanol (v/v) solution modified sample. This could more strongly confirm the existence of cationic block copolymer PBA-*b*-P*q*DMAEMA in/on PP film surface than FTIR spectrum.

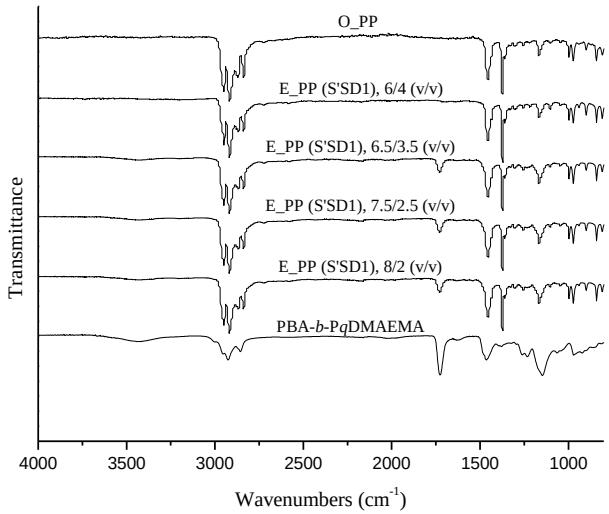

Figure 4.62. IR spectra of O_PP and E_PP films modified in a variety of o-xylene/1-propanol solvents (v/v): 101.6 ± 0.1 °C, 25 g/L PBA-*b*-P*q*DMAEMA/mutual solvent, 1 min, S'SD1, water eluted at room temperature for 2.5 h.

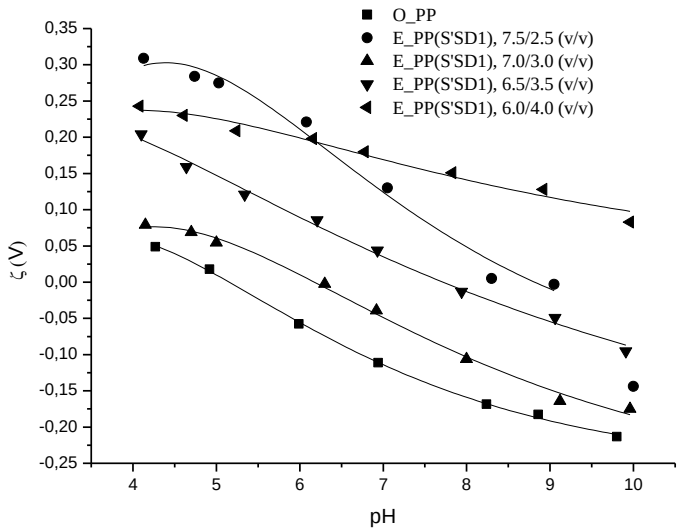

Figure 4.63. Zeta potential of O_PP and E_PP films modified in a variety of o-xylene/1-propanol solvent (v/v): 101.6 ± 0.1 °C, 25 g/L PBA-*b*-P*q*DMAEMA/mutual solvent, 1 min, S'SD1, water eluted at room temperature for 2.5 h.

Moreover, it is interesting to mention one occasional case on the basis of former conclusions. In this case, 6.5/3.5 o-xylene/1-propanol mixture was used to prepare modifier solution, after being immersed into modifier solution at 101.6 ± 0.1 °C for 1 min, the swollen and

impregnated PP film was immediately removed into o-xylene at room temperature for 14.5 h (to distinguish with E_PP (SD2) samples, this sample was recorded as E_PP (SD2 for 14.5 h)). It was found that this sample surface showed as good as wettability as E_PP (D). Compared with O_PP, the IR spectrum curves of both E_PP (D) and E_PP (SD2 for 14.5 h) showed an obvious new peak with very similar strength at 1732 cm^{-1}; and it can be deduced that this peak was corresponding to ester group from PBA-*b*-P*q*DMAEMA from Figure 4.64. Moreover, outer surface zeta potentials of O_PP, E_PP (D) and E_PP (SD2 for 14.5 h) in the pH range of 4 ~ 11 have been compared in Figure 4.65. It was clear to see that either E_PP (D) or E_PP (SD2 for 14.5 h) showed much more positive and less negative surface charges than O_PP, because of the existence of cationic modifier PBA-*b*-P*q*DMAEMA. In addition, the absolute values of these two modified samples had not much difference. Overall, E_PP (SD2 for 14.5 h) showed similar modification efficiency with E_PP (D). Details will be discussed in Chapter 5.

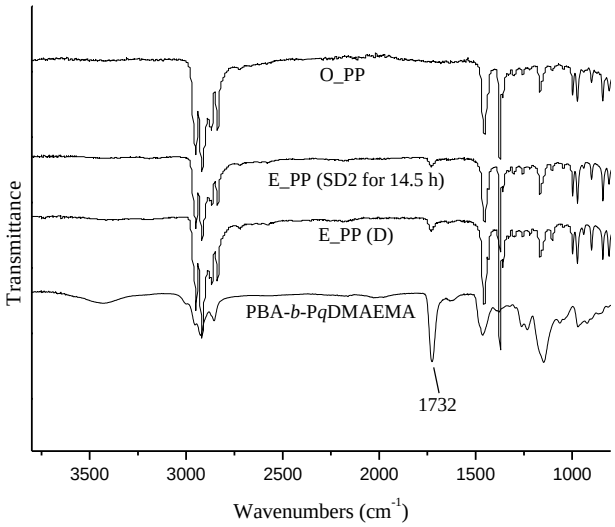

Figure 4.64. IR spectra of O_PP and E_PP deswollen with vacuum dry (E_PP (D)) and oxylene 14.5 h-vacuum dry (E_PP (SD2 for 14.5 h)) respectively: 25 g/L PBA-*b*-P*q*DMAEMA/mutual solvent (o-xylene/1-propanol, 6.5/3.5, v/v), 101.6 ~ 8 °C, 1 min.

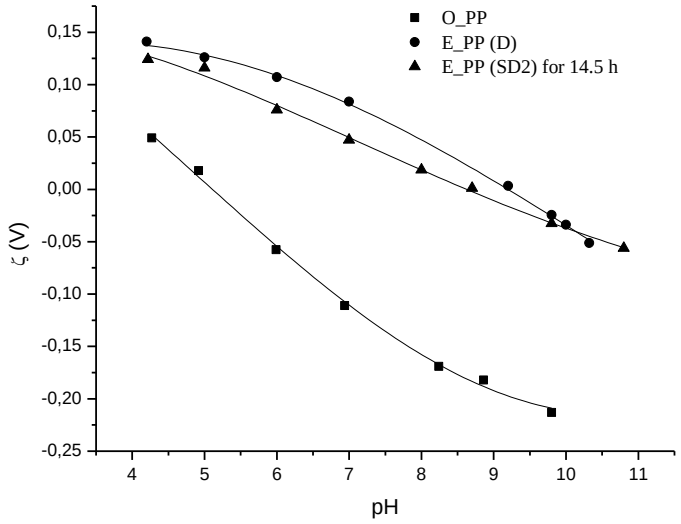

Figure 4.65. Zeta potential of O_PP and E_PP treated with different deswelling ways: 25 g/L PBA-*b*-P*q*DMAEMA/mutual solvent (o-xylene/1-propanol, 6.5/3.5, v/v), 101.6 ~ 8 °C, 1 min.

4.5. Influence of nonionic (macro)molecule structure onto entrapment behavior and efficiency

To hydrophilically modify PP membrane surfaces via entrapment strategy, a family of homopolymers (PEOs, with average molar masses between 400 and 200,000 g/mol) and various amphiphilic (macro)molecules have been used. The details on these amphiphilic modifiers are shown in Table 4.14.

The solvent 1,2-dichloroethane had been selected because its solubility parameter (18.20) is close to that of PP (18.80) (Table 4.9). It should be noted that for PEO homopolymers, saturated solutions have been used because the polymers were not soluble at the target concentration of 25 g/L. PP membranes treated by the solutions of the homo- and block copolymers under the same entrapment process conditions (cf. Chapter 3, Figure 3.1a) were characterized by gravimetric change, water contact angle and IR spectroscopy firstly. On the

basis of these results, several significantly modified membranes were chosen for further analysis of water flux and static protein adsorption. At last, the formation of reverse micelles by the most promising Pluronic® modifiers was investigated using the pyrene-fluorescence method in 1,2-dichloroethane and ^{1}H NMR spectroscopy in d-chloroform.

Table 4.14. Structure of amphiphilic modifiers selected for this study.

Modifier	Abbrevation of chemical structure	M_w (g/mol)	Alkyl or PPO block(s), $M_{w,total}$ (g/mol)	PEO content (wt%)
Octaethylene glycol monooctadecyl ether	$C_{18}EO_8$	623	270	54
PEG400 distearate	$C_{18}EO_8C_{18}$	950	550	42
PEG6000 distearate	$C_{18}EO_{136}C_{18}$	6550	550	92
PE10100	$EO_4PO_{54}EO_4$	3500	3130	10
PE10300	$EO_{17}PO_{60}EO_{17}$	4950	3480	30
PE10500	$EO_{37}PO_{56}EO_{37}$	6500	3250	50
F127	$EO_{100}PO_{65}EO_{100}$	12600	3780	70
F108	$EO_{132}PO_{50}EO_{132}$	14600	2920	80
PE6400	$EO_{13}PO_{30}EO_{13}$	2900	1740	40
RPE1740	$PO_{14}EO_{23}PO_{14}$	2650	1620	40

4.5.1. Gravimetric change due to entrapment modification process, wetting by water from contact angle and surface composition from IR spectroscopy

Figure 4.66 shows the gravimetric change and water contact angle (CA) achieved with all homopolymer PEGs and amphiphilic copolymers for entrapment modification of PP membranes. Figure 4.66a compares the gravimetric change with PEOs from low molecular weight (400 g/mol) to large molecular weight (200 kg/mol). The weight gain increased with molecular weight, but water contact angles of all these PEO treated PP samples were still higher than 130°, as that of original PP. PEO-containing amphiphilic modifiers, such as

diblock $C_{18}EO_8$, tri-block $C_{18}EO_8C_{18}$ and PE10500, all with PEO contents around 50%, were used for PP membrane surface modification (Figure 4.66b). When compared with PEG200k, although these three amphiphilic modifiers have much lower molecular weight, the gravimetric increases were larger than for PEG200k, and the contact angles were lower than 60° (for E_PP/ $C_{18}EO_8$, water drop spread immediately), indicating that the PP surface was hydrophilically modified. Figure 4.66c is a comparison of two kinds of PEO-containing tri-block copolymers, i.e., Pluoronic® PE6400 and RPE1740. These two polymers have the same PEO content (40 wt%), and the difference is that PE6400 is PEO end-capped while RPE1740 has the reverse structure, i.e., it is PPO end-capped. Both modified PP membranes showed similar gravimetric increase, but E_PP/PE6400 was relatively more hydrophilic compared with E_PP/RPE1740; the latter one was still very hydrophobic. Moreover, the effect of PEO content of amphiphilic modifiers was also studied (Figure 4.66d and e). For the Pluronic® series (PEO-PPO-PEO), the weight of modified PP membranes increased with PEO content or molar mass, except for PE10100. This might be because PE10100 is water insoluble, so that the deposited PE10100 on the PP surface could not be washed out completely during the water elution step. However, the corresponding CA data were against the intuition: PE10300 and PE10500 were most efficient for PP surface hydrophilic modification, while F127 and F108 containing much longer PEO chains also modified PP, but still yielded hydrophobic properties (CA > 130°). An analogous result was obtained with the other amphiphilic polymers, the PEG distearates with the same hydrophobic alkyl chain length but a large difference in PEG content (Figure 4.66e): PEG400 distearate with 42% PEG content was much more effective for hydrophilic surface modification than PEG6000 distearate with 92% PEG content.

The corresponding IR spectra of PP membranes after surface entrapment modification with PEOs and amphiphilic substances were measured to identify the change of PP surface

chemical structure (see Figure 4.67). Figure 4.67a shows spectra of PP after treatments with the family of PEOs. Compared with unmodified PP, when the PEG molecular weight was larger than 10 kg/mol, at the wavenumber of 1110 cm^{-1}, one peak corresponding to the ether group of PEO appeared, and the intensity of this peak increased with PEO molecular weight. It seemed that there was PEO on the PP membrane surface, as also indicated by the gravimetric change (cf. Figure 4.66a). In accordance with gravimetric change and CA data (cf. Figure 4.66b-d), the ether peak (at 1110 cm^{-1}) was clearly detected in modified membranes E_PP obtained with $C_{18}EO_8$, $C_{18}EO_8C_{18}$, PE10300 and PE10500 (Figure 4.67b and c), and intensities were larger than those for, e.g., E_PP/PEG200k (Figure 4.67b-d). Also one ester peak (at 1737 cm^{-1}) from $C_{18}EO_8C_{18}$ could be detected (cf. Figure 4.67b). However, for the not well hydrophilically modified membranes E_PP obtained with PE6400, RPE1740, PE10100, F127 and F108, the obvious ether peak at 1110 cm^{-1} was also observed (Figure 4.67c and d). For membrane E_PP/$C_{18}EO_{136}C_{18}$, we could only detect the ether peak, but no ester peak (Figure 4.67e). IR intensities were similar to those for membranes E_PP/PEO (and smaller than for the strongly modified membranes; cf. Figure 4.67d), so that this could be due to small amounts of adsorbed modifier. Based on all results it can be concluded that PEO homopolymers are ineffective for PP membrane surface hydrophilic modification under entrapment conditions, although some deposited or adsorbed PEO had been detected. For the amphiphilic PEO-containing modifiers, significant differences have been observed.

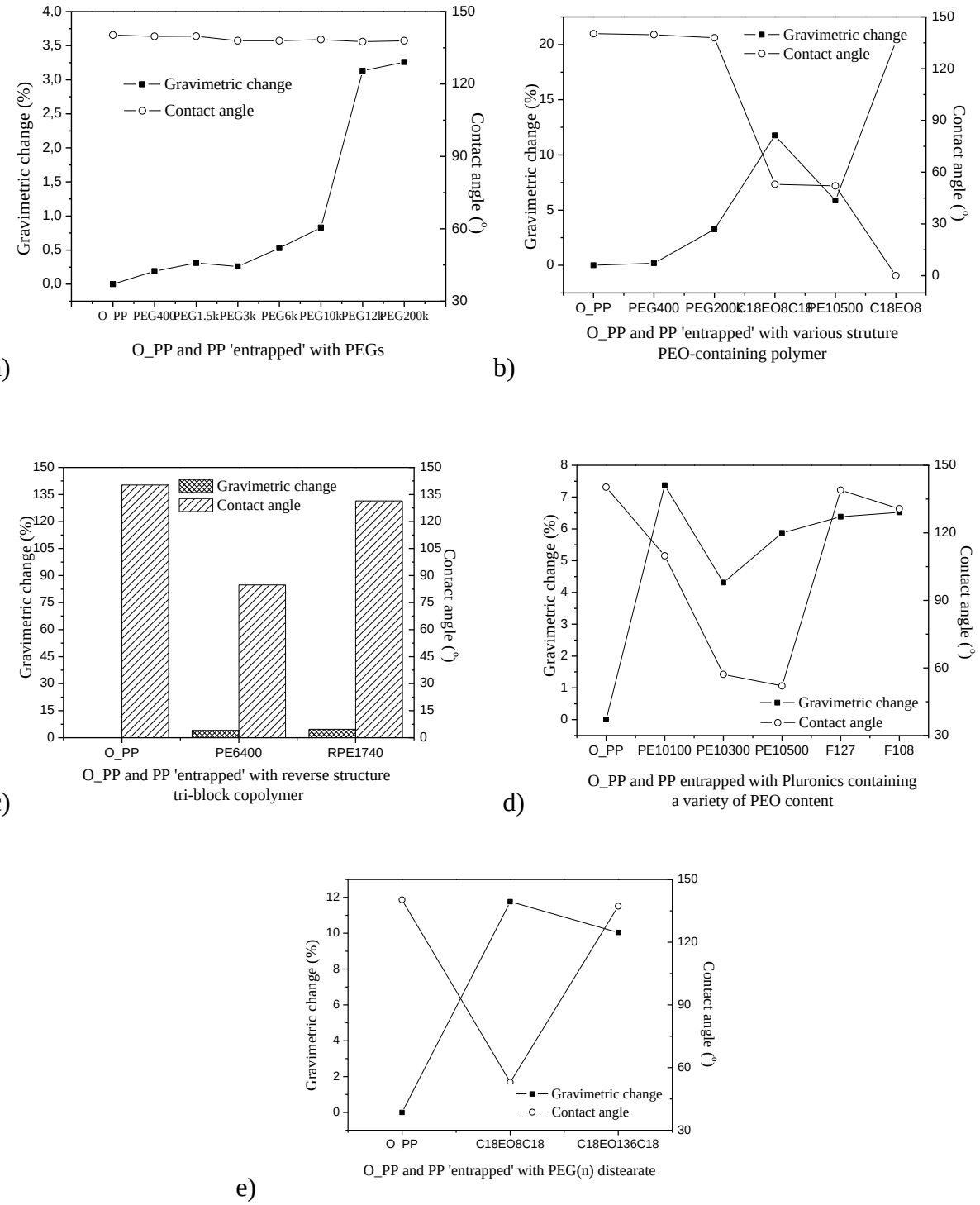

Figure 4.66. Gravimetric change and contact angles of unmodified PP membrane (O_PP) and PP membranes after treatment with various modifiers (cf. Table 4.14) under entrapment conditions: a) PEOs of varied molecular weights 4~200 kg/mol; b) homo- and di-/tri-block copolymers with 40 ~ 50 wt% PEO content; c) pair of PEO-ending and PPO-ending triblock copolymers with similar molar mass; d) PEO-PPO-PEO triblock copolymers with varied PEO content; e) PEG distearates with different PEG content.

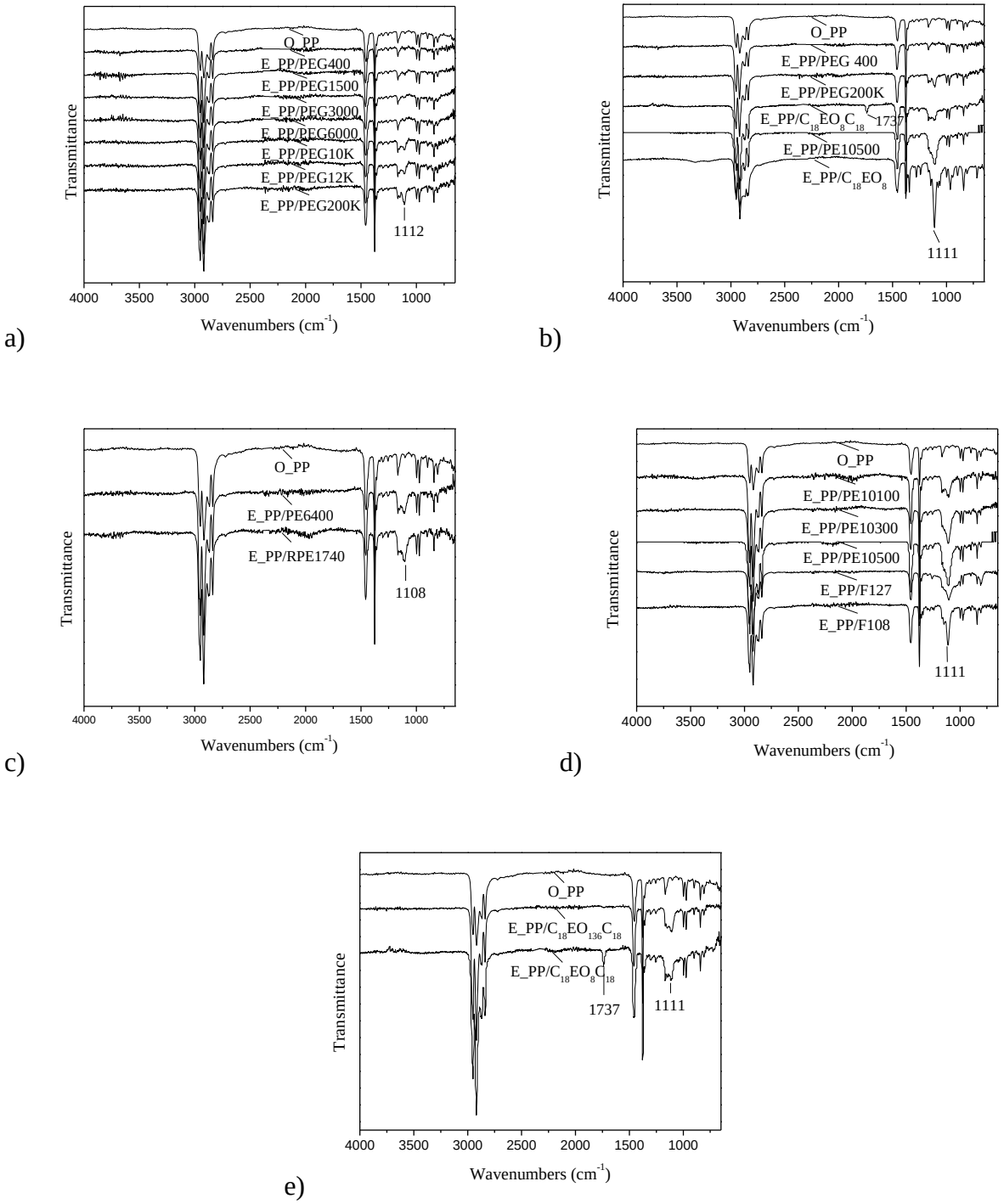

Figure 4.67. IR spectra of unmodified PP membrane (O_PP) and PP membranes after treatment with various modifiers (cf. Table 4.14) under entrapment conditions: a) PEOs of varied molecular weights 4 ~ 200 kg/mol; b) homo- and di-/tri-block copolymers with 40 ~ 50 wt% PEO content; c) pair of PEO-ending and PPO-ending triblock copolymers with similar molar mass; d) PEO-PPO-PEO triblock copolymers with varied PEO content; e) PEG distearates with different PEG content.

4.5.2. Water permeability and protein adsorption

Membrane performance (water flux, wettability inside membrane pores) and anti-fouling properties of functionalized PP membranes were examined (see Figure 4.68). The tendencies were generally consistent with the results of the surface characterizations shown in the previous section. Effectively hydrophilically modified membranes E_PP obtained with $C_{18}EO_8$, $C_{18}EO_8C_{18}$ and PE10500 showed larger water permeability and lower protein adsorption than the unmodified PP membrane (Figure 4.68a). It seemed that modifiers with small molar mass were much more effective than those with larger molar mass. Membrane E_PP/PE10300 had much higher water permeability compared with membrane O_PP. On the other hand, its anti-protein fouling property was only moderate, and this might be caused by the relatively low PEO content of PE10300. In contrast, the not effectively modified membranes E_PP obtained with PE6400, RPE1740, PE10100, F127, F108 and $C_{18}EO_{136}C_{18}$ had relatively low water permeability and high BSA adsorption tendency (Figure 4.68b-d).

Overall, the best modification efficiency with respect to membrane performance has been achieved with modifiers containing similar amounts of PEO and PPO.

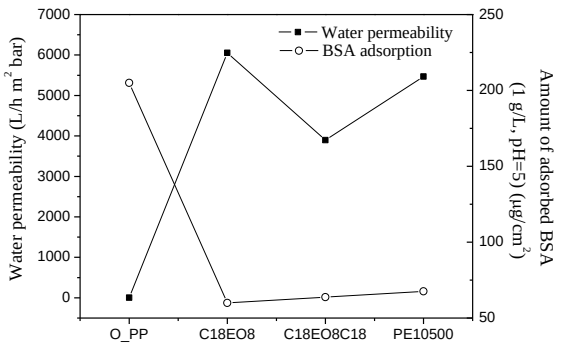

O_PP and PP entrapped of di-/tri-block amphiphilic molecules

a)

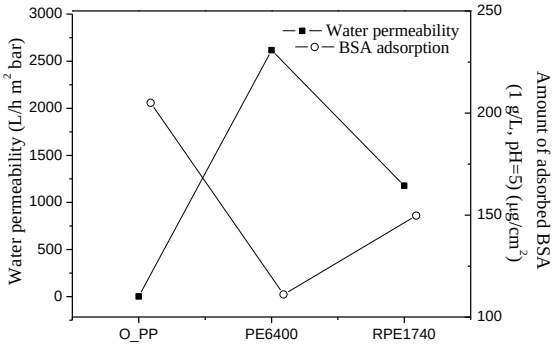

O_PP and PP 'entrapped' with reverse structure triblock PEO/PPO copolymers

b)

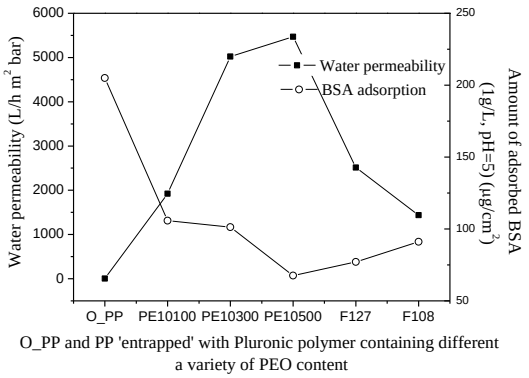

c)

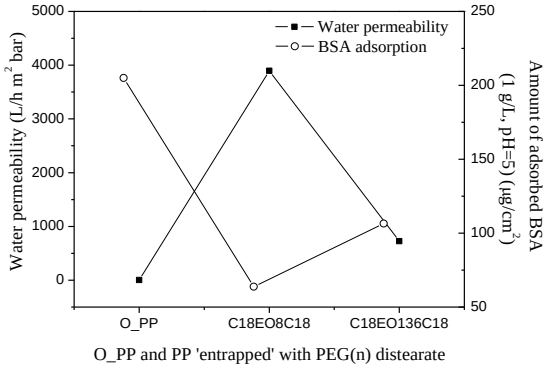

d)

Figure 4.68. Water permeability and adsorbed BSA amounts unter static conditions of unmodified PP membrane (O_PP) and PP membranes after treatment with various modifiers under entrapment conditions (membranes have not been prewetted, e.g. with ethanol, before water flux measurements, therefore the values for O_PP were very low; but membranes have been wetted with buffer, in case of O_PP before also in ethanol, before protein adsorption tests): a) di-/tri-block amphiphilic modifiers with 40 ~ 50% PEO content ($C_{18}EO_8$, $C_{18}EO_8C_{18}$ and PE10500); b) PEO-ending and PPO-ending reverse structure Pluronics®; c) various PEO-PPO-PEO polymers with different PEO content; d) PEG distearates with different PEG content.

4.5.3. Analysis of critical micelle concentration

All analyses shown in the previous sections indicated that the amphiphilic copolymers containing around 50% PEO showed the best surface modification efficiency. With respect to Ruckenstein's theory of ''two-liquid adsorptive entrapment" (cf. Section 2.4.1), the amphiphilic properties in terms of self-aggregation in 1,2-chloroethane or chloroform, respectively, were examined by using the pyrene-probe fluorescence method or ^{1}H NMR spectroscopy. In addition, some CMC values for modifiers in aqueous solutions were also measured with the pyrene-probe method. This should help to identify the relationship between the structure of the amphiphilic (macro)molecules and their entrapment behavior, in particular the influence of adsorption/aggregation in the embedding step.

4.5.3.1. Pyrene probe method

Pyrene is one of the aromatic hydrocarbons which show a significant fine structure in its fluorescence spectrum in solution [169]. For solutions of amphiphiles in water, the amphiphile concentration where the "III/I ratio" suddenly increases is related to a microenvironment of the pyrene which is much more nonpolar; this can be explained by the uptake of pyrene in the hydrophobic core of a micelle, i.e., this concentration is the critical micelle concentration (CMC). In a nonpolar solvent, surfactant aggregates can form a polar core and less polar shell in contact with the solvent, i.e., the respective critical concentration is called reverse CMC (RCMC).

Solutions were prepared with concentrations in the range of 10^{-6} ~ 100 g/L; results are shown in Figure 4.69 and Table 4.15, where the concentrations are expressed on a molar basis. Completely different from their behavior in aqueous solution (very low CMC, ~ 10 µM [170-175]), it was impossible to find a RCMC for $C_{18}EO_8$ until 100 g/L. However, the tri-block amphiphilic substance $C_{18}EO_8C_{18}$ had a RCMC of 7970 µM (< 1 g/L), and the tri-block copolymer PE10500 showed a RCMC of 640 µM (< 10 g/L). The RCMC values of Pluronics® with a variation of the PEO content in the range 10 ~ 80% had the order PE10500 < PE10300 < PE10100 < F127 and F108 (cf. Table 4.15). Actually, we could not identify a RCMC for Pluronics® F127 and F108 until the highest concentration of 100 g/L. Clearly, Pluronic® PE10500 with 50% PEO showed the lowest RCMC. The solvent had been dried and the maximum water content was 0.02%. This corresponds to a maximum of 0.002 g per gram PE10500 at a concentration of 10 g/L in dichloroethane, or corresponds to < 0.01 mol water per mol ethyleneoxide. When adding water into solutions of PE10500 at concentrations below the RCMC, it was observed that a clear solution became to be an emulsion at about 0.3% water content. Below that water content, no significant change of the estimated RCMC values has been observed. Some literatures reported lower CMC values for PE10500 (385 ~ 461 µM)

than for F127 (555 µM) (cf. Table 4.15), although PE10500 has shorter PPO blocks [176,177]. We obtained experimentally a similar CMC for PE10500 (476 µM, Figure 4.69a), but a much smaller CMC for F127 (81 µM, cf. Figure 4.69a).

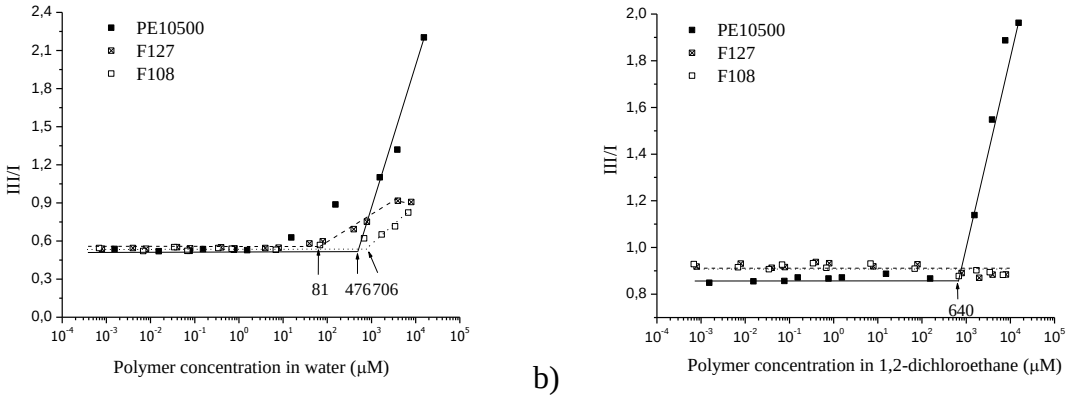

a) b)

Figure 4.69. III/I ratios of pyrene-fluorescence spectra as a function of polymer concentration for PE10500, F127 and F108 in aqueous (a) and nonaqueous (b) solution, respectively (T = 23 ^{o}C).

Table 4.15. CMC (from literature) and RCMC (from experiments) values for amphiphilic modifiers estimated from pyrene probe fluorescence at room temperature.

Modifier	Abbreviation of chemical structure	CMC in water (µM)[a]	RCMC in 1,2-dichloroethane (µM)
Octaethylene glycol monooctadecyl ether	$C_{18}EO_8$	~ 10 [b]	> 10^5
PEG400 distearate	$C_{18}EO_8C_{18}$	- [c]	7970
PE10100	$EO_4PO_{54}EO_4$	- [c]	13058
PE10300	$EO_{17}PO_{60}EO_{17}$	141	4069
PE10500	$EO_{37}PO_{56}EO_{37}$	461	640
F127	$EO_{100}PO_{65}EO_{100}$	555	> 10^4
F108	$EO_{132}PO_{50}EO_{132}$	3082	> 10^4

[a] CMC data at T = 25 ^{o}C from literature [170-177].

[b] the value has been estimated from a from a known value for C_iEO_8 (i = 14, CMC = 9.7 µM [170,171,173] based on the well accepted trend that "the CMC decreases with increasing length of the hydrocarbon chain" [171,172,174,175].

[c] PEG400 distearate and PE10100 are not soluble in water at 25 °C, therefore, there are no CMC data from literature and own experiments.

4.5.3.2. ^{1}H NMR method

The NMR method seems to be particularly suitable for the investigation of micellar solutions [178,179], and, consequently, the technique has also been used to study the micellization of Pluronics® in aqueous solutions [180-182]. The intrinsic probes, for example, the chemical shift of the PO-CH_3 signal, are very sensitive to the local environment and can therefore be used to characterize the concentration-dependent aggregation process. Therefore, to support the results obtained with the pyrene-probe method, ^{1}H NMR has been also applied to analyze the reverse micelle formation of PE10500, F127 and F108. However, d-chloroform had to be used as solvent. Therefore, solutions of the PEO-PPO-PEO tri-block copolymers in chloroform were first analyzed by the pyrene-fluorescence method. It was found that RCMC of PE10500 was 5880 µM (ca. 38 g/L) while the values for F127 and F108 in chloroform were larger than 200 g/L. The value for PE10500 was about 10 times larger than in 1,2-dichloroethane, but the trend for the three block copolymers was nearly the same. This can be related to the higher polarity of chloroform than 1,2-dichloroethane. Nevertheless, the ^{1}H NMR spectra of Pluronic® PE10500, F127 and F108 solutions in d-chloroform with various concentrations, i.e., 0.1, 1, 5, 10, 25, 50, and 100 g/L, were measured at room temperature, two exemplaric cases are shown in Figure 4.70.

The characteristic resonance signals for PEO-PPO-PEO are a triplet at 1.16 ppm (for the PO-CH_3 protons), a signal at 3.4 ~ 3.55 ppm (attributed to PO-CH_2-/PO-CH- units) and a peak at 3.6 ~ 3.65 ppm (for the protons EO-CH_2-). The corresponding chemical shifts of the signals have been taken from NMR spectra and the changes as function of modifier concentration are summarized in Figure 4.71.

It can be seen that the chemical shift of the protons in EO-CH_2- and also in PO-CH_2 and PO-CH_3 had changed to lower values with increasing concentrations. For F127 and F108 this decrease was continuous in the entire concentration range. However, the values for PE10500 decreased initially but became almost stable at higher polymer concentration. This indicated that the functional groups are experiencing a progressively less polar or more nonpolar environment.

The first inflection point in the curves of chemical shift vs. concentration should correspond to the RCMC, because the environment became constant, i.e., independent of overall solution polarity. We noticed, that the thus obtained RCMC for PE10500 in d-chloroform was about 50 g/L, i.e., in reasonable agreement with the value obtained with the pyrene-probe method in the same solvent (ca. 38 g/L; cf. above). And the value was much larger than that in dichloroethane (< 10 g/L), as already mentioned and explained with the more polar nature of chloroform [177]. The maximum water content in chloroform was 0.02%. Because the RCMC was higher than in dichloroethane, the maximum ratio of water to ethyleneoxide was even lower in chloroform than in the dichloroethane case discussed above.

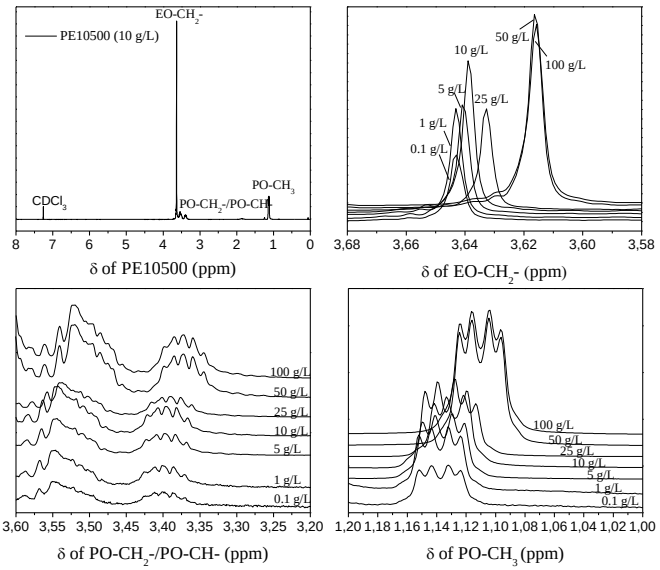

a)

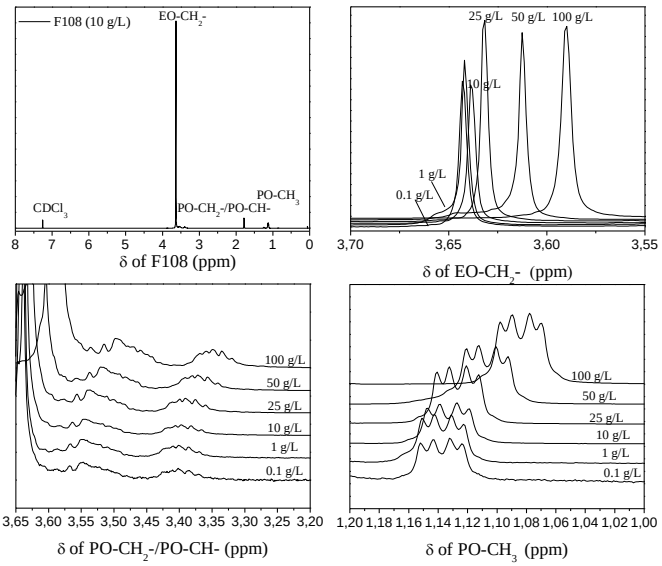

b)

Figure 4.70. Original ^{1}H NMR spectra of PE10500 (a) and F108 (b) in d-chloroform: left above) overview for 10 g/L; other graphs) effect of polymer concentration in the chemical shift regions of EO-CH_2- (3.55 ~ 3.80 ppm), PO-CH_2-/PO-CH- (3.20 ~ 3.65 ppm) and PO-CH_3 (1.00 ~ 1.20 ppm).

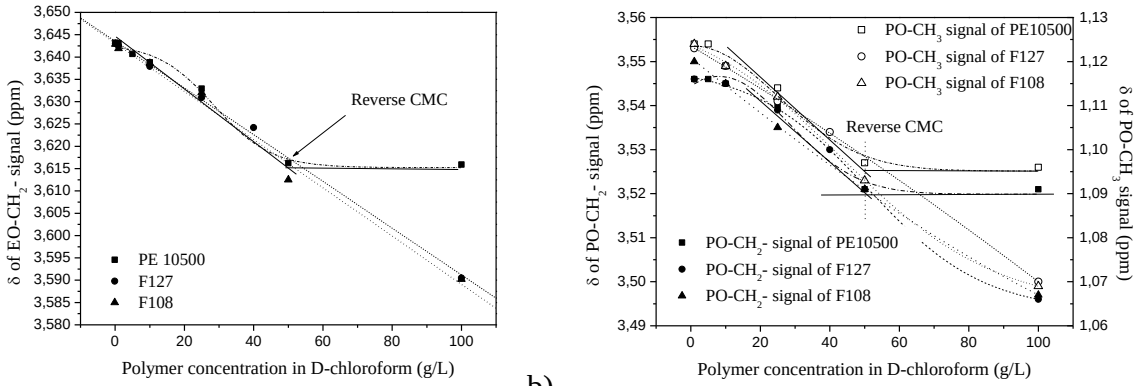

a) b)

Figure 4.71. Concentration-dependent chemical shifts from ^{1}H NMR spectra for protons in EO-CH_2- (a) and PO-CH_2-/PO-CH_3 (b), for solutions of PE10500, F127 and F108 in d-chloroform.

Overall, the most important results are that large differences with respect to their aggregation behavior in nonpolar or moderately polar solvents have been identified by two independent methods, and that Pluronic® PE10500 showed consistently the lowest CMC (on molar basis), i.e., the largest aggregation tendency among the polymeric modifiers.

Chapter 5

Discussion

The discussion of this chapter will focus on two main aspects. On one hand, it is on the effects of modification condition on the feasibility and efficiency of entrapment technique with respect to different (non)porous membrane substrate, based on the results obtained from different sections of Chapter 4, respectively. On the other hand, it is on the intrinsic reasons, which result to various modification conditions with respect to the type of polymer substrate, modifier etc.

5.1. Factors of modification conditions in different entrapment systems

5.1.1. PES microfiltration membrane surface modification

5.1.1.1. Effects on entrapment modification efficiency

Effect of solvent. According to Hansen solubility parameters, several organic solvents, such as NMP, DMAc, DMF, DMSO were selected as good solvent for swelling PES membrane before or during embedment of modifier. It was found that these pure solvents can dissolve PES membrane or made the membrane become dense films. Therefore, water, a solvent that is miscible with the above solvent but is a nonsolvent for PES membrane was chosen to dilute the organic solvent. For a mutual solvent, the general cohesive energy density (δ_{sm}) can be obtained from Eq. 5.1,

$$\delta_{sm} = \emptyset_1\delta_1 + \emptyset_2\delta_2 \quad (5.1)$$

Therein, Φ_1 and Φ_2 represent the volume fraction of different components respectively. Hence, the energy from dispersion bonds, dipolar intermolecular force and hydrogen bonds between molecules can be expressed as a sum of different components, as expressed in Eq. 5.2 ~ 5.4.

$$\delta_d = \emptyset_1\delta_{d1} + \emptyset_2\delta_{d2} \quad (5.2)$$

$$\delta_p = \emptyset_1\delta_{p1} + \emptyset_2\delta_{p2} \quad (5.3)$$

$$\delta_h = \emptyset_1\delta_{h1} + \emptyset_2\delta_{h2} \quad (5.4)$$

Combined with Eq. 2.5 (Section 2.2.1), solubility parameters of families of water diluted solvents have been calculated (Table 7.1 in Appendix). It should be noted that the Hansen solubility parameters of the mutual solvents were calculated from volume fraction (cf. Table 7.1), while the water diluted solvents were prepared via mixture of different volume ratios of solvents. Therefore, the calculated Hansen solubility parameters in Table 7.2.1 ~ 7.2.3 were used approximately for those solvents. In terms of those solubility parameters, appearance of PES samples treated by solvents, as well as permporometry analyses results (cf. Figure 4.4, Figure 4.5), 8/2(v/v) organic solvent/water can be taken as the critical mixture volume ratio and 7/3 (v/v) could be much "safer" to PES membrane.

Therefore, the mutual solvents with high content of organic component have been used for preparing modification solution (20 g/L). In case of TEG/water system, the higher water content was used considering the worse solubility of TEG to modifiers. For comparison of surface wettability of modified membranes, it was found that DMSO/H_2O was better than NMP/H_2O (cf. Table 4.1, Figure 4.7) and DMF/H_2O (cf. Figure 4.8) with the same volume ratio. From Table 7.1, it can be seen that NMP and DMF have better solubility to PES membrane, the worse modification efficiency from them could be due to more serious damage on membrane surface than by DMSO. It was surprising that the sample was damaged (e.g. shrunk, became partly transparent or partly dissolved etc.) when vacuum dried directly

after taking membrane out from modification solution, although the membrane shape and structure can keep well from pure mutual solvent. That is why we could not obtain the corresponding characterization data of "modification treated" samples such as PES-301 ~ 306#, PES-313#, 315#, 317#, 319# etc. It was supposed that this could be related to the effect of modifier and the different boiling point/vapor pressure of water and organic component. In the modification solution, water molecules bind with either organic solvent or the modifier molecules, and in some cases, modifier has very low solubility in organic solvent. For this reason, the ratio of organic solvent/water in solution could be higher than that in pure solvent. In addition, under vacuum dry at 45 °C, water, which has much lower boiling point or higher vapor pressure than NMP (202 °C), DMAc (165 °C), DMF (153 °C) and DMSO (189 °C), could be firstly evaporated, therefore, the residual content of organic component existed in membrane became higher and higher till damaged membrane. To solve this problem, three ways can be adopted: decreasing organic solvent content, soaking into water solution before vacuum drying, and decreasing concentration respectively. Modification efficiency was very low using low organic solvent content, even when the concentration of PEG or PEO-containing modifier was as high as 20 g/L, as shown in Figure 4.7 and Figure 4.11. The second way related to the deswelling method, is discussed in following. The third way related to deswelling process will be discussed subsequently.

Effect of deswelling method. The deswelling method, performed as quenching impregnated sample into excess of water, is anticipated to replace and extract organic solvent in swelling region to reach an entrapment. Moreover, this method could avoid the water-organic solvent phase separation and membrane damage during directly vacuum drying, connecting to the question left in the previous paragraph. The cases in Figure 4.8, Table 4.2 etc. confirmed that, under water treatment before dry, it was possible to use high organic content water-diluted solvent, e.g. DMSO/H_2O (8/2, v/v) as good solvent for PES swelling and embedment without

damaging membrane judged from appearance. More advantages will be discussed in other sections.

Effect of solution (concentration, modifier etc.). As discussed in the first part of this section, it was found that low organic content of water-diluted solvent is ineffective for membrane surface modification (20 g/L concentration). By contrast, high organic content with low modifier concentration has been tested for modification, and it has been found that the surface wettability was improved even at 1 g/L solution modification. This comparison confirms that the swelling degree is more important than concentration for modification, although the modification increases with concentration (cf. Table 4.2).

PEO-containing modifiers, such as homopolymer, diblock amphiphilic molecules, triblock amphiphilic molecules end-capped with hydrophobic alkyl group, triblock amphiphilic polymer Pluronic® have been used for PES membrane surface hydrophilicity modification. However, as shown in Figure 4.8, the PEO chain length did not show evident influence on surface wettability, but the type of organic solvent showed more importance in modification, as confirmed in the first part (Page 126 ~ 128). The structure influence in Figure 4.9 was not very clear because modification efficiency was too weak to be analyzed by contact angle measurement.

E2 procedure for PES membrane surface modification. Entrapment of functional groups into polymer surface is on the basis of the reversible swelling/deswelling property of polymer. For this reason, it was considered to firstly swell polymer with water-diluted organic solvent, and then entrap the modifier into swelling region with rapid deswelling in the modifier aqueous solution, called procedure E2. It has been concluded from Section 4.1.1.2 that the swelling time in a relative strong solvent is the key to dominate the feasibility of entrapment modification, rather than structure or PEO chain length of modifiers as well as

embedment time. Additionally, water treatment before drying is important to decrease modifier adsorption on membrane surface and pores. For instance, in 7/3 NMP^2/H_2O, when the swelling time was longer than four hours, the corresponding samples showed better surface wettability than unmodified PES or PES treated with too short time for swelling. That indicated that prolonging swelling time is benefit to increase swelling degree, so that the polymer substrate surface has enough space for diffusion of more modifiers to achieve higher hydrophilic modification efficiency (cf. Figure 4.14). Similar to the effect of swelling time on entrapment modification, increasing temperature is another efficiency way to promote swelling and further modifier molecular diffusion into polymer substrate.

5.1.1.2. Comparison of E1 and E2 entrapment procedures

E1 and E2 are different procedures for PES membrane surface modification. In case of E1, the swelling and embedment of modifiers happen in parallel, and then followed by deswelling step to fix the modifier into membrane surface; in case of E2, swelling membrane in solvent was initially performed, and then entrapment of modifiers (including embedment/chain entanglement, and fixation in parallel) was accomplished in modifier solution. E1 has been studied and reported for several times, and it is well known that the solvent selection is the difficulty in E1 procedure. The solvents for swelling (I) and deswelling (II) are chosen in terms of different principles. Solvent I should be good solvent for base polymer, in parallel can well dissolve modifier, and normally it is water soluble solvent. Solvent II is a nonsolvent for base polymer but should be miscible with solvent I for solvent replacement and extraction, however, which is also a good solvent for modifier so that can result to the leaching of modifiers. Therefore, the small molecules are not very efficient for entrapping into polymer surface. However, in E2 procedure, the swelling and embedment processes were separated and isolated. So the solvent I will not be limited by modifier (e.g. entrapping PEG into nonpolar polymer surface), and the design of entrapment with deswelling behaviour can

avoid the molecular leaching phenomena. Moreover, water or aqueous solution for entrapment of polar PES membrane surface has less negative impact on environment than many organic solvents. However, the second step in water solution for entrapment and deswelling is much more complicated than E1. It is hard to say, leaching of modifier and collapse of swelling polymer, which is faster. Only when the entrapment of modifier dominates this process, it is possible to acquire well modified surface. Otherwise, the modification efficiency could be very low if deswelling quickly happens before leaching. So far, there is no other study to confirm the intrinsic behavior of E2 in water solution. The present experiments are too limited to make a reliable conclusion.

Although there were no corresponding comparable modification conditions of procedures E1 and E2, it can be generally concluded that much better wettability surface can be achieved from E1 than E2. CA values of many E1_PES samples were at least 10° less than unmodified PES membrane. Considering MicroPES® is made from a sulfonated PES polymer cast [183], which owns a CA lower than 50°, therefore, the CA decrease of 10° confirms that surface hydrophicility is really improved. A similar result has been acquired by Kouwonu, who modified PES MF surface via photografting of acrylic acid (AA), and the CA of modified PES decreased from 55 ± 4° to 44 ± 1° [4]. In addition, there are still several common points between E1 and E2. 1) Both of the effective modified cases confirmed the importance of 'swelling' degree. In E1, it was found that high organic content solvent but low modifier concentration can yield better modification efficiency than low organic content but high modifier concentration system. In E2 procedure, it was found that, the longer swelling time is, the better is surface wettability. 2) Either homo or amphiphilic (macro)molecules can be entrapped into PES membrane surface. But the modification efficiency seemed independent of either PEG/PEO chain length or membrane structure. 3) Immediately drying after the embedment (in E1)/entrapment (in E2) step could result in adsorption/deposition of modifier

onto membrane surface (cf. Figure 4.11 and Table 4.3). These three common points validate that the swelling degree and deswelling way dominate the feasibility of an entrapment modification. Other conditions, such as modifier or concentration can be adjusted to reach better modification efficiency.

5.1.2. Entrapment of nonionic poly(ethylene oxide) alkyl-based amphiphilic molecules into PP microfiltration membrane surface

5.1.2.1. Effect of modification conditions

1,2-dichloroethane (DCE) was selected as good solvent for PP membrane with respect to Hansen solubility parameter, which is close to that of PP. Moreover, DCE soaked PP appeared unchanged compared with PP treated by o-xylene and benzene (cf. Table 4.9). As anticipated, characterizations from permporometry, SEM and XRD verified that DCE had gentle influence on membrane pore structure, but decreased crystalline content of PP. Figure 4.23 showed only DCE treated PP (S_PP) has a slight decrease of average pore diameter; this decrease might be due to the collapse of PP chain under vacuum. Similar with permporometry results, pore morphology has no change after DCE treated at room temperature for 20 h (cf. Figure 4.24a vs. b). Figure 4.27 showed primary crystal structure of the PP such as crystalline lattice did not change. The average crystalline size only slightly decreased according to analysis using the Scherrer equation [184]. But the crystalline degree Xc of PP after DCE treatment decreased by about 9 % (cf. Table 4.27). This change implied the DCE might somehow damage the polymer crystal structure. However, the change of crystal degree is not that large considering the problem of calculation error.

Two kinds of nonionic poly(ethylene oxide) alkyl-based surfactants, $C_{18}EO_8$, $C_{18}EO_8C_{18}$ as well as $C_{18}EO_{136}C_{18}$ have been used for PP microfiltration membrane surface modification

with E1 procedure. As concluded from section 4.2.2, the surface hydrophilic modification seems not depending on PEG chain length (cf. Table 4.5), $C_{18}EO_8$ and $C_{18}EO_8C_{18}$ are much more efficient than $C_{18}EO_{136}C_{18}$, and details will be discussed in the following. High concentration and long swelling/embedment were expected to lead to high modification efficiency (cf. Figure 4.19 ~ 20). Temperature in the range of 20 ~ 30 °C would not influence the modification results so much. Amphiphilic molecule $C_{18}EO_8C_{18}$ is water insoluble at room temperature. Taking into account all these investigations, $C_{18}EO_8$ was selected as a model modifier for PP microfiltration membrane surface modification. The comprehensive characterizations of membrane structure, polymer substrate structure, inner pore wall and outer surface property (wettability, charge property) as well as antifouling and stability will be discussed below.

5.1.2.2. Entrapment of $C_{18}EO_8$

Entrapment modification with pore-narrowing. $C_{18}EO_8$ is a small molecular with M_w less than 1000 g/mol. However, the average pore diameter of E_PP/$C_{18}EO_8$ decreased by more than 50 nm after modification. Assuming an even coverage of the specific surface area (29.6 m^2/g) with $C_{18}EO_8$, it was estimated from gravimetric increase that the average thickness of $C_{18}EO_8$ layer on the PP surface was about 7 nm. However, a thicker layer of $C_{18}EO_8$ on pore walls was estimated as about 25 nm from Figure 4.23. It was of interest that changes of pore size would result from such degree of modification, presumably also leading to blocking of a fraction of small pores. The presumption of pore blocking was further directly confirmed by surface morphology (cf. Figure 4.24c). Nevertheless, a more careful inspection of the morphology underneath the "cover-layer" of E_PP revealed that the pore shape, pore size as well as pore morphology looked very much like that of O_PP. This suggested that the shape of the size distribution in the macropore range was essentially unchanged, and this is in accordance with the results from permporometry (cf. Figure 4.23). Overall, morphology of

E_PP remained essentially unchanged after entrapment of $C_{18}EO_8$, this could be one advantage of entrapment modification compared with some of the chemical modification methods always bearing the risk that the base polymer is etched, e.g. by plasma or high-energy UV, and change of pore shape and increase in pore size may result [52,185].

Entrapment region. Existence of C_8EO_{18} of E_PP on/in an otherwise essentially unchanged PP membrane can be verified each other from crystalline structure of XRD and DSC. Moreover, the crystalline and amorphous region of crystal PP can be analyzed by IR spectrum. It is known that the peak at wavenumber of 973 cm^{-1} is contributed by amorphous domains, and the peak at 998 cm^{-1} is contributed by crystal domains. It is noticed from Figure 4.29 that after modification, the intensity of 973 cm^{-1} peak was more than two times higher than that at 998 cm^{-1}. This ratio is much bigger than that of unmodified PP. It implies that the modifier mainly present into amorphous region. This might because the soft amorphous chains are easily to be loose during swelling in good solvent, so that the modifiers can diffuse and embed into this region. This result confirmed the importance of 'swelling' of polymer substrate during embedment step.

Wettability and antifouling property. The existence of hydrophilic chains (oligoethylene glycol) of the amphiphilic $C_{18}EO_8$ on the membrane surface facilitated the reduction of interfacial tension with water (cf. Figure 4.30, 4.31). This improved not only the wetting of the pores but also the protein resistance (cf. Figure 4.32, 4.34 and Figure 4.35, 4.36). It should be noted that in dry state a decrease of average pore size was measured (cf. Figure 4.23) and further qualitatively confirmed by electron microscopy (cf. Figure 4.24, Figure 4.25). On the other hand, not only the wetting of the outer membrane surface but also uptake of water in the dry membrane had been largely improved by the modification (cf. Figure 4.30). Therefore, the increased water permeability and the elimination of the off-set pressure could also be related to the improved wetting of the originally hydrophobic PP pores with

water. This latter result could be related to the improved wetting of the originally hydrophobic PP pores. Therefore, a gas flow through pore dewetting with water filled membranes has been measured, but it seems that the relationship between surface wettability and gas permeation is not yet clear. Overall, the results of contact angle, zeta potential and water permeability are evidence for the entrapment of $C_{18}EO_8$ in PP surface and inner pore wall, where the exposed hydrophilic oligoethylene glycol is dominating the interface properties, which results in better protein antifouling capacity. However, similar to many other "grafting-to" modifications with PEGs [186,187], a complete shielding of the surface to protein adsorption has not been reached.

Stability study. In surface engineering, physical methods always face the problem of limited stability. Several previous studies of entrapment strategy on polymer surface revealed that the surface modification could persist for at least 1 week in water [114,116,121,122]. Overall, the physically entrapped modifier tended to leach out from the PP surface and to dissolve into water. This tendency was increased by flow though the membrane. This is the reason why water permeability of membranes E_PP decreased after the first water flux measurement for longer periods. However, it was also found that $C_{18}EO_8$-modified PP membrane surface still remained significant hydrophicility after 8 weeks extensive leaching, and the better antifouling property than that of O_PP. These results confirm that the chain entanglement of modifier into PP surface rather than coating is the main reason to keep modification efficiency in certain degree.

5.1.3. Entrapment of PNIPAAm-based macromoleclues into PP membrane and plate surface

5.1.3.1. Factors affecting the modification efficiency

Different with modification condition used in 5.1.2., THF was selected as good solvent for either Membrana PP membrane or PNIPAAm-based polymers with respect to the solubility of modifiers and modification efficiency (Figure 4.41, Table 4.10), although the membrane was slightly deformed by the treatment of THF.

CA result in Figure 4.42 indicated that both homopolymer PNIPAAm and block copolymer cP1 with balanced hydrophilic/hydrophobic structure are much more effective than cP2. And this surface modification efficiency is independent of hydrophilic PNIPAAm chain length. Like shown in studies of PES surface modification (Section 4.1.2.1) as well as PP surface modification with various PEO-based modifiers (Section 4.5), the modification efficiency is not mainly due to the hydrophilic chain length.

Additionally, Figure 4.42 shows that the water soaking step before drying is beneficial to obtain better homogeneous hydrophilically modified surface than immediately drying or deswelling. This could be related to the configuration of macromolecules in/on membrane surface. Macromolecules in a good solvent can be described as random coil which could entangle with each other at quite low concentrations. Therefore, during the swelling/embedment process, the modifier macromolecular chains should anchor in the PP and entangle with PP chains irregularly. This could be the reason why directly dried membrane surface of EPP/cP1 showed less hydrophilicity than EPP/hP, because the hydrophilic PNIPAAm segments could be covered by hydrophobic PBA block, due to the same random arrangement as in solution (see Figure 5.1a). However, during the water treatment, a water/oil-like interface forms, so that the hydrophilic blocks tend to stretch into the water phase and will be exposed from the solvent-swollen (“oil-like”) membrane surface (see Figure 5.1b). This model would be compatible to the findings and discussion in Section

4.2.2 and 5.2.1.1., where dichloroethane had been the swelling solvent. However, THF used in this study is miscible with water. Hence, water will also function as deswelling agent for the PP membrane surface because it is nonsolvent for PP but can extract the THF from the swelling region (cf. Section 2.4.1). Often one serious negative consequence is that if water has a good solubility for the modifier it would quickly leach out from the surface. In this study, hP, cP1 and cP2 are amphiphilic but not water-soluble. Hence, in the process of extraction of THF by water, the macromolecules tend to move to the membrane/water interface, but are not leached out of the PP surface. In parallel, lack of THF results to the polymer collapse and deswell. In conclusion, water acts not only as nonsolvent of PP but also for orienting the hydrophilic blocks of the modifier on the polymer surface. This explains the better surface wettability after water treatment (cf. Figure 4.42); this is the preferred deswelling way. Combined with results from Section 4.5, cP1 with balanced hydrophilic/hydrophobic structure would be the better modifier than hP, because it is anticipated that the hydrophobic PBA block could act as anchor in the PP and the modified membrane should have a better stability.

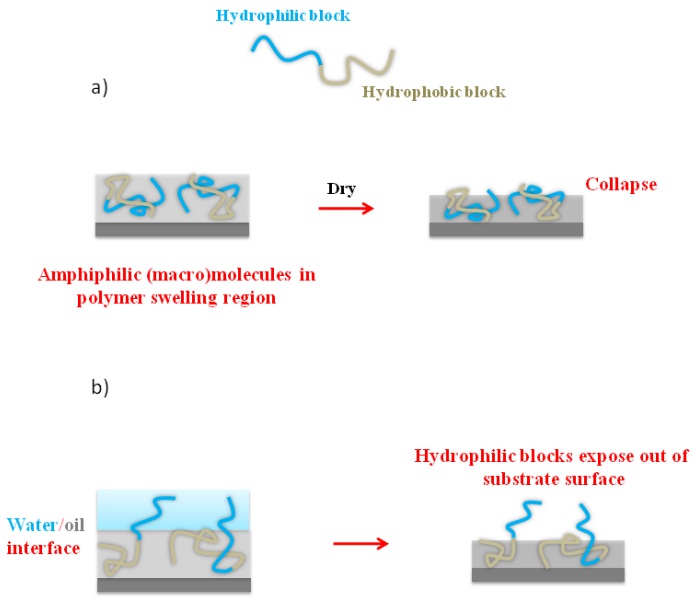

Figure 5.1. Schematic depictions of water/solution and membrane/solution interface under different process conditions: a) dry directly; b) expose to water before drying.

5.1.3.2. Thermo-responsivity of modified PP MF membrane

Thermo-responsive property of PNIPAAm can be depicted as hydration-dehydration and volume transition in parallel with surrounding lower critical solution temperature of water (or aqueous solution). Normally, the LCST of PNIPAAm in water is in the range of 31 ~ 34 °C [188]. It was confirmed that when T < LCST, H-bonds of water with amide groups (-NH and C=O) form a stable hydration shell around the hydrophobic groups (isopropyl), which leads to large water uptake; while when T > LCST, H-bonds are weakened and "hydrophobic" PNIPAAm-PNIPAAm interactions (driven by dehydration of isopropyl groups) dominate resulting in the release of water [160,189]. Hence, the change of PP surface contact angle with temperature confirmed that the modified PP processed thermo-responsibility based on surface-entrapped PNIPAAm (cf. Figure 4.47). This is a strong support for the assumption that PNIPAAm blocks are oriented toward the PP surface and are free to move in the interphase region because surfaces with too short PNIPAAm segments do not show thermo-responsive behavior [190,191].

In addition, the phenomena of discontinuous change of water permeability with temperature and its large absolute change around 31 ~ 32 °C (cf. Figure 4.48) can be explained by the temperature-responsive volume change of PNIPAAm in combination with its effect onto pore surface wettablity. The LSCT of PP-anchored PBA-*b*-PNIPAAm in pure water could be estimated to be 31 ~ 32 °C that the water permeability was much lower at ~ 20 °C can be explained by pore narrowing by the "grafted" swollen PNIPAAm coils on the pore walls. That water permeability was, irrespective the smaller characteristic pore size in dry state (cf. Figure 4.44), almost the same at ~ 30 °C can be related to the improved wetting as compared with PP. The volume phase transition of PNIPAAm close to LCST – PNIPAAm chains stretch or coils expand when temperature is below LCST, while the polymer collapses/shrinks when temperature is above LCST – leads in this case to a more open pore at

T > 32° C, and this can be related to the fact, that the “grafted” PNIPAAm is freely mobile to expand into the pore at T < LCST and collaps to the pore wall at T > LCST. Similar PNIPAAm based grafted membranes had been designed to obtain temperature-manipulated membrane pores for separation [192-194], and such so-called ”on-off valve” models have in common, that the reversible swelling or shrinking of PNIPAAm causes a regulation of the effective membrane pore size [34,195-197].

The hydration/dehydration transition property of PNIPAAm can be further applied in BSA elution (cf. Figure 4.50), and it can be seen that the water elution step at temperature lower than LCST was beneficial for protein desorption, because the grafted PNIPAAm chains showed more hydrophilic properties and stretched out so that they could ‘shake off’ bound proteins [198]. Overall, the effects with respect to water flux were relatively small because the change of flux through a MF membrane with ~ 0.2 µm pore diameter due to formation of an adsorbed protein layer (with a thickness of a few nm) is small.

5.1.3.3. PP plate surface

To well understand the entrapment efficiency on polymer surface without disturbance of pore effect, nonporous PP plate was used as substrate. For this reason, analogous experiments had been performed to modify non-porous PP plates by surface entrapment. It should be noted that, due to the fully accessible outer surface, solvent exchange, rinsing and washing/extraction steps were much faster and more efficient than for the interior of a porous structure. Also, influence of the pore structure on characterization results can be excluded. As anticipated, the E_PP/cP1 plates surface showed as good as wettability like cP1 modified PP membrane (Figure 4.52, 4.53). The well repeatable modification results from six different samples strongly proved the dominating effect of entrapment for modification without pore-blocking.

Thermo-sensitive zeta potential had been measured for either membrane (trans-membrane zeta potential) or plate (outer surface zeta potential). Generally speaking, zeta potential decreased with temperature. This has been confirmed by some literatures, but they found there was a linear relationship between zeta potential and temperature for microfluidic system [199-201]. Venditti et al. also confirmed that the change with temperature would be very weak in low concentration environment, such as 0.1 mM KCl solution. Additionally, the comparison of Figure 4.49 and Figure 4.54 revealed that the outer surface zeta potential showed more obvious response to temperature than that of inner pores, especially around the LCST. At present we have no direct data to verify whether this difference is caused by porous structure. Venditti once found that the substrate material had influence on temperature-dependent zeta potential [202], but in this case, the material should be the same. Moreover, it is still confused that the absolute values of modified PP membrane are positive under pH around 5.7, and the IEP shifted so much after modification (Figure 7.4. in Appendix-1).

Overall, different modification conditions used for entrapment of PNIPAAm-based polymers showed different entrapment behavior compared with that of PEO-based polymers for PP membrane surface modification. Successful entrapment of cP1 into PP plate surface indicated the feasibility of entrapment of modifier without effect of pore-blocking.

5.1.4. Entrapment of nonionic and cationic macromolecules into PP membrane and film surface

5.1.4.1 Influence of polymer substrate

It is known that the physical properties of a polymer depend not only on the type of monomer(s) comprising it, but also on the secondary and tertiary structures, i.e., the stereochemistry of the linkage, the chain length and its distribution, its ability to crystallize or

remain amorphous state under various conditions, and the shape or distribution of the shapes of the chain in the crystalline and amorphous states [76,203]. Discussion in section 5.1.3 confirms that the entrapment method is also feasible for surface modification without effect of pore-blocking. The further discussion would focus on effect of polymer substrates, which are made from the same monomer but with different bulk or solid states (Membranea PP membrane, Celgard PP membrane and Celgard PP film) (cf. Table 5.1).

Table 5.1. Basic physical parameters of different PP.

PP substrate	Porosity (%)	Nominal pore diameter (μm)	Thickness (μm)	Contact angle (°)
Membrana PP membrane	70	0.2	190	140.3
Celgard PP membrane [60, 135-137]	37~48	0.05×0.19	25	123.8
Celgard PP film	-	-	28	101

Under the same modification condition, the results for these three kinds of PP substrates are obviously different, as indicated by Figure 4.55. Therein, Membrana PP membrane surface acquired the best wettability, which was better than that for Celgard PP membrane, and Celgard PP film FS surface did not acquire hydrophilicity improvement. It is noticed that solubility parameter values for PP as reported in literatures cover a rather broad span, ranging from 7.9 to 9.4 $(cal \cdot cm^{-3})^{1/2}$ or 16.60 ~ 19.90 $(MPa)^{1/2}$ (cf. Table 4.9), which might be due to different measuring processes. But different crystalline degree, pore, crystalline type and size of PP material themselves should be the dominating reason resulting to different solubility of PP in the same solvent. Thereby, the different swelling degree of diverse PP substrates in even the same solution probably is the dominating reason for different modification efficiency. This presumption was further validated by a successful surface hydrophilic

modification for Celgard PP film under sufficient swelling condition (cf. Table 4.12, 4.13 and Figure 4.56).

5.1.4.2. Entrapment of cationic amphiphilic macromolecules (PBA-*b*-P*q*DMAEMA) into PP film surface

Swelling conditions. The swelling condition mainly depends on two aspects: solvent and temperature. In this section, mutual solvent with alcohol component was adopted considering the specific solubility of PBA-*b*-P*q*DMAEMA. The other organic component is o-xylene, used as good solvent for PP film. The detailed solvent selection process has been expressed in Section 4.4.2. In addition, the temperature is the other important factor to increase swelling degree. Irrespective to the former solvent selection conditions, influence of swelling time of PP film in tetraline, o-xylene and o-xylene/cyclohexane mixtures had been tested respectively, at room temperature (see Figure 7.5. in Appendix-1). It can be concluded that the swelling degree increases with swelling time, and it reaches saturated when time is long enough. However, the modification efficiency is too low considering such long swelling time. Hence, increase of temperature was considered to promote swelling efficiency. Taking the boiling points of mutual solvents (o-xylene/1-propanol) into account, the best suitable temperature was finally fixed as 101.6 ± 0.1 °C.

Study on deswelling way. Immediately vacuum drying is a high efficiency way to remove organic solvent aiming to deswell and fix the modifiers into polymer surface layer. But this method faces a serious problem of deposition. Therefore, in order to avoid or decrease surface deposition, other five deswelling ways have been tested except immediately dry, which have been detailed explained in Section 4.4.2 (Page 105 ~ 106). A comparison of effect of different deswelling ways on surface hydrophilic modification efficiency was shown in Figure 4.61. Two general conclusions can be obtained from this Figure. On one hand,

modification efficiency from surface wettability showed that E_PP (S'SD1) had better surface hydrophilicity than E_PP (SD1). On the other hand, E_PP (SD1) and E_PP (S'SD1) showed generally better hydrophilic improvement than E_PP (SD2), E_PP (S'SD2) and E_PP (S''SD2). Details are discussed in following.

In deswelling way of SD1, it was anticipated to replace mutual solvent from solution with the same pure solvent. However, the cool mutual solvent could just dilute the swelling region instead of extracting the mutual solvent (Figure 5.2a). Based on the theory of concentration difference, the modifier has the tendency to enter low concentration or pure mutual solvent. So it is impossible to exclude the deposition effect. But in the deswelling way of S'SD1, membrane was kept into the same solution at room temperature initially to make sure the modifier will not leach out of PP surface. At the same time, the swelling PP film could somehow collapse because of sudden low temperature; the collapsed sample was then immersed into pure mutual solvent for only replacement of solvent (Figure 5.2b). Both FTIR (cf. Figure 4.62) and zeta potential (cf. Figure 4.63) results confirmed the significant modification efficiency of E_PP (S'SD1). However, the entrapped modifier could leach out from membrane surface to the mutual solvent, but the tendency could be too low to affect modification efficiency during deswelling step in short time (5 min).

In deswelling way of E_PP (SD2), E_PP (S'SD2) and E_PP (S''SD2), only E_PP at low o-xylene content showed as good modification efficiency as E_PP (S'SD1). In this case, PBA-*b*-P*q*DMAEMA is not soluble in o-xylene, therefore the modifier could not leach out from membrane surface into o-xylene while PP film can reach a rapid collapse (Figure 5.2c). Although Figure 4.61 does not show expected result for E_PP (SD2) series samples, one occasional case of E_PP (SD2) in excessive o-xylene at room temperature for 14.5 h was prepared, and the characterizations of IR (cf. Figure 4.63) and outer surface zeta potential (cf.

Figure 4.65) strongly verified that the membrane surface obtained as good modification efficiency as E_PP (D).

Generally speaking, E_PP (S'SD1) surface can obtain good modification without deposition effect; while E_PP (SD2) can reach higher modification efficiency because of no leaching of PBA-*b*-P*q*DMAEMA during solvent-extraction.

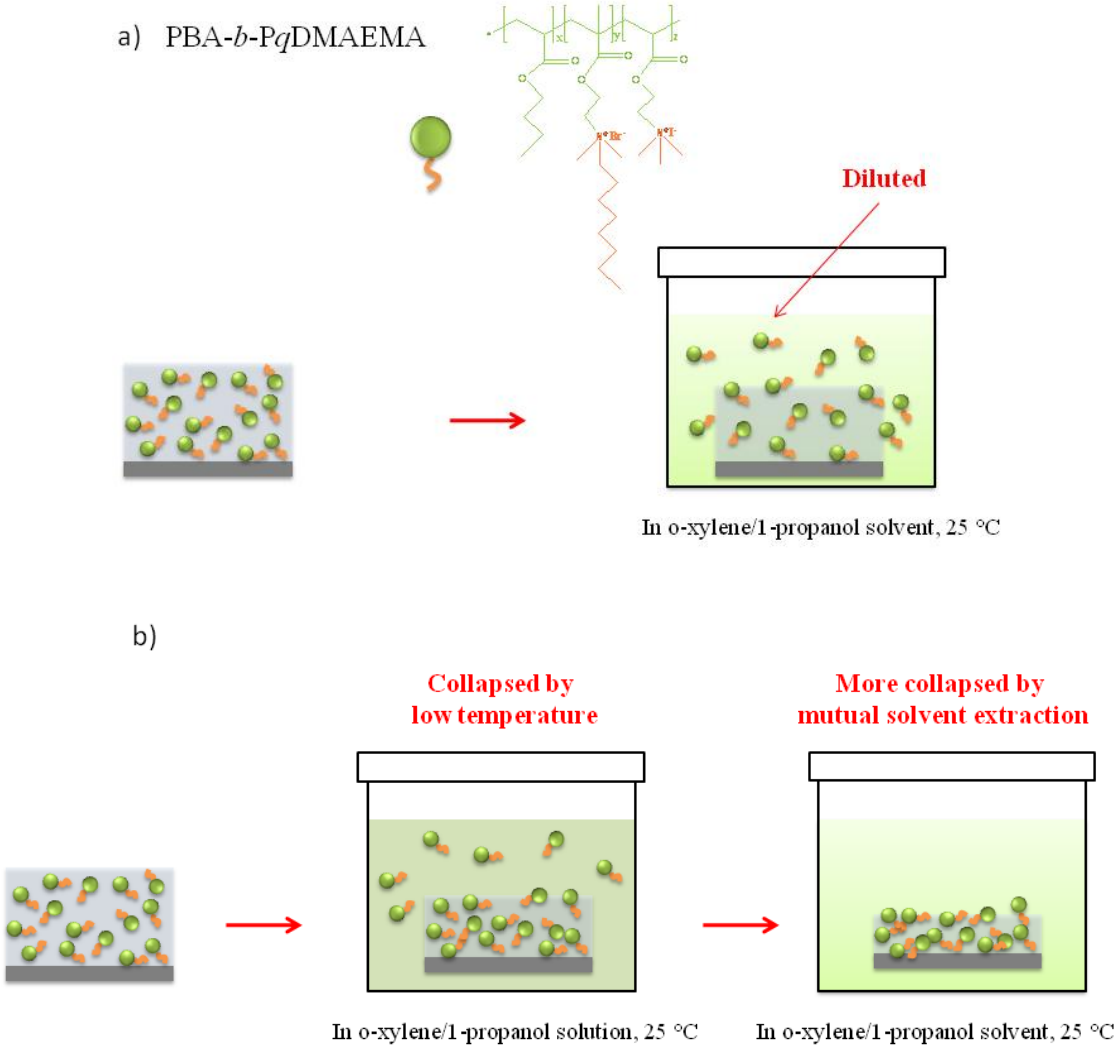

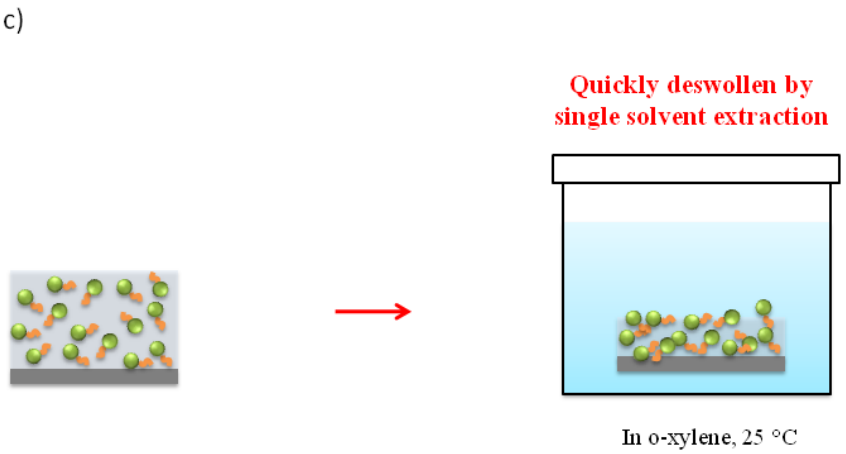

Figure 5.2. Schematic drawing of transition from swollen to deswollen structure for different treatment.

5.2. Discussion of entrapment for functionalization of polymer surface

5.2.1. General principles for polymer surface entrapment modification

In order to impart desirable properties such as hydrophilic, antifouling properties into polymer surface, entrapment of functional modifiers into polymer surface has been performed. Therein, according to different polymer substrates (i.e. PES MF membrane, PP MF membrane, film etc.), the modification conditions should be redesigned, otherwise, the modification efficiency was different (cf. Section 4.4.1, Figure 4.55). Combining the solubility effect of different modifier, the solvent selection for the same polymer substrate was different (cf. Section 4.2 and 4.3) and the further entrapment behavior could be different too (cf. Section 4.2, 4.5 vs. Section 4.3, Figure 5.1). It was also found that homopolymer PEG can entrap into PES membrane surface (Section 4.1, e.g. Figure 4.8) but has very low efficiency to entrap into PP membrane surface (Section 4.5, Figure 4.66a and Figure 4.67a).

However, another kind of homopolymer PNIPAAm could be well entrapped into PP membrane surface (Section 4.3, Figure 4.42). Taking all the above differences into account, it is interesting to seek the intrinsic factors behind the phenomena.

5.2.1.1 Factor of swelling

Swelling polymer substrate is the first important step of entrapment technique, which offers enough 'space' for diffusion and entanglement of modifiers. In the above investigations, it was really found the effect of swelling degree or suitable good solvent for polymer substrate on modification efficiency. For instance, as discussed in Section 5.1, much organic solvent content with low modifier concentration (8/2 DMSO/H_2O, 1 g/L F127 in Figure 4.8) was efficient for PES surface modification, even better than low organic solvent content with high modifier concentration (3/7 DMSO/H_2O, 20 g/L F127 in Figure 4.7). Similarly, Figure 4.55 showed same modification condition for different kinds of PP substrates finally yielded different surface modification efficiency. Furthermore, for PP film surface modification, much work has been done to find either suitable mutual solvent or the critical swelling temperature (Section 4.4). Overall, for different polymer substrates, aiming to swell but not dissolve polymer substrate in the very beginning of entrapment modification procedure, it is necessary to find the appropriate swelling condition, such as solvent or mutual solvent, corresponding temperature, swelling time etc. However, the limitation of molecular diffusion due to M_w of modifiers should not be ignored, as confirmed in Section 4.3. In Hubbell's suggestion, 18.5 kg/mol is the best suitable molecular weight [114].

One correlated problem is the selection of solvent. A good solvent should have a suitable solubility parameter close to that of polymer substrate. The polarity and the dissolution temperature to polymer substrate etc. are also important to be taken into account. Additionally, in case of mutual solvent system, the different boiling point or vapor pressure

should be taken into account to avoid phase separation during adding sample or vacuum dry. Many negative examples have been validated, such as unexpected damage of PES sample under immediate vacuum dry (Section 4.1), or sudden increase of mutual solvent temperature (Section 4.4, Table 4.13). Meanwhile, the solubility of solvent for modifier should not be ignored, as investigated in Section 4.3, Section 4.4. In some cases, the failure of surface modification might be due to the worse solubility of modifier into the solvent, as judged from Flory parameter χ, e.g. at 100 °C, χ of PEG in 1,2-dichloroethane is -0.31 when volume fraction of PEG is 1 [98]. In these cases, the modifiers in solvent are too big to enter swelling network. Generally speaking, all the above factors during the swelling of polymer substrate and solubility of modifier should be taken into account in the beginning of entrapment modification.

5.2.1.2. Factor of deswelling

Water treatment before vacuum drying was finally considered to be a suitable deswelling way from the study of PES and PP membrane surface modification. However, the function of water seems different in different modification systems, as depicted in Figure 5.1. In polar system, water acted as a deswelling solvent which can extract the swelling solvent so that polymer substrate collapses and can fix the anchoring modifier (Figure 5.1c). One more advantage of water replacement is effectively avoiding the negative influence of organic swelling solvent on polymer substrate, such as NMP to PES under vacuum dry. In water/oil interface, water soluble chains has the tendency to stretch into water phase and expose out of membrane surface, which is especially interesting when the modifier is amphiphilic one.

As discussed in 5.1.4.2, deswelling ways of the organic solvent extraction and extraction after pretreatment in cool solution were considered to be effective for PP film surface modification. The single organic solvent o-xylene acted like water in case of PES and PP

membrane surface modification, but one significant difference was that o-xylene could not dissolve modifier so that avoids the leaching phenomena of modifiers during deswelling step (Figure 5.2c). The other way is alternative to promote deswelling at low temperature and then extract good solvent with mutual solvent (Figure 5.2b). Both of these two approaches are positive and alternative, the former one seems much more quick and simple, but the latter one could well define surface modifier structure (stretch into extraction mutual solvent).

Overall, either water or organic solvent, even from cool solution to organic solvent extraction deswelling way is better than immediately vacuum dry. The selection of the deswelling solvent is limited by the type of swelling solvent and also modifier. O-xylene is a suitable choice if only considering the modification efficiency; however, a mutual solvent from modification solution might be a better choice to understand the entrapment behavior.

5.2.1.3. Factor of modifier strucutre

Either water-soluble homopolymer or amphiphilic polymers can successfully entrap into polar base polymer surface, as confirmed by literatures [116,124] and PES study in this dissertation. The molecular weight can influence the diffusion (during swelling) of modifiers or incorporation efficiency (during deswelling). However, in view of hydrophilic modification, the hydrophilic polymer or block in amphiphilic (macro)molecules have not shown much relationship to the final surface wettability, as confirmed in some cases in Section 4.1 and 4.3. More surprisingly, PEG cannot effectively entrap into nonpolar PP membrane surface. Taking the nonionic PEO-based (macro)molecules as an example, the relationship between modifier and entrapment feasibility & efficiency for nonpolar PP membrane surface is discussed.

All results have revealed that PEO homopolymers were not efficient for modification of PP via entrapment, while for the PEO-containing amphiphilic modifiers, the block copolymers

with similar chain length of hydrophilic and hydrophobic blocks were most effective for a hydrophilic surface modification of PP. The discussion will focus on four aspects related to functionalization efficiency: (i) the differences between homopolymer and amphiphilic copolymer; (ii) the effect of the unpolar end-capping component in amphiphilic modifiers on entrapment modification; (iii) the effects of PEO chain length on hydrophilic modification; (iv) the origin of the highest modification efficiency for a relatively balanced modifier structure and the relationships between aggregation tendency in solution and embedding efficiency.

Hubbell et al. indicated that the optimum molar mass of PEG for surface modification of, for instance, PET in aqueous solution of trifluoroacetic acid (18 ~ 20%) was 18.5 kg/mol [114]. Therefore, PEOs with various molar masses (400 ~ 200,000 g/mol) had been used for PP membrane surface modification, but we did not obtain any efficient modification of PP. All the previous research about entrapment of PEGs had focused on the surface modification of polar polymers. For the nonpolar PP used as substrate in this study, a nonpolar solvent, 1,2-dichloroethane, was chosen as good solvent for swelling PP (cf. 5.2.1.1). However, PEGs cannot well dissolve in such nonaqueous, nonpolar solvent. We can conclude that the entrapment of PEG is not feasible in nonpolar system because of the limited solubility. For the same reason, a direct comparison with the other modifiers in terms of efficiency is not possible. Therefore, no clear conclusions can be drawn with respect to the influences of the compatibility of PP and PEO and of PEO chain length on entrapment in PP.

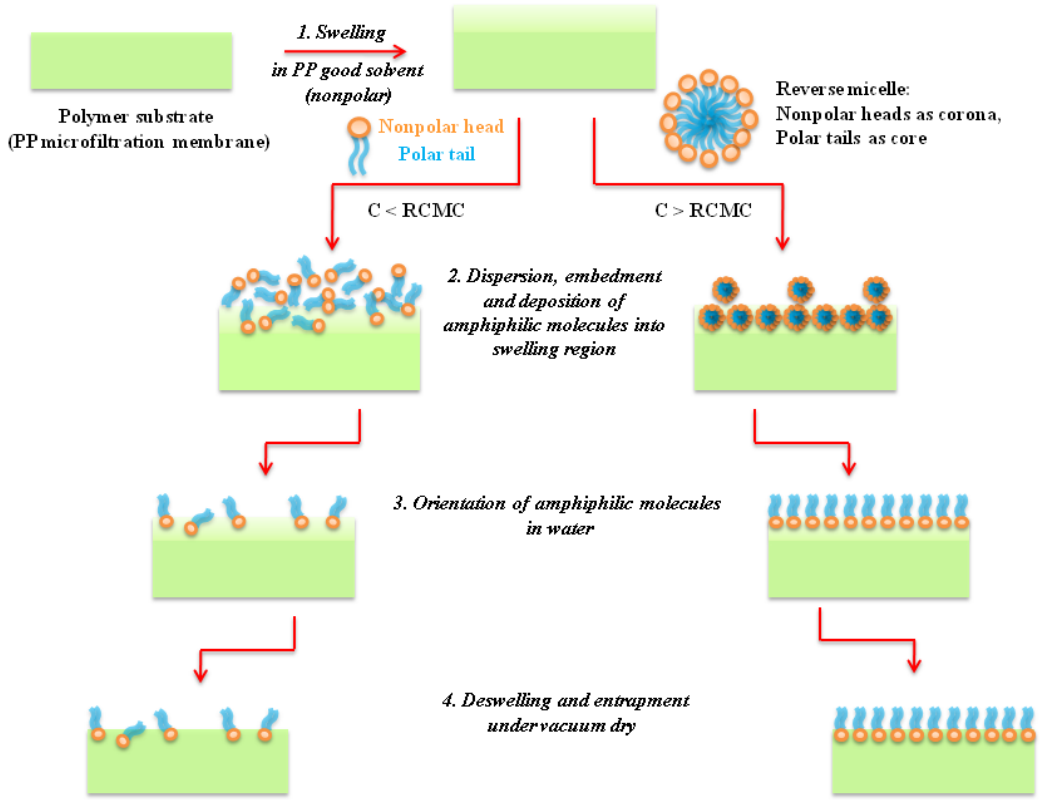

Figure 5.3. Schematic drawing of entrapment process with tri-block amphiphilic molecules at different concentrations.

On the other hand, several amphiphilic substances showed good hydrophilic modification for PP. Hence, the focus of the discussion is now on the influence of amphiphilic modifier structure; a schematic overview on the possible processes is given in Figure 5.3. In terms of Ruckenstein's view, during the first step of entrapment (embedding of amphiphilic polymer), the hydrophobic chains tend to be incorporate into the surface layer of the hydrophobic substrate while the hydrophilic chains are anticipated to be exposed out of the substrate surface [116]. Some other studies on the adsorption mechanism of Pluronics® PEO-*b*-PPO-*b*-PEO, on hydrophobic surfaces have concluded that the first step is the adsorption of hydrophobic PPO chains onto the hydrophobic surface (''hydrophobic interaction") so that the anchored flexible PEO chains (''tails") cause the hydrophilic modification [204-206].

However, these studies were all on PEO end-capped structures and polar aqueous solutions. Therefore, it was of interest to study the influence of the reverse structure of the tri-block copolymer, PPO-*b*-PEO-*b*-PPO, on resulting hydrophilicity and even stability. It was hypothesized that the two hydrophobic end blocks could entrap into base polymer surface leading to the middle hydrophilic chain exposed out of the surface as a ‘‘loop” rather than a ‘‘tail”. In this study, Pluronics® PE6400 and RPE1740, two polymers with similar molecular weight and same PEO content but opposite architecture were employed. After entrapment treatment, membrane E_PP/PE6400 showed better surface hydrophilicity and anti-fouling ability than membrane E_PP/RPE1740. This might be because the relatively short middle PEO block (Mw ~ 1000 g/ mol) can entangle with the PPO chains (Mw ~ 800 g/mL; cf. Table 4.14), so that this block could also embed into PP surface, rather than be exposed out of the surface. The PEO end-capped amphiphilic tri-block copolymer seemed to be more efficient to improve surface hydrophilicity than the PPO end-capped structure. Nevertheless, results with the smaller tri-block substances demonstrated that this limitation should not be generalized. For instance, we observed that PEG400 distearate ($C_{18}EO_8C_{18}$), i.e., end-capped with alkyl groups (M_w ~ 225 g/mL; cf. Table 4.14), can well improve PP surface hydrophilicity, water flux and anti-fouling properties. This might be because the alkyl chains were short and less flexible compared with the PPO segments of RPE1740, so that the PEG400 could be entirely exposed out of the PP surface and lead to hydrophilic properties.

With respect to PEO chain length in amphiphilic substances, it is well known that higher PEO content ensures higher hydrophilicity. However, the results were not consistent with such principle, i.e., membranes E_PP/F127 and E_PP/F108 were not hydrophilically modified irrespective the PEO content of the amphiphilic modifier of 70% and 80%. A similar result was obtained for PEG6000 distearate. In contrast, membranes entrapped with Pluronics® of lower PEO content, i.e., PE10300 and PE10500, had much higher surface hydrophilicity and

anti-fouling tendency. Apparently, amphiphilic triblock modifiers with relatively too long PEO chains or a too high PEO content lead to low efficiency or even unfeasibility of entrapment modification (the PEG homopolymers discussed above are the extreme case). Reasons for that should be due to the macromolecular conformation and aggregation tendency in organic solutions. Many studies on mechanisms of the adsorption of PEO-*b*-PPO-*b*-PEO from aqueous solution on hydrophobic surface had revealed that the adsorbed amounts suddenly increase when the polymer concentration reaches the CMC [207,208]. Therefore we thought that in nonaqueous solutions, the tendency to form reverse micelles could be important for the adsorption tendency to the nonpolar PP surface and to promote the embedding of modifier into PP.

Most studies on reverse micelle formation have been performed in oil/water emulsions. With the exception of [209], it was not yet found much published research on the formation of reverse micelles of PEO-PPO-PEO tri-block copolymers in pure nonaqueous solutions (i.e., without additional water content). Alexandridis et al. have done a series of systematic investigations of effects (e.g., polymer chemical composition, molar mass) on the reverse micellization of PEO-*b*-PPO-*b*-PEO in an organic solvent in the presence of some water [209-211]. It was found that, except the water, the effect of copolymer composition was also important for the formation of reverse micelles. The relative size of the ‘‘solvophobic” PEO block (rather than the PPO block size) should be the controlling parameter in the tendency of the polyoxyalkylene block copolymers to form micelles in organic solvents, just as the size of the hydrophobic PPO block is most important for the micellization in aqueous solutions. Following this conclusion, PEO-*b*-PPO-*b*-PEO with large PEO blocks should have a larger tendency to form micelles. Hence, for instance, Pluronics® F108 and F127 should have a lower RCMC value compared with PE10500. However, this is not in agreement with our experimental results; we could not find a RCMC in the range up to ~ 100 g/L in 1,2-

dichloroethane (and up to ~ 200 g/L in chloroform) for Pluronics® F127 and F108, but we did find RCMC for some other tri-block copolymers with shorter PEO chains (Pluronics® PE10100, PE10300, and PE10500, and PEG400 distearate; cf. Table 4.15). The lowest RCMC values were found for PE10500 and PEG400 distearate, both containing about 50% PEO. Therefore, it seems that the relative PEO size is not the key factor for self-association in pure organic solvents. It should also be considered that the intrinsic driving force for (reverse) micellization is the entropy gain of the system. In aqueous solution, the so called ‘‘hydrophobic effect” is due to the entropy gain by release of clustered water and dominates the decrease of free energy; this promotes the aggregation of amphiphilic macromolecules [212]. In nonaqueous solutions, there is no hydrophobic effect; and the only evidence for promoting the aggregation of “solvophobic” PEO blocks in nonpolar solutions found from literature is due to the presence of additional water or some other water-soluble polar components [209-211,213,214].

In study of section 4.5, the liquid system was ‘‘nonaqueous” nonpolar. The maximum additional water amounts corresponded in the range of the estimated RCMC to much less than 0.15 mol water/mol EO in dichloroethane solution, and much less than 0.05 mol water/mol EO in chloroform, and tests had proven that the RCMC values were not sensitive to small but significant changes of water content in this very low range. Therefore, the effect of water to promote aggregation should be excluded. As noted previously, the modifiers PE10500 and PEG400 distearate had very low RCMC (generally < 10 g/L), and these values were much lower than the concentrations used for entrapment modification (25 g/L). It can be well understood that the reverse micelle of the tri-block amphiphilic (macro)molecules with nonpolar corona (PPO/alkyl blocks) and polar core (PEO/PEG blocks) is easier to incorporate into nonpolar PP polymer chains than random macromolecules. Hence, the presence of reverse micelles seems to promote the embedment of amphiphilic modifiers into nonpolar PP

surface. Furthermore, during the subsequent step in water (not for deswelling as mentioned in other work [114-118,121,122,124], because the organic solvent cannot be replaced by water), it is expected that a reorientation of tri-block amphiphilic (macro)molecules at the interface of oil/water happens so that the inner PEO/PEG chains tend to stretch into the water phase. Consequently, we deduce that, in nonaqueous and nonpolar microenvironment, the relatively balanced structure of the two different kinds of blocks of amphiphilic modifiers was most important for formation of reverse micelles. It presumably increases the adsorption tendency and promotes the subsequent embedment of modifier into the PP surface (cf. Figure 5.3). Brandani and Stroeve also mentioned the importance of a balanced structure of Pluronics® in adsorption although their study was focused on aqueous systems [207].

Moreover, another special case was found in entrapment process, $C_{18}EO_8$, different with the above tri-block amphiphilic (macro)molecules. This diblock amphiphilic substance was very effective to improve PP membrane surface hydrophilicity and anti-fouling properties (cf. Section 4.2.3), but it cannot form reverse micelles at 25 g/L (and even up to 100 g/L, cf. Table 4.15). As described in the literature, there were very few aggregates of $C_{18}EO_8$ in pure nonpolar solvent (heptane or decane) even when the amphiphilic concentration was above RCMC (60~70 g/L or ~ 3×10^5 μM) [209,215]. Thereby, we believe that for this small diblock amphiphilic molecule, the key fact to promote incorporation into nonpolar PP surface is its flexibility and good, more or less random, dispersion into the PP surface.

5.2.2. Evaluation and argument of entrapment: Coating? Adsorption/deposition?

Entrapment is one type of physical methods for introducing functional species into polymer substrate. It is necessary to clarify the difference between entrapment and other physical

surface modification techniques, such as coating. In case of Hubbell's research, angle resolved studies were done on the modified surface with the electron energy analyzer at different angles from surface normal ranging from 0° to 75° in steps of 15°, and they detected the existence of PEO rich in the upper PET surface region of 5 ~ 20 nm. From this result, we can believe that the molecular entanglement is achieved. Hubbell depicted this surface structure as "surface physical interpenetrating networks", which was "in" the substrate upper surface region [115]. By contrast, coating functional species 'onto' substrate surface is realized via the physical interactions between molecular and substrate surface, such as hydrophobic-hydrophobic interaction or hydrogen bond interaction etc (cf. Figure 5.4) [205,207]. The coating layer and substrate are two separated phases. On the other hand, entrapment as surface modification strategy especially focuses on polymer surface engineering because of its reversible swelling/deswelling property; whereas coating has more wide applications on many surfaces, such as glass, Au, silicon wafer as well as polymer surfaces [202,216,217]. Therefore, in this dissertation, the method of incorporation of modifier to polymer surface is preferred to be "entrapment", rather than "coating".

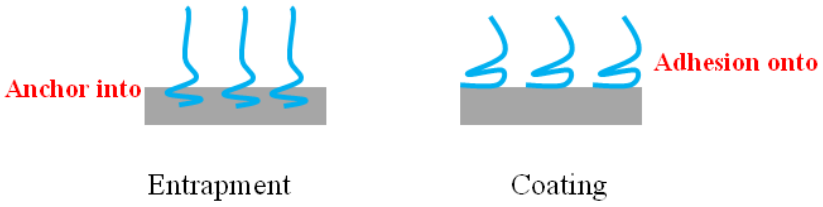

Figure 5.4 Schematic drawing of difference between entrapment and coating.

Similar to XPS results, in case of e.g. $C_{18}EO_8$-modified PP surface, it has been found that the modifiers existed mainly in amorphous region of polymer surface, which part was more easily to be swollen and loose to form larger space for modifiers (cf. Figure 4.29) than crystalline region. This result proved the swelling function and the further entrapment rather

than coating. The case in Section 4.4 has strongly validated that film surface modification is dominated by molecular entanglement under the deswelling way of solvent extraction.

Nevertheless, there is still an argument of surface adsorption/deposition on membrane surface. Ruckenstein once mentioned that the modification was from deposition [116]. The existence of PEGs or $C_{18}EO_{136}C_{18}$ on PP membrane surface has been detected from gravimetric change, ATR-FTIR, but there is no surface wettability improvement (cf. Figure 4.66a, Figure 4.66e, Figure 4.68 in Section 4.5). That means these modifiers could attach or deposit on membrane surface or even pores, but the amount is too small to affect surface property. The inefficient attachment or adsorption of modifier onto polymer substrate surface can be explained theoretically by the non-adsorbing model in Figure 2.5, which is mainly due to the weak interaction between modifier and polymer surface, as judged by Flory parameter χ. For example, in 1,2-dichloroethane, χ_{PEG} is -0.31, which is much smaller than χ_{PP} of 0.97 [98], therefore, this polymer cannot adsorb onto PP surface. On the other hand, for $C_{18}EO_8$ efficient modified PP, pore-blocking can be detected and deduced from gravimetric change, permporometry, SEM as well as water flux (cf. Section 4.2.3). However, the influence of pore-narrowing is much small when macromolecule cP1 was used as modifier (cf. Figure 4.44 in Section 4.3). On behalf of pore-narrowing, the possible presence of outer surface adsorption/deposition could not be excluded. But different with the inefficient attachment of PEGs on membrane surface, the pore-narrowing might be from the modifier molecular interactions and aggregation, like cake layer formation process of protein on membrane surface. But this deposition is accompanied by entrapment process.

Considering the adsorption/deposition is hard to be absolutely avoided especially in case of porous membrane surface modification, it is possible to think about utilize this property combination with entrapment for surface modification. For example, $C_{18}EO_8C_{18}$ and cP1 are amphiphilic but not well water soluble at room temperature, for this reason, there should be

no molecular leaching during deswelling process in water. That is to say, there could be much non-entrapped modifiers deposited on membrane surface even after water elution for 2.5 h at room temperature (cf. Figure 4.22). It has been reported in some literatures that the stability of coating layer is dependent on the (ir)reversibility of the non-covalent attachment [218-220]. Thereby, adopting such amphiphilic molecules - which own hydrophilicity but worse water soluble - as modifiers can acquire better stability than e.g. $C_{18}EO_8$-modified PP membrane in water (Figure 4.37 ~ 4.39).

In conclusion, swelling and deswelling are two important steps to decide the feasibility and efficiency of entrapment of modifiers into polymer substrate. The principle of swelling solvent selection is relaying on the property of polymer substrate and type of modifier; the deswelling solvent selection and the modifier configuration on the interface of membrane are related to the type of swelling solvent. The modifier structure can affect final membrane/air interface structure and property. Adsorption/deposition accompanying with entrapment in some cases, can be utilized for enhancing water stability concerning the specific modifier property. On the basics of the above principles, entrapment functionalization can be flexibly and widely applied in membrane technology and other fields in order to tailor base polymers to the requirements of certain applications.

Chapter 6

Conclusion and outlook

6.1. Conclusion of this dissertation

Polar PES (MF membrane) and nonpolar PP (MF membranes from different company, plate, film) have been used as substrate, a family of hydrophilic homopolymer PEG with a M_w range of 400 ~ 200,000 g/mol, nonionic amphiphilic (macro)molecules of di-/tri-block structures and different end-group for triblock amphiphilic (macro)molecules, PNIPAAm-based thermo-responsive homopolymer/block copolymers, as well as cationic block copolymer have been used as modifier for membrane surface functionalization. Entrapment technique was carried out through the whole dissertation for incorporating the above modifiers into PES or PP surface, to impart desirable functional properties such as hydrophilicity, thermo-responsive and cationic surface respectively. The general results can be concluded as:

i. The entrapment method has been initially performed as reported in literatures for polar PES membrane surface modification. The surface wettability can be further improved by successful entrapment of series PEG or PEO-based amphiphilic polymers. Controlling the condition with high organic solvent content in water-diluted solvent is more important than high concentration. Moreover, E1 procedure is decided for the whole project because of the higher efficiency compared with E2. Therein, E1 is performed by diffusing modifiers during swelling process in organic solution, and following solvent evaporation for entrapment; while E2 is performed by swelling in organic solvent firstly, and then the modifiers are anticipated to diffuse and entrap

into polymer substrate surface in aqueous solution.

ii. A simple, effective surface engineering method, entrapment of the amphiphilic modifier $C_{18}EO_8$, was shown to yield strong improvements of surface hydrophilicity and pore wetting of PP microfiltration membranes. This contributed also to improve antifouling properties. One advantage of this entrapment technique as compared to many chemical strategies was the only very slight negative influence on membrane and polymer structure. By combination of various characterization methods, it has been confirmed that both outer membrane surface and inner pore walls were modified, i.e., the entrapment method has the potential for achieving a relatively homogeneous modification. Moreover, while former entrapment studies mainly stressed a "two-liquid" sequence and focused on polar solvent systems, our work is different in that it is generally applicable to nonpolar systems by using amphiphilic molecules as modifier through a "one-liquid" process. Therefore, the range of entrapment study can be expanded to any polymer substrate when suitable solvent and modifier are identified. In this study, the feasibility of entrapment technique for PP microfiltration membrane surface hydrophilic modification had been demonstrated.

iii. It is further demonstrated that a thermo-responsive PP microfiltration membrane can be fabricated via simple surface entrapment of PNIPAAm-containing macromolecules, preferably an amphiphilic block copolymer PBA-*b*-PNIPAAm (cP1) with a balanced hydrophilic/hydrophobic structure. A modifier concentration of 20 g/L in THF, at 20 °C for 20 h, and immersion for 20 min in water for deswelling before drying were found to be the best suited conditions for this PP surface modification. Those conditions could serve as starting point for further optimization, e.g., to decrease modification time. The results with nonporous PP plates, surface modified under the same conditions, also confirmed that the modification efficiency

was not dominated by a simple deposition of the modifier in the membrane pores. Significant surface hydrophilization as well as switchable properties with respect to wettability had been achieved. Moreover, the LCST of a non-water soluble amphiphilic block copolymer, PBA-*b*-PNIPAAm (cP1), in pure water had been estimated in terms of an abrupt water permeability change at 31~32 °C. In conclusion, this study further validated that a relatively balanced hydrophilic/hydrophobic chain/segment length, is very efficient for PP surface modification. The results for deswelling under different conditions confirm that water-miscible organic solvents are much preferred to be selected as swelling solvent than nonpolar solvents, if this is possible considering the solubility of the modifier.

iv. On the basis of above results and conclusions, hydrophobic nonionic PP film surface was imparted with hydrophilic and charged property with entrapment of PBA-*b*-P*q*DMAEMA. A series of solvent replacement and extraction methods have been compared, and finally S'SD1 and SD2 are selected to be most suitable way for effective deswelling without deposition or leaching. Here S'SD1 is a treatment process of replacing impregnating PP with modifier into "solution at room temperature for 5 min – corresponding mutual solvent at room temperature for 5 min – vacuum dry", and SD2 is a deswelling treatment process of replacing impregnating PP with modifier into "o-xylene at room temperature for 5 min – vacuum dry". These results strongly confirmed that the modification is from entanglement of modifier chains with polymer substrate.

Furthermore, the mechanism of entrapment behavior has been investigated from the selection of swelling solvent, deswelling solvent/solution, as well as the modifier. The whole entrapment process includes two steps of first diffusion (embedment) in swelling region, and subsequently anchoring (entrapment). It has been revealed that the PEG or other hydrophilic

block chain length has not direct contribution to the resulting hydrophilic modification, instead, too long chain length will limit the diffusion efficiency of modifiers into swelling polymer surface. The possibility of entrapping homopolymer or amphiphilic (macro)molecules is up to polarity of solution environment, which also decides the different entrapment behavior and interface configuration of modifiers. In polar environment, the polar and hydrophilic homopolymers or molecules are well soluble in solvent so that they can enter swelling network with solution droplet. In nonpolar environment, it can be concluded that in nonpolar solution system (e.g. 1,2-dichloroethane), 1) amphiphilic (macro)molcecules are more efficient for improve PP surface hydrophicility and antifouling capacity than PEG homopolymer; 2) diblock and small amphiphilic molecules tend to disperse and subsequently entrapped into PP surface; 3) the hydrophilically end-capped structure of amphiphilic tri-block macromolecules was better suited than the reverse, hydrophobically end-capped structure. More importantly, the relative balance of hydrophilic and hydrophobic chain lengths within the macromolecule seems to be the most important fact to decide upon the embedment behavior during entrapment modification process. The balance structure of hydrophilic/hydrophobic blocks, which promotes macromolecule self-association to form nonpolar shell reverse micelles, is the basis for a high modification efficiency.

6.2. Outlook of future work

Adaptations and applications of entrapment modification strategy could be done with various block copolymer modifiers rendering membrane and other material's surfaces more functional, according to the principles deduced and confirmed previously in this project. As to film surface modification, it is interesting to obtain more surface information after

modification, such as morphology (from AFM) and surface chemical composition (XPS) because of the sensitivity limitation of FTIR. It is interesting to investigate the structure of ionic amphiphilic polymer, such as PBA-*b*-P*q*DMAEMA in mutual solvent, this could be helpful to understand the influence of ionic modifiers on embedment/entrapment efficiency. In addition, E2 procedure might be interesting to do more detailed research work. This would be helpful to understand the entrapment behavior.

References

[1] M. Ulbricht, Advanced functional polymer membranes, Polymer 47 (2006) 2217-2262.

[2] M.A.C. Stuart, W.T.S. Huck, J. Genzer, M. Muller, C. Ober, M. Stamm, G.B. Sukhorukov, I. Szleifer, V.V. Tsukruk, M. Urban, F. Winnik, S. Zauscher, I. Luzinov, S. Minko, Emerging applications of stimuli-responsive polymer materials, Nature Material 9 (2010) 101-113.

[3] M. Motornov, S. Ro, R. Lupitskyy, E. MacWilliams, O. Hoy, I. Luzinov, S. Minko, Stimuli-responsive colloidal systems from mixed brush-coated nanoparticles, Advanced Functional Materials 17 (2007) 2307-2314.

[4] Y. Kouwonou, R. Malaisamy, K.L. Jones, Modification of PES membrane: reduction of biofouling and improved flux recovery, Separation Science and Technology 43 (2008) 4099-4112.

[5] H. Susanto, M. Ulbricht, Photografted thin polymer hydrogel layers on PES ultrafiltration membranes: characterization, stability, and influence on separation performance, Langmuir 23 (2007) 7818-7830.

[6] K.J. Choi, E.H. Hwang, Y.W. Rhee, T.S. Hwang, Preparation and properties of aminated poly(ethersulfone) ion-exchange membrane by UV irradiation method, Polymer (Korea) 32 (2008) 70-76.

[7] S.X. Liu, J.T. Kim, S. Kim, Effect of polymer surface modification on polymer-protein interaction via hydrophilic polymer grafting, Journal of Food Science 73 (2008) E143-E150.

[8] S.X. Liu, J.T. Kim, S. Kim, M. Singh, The effect of polymer surface modification via interfacial polymerization on polymer-protein interaction, Journal of Applied Polymer Science 112 (2009) 1704-1715.

[9] R. Malaisamy, D. Berry, D. Holder, L. Raskin, L. Lepak, K.L. Jones, Development of reactive thin film polymer brush membranes to prevent biofouling, Journal of Membrane Science 350 (2010) 361-370.

[10] M. Kral, A. Ogino, K. Narushima, N. Inagaki, M. Yamashita, M. Nagatsu, Low-temperature nitrogen introduction onto polyurethane surface using surface-wave

excited N_2/H_2 plasma, Japanese Journal of Applied Physics, Part 1: Regular Papers and Short Notes and Review Papers 46 (2007) 7470-7474.

[11] K.R. Kull, M.L. Steen, E.R. Fisher, Surface modification with nitrogen-containing plasmas to produce hydrophilic, low-fouling membranes, Journal of Membrane Science 246 (2005) 203-215.

[12] H.U. Lee, S.Y. Park, Y.H. Kang, S.Y. Jeong, S.H. Choi, K.Y. Jahng, C.R. Cho, Surface modification of and selective protein attachment to a flexible microarray pattern using atmospheric plasma with a reactive gas, Acta Biomaterialia 6 (2010) 519-525.

[13] B. Van Der Bruggen, Chemical modification of polyethersulfone nanofiltration membranes: A review, Journal of Applied Polymer Science 114 (2009) 630-642.

[14] T. Vatuňa, P. Špatenka, J. Píchal, J. Koller, L. Aubrecht, J. Wiener, PES fabric plasma modification, Czechoslovak Journal of Physics 54 (2009) C475-C482.

[15] A. Vesel, XPS study of surface modification of different polymer materials by oxygen plasma treatment, Informacije MIDEM 38 (2008) 257-265.

[16] A. Vesel, M. Mozetic, Surface functionalization of organic materials by weakly ionized highly dissociated oxygen plasma, Journal of Physics: Conference Series 162 (2009).

[17] D.S. Wavhal, E.R. Fisher, Hydrophilic modification of polyethersulfone membranes by low temperature plasma-induced graft polymerization, Journal of Membrane Science 209 (2002) 255-269.

[18] D.S. Wavhal, E.R. Fisher, Modification of porous poly(ether sulfone) membranes by low-temperature CO_2-plasma treatment, Journal of Polymer Science, Part B: Polymer Physics 40 (2002) 2473-2488.

[19] M.L. Steen, A.C. Jordan, E.R. Fisher, Hydrophilic modification of polymeric membranes by low temperature H_2O plasma treatment, Journal of Membrane Science 204 (2002) 341-357.

[20] L.P. Zhu, B.K. Zhu, L. Xu, Y.X. Feng, F. Liu, Y.Y. Xu, Corona-induced graft polymerization for surface modification of porous polyethersulfone membranes, Applied Surface Science 253 (2007) 6052-6059.

[21] E.S.A. Hegazy, H.A. AbdEl-Rehim, H. Kamal, K.A. Kandeel, Advances in radiation grafting, Nuclear Instruments and Methods in Physics Research, Section B: Beam Interactions with Materials and Atoms 185 (2001) 235-240.

[22] S. Kroll, L. Meyer, A.M. Graf, S. Beutel, J. Glökler, S. Döring, U. Klaus, T. Scheper, Heterogeneous surface modification of hollow fiber membranes for use in micro-reactor systems, Journal of Membrane Science 299 (2007) 181-189.

[23] T. He, M.H.V. Mulder, H. Strathmann, M. Wessling, Preparation of composite hollow fiber membranes: Co-extrusion of hydrophilic coatings onto porous hydrophobic support structures, Journal of Membrane Science 207 (2002) 143-156.

[24] G.L. Tao, A.J. Gong, J.J. Lu, H.J. Sue, D.E. Bergbreiter, Surface functionalized polypropylene: synthesis, characterization, and adhesion properties, Macromolecules 34 (2001) 7672-7679.

[25] R. Dhamodharan, A. Nisha, K. Pushkala, T.J. McCarthy, Investigation of the mercat reaction as a tool for the introduction of nitrogen surface functionality on linear low-density polyethylene (LLDPE) and polypropylene (PP), Langmuir 17 (2001) 3368-3374.

[26] H.M. Ma, R.H. Davis, C.N. Bowman, A novel sequential photoinduced living graft polymerization, Macromolecules 33 (1999) 331-335.

[27] C.H. Bamford, K.G. Al-Lamee, Studies in polymer surface functionalization and grafting for biomedical and other applications, Polymer 35 (1994) 2844-2852.

[28] T. Rieser, K. Lunkwitz, S. Berwald, J. Meier-Haack, M. Müller, F. Cassel, Z. Dioszeghy, F. Simon, Surface modification of microporous polypropylene membranes by polyelectrolyte multilayers, ACS Symposium Series, 744 (1999) 189-204.

[29] T. Czvikovszky, H. Hargitai, Electron beam surface modifications in reinforcing and recycling of polymers, Nuclear Instruments and Methods in Physics Research, Section B: Beam Interactions with Materials and Atoms 131 (1997) 300-304.

[30] J.W. Lee, T.H. Kim, S.H. Kim, C.Y. Kim, Y.H. Yoon, J.S. Lee, J.G. Han, Investigation of ion bombarded polymer surfaces using SIMS, XPS and AFM, Nuclear Instruments and Methods in Physics Research, Section B: Beam Interactions with Materials and Atoms 121 (1997) 474-479.

[31] P.Y. Apel, A.Y. Didyk, A.G. Salina, Physico-chemical modification of polyolefins irradiated by swift heavy ions, Nuclear Instruments and Methods in Physics Research, Section B: Beam Interactions with Materials and Atoms 107 (1996) 276-280.

[32] D. Klein, E. Tomasella, V. Labed, C. Meunier, P. Cetier, M.C. Robé, A. Chambaudet, Radon 222 permeation through different polymers (PVC, EVA, PE and PP) after exposure to gamma radiation or surface treatment by cold plasma, Nuclear

Instruments and Methods in Physics Research Section B: Beam Interactions with Materials and Atoms 131 (1997) 392-397.

[33] R.Q. Kou, Z.K. Xu, H.T. Deng, Z.M. Liu, P. Seta, Y.Y. Xu, Surface modification of microporous polypropylene membranes by plasma-induced graft polymerization of α-Allyl Glucoside, Langmuir 19 (2003) 6869-6875.

[34] L. Liang, M. Shi, V.V. Viswanathan, L.M. Peurrung, J.S. Young, Temperature-sensitive polypropylene membranes prepared by plasma polymerization, Journal of Membrane Science 177 (2000) 97-108.

[35] N. Shahidzadeh-Ahmadi, M.M. Chehimi, F. Arefi-Khonsari, N. Foulon-Belkacemi, J. Amouroux, M. Delamar, A physicochemical study of oxygen plasma-modified polypropylene, Colloids and Surfaces A: Physicochemical and Engineering Aspects 105 (1995) 277-289.

[36] M. Collaud Coen, P. Groening, L. Schlapbach, Plasma treatment and plasma polymerisation: How to design surfaces for specific applications, Vide: Science, Technique et Applications 291 SUPPL. 2 (1999) 162-167.

[37] A. Nihlstrand, T. Hjertberg, K. Johansson, Plasma treatment of polyolefins: Influence of material composition: 1. Bulk and surface characterization, Polymer 38 (1997) 3581-3589.

[38] A. Nihlstrand, T. Hjertberg, Plasma treatment of polyolefins: Influence of plasma parameters and material composition on paint adhesion, American Chemical Society, Polymer Preprints, Division of Polymer Chemistry 38 (1997) 1055-1056.

[39] A. Nihlstrand, T. Hjertberg, K. Johansson, Adhesion properties of oxygen plasma-treated polypropylene-based copolymers, Polymer 38 (1997) 1557-1563.

[40] A. Nihlstrand, T. Hjertberg, K. Johansson, Plasma treatment of polyolefins: Influence of material composition: 2. Lacquer adhesion and locus of failure, Polymer 38 (1997) 3591-3599.

[41] S.A. Piletsky, H. Matuschewski, U. Schedler, A. Wilpert, E.V. Piletska, T.A. Thiele, M. Ulbricht, Surface functionalization of porous polypropylene membranes with molecularly imprinted polymers by photograft copolymerization in water, Macromolecules 33 (2000) 3092-3098.

[42] Z.M. Liu, Z.K. Xu, M. Ulbricht, Surface modification of polypropylene microporous membrane by tethering polypeptides, Chinese Journal of Polymer Science (English Edition) 24 (2006) 529-538.

[43] D. He, M. Ulbricht, Tailored "grafting-from" functionalization of microfiltration membrane surface photo-initiated by immobilized iniferter, Macromolecular Chemistry and Physics 210 (2009) 1149-1158.

[44] H. Yang, M. Ulbricht, Synthesis and performance of PP microfiltration membranes grafted with polymer layers of different structure, Macromolecular Materials and Engineering 293 (2008) 419-427.

[45] A.H.M. Yusof, M. Ulbricht, Polypropylene-based membrane adsorbers via photo-initiated graft copolymerization: Optimizing separation performance by preparation conditions, Journal of Membrane Science 311 (2008) 294-305.

[46] D. He, H. Susanto, M. Ulbricht, Photo-irradiation for preparation, modification and stimulation of polymeric membranes, Progress in Polymer Science 34 (2009) 62-98.

[47] A.H.M. Yusof, M. Ulbricht, Structure variations of the grafted functional polymer brush enhance membrane adsorber performance, Desalination 236 (2009) 16-22.

[48] A.H.M. Yusof, M. Ulbricht, Effects of photo-initiation and monomer composition onto performance of graft-copolymer based membrane adsorbers, Desalination 200 (2006) 462-463.

[49] D. He, M. Ulbricht, Surface-selective photo-grafting on porous polymer membranes via a synergist immobilization method, Journal of Materials Chemistry 16 (2006) 1860-1868.

[50] H. Yang, D. Lazos, M. Ulbricht, Thin, highly crosslinked polymer layer synthesized via photoinitiated graft copolymerization on a self-assembled-monolayer-coated gold surface, Journal of Applied Polymer Science 97 (2005) 158-164.

[51] M. Ulbricht, H. Yang, Porous polypropylene membranes with different carboxyl polymer brush layers for reversible protein binding via surface-initiated graft copolymerization, Chemistry of Materials 17 (2005) 2622-2631.

[52] Q. Yang, Z.K. Xu, Z.W. Dai, J.L. Wang, M. Ulbricht, Surface modification of polypropylene microporous membranes with a novel glycopolymer, Chemistry of Materials 17 (2005) 3050-3058.

[53] A. Delcorte, P. Bertrand, E. Wischerhoff, A. Laschewsky, Adsorption of polyelectrolyte multilayers on polymer surfaces, Langmuir 13 (1997) 5125-5134.

[54] C.G.P.H. Schroen, M.C. Wijers, M.A. Cohen-Stuart, A. Van der Padt, K. Van 't Riet, Membrane modification to avoid wettability changes due to protein adsorption in an emulsion/membrane bioreactor, Journal of Membrane Science 80 (1993) 265-274.

[55] F. Peñacorada, A. Angelova, H. Kamusewitz, J. Reiche, L. Brehmer, Scanning force microscopy and wetting study of the surface modification of a polypropylene membrane by means of Langmuir-Blodgett film deposition, Langmuir 11 (1995) 612-617.

[56] D.E. Bergbreiter, Polyethylene surface chemistry, Progress in Polymer Science 19 (1994) 529-560.

[57] R.M. France, R.D. Short, Plasma treatment of polymers:the effects of energy transfer from an argon plasma on the surface chemistry of polystyrene, and polypropylene. a high-energy resolution X-ray photoelectron spectroscopy study, Langmuir 14 (1998) 4827-4835.

[58] A. Bhattacharya, J.W. Rawlins, P. Ray, Polymer grafting and crosslinking, John Wiley & Sons, Inc., New Jersey, 2009.

[59] Z.P. Fang, Y.H. Song, L. Shen, Polymer physics, Zhejiang University, Hangzhou, 2005.

[60] X.-J. Yang, T. Fane, Effect of membrane preparation on the lifetime of supported liquid membranes, Journal of Membrane Science 133 (1997) 269-273.

[61] A. Kloczkowski, Theoretical models for polymer chains, in: J.E. Mark (Ed.), Physical Properties of Polymers Handbook, AIP Press, New York, 1996.

[62] P.J. Flory, Theory of elasticity of polymer networks. The effect of local constraints on junctions, The Journal of Chemical Physics 66 (1977) 5720-5729.

[63] L.H. Sperling, D.W. Friedman, Synthesis and mechanical behavior of interpenetrating polymer networks: Poly(ethyl acrylate) and polystyrene, Journal of Polymer Science Part A-2: Polymer Physics 7 (1969) 425-427.

[64] L.H. Sperling, Interpenetrating polymer networks and related materials, Journal of Polymer Science: Macromolecular Reviews 12 (1977) 141-180.

[65] S.J. Kim, S.G. Yoon, I.Y. Kim, S.I. Kim, Swelling characterization of the semiinterpenetrating polymer network hydrogels composed of chitosan and poly(diallyldimethylammonium chloride), Journal of Applied Polymer Science 91 (2004) 2876-2880.

[66] S.J. Kim, S.G. Yoon, S.I. Kim, Synthesis and characteristics of interpenetrating polymer network hydrogels composed of alginate and poly(diallydimethylammonium chloride), Journal of Applied Polymer Science 91 (2004) 3705-3709.

[67] S.J. Kim, S.G. Yoon, S.I. Kim, Synthesis and characterization of an interpenetrating polymer network composed of poly(methacrylic acid) and poly(vinyl alcohol), Polymer International 54 (2005) 149-152.

[68] S. Goswami, S. Nad, D. Chakrabarty, Modification of novolac resin by interpenetrating network formation with poly(butyl acrylate), Journal of Applied Polymer Science 97 (2005) 2407-2417.

[69] C.J. McDonald, P.B. Smith, J.A. Roper, D.I. Lee, J.G. Galloway, NMR linewidth study of a latex interpenetrating network, Colloid & Polymer Science 269 (1991) 227-241.

[70] S. Goswami, D. Chakrabarty, Synthesis and characterization of sequential interpenetrating polymer networks of novolac resin and poly(ethyl acrylate), Journal of Applied Polymer Science 99 (2006) 2857-2867.

[71] C.E.C. Jr., Introduction to polymer chemistry, CRC Press, New York, 2007.

[72] http://www.nexans.be/eservice/Belgiumen/navigate_232142.

[73] L.H. Sperling, Introduction to physical polymer science, Wiley, New York, 1986.

[74] H. Tadokoro, Structure of crystalline polymers, Wiley, New York, 1979.

[75] K. Mezghani, P.J. Phillips, Crysallization kinetics of polymers, in: J.E. Mark (Ed.), Physical Properties of Polymers Handbook, AIP Press, New York, 1996.

[76] R.B. Seymour, C.E. Carraher, Structure-property relationships in polymers, Plenum Publishing, New York, 1984.

[77] Z.P. Fang, Y.H. Song, L. Shen, Polymer physics, Zhejiang University, Hangzhou, 2005.

[78] C.M. Hansen, The three dimensional solubility parameter and xolvent diffusion coefficient: their importance in surface coating formulation, vol. Doctor, Danish Technical Press, Copenhagen, 1967.

[79] C.M. Hansen, The universality of the solubility parameter, Industrial & Engineering Chemistry Product Research and Development 8 (1969) 2-11.

[80] C.M. Hansen, The three dimensional solubility parameter - key to paint component affinities I. - solvents, plasticizers, polymers, and resins, J. Paint Techn. 39 (1967) 104-117.

[81] C.M. Hansen, The three dimensional solubility parameter - key to paint component affinities II. - dyes, emulsifiers, mutual solubility and compatibility, and pigments, J. Paint Techn. 39 (1967) 511-514.

[82] C.M. Hansen, On application of the three dimensional solubility parameter to the prediction of mutual solubility and compatibility, Faerg och Lack 13 (1967) 132-138.

[83] C.M. Hansen, Solvent selection by computer, in: R.W. Tess (Ed.), Advances in Chemistry Series, American Chemical Society, Washington, 1973.

[84] C.M. Hansen, E. Wallström, On the use of cohesion parameters to characterize surfaces, J. Adhesion 15 (1983) 275-286.

[85] R.F. Blanks, Thermodynamics of polymer solutions, Polymer-Plastics Technology and Engineering 8 (1977) 13 - 33.

[86] M.T. Shaw, Studies of polymer-polymer solubility using a two-dimensional solubility parameter approach, Journal of Applied Polymer Science 18 (1974) 449-472.

[87] V. Brucato, G. Titomanlio, Movement of phase-transition front in a constant-wall-temperature slab, Industrial & Engineering Chemistry Research 26 (1987) 1722-1724.

[88] B. Schneier, An equation for calculating the solubility parameter of random copolymers, Journal of Polymer Science Part B: Polymer Letters 10 (1972) 245-251.

[89] P.E. Froehling, L.T. Hillegers, Solubility parameters of ternary solvent mixtures; calculation of the solvent composition with maximum polymer interaction, Polymer 22 (1981) 261-262.

[90] Z. Rigbi, Prediction of swelling of polymers in 2 and 3 component solvent mixtures, Polymer 19 (1978) 1229-1232.

[91] W. Zeng, Y. Du, Y. Xue, H. Frisch, Solubility parameters, Physical properties of polymers handbook, 2007, pp. 289-303.

[92] P.J. Flory, Constitution of three-dimensional polymers and the theory of gelation, The Journal of Physical Chemistry 46 (1942) 132-140.

[93] M.L. Huggins, Some properties of solutions of long-chain compounds, The Journal of Physical Chemistry 46 (1942) 151-158.

[94] M.L. Huggins, Theory of solutions of high polymers1, Journal of the American Chemical Society 64 (1942) 1712-1719.

[95] M.L. Huggins, The viscosity of dilute solutions of long-chain molecules. IV. dependence on concentration, Journal of the American Chemical Society 64 (1942) 2716-2718.

[96] M.L. Huggins, Solutions of long chain compounds, The Journal of Chemical Physics 9 (1941) 440-440.

[97] P.J. Flory, Principle of polymer chemistry, Corncell University Press, Ithaca, 1953.

[98] R.A. Orwoll, P.A. Arnold, Polymer-solvent interaction parameter χ, in: J.E. Mark (Ed.), Physical properties of polymers handbook, AIP Press, New York, 2007, pp. 177-196.

[99] J. Goodwin, Colloids and interfaces with surfactants and polymers 2nd ed., Wiely, Chichester, 2009.

[100] J.M.H.M. Scheutjens, G.J. Fleer, Statistical theory of the adsorption of interacting chain molecules. 1. Partition function, segment density distribution, and adsorption isotherms, The Journal of Physical Chemistry 83 (1979) 1619-1635.

[101] P.G. de Gennes, Conformations of polymers attached to an interface, Macromolecules 13 (1980) 1069-1075.

[102] P.G. de Gennes, Polymers at an interface; a simplified view, Advances in Colloid and Interface Science 27 (1987) 189-209.

[103] J. You, J.A. Yoon, J. Kim, C.-F. Huang, K. Matyjaszewski, E. Kim, Excimer emission from self-assembly of fluorescent diblock copolymer prepared by atom transfer radical polymerization, Chemistry of Materials (2010) 4426-4434.

[104] R.J. Bergeron, O. Phanstiel, G.W. Yao, S. Milstein, W.R. Weimar, Macromolecular self-assembly of diketopiperazine tetrapeptides, Journal of the American Chemical Society 116 (1994) 8479-8484.

[105] C. Cecutti, B. Focher, B. Perly, T. Zemb, Glycolipid self-assembly: micellar structure, Langmuir 7 (1991) 2580-2585.

[106] L. Cusack, S.N. Rao, J. Wenger, D. Fitzmaurice, Self-assembly of heterosupermolecules, Chemistry of Materials 9 (1997) 624-631.

[107] J. Das, J.M.J. Fréchet, A.K. Chakraborty, Self-assembly of dendronized polymers, The Journal of Physical Chemistry B 113 (2009) 13768-13775.

[108] T. Guo, P. Nikolaev, A.G. Rinzler, D. Tomanek, D.T. Colbert, R.E. Smalley, Self-assembly of tubular fullerenes, The Journal of Physical Chemistry 99 (1995) 10694-10697.

[109] B. Ozbas, P. Schneider Joel, J. Pochan Darrin, Hydrogels constructed via β-Hairpin peptide self-assembly, Advances in biopolymers, American Chemical Society 935 (2006) 284-297.

[110] K.-M. Park, S.-Y. Kim, J. Heo, D. Whang, S. Sakamoto, K. Yamaguchi, K. Kim, Designed self-assembly of molecular necklaces, Journal of the American Chemical Society 124 (2002) 2140-2147.

[111] R.-S. Shih, C.-H. Lu, S.-W. Kuo, F.-C. Chang, Hydrogen bond-mediated self-assembly of polyhedral oligomeric silsesquioxane-based supramolecules, The Journal of Physical Chemistry C 114 (2010) 12855-12862.

[112] H. Yang, P. Jiang, Large-scale colloidal self-assembly by doctor blade coating, Langmuir 26 (2010) 13173-13182.

[113] R.I. Hancock, Macromolecular surfactants, in: T. Tadros (Ed.), Surfactants, Academic Press, London, 1984, pp. 287-321.

[114] N.P. Desai, J.A. Hubbell, Solution technique to incorporate polyethylene oxide and other water-soluble polymers into surfaces of polymeric biomaterials, Biomaterials 12 (1991) 144-153.

[115] N.P. Desai, J.A. Hubbell, Surface physical interpenetrating networks of poly(ethylene terephthalate) and poly(ethylene oxide) with biomedical applications, Macromolecules 25 (1992) 226-232.

[116] E. Ruckenstein, D. Byungip Chung, Surface modification by a two-liquid process deposition of A-B block copolymers, Journal of Colloid and Interface Science 123 (1988) 170-185.

[117] R.A. Quirk, M.C. Davies, S.J.B. Tendler, W.C. Chan, K.M. Shakesheff, Controlling biological interactions with poly(lactic acid) by surface entrapment modification, Langmuir 17 (2001) 2817-2820.

[118] R.A. Quirk, M.C. Davies, S.J.B. Tendler, K.M. Shakesheff, Surface engineering of poly(lactic acid) by entrapment of modifying species, Macromolecules 33 (2000) 258-260.

[119] R.M. Rasal, A.V. Janorkar, D.E. Hirt, Poly(lactic acid) modifications, Progress in Polymer Science 35 (2010) 338-356.

[120] J. Zhang, C.J. Roberts, K.M. Shakesheff, M.C. Davies, S.J.B. Tendler, Micro- and macrothermal analysis of a bioactive surface-engineered polymer formed by physical entrapment of poly(ethylene glycol) into poly(lactic acid), Macromolecules 36 (2003) 1215-1221.

[121] H. Zhu, A. Ji, R. Lin, C. Gao, L. Feng, J. Shen, Surface engineering of poly(D,L-lactic acid) by entrapment of chitosan-based derivatives for the promotion of chondrogenesis, Journal of Biomedical Materials Research 62 (2002) 532-539.

[122] H. Zhu, A. Ji, J. Shen, Surface engineering of poly (DL-lactic acid) by entrapment of biomacromolecules, Macromolecular Rapid Communications 23 (2002) 819-823.

[123] Z. Liu, Y. Jiao, Z. Zhang, C. Zhou, Surface modification of poly(L-lactic acid) by entrapment of chitosan and its derivatives to promote osteoblasts-like compatibility, Journal of Biomedical Materials Research Part A 83A (2007) 1110-1116.

[124] Z.F. Li, E. Ruckenstein, Two liquid adsorptive entrapment of a pluronic polymer into the surface of polyaniline films, Journal of Colloid and Interface Science 264 (2003) 370-377.

[125] Z.G. Li, S. Miyake, M. Kumagai, H. Saito, Y. Muramatsu, Hard nanocomposite Ti-Cu-N films prepared by d.c. reactive magnetron co-sputtering, Surface and Coatings Technology 183 (2004) 62-68.

[126] R. Langer, Drug delivery and targeting, Nature 392 (1998) 5-10.

[127] D.E. Bergbreiter, H.N. Gray, Studies of Two-Dimensional Morphology at Surface-Functionalized Polyethylene Films, Macromolecules 28 (1995) 8302-8307.

[128] D.E. Bergbreiter, B.C. Ponder, G. Aguilar, B. Srinivas, Temperature-responsive surface-functionalized polyethylene films, Chemistry of Materials 9 (1997) 472-477.

[129] D.E. Bergbreiter, B. Srinivas, Surface selectivity in blending polyethylene-poly(ethylene glycol) block cooligomers into high-density polyethylene, Macromolecules 25 (1992) 636-643.

[130] D.E. Bergbreiter, B. Walchuk, B. Holtzman, H.N. Gray, Polypropylene surface modification by entrapment functionalization, Macromolecules 31 (1998) 3417-3423.

[131] H. Chen, Y. Zhu, Y. Zhang, J. Xu, Synthesis and characterization of a macromolecular surface modifier for polypropylene, Journal of Applied Polymer Science 102 (2006) 3413-3419.

[132] H.J. Chen, X.H. Shi, Y.F. Zhu, Y. Zhang, J.R. Xu, Polypropylene surface modification by entrapment of polypropylene-graft-poly(butyl methacrylate), Applied Surface Science 254 (2008) 2521-2527.

[133] M. Xu, J. Qiu, Y. Lin, X. Shi, H. Chen, T. Xiao, Surface biocompatible modification of polypropylene by entrapment of polypropylene-block-poly(vinylpyrrolidone), Colloids and Surfaces B: Biointerfaces 80 200-205.

[134] M. Ulbricht, O. Schuster, W. Ansorge, M. Ruetering, P. Steiger, Influence of the strongly anisotropic cross-section morphology of a novel polyethersulfone microfiltration membrane on filtration performance, Separation and Purification Technology 57 (2007) 63-73.

[135] A.M. Barbe, P.A. Hogan, R.A. Johnson, Surface morphology changes during initial usage of hydrophobic, microporous polypropylene membranes, Journal of Membrane Science 172 (2000) 149-156.

[136] I. Gancarz, M. Bryjak, J. Kunicki, A. Ciszewski, Microwave plasma-initiated grafting of acrylic acid on Celgard 2500 membrane to prepare alkaline battery separators—Characteristics of process and product, Journal of Applied Polymer Science 116 (2010) 868-875.

[137] A. Schäfer, M.M. Hossain, Extraction of organic acids from kiwifruit juice using a supported liquid membrane process, Bioprocess and Biosystems Engineering 16 (1996) 25-33.

[138] E. Berndt, M. Ulbricht, Synthesis of block copolymers for surface functionalization with stimuli-responsive macromolecules, Polymer 50 (2009) 5181-5191.

[139] E. Berndt, S. Behnke, M. Ulbricht, Influence of alkyl chain length and molecular weight on the surface functionalization via adsorption/entrapment with biocidal cationic block copolymers, Macromolecular Chemistry and Physics (2010) in revision.

[140] D. Moeckel, E. Staude, M. Dal-Cin, K. Darcovich, M. Guiver, Tangential flow streaming potential measurements: Hydrodynamic cell characterization and zeta potentials of carboxylated polysulfone membranes, Journal of Membrane Science 145 (1998) 211-222.

[141] K. Rodemann, E. Staude, Electrokinetic characterization of porous membranes made from epoxidized polysulfone, Journal of Membrane Science 104 (1995) 147-155.

[142] C. Lettmann, D. Moeckel, E. Staude, Permeation and tangential flow streaming potential measurements for electrokinetic characterization of track-etched microfiltration membranes, Journal of Membrane Science 159 (1999) 243-251.

[143] J.M.M. Peeters, M.H.V. Mulder, H. Strathmann, Streaming potential measurements as a characterization method for nanofiltration membranes, Colloids and Surfaces A: Physicochemical and Engineering Aspects 150 (1999) 247-259.

[144] C. Geismann, A. Yaroshchuk, M. Ulbricht, Permeability and electrokinetic characterization of poly(ethylene terephthalate) capillary pore membranes with grafted temperature-responsive polymers, Langmuir 23 (2007) 76-83.

[145] P.C. Hiemenz, Principles of colloid and surface chemistry, Marcel Dekker, Inc., New York, 1977.

[146] p.m.P.B. COULTERTM SA 3100TM series surface area and pore size analyzers, Coulter Corporation, Miami, 1996.

[147] G. Ganesh, T.K.S. Kumar, S.T.K. Pandian, C. Yu, Rapid staining of proteins on polyacrylamide gels and nitrocellulose membranes using a mixture of fluorescent dyes, Journal of Biochemical and Biophysical Methods 46 (2000) 31-38.

[148] N.T. Hayner, J. Driscoll, L. Ferayorni, G. Spies-Karotkin, H.O. Jauregui, Ponceau S: A sensitive method for protein determination in freshly isolated and cultured cells, Methods in Cell Science 7 (1982) 77-80.

[149] T. McPherson, A. Kidane, I. Szleifer, K. Park, Prevention of protein adsorption by tethered poly(ethylene oxide) layers: Experiments and single-chain mean-field analysis, Langmuir 14 (1998) 176-186.

[150] F. Auriemma, C. De Rosa, Stretching isotactic polypropylene: from cross-β to crosshatches, from γ form to α form, Macromolecules 39 (2006) 7635-7647.

[151] J. Huang, X.L. Wang, W.S. Qi, X.H. Yu, Temperature sensitivity and electrokinetic behavior of a N-isopropylacrylamide grafted microporous polyethylene membrane, Desalination 146 (2002) 345-351.

[152] J.N. Israelachvili, Intermolecular & surface forces (2nd edition), Acad. Press, Darmstadt, 1992.

[153] H.J. Jacobasch, Interfaces, surfactants and colloids in engineering, Steinkopff, Leipzig 1996.

[154] M. Ulbricht, H. Matuschewski, A. Oechel, H.G. Hicke, Photo-induced graft polymerization surface modifications for the preparation of hydrophilic and low-protein-adsorbing ultrafiltration membranes, Journal of Membrane Science 115 (1996) 31-47.

[155] K. Rezwan, L.P. Meier, M. Rezwan, J. Voeroes, M. Textor, L.J. Gauckler, Bovine serum albumin adsorption onto colloidal Al_2O_3 Particles: a new model based on zeta potential and UV-Vis measurements, Langmuir 20 (2004) 10055-10061.

[156] P. Bacchin, P. Aimar, R.W. Field, Critical and sustainable fluxes: Theory, experiments and applications, Journal of Membrane Science 281 (2006) 42-69.

[157] S.M. Alan, R.V. Wolf, H.A. Haim, The solubility parameter of polypropylene, Journal of Applied Polymer Science 12 (1968) 1621-1624.

[158] A.F.M. Barton, Handbook of Polymer Liquid Interaction Parameters and Other Solubility Parameters, CRC Press, New York, 1990.

[159] R.A. Hayes, The relationship between glass temperature, molar cohesion, and polymer structure, Journal of Applied Polymer Science 5 (1961) 318-321.

[160] S.Y. Kim, T. Kanamori, T. Shinbo, Preparation of thermal-responsive poly(propylene) membranes grafted with N-isopropylacrylamide by plasma-induced polymerization and their water permeation, Journal of Applied Polymer Science 84 (2002) 1168-1177.

[161] W. Wang, X. Tian, Y. Feng, B. Cao, W. Yang, L. Zhang, Thermally On-Off Switching Membranes Prepared by Pore-Filling Poly(N-isopropylacrylamide) Hydrogels, Industrial & Engineering Chemistry Research 49 (2010) 1684-1690.

[162] A. Borrás, C. López, V. Rico, F. Gracia, A.R. González-Elipe, E. Richter, G. Battiston, R. Gerbasi, N. McSporran, G. Sauthier, E. György, A. Figueras, Effect of Visible and UV Illumination on the Water Contact Angle of TiO_2 Thin Films with Incorporated Nitrogen, The Journal of Physical Chemistry C 111 (2007) 1801-1808.

[163] I.H. Huisman, B. Dutré, K.M. Persson, G. Trägårdh, Water permeability in ultrafiltration and microfiltration: Viscous and electroviscous effects, Desalination 113 (1997) 95-103.

[164] H. Darcy, Les Fontaines Publiques de la Ville de Dijon ('The Public Fountains of the Town of the Dijon'), (1856).

[165] J.S. Kang, K.Y. Kim, Y.M. Lee, Preparation of PVP immobilized microporous chlorinated polyvinyl chloride membranes on fabric and their hydraulic permeation behavior, Journal of Membrane Science 214 (2003) 311-321.

[166] M.S. Kang, B. Chun, S.S. Kim, Surface modification of polypropylene membrane by low-temperature plasma treatment, Journal of Applied Polymer Science 81 (2001) 1555-1566.

[167] Y. Dong, Characterization technique of polymer materials, China Petrochemical Press Beijing, 1997.

[168] J.H. Hildebrand, R.L. Scott, Solubility of non-electrolytes, Dover, New York, 1964.

[169] K. Kalyanasundaram, J.K. Thomas, Environmental effects on vibronic band intensities in pyrene monomer fluorescence and their application in studies of micellar systems, Journal of the American Chemical Society 99 (1977) 2039-2044.

[170] J. Aguiar, P. Carpena, J.A. Molina-BolIvar, C.C. Ruiz, On the determination of the critical micelle concentration by the pyrene 1:3 ratio method, Journal of Colloid and Interface Science 258 (2003) 116-122.

[171] N. Hamada, Y. Einaga, Effects of hydrophobic chain length on the characteristics of the micelles of octaoxyethylene tetradecyl $C_{14}E_8$, hexadecyl $C_{16}E_8$, and Octadecyl $C_{18}E_8$ ethers, The Journal of Physical Chemistry B 109 (2005) 6990-6998.

[172] T. Imae, Nonionic rodlike micelles in dilute and semidilute solutions: intermicellar interaction and the scaling law, The Journal of Physical Chemistry 92 (1988) 5721-5726.

[173] S.-Y. Lin, Y.-Y. Lin, E.-M. Chen, C.-T. Hsu, C.-C. Kwan, A Study of the equilibrium surface tension and the critical micelle concentration of mixed surfactant solutions, Langmuir 15 (1999) 4370-4376.

[174] D. Myers, Surfactant science and technology, VCH publishers, Inc. 1988.

[175] S. Yoshimura, S. Shirai, Y. Einaga, Light-scattering characterization of the wormlike micelles of hexaoxyethylene dodecyl $C_{12}E_6$ and hexaoxyethylene tetradecyl $C_{14}E_6$ ethers in dilute aqueous solution, The Journal of Physical Chemistry B 108 (2004) 15477-15487.

[176] P. Alexandridis, T. Alan Hatton, Poly(ethylene oxide)-poly(propylene oxide)-poly(ethylene oxide) block copolymer surfactants in aqueous solutions and at interfaces: thermodynamics, structure, dynamics, and modeling, Colloids and Surfaces A: Physicochemical and Engineering Aspects 96 (1995) 1-46.

[177] P. Alexandridis, J.F. Holzwarth, T.A. Hatton, Micellization of poly(ethylene oxide)-poly(propylene oxide)-poly(ethylene oxide) triblock copolymers in aqueous solutions: thermodynamics of copolymer association, Macromolecules 27 (1994) 2414-2425.

[178] D.M. Moebius, R., Novel mehods to study interficial layers: NMR methods for studies of organic adsorption layers, Elsevier science B.V., Amsterdam, 2001.

[179] O. Söderman, P. Stilbs, NMR studies of complex surfactant systems, Progress in Nuclear Magnetic Resonance Spectroscopy 26 (1994) 445-482.

[180] J. Ma, C. Guo, Y. Tang, J. Xiang, S. Chen, J. Wang, H. Liu, Micellization in aqueous solution of an ethylene oxide-propylene oxide triblock copolymer, investigated with 1H NMR spectroscopy, pulsed-field gradient NMR, and NMR relaxation, Journal of Colloid and Interface Science 312 (2007) 390-396.

[181] J.-h. Ma, C. Guo, Y.-l. Tang, H. Zhang, H.-z. Liu, Probing paeonol-Pluronic polymer interactions by ^{1}H NMR spectroscopy, The Journal of Physical Chemistry B 111 (2007) 13371-13378.

[182] G. Wanka, H. Hoffmann, W. Ulbricht, Phase diagrams and aggregation behavior of poly(oxyethylene)-poly(oxypropylene)-poly(oxyethylene) triblock copolymers in aqueous solutions, Macromolecules 27 (1994) 4145-4159.

[183] http://www.membrana.de/industrial/product/micropes_flat.htm.

[184] M. Meier, Measuring crystallite size using X-ray diffraction University of California, Davis, 2005.

[185] H.I. Kim, S.S. Kim, Plasma treatment of polypropylene and polysulfone supports for thin film composite reverse osmosis membrane, Journal of Membrane Science 286 (2006) 193-201.

[186] D. Lazos, S. Franzka, M. Ulbricht, Size-selective protein adsorption to polystyrene surfaces by self-assembled grafted poly(ethylene glycols) with varied chain lengths, Langmuir 21 (2005) 8774-8784.

[187] E.S. Pagac, D.C. Prieve, Y. Solomentsev, R.D. Tilton, A comparison of polystyrene-poly(ethylene oxide) diblock copolymer and poly(ethylene oxide) homopolymer adsorption from aqueous solutions, Langmuir 13 (1997) 2993-3001.

[188] L. Liang, X. Feng, J. Liu, P.C. Rieke, G.E. Fryxell, Reversible surface properties of glass plate and capillary tube grafted by photopolymerization of N-isopropylacrylamide, Macromolecules 31 (1998) 7845-7850.

[189] I. Lokuge, X. Wang, P.W. Bohn, Temperature-controlled flow switching in nanocapillary array membranes mediated by poly(N-isopropylacrylamide) polymer brushes grafted by atom transfer radical polymerization Langmuir 23 (2007) 305-311.

[190] K.N. Plunkett, X. Zhu, J.S. Moore, D.E. Leckband, PNIPAM chain collapse depends on the molecular weight and grafting density, Langmuir 22 (2006) 4259-4266.

[191] X. Zhu, C. Yan, F.M. Winnik, D. Leckband, End-grafted low-molecular-weight PNIPAM does not collapse above the LCST, Langmuir 23 (2007) 162-169.

[192] H. Yim, M.S. Kent, S. Satija, S. Mendez, S.S. Balamurugan, S. Balamurugan, G.P. Lopez, Evidence for vertical phase separation in densely grafted, high-molecular-weight poly(N-isopropylacrylamide) brushes in water, Physical Review E - Statistical, Nonlinear, and Soft Matter Physics 72 (2005) 1-7.

[193] S. Mendez, J.G. Curro, J.D. McCoy, G.P. Lopez, Computational modeling of the temperature-induced structural changes of tethered poly(N-isopropylacrylamide) with self-consistent field theory, Macromolecules 38 (2005) 174-181.

[194] S. Balamurugan, S. Mendez, S.S. Balamurugan, M.J. O'Brien Ii, G.P. López, Thermal response of poly(N-isopropylacrylamide) brushes probed by surface plasmon resonance, Langmuir 19 (2003) 2545-2549.

[195] S.J. Lue, J.J. Hsu, C.H. Chen, B.C. Chen, Thermally on-off switching membranes of poly(N-isopropylacrylamide) immobilized in track-etched polycarbonate films, Journal of Membrane Science 301 (2007) 142-150.

[196] I. Lokuge, X. Wang, P.W. Bohn, Temperature-controlled flow switching in nanocapillary array membranes mediated by poly(N-isopropylacrylamide) polymer brushes grafted by atom transfer radical polymerization, Langmuir 23 (2007) 305-311.

[197] A. Friebe, M. Ulbricht, Controlled pore functionalization of poly(ethylene terephthalate) track-etched membranes via surface-initiated atom transfer radical polymerization, Langmuir 23 (2007) 10316-10322.

[198] H. Guo, J. Huang, X. Wang, The alternate temperature-change cleaning behaviors of PNIPAAm grafted porous polyethylene membrane fouled by proteins, Desalination 234 (2008) 42-50.

[199] B.J. Kirby, E.F. Hasselbrink Jr, Zeta potential of microfluidic substrates: 1. Theory, experimental techniques, and effects on separations, Electrophoresis 25 (2004) 187-202.

[200] B.J. Kirby, E.F. Hasselbrink Jr, Zeta potential of microfluidic substrates: 2. Data for polymers, Electrophoresis 25 (2004) 203-213.

[201] A. Revil, P.A. Pezard, P.W.J. Glover, Streaming potential in porous media 1. Theory of the zeta potential, Journal of Geophysical Research B: Solid Earth 104 (1999) 20021-20031.

[202] R. Venditti, X. Xuan, D. Li, Experimental characterization of the temperature dependence of zeta potential and its effect on electroosmotic flow velocity in microchannels, Microfluidics and Nanofluidics 2 (2006) 493-499.

[203] Z.P. Fang, Y.H. Song, L. Shen, Polymer physics, Zhejiang University, Hangzhou, 2005.

[204] M.A. Bevan, D.C. Prieve, Forces and hydrodynamic interactions between polystyrene surfaces with adsorbed PEO-PPO-PEO, Langmuir 16 (2000) 9274-9281.

[205] P. Brandani, P. Stroeve, Adsorption and desorption of PEO-PPO-PEO triblock copolymers on a self-assembled hydrophobic surface, Macromolecules 36 (2003) 9492-9501.

[206] H. Motschmann, M. Stamm, C. Toprakcioglu, Adsorption kinetics of block copolymers from a good solvent: A two-stage process, Macromolecules 24 (1991) 3681-3688.

[207] P. Brandani, P. Stroeve, Kinetics of adsorption and desorption of PEO-PPO-PEO triblock copolymers on a self-assembled hydrophobic surface, Macromolecules 36 (2003) 9502-9509.

[208] I. Goldmints, J.F. Holzwarth, K.A. Smith, T.A. Hatton, Micellar dynamics in aqueous solutions of PEO-PPO-PEO block copolymers, Langmuir 13 (1997) 6130-6133.

[209] P. Alexandridis, K. Andersson, Effect of solvent quality on reverse micelle formation and water solubilization by poly(ethylene oxide)/poly(propylene oxide) and poly(ethylene oxide)/poly(butylene oxide) block copolymers in xylene, Journal of Colloid and Interface Science 194 (1997) 166-173.

[210] P. Alexandridis, K. Andersson, Reverse micelle formation and water solubilization by polyoxyalkylene block copolymers in organic solvent, Journal of Physical Chemistry B 101 (1997) 8103-8111.

[211] B. Svensson, U. Olsson, P. Alexandridis, K. Mortensen, A SANS investigation of reverse (water-in-oil) micelles of amphiphilic block copolymers, Macromolecules 32 (1999) 6725-6733.

[212] P. Alexandridis, T. Alan Hatton, Poly(ethylene oxide)poly(propylene oxide)poly(ethylene oxide) block copolymer surfactants in aqueous solutions and at interfaces: thermodynamics, structure, dynamics, and modeling, Colloids and Surfaces A: Physicochemical and Engineering Aspects 96 (1995) 1-46.

[213] R. Zhang, J. Liu, J. He, B. Han, Z. Liu, T. Jiang, W. Wu, L. Rong, H. Zhao, B. Dong, G.H. Hu, Compressed ethylene-assisted formation of the reverse micelle of PEO-PPO-PEO copolymer, Macromolecules 36 (2003) 1289-1294.

[214] R. Zhang, J. Liu, J. He, B. Han, X. Zhang, Z. Liu, T. Jiang, G. Hu, Compressed CO_2-assisted formation of reverse micelles of PEO-PPO-PEO copolymer, Macromolecules 35 (2002) 7869-7871.

[215] P. Jones, E. Wyn-Jones, G.J.T. Tiddy, Kinetic and equilibrium studies associated with the aggregation of non-ionic surfactants in non-polar solvents, Journal of the Chemical Society, Faraday Transactions 1: Physical Chemistry in Condensed Phases 83 (1987) 2735-2749.

[216] Y. Qiu, Y. Liu, L. Wang, L. Xu, R. Bai, Y. Ji, X. Wu, Y. Zhao, Y. Li, C. Chen, Surface chemistry and aspect ratio mediated cellular uptake of Au nanorods, Biomaterials 31 (2010) 7606-7619.

[217] H. Thissen, T. Gengenbach, R. du Toit, D.F. Sweeney, P. Kingshott, H.J. Griesser, L. Meagher, Clinical observations of biofouling on PEO coated silicone hydrogel contact lenses, Biomaterials 31 (2010) 5510-5519.

[218] L.E.S. Brink, S.J.G. Elbers, T. Robbertsen, P. Both, The anti-fouling action of polymers preadsorbed on ultrafiltration and microfiltration membranes, Journal of Membrane Science 76 (1993) 281-291.

[219] V. Chen, A.G. Fane, C.J.D. Fell, The use of anionic surfactants for reducing fouling of ultrafiltration membranes: Their effects and optimization, Journal of Membrane Science 67 (1992) 249-261.

[220] A.V.R. Reddy, D.J. Mohan, A. Bhattacharya, V.J. Shah, P.K. Ghosh, Surface modification of ultrafiltration membranes by preadsorption of a negatively charged polymer: I. Permeation of water soluble polymers and inorganic salt solutions and fouling resistance properties, Journal of Membrane Science 214 (2003) 211-221.

Chapter 7

Appendix

Appendix-1 Figures and tables

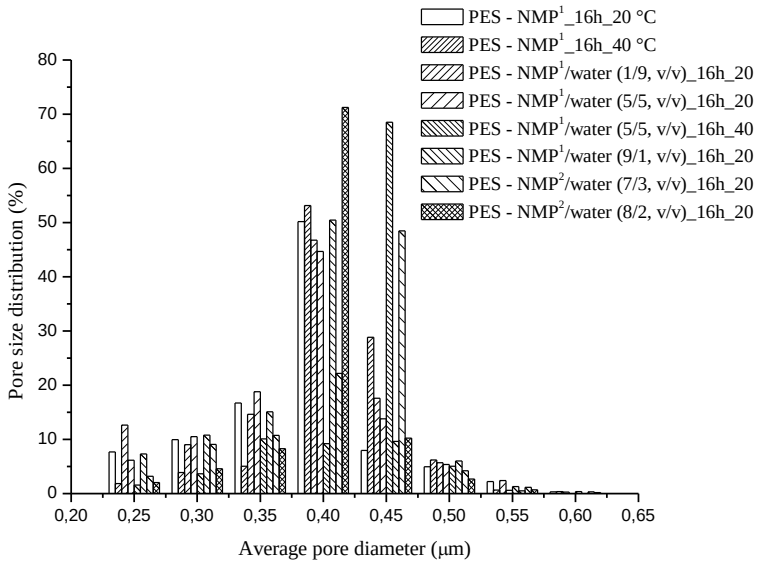

a)

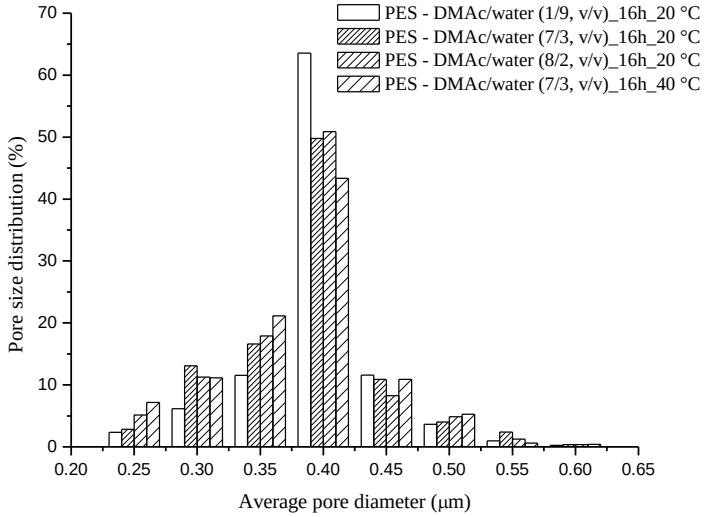

b)

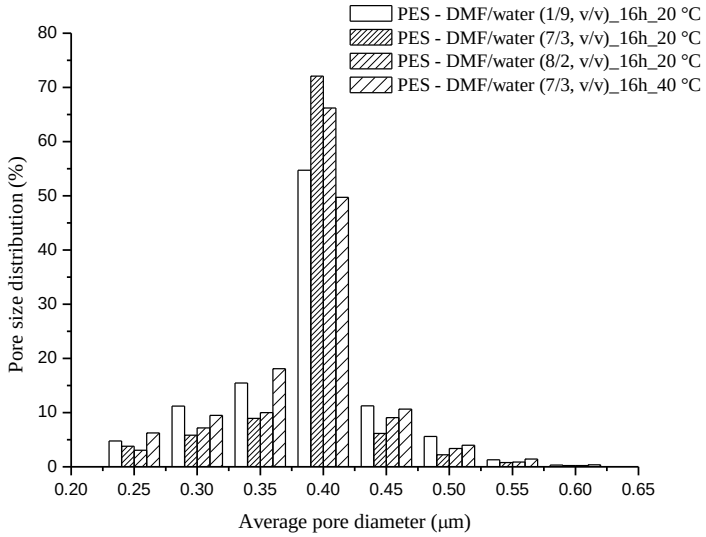
PES - DMF/water (1/9, v/v)_16h_20 °C
PES - DMF/water (7/3, v/v)_16h_20 °C
PES - DMF/water (8/2, v/v)_16h_20 °C
PES - DMF/water (7/3, v/v)_16h_40 °C
Pore size distribution (%)
Average pore diameter (μm)

c)

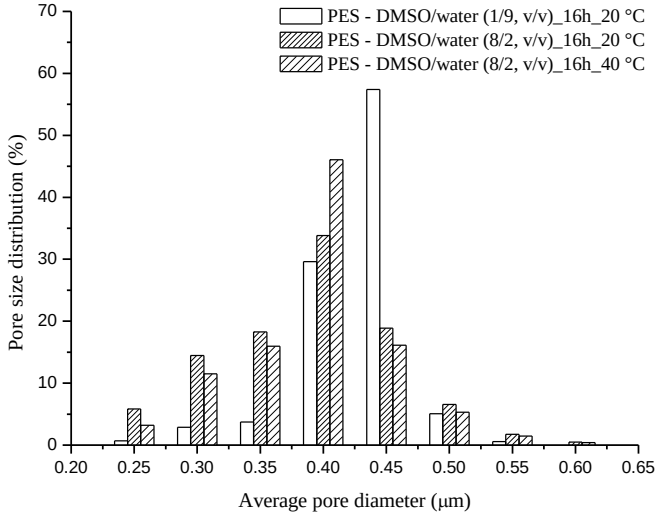
PES - DMSO/water (1/9, v/v)_16h_20 °C
PES - DMSO/water (8/2, v/v)_16h_20 °C
PES - DMSO/water (8/2, v/v)_16h_40 °C
Pore size distribution (%)
Average pore diameter (μm)

d)

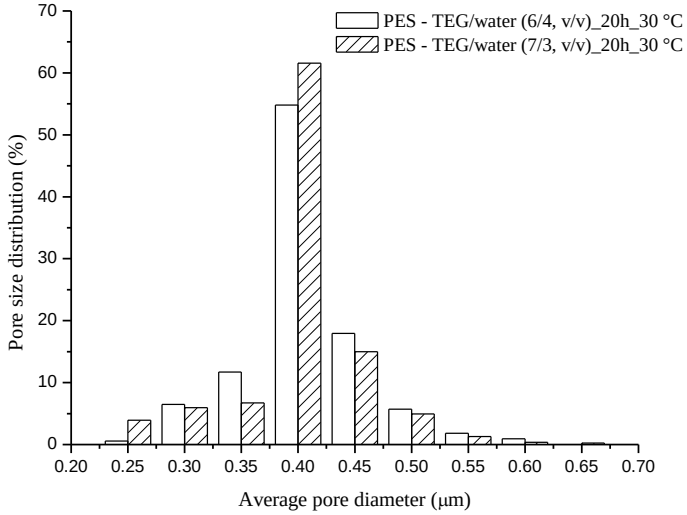
PES - TEG/water (6/4, v/v)_20h_30 °C
PES - TEG/water (7/3, v/v)_20h_30 °C
Pore size distribution (%)
Average pore diameter (μm)

e)

Figure 7.1. Effect of solvent or mutual solvent on membrane structure: a) NMP[1], NMP[1] and NMP[2]/water mixtures; b) DMAc/water mixtures; c) DMF/water mixtures; d) DMSO/water mixtures; e) 20 g/L $C_{18}EO_{136}C_{18}$ in TEG/water solutions, vacuum dry directly.

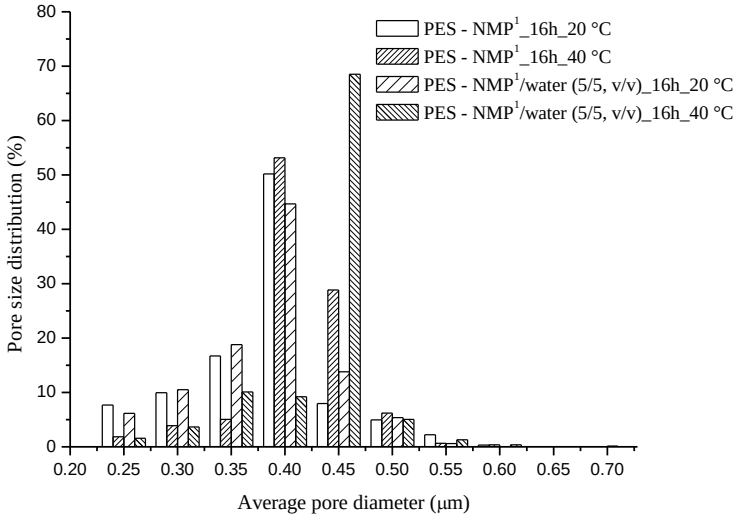

Figure 7.2. Effect of temperature on pore structure.

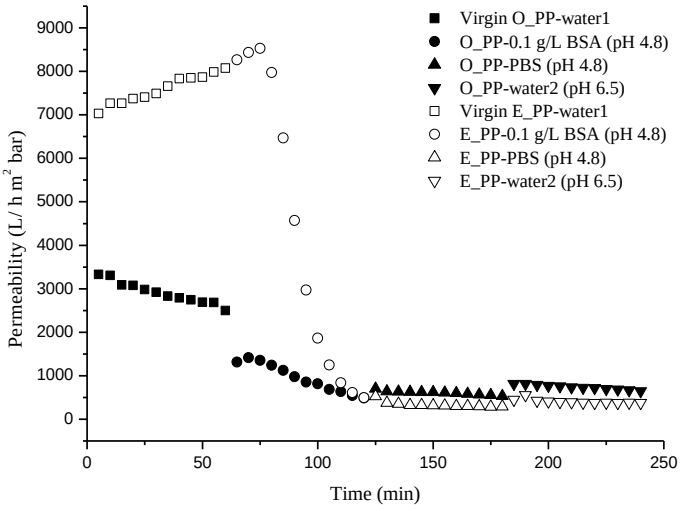

a)

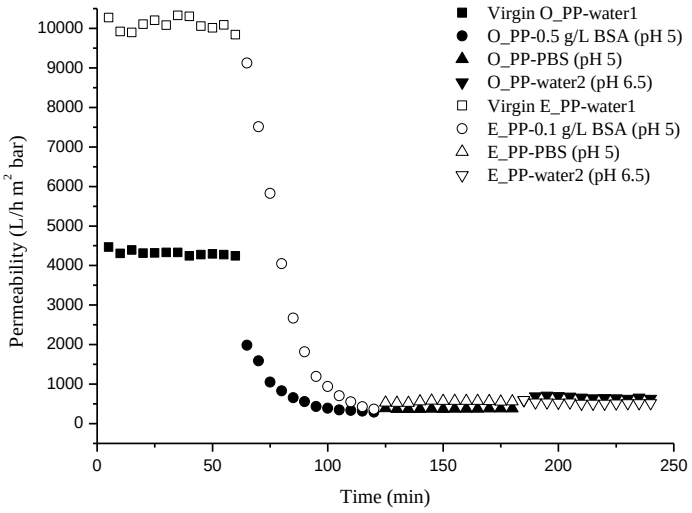

b)

Figure 7.3. Subsequent measurements of fluxes for water, for a 0.1, 0.5 and 1 g/L BSA solution (pH = 5), for buffer (PBS, pH 5) and again for water, through original (O_PP) and modified membranes (E_PP), at a constant trans-membrane pressure (1 bar), respectively. therein, a) 0.1 g/L BSA (pH 4.8); b) 0.5 g/L BSA (pH 5).

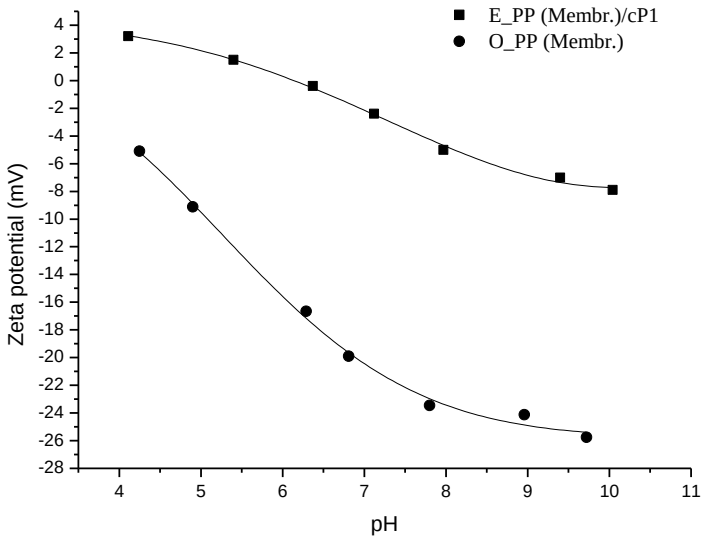

a)

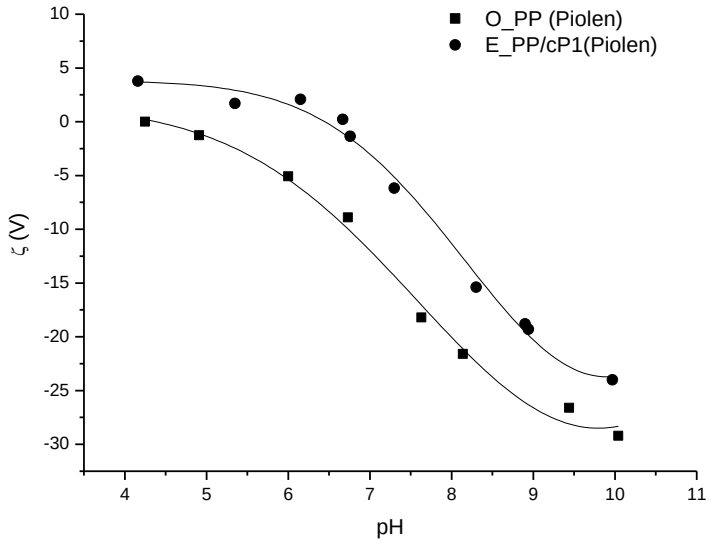

b)

Figure7.4. Zeta potential as a function of pH of original and cP1-modified PP membranes and plates at room temperature: a) PP membranes; b) PP plates.

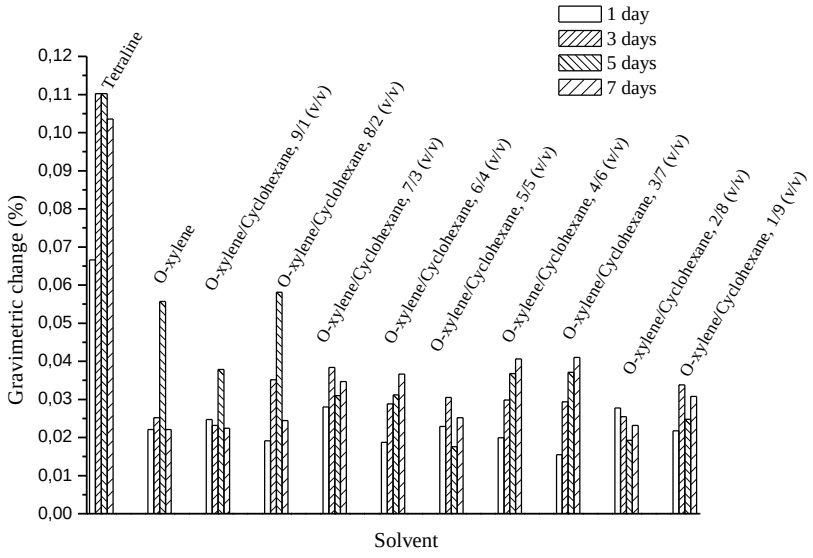

Figure 7.5. Swelling degree of Celgard PP film in different solvents in 7 days.

Table 7.1. Solubility parameter of some solvents and mutual solvents at 25 °C.

	δ $\sqrt{MPa}$	δ_d $\sqrt{MPa}$	δ_p $\sqrt{MPa}$	δ_h $\sqrt{MPa}$	$\lvert\delta_{PES} - \delta_{solvent}\rvert$ $\sqrt{MPa}$
PES	21.90	17.60	10.40	7.80	
H_2O	47.90	15.50	16.00	42.30	
DMAc	22.70	16.80	11.40	10.20	0.80
DMAc: H_2O (9:1)	24.26	16.67	11.86	13.41	2.56
DMAc: H_2O (8:2)	26.49	16.54	12.32	16.62	4.59
DMAc: H_2O (7:3)	28.74	16.41	12.78	19.83	6.84
DMAc: H_2O (6:4)	31.16	16.28	13.24	23.04	9.26
DMAc: H_2O (5:5)	33.73	16.15	13.70	26.25	11.83
DMAc: H_2O (4:6)	36.40	16.02	14.16	29.46	14.50
DMAc: H_2O (3:7)	39.16	15.89	14.62	32.67	17.26
DMAc: H_2O (2:8)	41.99	15.76	15.08	35.88	20.09
DMAc: H_2O (1:9)	44.87	15.63	15.54	39.09	22.07
NMP	22.90	18.00	12.30	7.20	1.00
NMP: H_2O (9:1)	24.30	17.75	12.67	10.71	2.40
NMP: H_2O (8:2)	26.05	17.50	13.04	14.22	4.15
NMP: H_2O (7:3)	28.14	17.25	13.41	17.73	6.24
NMP: H_2O (6:4)	30.50	17.00	13.78	21.24	8.60
NMP: H_2O (5:5)	33.06	16.75	14.15	24.75	11.16
NMP: H_2O (4:6)	35.80	16.50	14.52	28.26	13.90
NMP: H_2O (3:7)	38.67	16.25	14.89	31.77	16.77
NMP: H_2O (2:8)	41.64	16.00	15.26	35.28	19.74
NMP: H_2O (1:9)	44.69	15.75	15.63	38.79	22.79
DMF	24.80	17.40	13.70	11.20	2.90
DMF: H_2O (9:1)	26.36	17.21	13.93	14.31	4.46
DMF: H_2O (8:2)	29.17	17.02	14.16	17.42	6.27
DMF: H_2O (7:3)	30.20	16.83	14.39	20.53	8.30
DMF: H_2O (6:4)	31.70	16.64	13.02	23.64	9.80
DMF: H_2O (5:5)	34.74	16.45	14.85	26.75	12.84
DMF: H_2O (4:6)	37.19	16.26	15.08	29.86	15.29
DMF: H_2O (3:7)	39.74	16.07	15.31	32.97	17.84
DMF: H_2O (2:8)	42.37	15.88	15.54	36.08	20.47
DMF: H_2O (1:9)	45.06	15.69	15.77	39.19	23.16
DMSO	26.70	18.04	16.40	10.20	4.80
DMSO: H_2O (9:1)	27.64	17.79	16.36	13.41	5.74
DMSO: H_2O (8:2)	29.15	17.53	16.32	16.62	7.25
DMSO: H_2O (7:3)	30.93	17.28	16.28	19.83	9.03
DMSO: H_2O (6:4)	32.93	17.02	16.24	23.04	11.93
DMSO: H_2O (5:5)	35.11	16.77	16.20	26.25	13.21
DMSO: H_2O (4:6)	37.44	16.52	16.16	29.46	15.54
DMSO: H_2O (3:7)	39.40	16.26	16.12	32.67	17.50
DMSO: H_2O (2:8)	42.45	16.01	16.08	35.88	20.55
DMSO: H_2O (1:9)	45.09	15.75	16.04	39.09	23.59

Table 7.1. Solubility parameter of some solvents and mutual solvents at 25 °C (continued).

	δ $\sqrt{MPa}$	δ_d $\sqrt{MPa}$	δ_p $\sqrt{MPa}$	δ_h $\sqrt{MPa}$	$\lvert\delta_{PES} - \delta_{solvent}\rvert$ $\sqrt{MPa}$
TEG	27.50	16.00	12.50	18.60	5.60
TEG: H_2O (9:1)	29.31	15.95	12.85	20.97	7.41
TEG: H_2O (8:2)	31.17	15.90	13.20	23.34	9.27
TEG: H_2O (7:3)	33.10	15.85	13.55	25.71	11.20
TEG: H_2O (6:4)	35.09	15.80	13.90	28.08	13.19
TEG: H_2O (5:5)	37.12	15.75	14.25	30.45	15.22
TEG: H_2O (4:6)	39.20	15.70	14.60	32.82	17.30
TEG: H_2O (3:7)	41.31	15.65	14.95	35.19	19.41
TEG: H_2O (2:8)	43.45	15.60	15.30	37.56	21.55
TEG: H_2O (1:9)	45.62	15.55	15.65	39.93	23.72

Table 7.2.1. Solvent-resistant test of PES 2F membrane for 16 h – 20 °C.

Sample No.	PES-1#	PES-2#	PES-3#	PES-4#	PES-5#	PES-6#	PES-7#	PES-8#	PES-9#	PES-10#
Solvent /mutual solvent (v/v)	DMSO	DMSO:H_2O 9/1	DMSO:H_2O 8/2	DMSO:H_2O 7/3	DMSO:H_2O 6/4	DMSO:H_2O 5/5	DMSO:H_2O 4/6	DMSO:H_2O 3/7	DMSO:H_2O 2/8	DMSO:H_2O 1/9
Sample No.	PES-11#	PES-12#	PES-13#	PES-14#	PES-15#	PES-16#	PES-17#	PES-18#	PES-19#	PES-20#
Solvent /mutual solvent (v/v)	DMAc	DMAc:H_2O 9/1	DMAc:H_2O 8/2	DMAc:H_2O 7/3	DMAc:H_2O 6/4	DMAc:H_2O 5/5	DMAc:H_2O 4/6	DMAc:H_2O 3/7	DMAc:H_2O 2/8	DMAc:H_2O 1/9
Sample No.	PES-21#	PES-22#	PES-23#	PES-24#	PES-25#	PES-26#	PES-27#	PES-28#	PES-29#	PES-30#
Solvent /mutual solvent (v/v)	DMF	DMF:H_2O 9/1	DMF:H_2O 8/2	DMF:H_2O 7/3	DMF:H_2O 6/4	DMF:H_2O 5/5	DMF:H_2O 4/6	DMF:H_2O 3/7	DMF:H_2O 2/8	DMF:H_2O 1/9
Sample No.	PES-31#	PES-32#	PES-33#	PES-34#	PES-35#	PES-36#	PES-37#	PES-38#	PES-39#	PES-40#
Solvent /mutual solvent (v/v)	NMP[1]	NMP[1]:H_2O 9/1	NMP[1]:H_2O 8/2	NMP[1]:H_2O 7/3	NMP[1]:H_2O 6/4	NMP[1]:H_2O 5/5	NMP[1]:H_2O 4/6	NMP[1]: H_2O 3/7	NMP[1]:H_2O 2/8	NMP[1]:H_2O 1/9
Sample No.	PES-41#	PES-42#	PES-43#	PES-44#	PES-45#	PES-46#	PES-47#	PES-48#	PES-49#	PES-50#
Solvent /mutual solvent (v/v)	NMP[2]	NMP[2]:H_2O 9/1	NMP[2]:H_2O 8/2	NMP[2]:H_2O 7/3	NMP[2]:H_2O 6/4	NMP[2]:H_2O 5/5	NMP[2]:H_2O 4/6	NMP[2]:H_2O 3/7	NMP[2]:H_2O 2/8	NMP[2]:H_2O 1/9
Sample No.	PES-51#	PES-52#	PES-53#	PES-54#	PES-55#	PES-56#	PES-57#	PES-58#	PES-59#	PES-60#
Solvent /mutual solvent (v/v)	Acetone	Acetone:H_2O 9/1	Acetone:H_2O 8/2	Acetone:H_2O 7/3	Acetone:H_2O 6/4	Acetone:H_2O 5/5	Acetone:H_2O 4/6	Acetone:H_2O 3/7	Acetone:H_2O 2/8	Acetone:H_2O 1/9
Sample No.	PES-61#	PES-62#	PES-63#	PES-64#	PES-65#	PES-66#	PES-67#	PES-68#	PES-69#	PES-70#
Solvent /mutual solvent (v/v)	TEG	TEG:H_2O 9/1	TEG:H_2O 8/2	TEG:H_2O 7/3	TEG:H_2O 6/4	TEG:H_2O 5/5	TEG:H_2O 4/6	TEG:H_2O 3/7	TEG:H_2O 2/8	TEG:H_2O 1/9

Table 7.2.2. Solvent-resistant test of PES 2F membrane for 16 h – 30 °C.

Sample No.	PES-71#	PES-72#	PES-73#	PES-74#	PES-75#	PES-76#	PES-77#	PES-78#	PES-79#	PES-80#
Solvent /mutual solvent (v/v)	DMSO	DMSO:H_2O 9/1	DMSO:H_2O 8/2	DMSO:H_2O 7/3	DMSO:H_2O 6/4	DMSO:H_2O 5/5	DMSO:H_2O 4/6	DMSO:H_2O 3/7	DMSO:H_2O 2/8	DMSO:H_2O 1/9
Sample No.	PES-81#	PES-82#	PES-83#	PES-84#	PES-85#	PES-86#	PES-87#	PES-88#	PES-89#	PES-90#
Solvent /mutual solvent (v/v)	DMAc	DMAc:H_2O 9/1	DMAc:H_2O 8/2	DMAc:H_2O 7/3	DMAc:H_2O 6/4	DMAc:H_2O 5/5	DMAc:H_2O 4/6	DMAc:H_2O 3/7	DMAc:H_2O 2/8	DMAc:H_2O 1/9
Sample No.	PES-91#	PES-92#	PES-93#	PES-94#	PES-95#	PES-96#	PES-97#	PES-98#	PES-99#	PES-100#
Solvent /mutual solvent (v/v)	DMF	DMF:H_2O 9/1	DMF:H_2O 8/2	DMF:H_2O 7/3	DMF:H_2O 6/4	DMF:H_2O 5/5	DMF:H_2O 4/6	DMF:H_2O 3/7	DMF:H_2O 2/8	DMF:H_2O 1/9
Sample No.	PES-101#	PES-102#	PES-103#	PES-104#	PES-105#	PES-106#	PES-107#	PES-108#	PES-109#	PES-200#
Solvent /mutual solvent (v/v)	NMP[1]	NMP[1]:H_2O 9/1	NMP[1]:H_2O 8/2	NMP[1]:H_2O 7/3	NMP[1]:H_2O 6/4	NMP[1]:H_2O 5/5	NMP[1]:H_2O 4/6	NMP[1]: H_2O 3/7	NMP[1]:H_2O 2/8	NMP[1]:H_2O 1/9
Sample No.	PES-201#	PES-202#	PES-203#	PES-204#	PES-205#	PES-206#	PES-207#	PES-208#	PES-209#	PES-210#
Solvent /mutual solvent (v/v)	NMP[2]	NMP[2]:H_2O 9/1	NMP[2]:H_2O 8/2	NMP[2]:H_2O 7/3	NMP[2]:H_2O 6/4	NMP[2]:H_2O 5/5	NMP[2]:H_2O 4/6	NMP[2]:H_2O 3/7	NMP[2]:H_2O 2/8	NMP[2]:H_2O 1/9
Sample No.	PES-211#	PES-212#	PES-213#	PES-214#	PES-215#	PES-216#	PES-217#	PES-218#	PES-219#	PES-220#
Solvent /mutual solvent (v/v)	Acetone	Acetone: H_2O 9/1	Acetone: H_2O 8/2	Acetone: H_2O 7/3	Acetone: H_2O 6/4	Acetone: H_2O 5/5	Acetone: H_2O 4/6	Acetone: H_2O 3/7	Acetone: H_2O 2/8	Acetone: H_2O 1/9
Sample No.	PES-221#	PES-222#	PES-223#	PES-224#	PES-225#	PES-226#	PES-227#	PES-228#	PES-229#	PES-230#
Solvent /mutual solvent (v/v)	TEG	TEG:H_2O 9/1	TEG:H_2O 8/2	TEG:H_2O 7/3	TEG:H_2O 6/4	TEG:H_2O 5/5	TEG:H_2O 4/6	TEG:H_2O 3/7	TEG:H_2O 2/8	TEG:H_2O 1/9

Table 7.2.3. Solvent-resistant test of PES 2F membrane for 16 h – 40 °C.

Sample No.	PES-231#	PES-232#	PES-233#	PES-234#	PES-235#	PES-236#	PES-237#	PES-238#	PES-239#	PES-240#
Solvent /mutual solvent (v/v)	DMSO	DMSO:H_2O 9/1	DMSO:H_2O 8/2	DMSO:H_2O 7/3	DMSO:H_2O 6/4	DMSO:H_2O 5/5	DMSO:H_2O 4/6	DMSO:H_2O 3/7	DMSO:H_2O 2/8	DMSO:H_2O 1/9
Sample No.	PES-241#	PES-242#	PES-243#	PES-244#	PES-245#	PES-246#	PES-247#	PES-248#	PES-249#	PES-250#
Solvent /mutual solvent (v/v)	DMAc	DMAc:H_2O 9/1	DMAc:H_2O 8/2	DMAc:H_2O 7/3	DMAc:H_2O 6/4	DMAc:H_2O 5/5	DMAc:H_2O 4/6	DMAc:H_2O 3/7	DMAc:H_2O 2/8	DMAc:H_2O 1/9
Sample No.	PES-251#	PES-252#	PES-253#	PES-254#	PES-255#	PES-256#	PES-257#	PES-258#	PES-259#	PES-260#
Solvent /mutual solvent (v/v)	DMF	DMF:H_2O 9/1	DMF:H_2O 8/2	DMF:H_2O 7/3	DMF:H_2O 6/4	DMF:H_2O 5/5	DMF:H_2O 4/6	DMF:H_2O 3/7	DMF:H_2O 2/8	DMF:H_2O 1/9
Sample No.	PES-261#	PES-262#	PES-263#	PES-264#	PES-265#	PES-266#	PES-267#	PES-268#	PES-269#	PES-270#
Solvent /mutual solvent (v/v)	NMP[1]	NMP[1]:H_2O 9/1	NMP[1]:H_2O 8/2	NMP[1]:H_2O 7/3	NMP[1]:H_2O 6/4	NMP[1]:H_2O 5/5	NMP[1]:H_2O 4/6	NMP[1]: H_2O 3/7	NMP[1]:H_2O 2/8	NMP[1]:H_2O 1/9
Sample No.	PES-271#	PES-272#	PES-273#	PES-274#	PES-275#	PES-276#	PES-277#	PES-278#	PES-279#	PES-280#
Solvent /mutual solvent (v/v)	NMP[2]	NMP[2]:H_2O 9/1	NMP[2]:H_2O 8/2	NMP[2]:H_2O 7/3	NMP[2]:H_2O 6/4	NMP[2]:H_2O 5/5	NMP[2]:H_2O 4/6	NMP[2]:H_2O 3/7	NMP[2]:H_2O 2/8	NMP[2]:H_2O 1/9
Sample No.	PES-281#	PES-282#	PES-283#	PES-284#	PES-285#	PES-286#	PES-287#	PES-288#	PES-289#	PES-290#
Solvent /mutual solvent (v/v)	Acetone	Acetone:H_2O 9/1	Acetone:H_2O 8/2	Acetone:H_2O 7/3	Acetone:H_2O 6/4	Acetone:H_2O 5/5	Acetone:H_2O 4/6	Acetone:H_2O 3/7	Acetone:H_2O 2/8	Acetone:H_2O 1/9
Sample No.	PES-291#	PES-292#	PES-293#	PES-294#	PES-295#	PES-296#	PES-297#	PES-298#	PES-299#	PES-300#
Solvent /mutual solvent (v/v)	TEG	TEG:H_2O 9/1	TEG:H_2O 8/2	TEG:H_2O 7/3	TEG:H_2O 6/4	TEG:H_2O 5/5	TEG:H_2O 4/6	TEG:H_2O 3/7	TEG:H_2O 2/8	TEG:H_2O 1/9

Note : NMP[1], purity is 65.5%; NMP[2], purity is 99.5%.

Table 7.3. One-step modification conditions for PES 2F membrane surface hydrophilic modification.

Sample No.	Solvent / mutual solvent (v/v)	Modifier	Conc. (g/L)	Time (h)	Temp. (°C)	Deswelling way
PES-301#	NMP[2]/H_2O (8/2)	$C_{18}EO_8C_{18}$	1	16	20	Vacuum dry 24 h
PES-302#	NMP[2]/H_2O (8/2)	$C_{18}EO_8C_{18}$	1	16	20	Water 20 min
PES-303#	NMP[2]/H_2O (8/2)	$C_{18}EO_{136}C_{18}$	1	16	20	Vacuum dry 24 h
PES-304#	NMP[2]/H_2O (8/2)	$C_{18}EO_{136}C_{18}$	1	16	20	Water 20 min
PES-305#	NMP[2]/H_2O (8/2)	PEG 6000	1	16	20	Vacuum dry 24 h
PES-306#	NMP[2]/H_2O (8/2)	PEG 6000	1	16	20	Water 20 min
PES-307#	DMF/H_2O (8/2)	$C_{18}EO_8$	1	16	20	Vacuum dry 24 h
PES-308#	DMF/H_2O (8/2)	$C_{18}EO_8$	1	16	20	Water 20 min
PES-309#	DMF/H_2O (8/2)	$C_{18}EO_8C_{18}$	1	16	20	Vacuum dry 24 h
PES-310#	DMF/H_2O (8/2)	$C_{18}EO_8C_{18}$	1	16	20	Water 20 min
PES-311#	DMF/H_2O (8/2)	$C_{18}EO_{136}C_{18}$	1	16	20	Vacuum dry 24 h
PES-312#	DMF/H_2O (8/2)	$C_{18}EO_{136}C_{18}$	1	16	20	Water 20 min
PES-313#	NMP[2]/H_2O (7/3)	PEG 6000	3	16	20	Vacuum dry 24 h
PES-314#	NMP[2]/H_2O (7/3)	PEG 6000	3	16	20	Water 20 min
PES-315#	NMP[2]/H_2O (7/3)	$C_{18}EO_{136}C_{18}$	3	16	20	Vacuum dry 24 h
PES-316#	NMP[2]/H_2O (7/3)	$C_{18}EO_{136}C_{18}$	3	16	20	Water 20 min
PES-317#	DMF/H_2O (7/3)	$C_{18}EO_8$	1	16	20	Vacuum dry 24 h
PES-318#	DMF/H_2O (7/3)	$C_{18}EO_8$	1	16	20	Water 20 min
PES-319#	DMF/H_2O (7/3)	$C_{18}EO_8C_{18}$	1	16	20	Vacuum dry 24 h
PES-320#	DMF/H_2O (7/3)	$C_{18}EO_8C_{18}$	1	16	20	Water 20min
PES-321#	DMF/H_2O (7/3)	$C_{18}EO_{136}C_{18}$	1	16	20	Vacuum dry 24 h
PES-322#	DMF/H_2O (7/3)	$C_{18}EO_{136}C_{18}$	1	16	20	Water 20 min
PES-323#	DMF/H_2O (7/3)	$C_{18}EO_{136}C_{18}$	10	16	30	Vacuum dry 24 h
PES-324#	DMF/H_2O (7/3)	$C_{18}EO_{136}C_{18}$	15	16	30	Vacuum dry 24 h
PES-325#	DMF/H_2O (7/3)	$C_{18}EO_{136}C_{18}$	20	16	30	Vacuum dry 24 h
PES-326#	DMAc/H_2O (7/3)	$C_{18}EO_{136}C_{18}$	20	16	20	Vacuum dry 24 h
PES-327#	DMAc/H_2O (7/3)	PEG6000	20	16	20	Vacuum dry 24 h
PES-328#	DMSO/H_2O (8/2)	PEG6000	20	16	20	Vacuum dry 24 h
PES-329#	NMP[2]/H_2O (6/4)	PEG6000	20	16	30	Vacuum dry 24 h
PES-330#	DMF/H_2O (6/4)	PEG6000	20	16	30	Vacuum dry 24 h
PES-331#	DMAc/H_2O (6/4)	PEG6000	20	16	30	Vacuum dry 24 h
PES-332#	DMSO/H_2O (6/4)	PEG6000	20	16	30	Vacuum dry 24 h
PES-333#	NMP[2]/H_2O (5/5)	PEG6000	20	16	30	Vacuum dry 24 h
PES-334#	DMF/H_2O (5/5)	PEG6000	20	16	30	Vacuum dry 24 h
PES-335#	DMAc/H_2O (5/5)	PEG6000	20	16	30	Vacuum dry 24 h
PES-336#	DMSO/H_2O (5/5)	PEG6000	20	16	30	Vacuum dry 24 h
PES-337#	DMSO/H_2O (6/4)	PEG6000	20	18	30	Vacuum dry 24 h
PES-338#	DMSO/H_2O (5/5)	PEG6000	20	18	30	Vacuum dry 24 h
PES-339#	DMSO/H_2O (4/6)	PEG6000	20	18	30	Vacuum dry 24 h
PES-340#	DMSO/H_2O (3/7)	PEG6000	20	18	30	Vacuum dry 24 h
PES-341#	DMSO/H_2O (4/6)	PEG35,000	20	20	30	Vacuum dry 24 h
PES-342#	DMSO/H_2O (4/6)	PEG35,000	20	20	30	Water 20 min

Table 7.3. One-step modification conditions for PES 2F membrane surface hydrophilic modification (continued).

Sample No.	Solvent / mutual solvent (v/v)	Modifier	Conc. (g/L)	Time (h)	Temp. (°C)	Deswelling way
PES-343#	DMSO/H_2O (4/6)	F108	20	20	30	Vacuum dry 24 h
PES-344#	DMSO/H_2O (4/6)	F108	20	20	30	Water 20 min
PES-345#	DMSO/H_2O (4/6)	F127	20	20	30	Vacuum dry 24 h
PES-346#	DMSO/H_2O (4/6)	F127	20	20	30	Water 20 min
PES-347#	DMSO/H_2O (3/7)	PEG35,000	20	20	30	Vacuum dry 24 h
PES-348#	DMSO/H_2O (3/7)	F108	20	20	30	Vacuum dry 24 h
PES-349#	DMSO/H_2O (3/7)	F127	20	20	30	Vacuum dry 24 h
PES-350#	NMP^2/H_2O (3/7)	F127	20	20	30	Vacuum dry 24 h
PES-351#	DMF/H_2O (8/2)	PEG35,000	1	18	30	Vacuum dry 24 h
PES-352#	DMF/H_2O (8/2)	PEG35,000	1	18	30	Water 20 min
PES-353#	DMF/H_2O (8/2)	F108	1	18	30	Vacuum dry 24 h
PES-354#	DMF/H_2O (8/2)	F108	1	18	30	Water 20 min
PES-355#	DMF/H_2O (8/2)	F127	1	18	30	Vacuum dry 24 h
PES-356#	DMF/H_2O (8/2)	F127	1	18	30	Water 20 min
PES-357#	DMF/H_2O (8/2)	L64	1	18	30	Vacuum dry 24 h
PES-358#	DMF/H_2O (8/2)	L64	1	18	30	Water 20 min
PES-359#	DMF/H_2O (8/2)	L64	20	18	30	Vacuum dry 24 h
PES-360#	DMF/H_2O (8/2)	L64	20	18	30	Water 20 min
PES-361#	DMSO/H_2O (8/2)	PEG35,000	1	18	30	Vacuum dry 24 h
PES-362#	DMSO/H_2O (8/2)	PEG35,000	1	18	30	Water 20 min
PES-363#	DMSO/H_2O (8/2)	F108	1	18	30	Vacuum dry 24 h
PES-364#	DMSO/H_2O (8/2)	F108	1	18	30	Water 20 min
PES-365#	DMSO/H_2O (8/2)	F127	1	18	30	Vacuum dry 24 h
PES-366#	DMSO/H_2O (8/2)	F127	1	18	30	Water 20 min
PES-367#	DMSO/H_2O (8/2)	L64	1	18	30	Vacuum dry 24 h
PES-368#	DMSO/H_2O (8/2)	L64	1	18	30	Water 20 min
PES-369#	DMSO/H_2O (3/7)	PE10100	1	18	30	Vacuum dry 24 h
PES-370#	DMSO/H_2O (3/7)	PE10100	1	18	30	Water 20 min
PES-371#	TEG/H_2O (7/3)	$C_{18}EO_{136}C_{18}$	20	20	30	Vacuum dry 24 h
PES-372#	TEG/H_2O (6/4)	$C_{18}EO_{136}C_{18}$	20	20	30	Vacuum dry 24 h
PES-373#	DMSO/H_2O (8/2)	PE10100	1	20	20	Vacuum dry 24 h
PES-374#	DMSO/H_2O (8/2)	PE10100	1	20	20	Water 20 min
PES-375#	DMSO/H_2O (8/2)	PE10100	10	20	20	Vacuum dry 24 h
PES-376#	DMSO/H_2O (8/2)	PE10100	10	20	20	Water 20 min
PES-377#	DMSO/H_2O (8/2)	PE10100	20	20	20	Vacuum dry 24 h
PES-378#	DMSO/H_2O (8/2)	PE10100	20	20	20	Water 20 min
PES-379#	DMSO/H_2O (8/2)	PEG200,000	1	20	20	Vacuum dry 24 h
PES-380#	DMSO/H_2O (8/2)	PEG200,000	1	20	20	Water 20 min
PES-381#	DMSO/H_2O (8/2)	PEG200,000	10	20	20	Vacuum dry 24 h
PES-382#	DMSO/H_2O (8/2)	PEG200,000	10	20	20	Water 20 min

Table 7.4. Two-step modification condition of PES membrane using NMP^2/H_2O (7/3, v/v) as good solvent.

Sample No.	Modifier aqueous solution	Conc. (g/L)	Time 1 (h)	Time 2 (h)	Termp. (°C)	Deswelling way
PES-383#	PEG6000/H_2O	20	0.5	0.5	20	Vacuum dry 24 h
PES-384#	PEG6000/H_2O	20	1	2	20	Vacuum dry 24 h
PES-385#	PEG6000/H_2O	20	3	3	20	Vacuum dry 24 h
PES-386#	PEG6000/H_2O	20	6	4	20	Vacuum dry 24 h
PES-387#	PEG6000/H_2O	20	10	15	20	Vacuum dry 24 h
PES-388#	PEG6000/H_2O	20	19	3	20	Vacuum dry 24 h
PES-389#	PEG6000/H_2O	20	22	5	20	Vacuum dry 24 h
PES-390#	PEG6000/H_2O	20	16	144	20	Vacuum dry 24 h
PES-391#	PEG6000/H_2O	20	16	0.5	20	Vacuum dry 24 h
PES-392#	PEG6000/H_2O	20	16	0.5	20	Water 20 min
PES-393#	PEG6000/H_2O	20	16	2.5	20	Vacuum dry 24 h
PES-394#	PEG6000/H_2O	20	16	2.5	20	Water 20 min
PES-395#	PEG6000/H_2O	20	10	4.0	20	Vacuum dry 24 h
PES-396#	PEG6000/H_2O	20	10	4.0	20	Water 20 min
PES-397#	PEG35,000/H_2O	20	20	4	30	Vacuum dry 24 h
PES-398#	F108/H_2O	20	20	3	30	Vacuum dry 24 h
PES-399#	F127/H_2O	20	20	2	30	Vacuum dry 24 h
PES-400#	PEG35,000/H_2O	20	20	2	20	Vacuum dry 24 h
PES-401#	F108/H_2O	20	20	2	20	Vacuum dry 24 h
PES-402#	F127/H_2O	20	20	2	20	Vacuum dry 24 h
PES-403#	PE10500/H_2O	20	20	2	20	Vacuum dry 24 h
PES-404#	L64/H_2O	20	20	2	20	Vacuum dry 24 h
PES-405#	RPE1740/H_2O	20	20	2	20	Vacuum dry 24 h

Appendix-2 Abbreviations

1. Abbreviations of various polymer substrates

   Original/unmodified polymers are abbreviated as „O_polymer“, such as O_PP, O_PES; solvent treated polymers are abbreviated as „S_polymer“, such as S_PP, S_PES; and entrapment modified polymers are abbreviated as „E_polymer“, such as E_PP.

   In this dissertation, two entrapment strategies have been tested, which are abbreviated as E1 and E2. In Section 4.1, E1_PES and E2_PES represents PES entrapment treated with two different procedures. In other sections for PP surface modification, only E1 was adopted, and all modified PP samples are abbreviated as E_PP.

   In addition, the abbrevation of E_PP/$C_{18}EO_8$, E_PP/cP1 means $C_{18}EO_8$ or cP1 entrapment modified PP.

2. Abbreviations of chemicals and polymers

BSA	bovine serum albumin
$C_{18}EO_8$	octaethyleneglycol monooctadecylether
$C_{18}EO_jC_{18}$	poly(ethylene glycol)(n) distearate (n = 400 g/mol or j = 8; n= 6000 g/mol or j = 136)
DCE	1,2-dichloroethane
d-chloroform	deuterochloroform
DMAc	dimethylacetamide
DMF	N, N-dimethylformamide
DMSO	dimethyl sulfoxide
EO	ethylene oxide
MF	Microfiltration

NMP	N-methyl-2-pyrrolidone
NIPS	nonsolvent induced phase separation
NPC	N-methylene phosphonic chitosan
PANI	polyaniline
PBA-*b*-PDMAEMA	poly(butyl acrylate)-*b*-poly((dimethylamino)ethyl(methacrylate)
PBA-*b*-P*q*DMAEMA	methyl and octyl groups quaternized PBA-*b*-PDMAEMA
PBA-*b*-PNIPAAm	poly(butyl acrylate) -*b*- poly(N-isopropylacrylamide)
PBS	phosphate buffer solution
PDL-LA	poly ($_{D, L}$-lactic acid)
PE	polyethylene
PEG	polyethylene glycol
PEO	polyethyleneoxide
PEOx	poly(ethyl oxazoline)
PES	polyethersulfone
PET	polyethylene terephthalate
PLA	poly(lactic acid)
PLL	poly($_{L}$-lysine)
PL-LA	poly($_{L}$-lactic acid)
PLL-RGD	poly($_{L}$-lysine)-GRGDS
Pluronic®	PEO-PPO-PEO (PE10100, PE10300, PE10500, L64, F127, F108) and PPO-PEO-PPO (RPE1740)
PMMA	polymethyl methacrylate
PMMA-b-PPY	poly(methyl methacrylate)-b-poly(1-pyrenyl methacrylate)
PNIPAAm	poly(N-isopropylacrylamide)

PO	propylene oxide
PPO	polypropyleneoxide
PS	polystyrene
PS-b-P2VP-b-PEO	poly(styrene-b-2-vinylpyridine-b-ethylene oxide)
PUR	polyurethane
PVP	polyvinyl pyrrolidone
PV-PS	poly(N-vinylpyrrolidone-styrene)
PV-PVA	poly(N-vinylpyrrolidone)-b-poly(vinyl acetate)
TEG	triethylene glycol
Tetraline	1,2,3,4-tetrahydronaphthalene
TFE	2,2,2-trifluotoethanol
THF	tetrahydrofuran

Appendix-3 List of publications during doctoral study

Publications

1. **Haofei Guo**, Mathias Ulbricht. Preparation of thermo-responsive polypropylene membrane via surface entrapment of poly(N-isopropylacrylamide)-containing macromolecules. Journal of Membrane Science, 2010. Submitted.

2. **Haofei Guo**, Mathias Ulbricht. The effects of (macro)molecular structure on hydrophilic surface modification of polypropylene membranes via entrapment. Journal of Colloid and Interface Science, 350: 99 - 109, 2010.

3. **Haofei Guo**, Mathias Ulbricht. Surface modification of polypropylene microfiltration membrane via entrapment of an amphiphilic alkyl oligoethyleneglycolether. Journal of Membrane Science, 349: 312 - 320, 2010.

Conference proceedings

Oral Papers in International Conferences

2010 **Haofei Guo**, Mathias Ulbricht. Influence of amphiphilic molecular structure on entrapment modification of polypropylene microfiltration membrane surface: a reverse micellization study. The 6th Zigmondy Colloquium, Chemnitz, Germany, 22nd - 24th March.

2009 **Haofei Guo**, Mathias Ulbricht. Antifouling modification of polypropylene micofiltration membrane surface via "polymer entrapping". Euromembrane 2009, Montpellier, France, 6th - 10th September.

Haofei Guo, Mathias Ulbicht. A mechamistic study of entrapment strategy for hydrophilic modification of polypropylene membrane surface. PERMEA 2009, Prague, Czech Republic, 7th - 11th June.

2008 **Haofei Guo**, Mathias Ulbicht. Antifouling surface modification of polypropylene microfiltration membrane with incorporation of amphiphilic stimuli-responsive block copolymer: a facile entrapment approach. 10th Network Young Membrains Berlin, Germany, 18th - 19th September.

Haofei Guo, Mathias Ulbricht. Entrapment of hydrophilic macromolecules for antifouling modification of polypropylene membrane surface: a mechanistic study. Gordon Research Conference: Membranes: Materials & Processes, New London, U. S. A., 9th - 15th August.

Poster Papers in International Conferences

2010 **Haofei Guo**, Mathias Ulbricht. Influence of amphiphilic molecular structure on entrapment modification of polypropylene microfiltration membrane surface: a reverse micellization study. European Membrane Society Summer School, Bucharest, Romania, 14th - 19th June.

2008 **Haofei Guo**, Mathias Ulbricht. Entrapment of hydrophilic macromolecules for antifouling modification of polypropylene membrane surface - A mechanistic study. Gordon Research Conference: Membranes: Materials & Processes, New London, U. S. A., 9th - 15th August.

Appendix-4 Curriculum Vitae

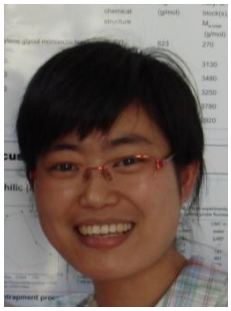

Name: Haofei Guo

Place/Date of Birth: Jiangsu, China/17 Sep 1981

Education

2007 – 2010 (Ph.D)	Technical Chemistry, University of Duisburg-Essen, Essen, Germany (Supervised by Prof. Dr. Mathias Ulbricht)
2003 – 2006 (M.Sc.)	Polymer Material Science and Engineering, Nanjing University of Technology, Nanjing, P. R. China (Supervised by Asst. Prof. Dr. Jian Huang)
1999 – 2003 (B.Sc.)	Polymer Material Science and Engineering, Nanjing University of Technology, Nanjing, P. R. China

Publication

Haofei Guo, Jian Huang, Xiaolin Wang. The alternate temperature-change cleaning behaviors of PNIPAAm grafted porous polyethylene membrane fouled by proteins. Desalination, 234: 42 - 45, 2008.

Patents in China

2006 Jian Huang, Xiaolin Wang, **Haofei Guo**. One hydrophilic modification strategy of polypropylene porous membrane surface with amphiphilic molecules. ZL 200610161542.2.

Jian Huang, Xiaolin Wang, **Haofei Guo**. One permanent hydrophilic modification strategy on polypropylene porous membrane surface. ZL 200610161541.8.

Awards

2009 ***"EMS Travel Award"*** from European Membrane Society (EMS). May.

"Best oral presentation" of EUROMEMBRNAE 2009, France. September.